Universität Bonn

Physikalisches Institut

Exploring the Web of Heterotic String Theories using Anomalies

Fabian Rühle

We investigate how anomalies can be used to infer relations among different descriptions of heterotic string theory. Starting from the observation that the construction mechanism of heterotic orbifold compactifications considered up to now prevents them from being resolved into fully smooth Calabi–Yau compactification manifolds, we use a new mechanism to obtain an orbifold which does not suffer from the aforementioned limitations. We explain in general how to resolve orbifolds into smooth Calabi–Yaus using toric geometry and gauged linear sigma models. The latter allow for studying the theory in various other regions of the string moduli space as well, which unveils interesting intermediate geometries. By following anomalies through the different regimes, we can match the orbifold theories to their smooth Calabi–Yau counterparts. In the process, we investigate discrete R and non-R orbifold symmetries and propose a mechanism for studying their fate in other regions of the moduli space. Finally, we introduce a novel anomaly cancelation mechanism in gauged linear sigma models, which manifests itself in target space as a description of compactification geometries with torsion and Neveu–Schwarz five branes.

Exploring the Web of Heterotic String Theories using Anomalies

Dissertation
zur
Erlangung des Doktorgrades (Dr. rer. nat.)
der
Mathematisch-Naturwissenschaftlichen Fakultät
der
Rheinischen Friedrich-Wilhelms-Universität Bonn

von
Fabian Rühle
aus
Herrenberg

Bonn, 30.07.2013

Dieser Forschungsbericht wurde als Dissertation von der Mathematisch-Naturwissenschaftlichen Fakultät der Universität Bonn angenommen und ist auf dem Hochschulschriftenserver der ULB Bonn
http://hss.ulb.uni-bonn.de/diss_online elektronisch publiziert.

Abstract

We investigate how anomalies can be used to infer relations among different descriptions of heterotic string theory. Starting from the observation that the construction mechanism of heterotic orbifold compactifications considered up to now prevents them from being resolved into fully smooth Calabi–Yau compactification manifolds, we use a new mechanism to obtain an orbifold which does not suffer from the aforementioned limitations. We explain in general how to resolve orbifolds into smooth Calabi–Yaus using toric geometry and gauged linear sigma models. The latter allow for studying the theory in various other regions of the string moduli space as well, which unveils interesting intermediate geometries. By following anomalies through the different regimes, we can match the orbifold theories to their smooth Calabi–Yau counterparts. In the process, we investigate discrete R and non-R orbifold symmetries and propose a mechanism for studying their fate in other regions of the moduli space. Finally, we introduce a novel anomaly cancelation mechanism in gauged linear sigma models, which manifests itself in target space as a description of compactification geometries with torsion and Neveu–Schwarz five branes.

Acknowledgments

First of all I thank my supervisor Prof. Hans Peter Nilles for giving me the opportunity to work in this fascinating, interesting, and challenging field of physics. I am especially grateful for his trust and confidence. Starting with accepting me in his group although I have not studied in Bonn, he gave me the opportunity of participating in the organization of international workshops and conferences, organizing and teaching tutorials, and supervising bachelor and master students. In this way, I learned a lot about the scientific field beyond pure research. My scientific advancement was driven by his view on physics as well as by the numerous conferences he enabled me to participate in. I further thank Priv. Doz. Stefan Förste for agreeing to be my second referee and for interesting discussions on various occasions.

I furthermore want to thank especially Prof. Stefan Groot Nibbelink, Michael Blaszczyk and Christoph Lüdeling for very fruitful collaborations and discussions. I also thank Nana Geraldine Cabo Bizet, Michael Ratz, Michele Trapletti, Patrick Vaudrevange, and Clemens Wieck for productive collaborations. I profited from discussions with Athanasios Chatzistavrakidis, James Gray, Hans Jockers, Sven Krippendorf, Damián Kaloni Mayorga Peña, Paul Oehlmann, and Matthias Schmitz, as well as from discussions with Ahmad Zein Assi during my stay at CERN. I also enjoyed conversations with my office neighbors Valéri Löwen, Claudia Stephan, and Clemens Wieck. In addition, I profited from the help of our bachelor student Pascal Cremer. I am indebted to Michael Blaszczyk and Christoph Lüdeling for proofreading this thesis.

My work was partially supported by the honors stipend of the Bonn Cologne Graduate school. I furthermore received support from the SFB-Tansregio TR33 "The Dark Universe" (Deutsche Forschungsgemeinschaft) and the European Union 7th network program "Unification in the LHC era" (PITN-GA-2009-237920). The latter also enabled me to spend three months at CERN for which I am particularly thankful.

On a private note, I especially enjoyed the company of Michael Blaszczyk and Christoph Lüdeling who showed me around in Bonn when I newly arrived here. I will always keep pleasant memories of our joint activities, especially watching soccer (either live at the FC Cologne stadium or on television) with Michael, playing squash with Christoph, and preparing food, playing cards, and leading on- and off-topic discussions with both. I am also thankful for fun hours on the tennis court with Hans Jockers.

In addition, I would like to thank Dr. Andreas Wisskirchen for his technical support and Dagmar Fassbender, Patrizia Zündorf, and Petra Weiss for their help with administrative issues. I also thank Eva Zimmermann, Michaela Mettler, and Christa Börsch for their organizational support concerning the Bethe Center.

Finally, I want to thank my parents for sparking my interest in science, my brother Bastian for his continuous support and memorable times outside of physics, and my girlfriend Anneli for everything.

CONTENTS

Chapter 1

⋯⋯⋯⋯⋯⋯⋯⋯⋯⋯⋯

INTRODUCTION

Son of man, you cannot say, or guess,
for you know only a heap of broken images

– TS Eliot, The Waste Land

Motivation

Up to now, four fundamental forces have been discovered in our universe which serve
as a good description for many observed processes. Arriving at this point was of course
a longstanding process during which our knowledge and our wit grew constantly. On
the theoretical side, new mathematical tools were developed for making complex con-
nections accessible. On the experimental side, fast technological progress and brilliant
ideas helped devising experiments of growing complexity culminating in the LHC. The
formulation of one of the fundamental forces, the electromagnetic force, was carried
out by Maxwell in the middle of the 19$^{\text{th}}$ century. As experiments became better, new
fundamental particles were discovered, which required the introduction of new phys-
ical forces. This led to the discovery of weak interactions. S. Glashow realized that
both electromagnetism and weak interactions could be described within one unifying
framework called electroweak interactions. As the accessible energy range grew even
further, the discovery of new particles led to the introduction of a third force called
strong force. The theoretical framework that was developed concurrently to these ex-
perimental advances is known as Quantum Field Theory.

One of the most important ingredients of this framework is the description of the
forces in terms of Abelian and non-Abelian gauge theories, called Yang–Mills theories.
In these theories, the interaction of particles is mediated by so-called gauge bosons.
The three fundamental forces discussed above are described by the gauge bosons of
$\text{SU}(3) \times \text{SU}(2) \times \text{U}(1)_Y$, which are the gauge groups of the strong and electroweak
interactions.

The other very important ingredient is the Higgs mechanism [1, 2], which is responsible for the spontaneous breakdown of the electroweak symmetry and for the masses of the fundamental particles. Until last year, this mechanism has only been a theoretical framework without experimental evidence. Yet, it was necessitated by the consistency of the model and many physicists believed in its existence, although it would take more than 50 years from its original postulation until its existence was announced by ATLAS [3] and CMS [4], two experiments at the LHC. The three fundamental forces together with their particle content are known as the Standard Model (SM) of particle physics.

The fourth fundamental force, gravity, is different. Its modern formulation was put forward by Einstein at the beginning of the last century and has remained basically unaltered. In this theory the mediation of the gravitational force is not described by gauge bosons but rather by properties of the spacetime itself.

Despite providing a complete picture of the fundamental interactions, and despite having withstood numerous experimental tests, the SM and the theory of gravity have shortcomings, all of which hint towards physics beyond the Standard Model.

Hierarchy problem   A hierarchy problem is a theoretical problem centered around the question why two physical scales are widely separated, which is considered unnatural without providing a convincing argument why one scale should be much smaller than the other. Usually, they are overcome by assuming the presence of new fields and symmetries. In the SM, one hierarchy problem deals with the question of why the electroweak breaking scale is so much lower than the scale of gravitational interactions called the Planck scale. The problem arises since the Higgs mass is expected to receive quadratic radiative corrections which drive its mass towards the Planck scale via the renormalization group (RG) running. Yet, its mass has been measured to be roughly seventeen orders of magnitude lower, which would require an unnatural, strong fine-tuning of the various contributions such that they cancel each other. A more convincing and more natural way of overcoming or ameliorating the problem is by introducing a symmetry that protects the Higgs mass from receiving too large corrections in the RG running. Another problem that requires explanation is the electric dipole moment of the neutron. Current measurements indicate that it is very small although a priori there is no theoretical reason why the term should be strongly suppressed. This is known as the strong CP problem. A third hierarchy problem of the SM is the wide separation of the masses of the elementary particles, ranging from the eV scale for the lightest neutrino to the multi-GeV scale for the top quark.

Cosmological problems   On the gravitational side there is the problem of dark energy. It is known that our universe undergoes an accelerated expansion [5]. For this result, Perlmutter, Schmidt, and Riess were awarded the Nobel Prize two years ago. This accelerated expansion can be described by adding a constant term proportional to the metric to Einstein's equations known as the cosmological constant. The cosmological constant describes dark energy, which was measured this year with unprecedented precision by the Planck satellite in combination with supernovae data to make up almost 70 percent of the total energy of the universe. When interpreting the cosmological constant term as vacuum energy in the framework of Quantum Field Theory, the result

deviates by 120 orders of magnitude from the experimental value. This problem lacks a convincing explanation within the framework of the SM.

New particles   There are experimental hints for the presence of new particles beyond those described by the SM. Most prominently, the observation of neutrino oscillations [6] requires the inclusion of three right-handed neutrinos. Since this particle does not carry a charge under the SM gauge group, it can be added to the SM without much alteration. Another hint is that the rotational curves of stars around the center of their galaxies differ strongly from their theoretical prediction. The results can be reconciled by assuming the presence of matter that is, however, not directly observed, hence the name dark matter. Since this matter cannot be seen directly, it has to interact weakly with the other SM particles, but it has to be heavy enough to alter the rotation due to gravitational effects. However, if the particles are heavy, one has to explain why they have not decayed into lighter particles in the course of the nearly fourteen billion years that our universe exists for.

Quantum theory of gravity   Motivated by the success of finding a unified description for what had previously been believed different phenomena, many physicists have tried to find a unified framework in which both the SM and the gravitational interactions can be described. However, when quantizing gravity by introducing a gauge boson that mediates the gravitational interactions, one encounters infinities which cannot be made sense of in a simple way. Yet, if we want to answer questions related to the Big Bang or to black holes, where all four fundamental forces are of the same strength and thus have to be treated simultaneously, we need a quantum theory of gravity.

Other open questions   Beyond the problems mentioned above, there are more fundamental questions which could be asked like: Why do we live in four spacetime dimensions? What sets the masses of the matter particle and the strengths of the four fundamental interactions? Why is the observed gauge group $SU(3) \times SU(2) \times U(1)_Y$? Clearly a more fundamental theory is needed for answering these kinds of questions.

Possible extensions   Many theories have been proposed to address the problems outlined above. An elegant way of solving the hierarchy problem related to the Higgs mass is to introduce a new symmetry called supersymmetry (SUSY). This theory relates the two different types of particles of the SM, bosons and fermions, to one another. By doing so, it not only treats the two kinds of particles in a more uniform way, but at the same time protects the Higgs mass from receiving quadratic corrections. However, since SUSY relates bosons to fermions, and since none of the known bosons has any of the known fermions as partner and vice versa, it requires the introduction of new particles. The resulting theory is known as the Minimal Supersymmetric Standard Model (MSSM). Some of the newly introduced particles could serve as dark matter candidates with SUSY providing a natural symmetry rendering them stable against decay. However, having not been observed to date, SUSY has to be broken at or above the energy scales we are currently testing with experiments. By gauging SUSY, the theory becomes invariant under local Lorenz transformations. Gauged SUSY is called supergravity (see e.g. [7–11]).

The other hierarchy problem related to the smallness of the electric dipole moment of the neutron can be explained in an elegant and natural way by postulating a global symmetry together with a new particle with distinct properties called axion [12].

The question of the presence of the right-handed neutrino can be combined elegantly with the question why the three fundamental forces of the Standard Model are of different strengths. Combined with SUSY, the running of the gauge couplings hints at a unification of all three gauge interactions at a scale of around 10^{16} GeV, known as the scale of grand unified theories (GUTs) [13]. This means that the difference of the fundamental forces stems from the fact that we are observing them at a very low energy scale. At a higher scale, they might all combine into one large gauge group, and the matter particles of the SM would then transform in more unified representations of these groups. Using that the Standard Model gauge group $SU(3) \times SU(2) \times U(1)_Y$ can be embedded into $SU(5)$, which can in turn be embedded into $SO(10)$, this provides a natural way of including the right-handed neutrino: in fact, all SM fermions plus the neutrino fit into one single irreducible representation, the spinorial representation **16** of $SO(10)$. The smallness of the mass of the left-handed neutrinos can then be explained using the seesaw mechanism [14], thus alleviating the third hierarchy problem.

However, the introduction of SUSY GUT theories also has new challenges that have to be overcome. Among them are proton stability and the question why flavor changing neutral currents and the Higgs μ term are so small. Also, while explaining the different strengths of the three SM forces, SUSY GUTs do not account for the different strengths of the gauge interactions as compared to gravity. One suggestion that has been put forward as an explanation is the introduction of extra dimensions. However, answering this question also ties into the question of finding a quantum theory of gravity.

String theory   String theory [15–18] is a theory which contains all of the mechanisms described above: SUSY, GUTs, and extra dimensions. Furthermore, it naturally includes the graviton as a mediator of the gravitational interactions. By introducing the string scale as one fundamental scale in the theory, it provides a finite UV completion to the SM including gravity. For all these reasons, string theory is particularly well-suited to address questions of physics beyond the Standard Model.

Superstring theory by itself requires ten spacetime dimensions for consistency. In addition, supersymmetry on the worldsheet of the string is required to remove unphysical tachyonic states from the string spectrum. This worldsheet supersymmetry extends to a supersymmetry of the ten-dimensional spacetime. String theory, being able to describe ten-dimensional gauge theory coupled to supergravity (SUGRA), is subject to strong consistency requirements. In general, super-Yang–Mills models coupled to SUGRA suffer from quantum anomalies rendering the theory inconsistent. In heterotic $E_8 \times E_8$ or $SO(32)$ string theory, two of the five known consistent and thus anomaly-free string theories, the particular choice of the gauge group necessitated by string theory yields in combination with an axionic field an anomaly-free ten-dimensional SUGRA theory. The gauge group E_8 is particularly appealing since it is the biggest exceptional Lie group.

However, the consistency requirements of string theory also present us with challenges. Neither do we observe ten spacetime dimensions nor do we live in a universe with an $E_8 \times E_8$ gauge group. Fortunately, both problems can be overcome simultaneously by assuming the extra six dimensions to be small and curled up (compact). Although the entire particle content and all symmetries are fixed uniquely in the ten-dimensional theory, the four-dimensional effective theory that we observe after compactification depends strongly on the properties of the compactification space. Thus, understanding the six-dimensional space is at the very heart of understanding the four-dimensional physics beyond the Standard Model that can be obtained from string theory. Requiring the theory to yield $\mathcal{N} = 1$ SUSY at low energies in four dimensions requires the compactification manifold to be of a special type called Calabi–Yau (CY) manifold [19]. These are complicated manifolds evading in most of the cases direct string calculations since properties needed for a full-fledged string analysis are unknown. However, there exist special singular points in the string moduli space, where these compactification manifolds become accessible to direct computation. The idea is to use these special points (orbifolds) [20–22] to study string theory and to learn something about its properties away from the orbifold point, where a direct computation is impossible.

Outline

There have been considerable advances in string theory towards the description of a realistic model of particle physics. This holds true for both string theory on orbifolds, where direct string computations can be performed within the framework of conformal field theory (CFT), as well as for string theory on smooth CY manifolds, where the analysis has to be carried out in the heterotic supergravity approximation which requires knowledge of the topological quantities of the compactification space. Since we want to calculate quantities on the orbifold and subsequently transfer them to the smooth CY, we require a tool that is universal and that can thus be used for connecting the theories in the different regimes; this is where anomalies come in. Since we know that string theory is a consistent theory in ten dimensions, it needs to yield a consistent theory after compactification to four dimensions as well, given that the compactification space is chosen such that it fulfills all string theory requirements. Being consistent especially requires the absence of anomalies. Thus by studying anomalies, relations across different regions in string moduli space can be established. By virtue of 't Hooft anomaly matching, we can use anomalies as (perturbatively) protected quantities. In this thesis we follow this approach and structure our results as follows:

Chapter 2 In this review chapter we introduce the concept of Calabi–Yau manifolds and orbifolds. We discuss their basic properties and explain how relevant information on the geometry and the massless matter spectrum can be extracted. The chapter serves to set our notation and introducing the less familiar reader to the techniques required for carrying out calculations on heterotic string compactification spaces. On the orbifold, this is done via conformal field theories, while on the CY we introduce cohomologies.

Chapter 3   In this chapter we explain how to connect the geometry of the singular orbifold with the smooth geometry of the CY via a so-called toric blowup. We introduce the language of gauged linear sigma models (GLSMs) and show how to use them for the description of the orbifold resolution process. We link our new findings to previous results that employed other techniques and point out the differences. Foremost, our GLSM approach has the advantage that we are not confined to either the orbifold or the blowup compactification spaces, but instead we can in principle access the entire moduli space of the compactification manifold, which allows for uncovering fascinating intermediate and non-geometric compactification spaces that correspond to neither pure orbifolds nor smooth CY manifolds.

Chapter 4   Here we introduce the basic concepts of anomalies. Like chapter 2, this is mostly a review chapter where we collect known results on anomalies, discuss the necessary tools for calculations with anomalies, and introduce our convention. We will make extensive use of the concepts introduced here in the rest of our discussions.

Chapter 5   We discuss how to relate the various consistency requirements of the orbifold to those of the smooth blowup CY. For most of the orbifold consistency requirements, we identify their counterpart in blowup. The most important part in the match are the field redefinitions which relates orbifold states that acquire a vacuum expectation value (VEV) to blowup states. These field redefinitions allow for relating the real part of the orbifold blowup mode to the Kähler parameters controlling the size of the resolution and the imaginary part to the axions involved in anomaly cancelation. By making extensive use of this field redefinition, we establish for the first time a complete match of an orbifold theory with its CY counterpart for the example of the $\mathbb{Z}_7$ orbifold. In this match we follow the anomalies from the orbifold point to the blowup and match both the anomaly polynomial as well as the massless matter spectrum. For the latter, we explain how to use a local version of the Hirzebruch–Riemann–Roch (HRR) index theorem, which gives the chiral part of the massless spectrum, to infer the complete massless spectrum and to match it to the orbifold. Being able to match the spectrum and the anomalies, we can set out to investigate how quantities on the orbifold side are transferred to the CY side. We find that fields with non-perturbative orbifold mass terms are identified as exactly massless fields in blowup. Furthermore, we study R symmetries on the orbifold and find that the blowup sees a different R symmetry.

Chapter 6   Here we deal with the question how string models can be constructed that yield viable phenomenology in both the orbifold and the blowup regime. Making use of the match between the consistency requirements in both regimes established in the previous chapter, we argue that the orbifold constructions used up to this point do not allow for viable phenomenology in full resolution. The argument is made again by analyzing the anomalies and realizing that the full resolution process introduces a hypercharge anomaly which is canceled at the cost of rendering the hypercharge massive. Having identified the source of the problem we discuss possible ways around. We first propose to use our GLSM description of heterotic orbifolds to arrive at a geometry where the critical orbifold fixed points remain unresolved, leaving the hypercharge anomaly-free. As another way around, we construct for the first time a phenomeno-

logically viable orbifold model based on the concept of non-local GUT breaking, which requires the construction of a compactification space with a nontrivial fundamental group. We study its phenomenological properties and find that these types of models compare well with the other string models that resemble the MSSM closest.

Chapter 7   Based on the results of R symmetries and the problem of connecting them between the orbifold and the CY regime, we study R symmetries from the GLSM point of view. We explain how discrete R and non-R symmetries can be identified, and propose a mechanism to analyze the charges of the massless matter states under the discrete symmetries at different points in moduli space.

Chapter 8   In this chapter we study anomalies on the worldsheet. Since the GLSM is a chiral theory, there are in general gauge anomalies. We identify a novel mechanism for the cancelation of these anomalies via the introduction of field-dependent, logarithmic Fayet–Iliopoulos terms on the worldsheet. This novel mechanism opens up a whole new class of models that can be studied in the GLSM formalism: we provide arguments that these new terms can be interpreted from the target space perspective as describing compactification manifolds with torsion and Neveu–Schwarz five (NS5) branes. A proper understanding of both is necessary since practically all MSSM-like string models require either torsion or both torsion and NS5 branes. Including these new terms changes the compact target space topology rather drastically. By including NS5 branes, the curves that are wrapped by the NS5 branes become inaccessible in target space. In cases where the new terms describe anti-NS5 branes rather than NS5 branes, the topology change is even more drastic since the target space seems to decompactify. This is discussed in various examples.

Chapter 9   In the last chapter we present our conclusions. Furthermore, we point out the questions that remain open and those which newly opened up during our analysis, and propose research directions based on our new findings.

List of publications

This thesis is based on results published in these papers which appeared in peer-reviewed journals:

- S. Groot Nibbelink, J. Held, F. Ruehle, M. Trapletti, and P. K. S. Vaudrevange "Heterotic Z(6-II) MSSM Orbifolds in Blowup," *JHEP* **0903** (2009) 005

- M. Blaszczyk, S. Nibbelink Groot, M. Ratz, F. Ruehle, M. Trapletti, and P. K. S. Vaudrevange "A Z2xZ2 standard model," *Phys.Lett.* **B683** (2010) 340–348

- M. Blaszczyk, S. Groot Nibbelink, F. Ruehle, M. Trapletti, and P. K. S. Vaudrevange "Heterotic MSSM on a Resolved Orbifold," *JHEP* **1009** (2010) 065

- M. Blaszczyk, S. Groot Nibbelink, and F. Ruehle "Green-Schwarz Mechanism in Heterotic (2,0) Gauged Linear Sigma Models: Torsion and NS5 Branes," *JHEP* **1108** (2011) 083

- M. Blaszczyk, N. G. Cabo Bizet, H. P. Nilles, and F. Ruehle "A perfect match of MSSM-like orbifold and resolution models via anomalies," *JHEP* **1110** (2011) 117

- M. Blaszczyk, S. Groot Nibbelink, and F. Ruehle "Gauged Linear Sigma Models for toroidal orbifold resolutions," *JHEP* **1205** (2012) 053

- C. Lüdeling, F. Ruehle, and C. Wieck "Non-Universal Anomalies in Heterotic String Constructions," *Phys.Rev.* **D85** (2012) 106010

Chapter 2

....

Heterotic String Compactification Spaces

In this chapter we lay the foundation for the discussion of particle physics models derived from (heterotic) string theory. In the first section, we explain the construction mechanism underlying heterotic string theory. As we shall see, phenomenological theories require string theory to be compactified on special types of complex three-dimensional manifolds called Calabi–Yau manifolds. Before we can discuss these manifolds, we need to introduce the necessary topological tools needed for the treatment of these spaces. This is done in section 2.2. Equipped with these tools, we investigate the properties of CY manifolds in section 2.3. In the last section we discuss string theory on a very special class of CY manifolds, so-called orbifolds.

2.1 Heterotic string theory

There are five known consistent ten-dimensional string constructions which are called *Type I, Type IIA/B*, and *Heterotic $E_8 \times E_8/SO(32)$ string theory*. In our analysis we will be dealing with the two heterotic string theories [23–25]. They can be described in terms of conformal field theories (CFTs) on the two-dimensional string worldsheet and its embedding into our spacetime, the so-called target space. Heterotic string theory is a theory of closed strings only. Hence the worldsheet that the string swipes out is a closed Riemann surface. Cancelation of the conformal anomaly requires the bosonic string to live in 26 dimensions. Another drawback of this theory is that it contains only worldsheet and target space bosons; however, we also need target space fermions in order to describe the matter particles of our universe. Another problem of the theory is that it has a tachyonic state in its spectrum, signaling an instability.

A solution to the last two problems is to include worldsheet fermions in the theory, which arise as the superpartners of the worldsheet bosons. These supersymmetric

string theories are called superstring theories. The worldsheet fermions give rise to target space bosons and fermions, depending on their boundary conditions. Furthermore, the tachyonic state is projected out since it lacks a superpartner. Canceling the conformal anomaly of the superstring requires the target space to be ten-dimensional. Albeit ten dimensions are less than 26, the introduction of superstrings has not solved the problem of string theory requiring more spacetime dimensions than we actually perceive. This problem is overcome by compactifying the six extra spatial dimensions on a compact manifold which is small enough to evade our perception but still part of the string target space. As we will explain in the next subsection, the low-energy massless spectrum of the 10D heterotic string theory is completely fixed. It is the geometry of the compactification manifold that determines the 4D physics which comes out of string theory.

Before we go deeper into the discussion of the compactification spaces, we would like to line out the heterotic string theory construction. On the closed worldsheet, we can split the string into left- and right-moving parts. In two dimensions, we can choose a different amount of SUSY for Majorana spinors of different chirality. The amount of left- and right-chiral supersymmetry is labeled as $\mathcal{N} = (\mathcal{N}_L, \mathcal{N}_R)$. As its name suggests, the idea of heterotic string theory is to treat left- and right-moving strings differently: supersymmetry is only introduced for the right-moving string modes. Heterotic string theories with $\mathcal{N} = (0,1)$ worldsheet supersymmetry thus lead to a 26-dimensional bosonic string theory in the left-moving sector and a 10-dimensional superstring theory in the right-moving sector. This means that the left-moving string has 16 additional bosonic degrees of freedom as compared to the right-moving string, which are severely constrained by string theory. Note furthermore that the worldsheet supersymmetry does not necessarily lead to (low-energy) target space supersymmetry. Since we want to describe in the end phenomenologically interesting models in four dimensions, we actually want an effective 4D theory with $\mathcal{N} = 1$ SUSY to make use of the advantages of SUSY GUTs outlined in chapter 1. The stringent conditions for $\mathcal{N} = 1$ SUSY in 4D that have to be imposed on the real six-dimensional manifold on which the 10D theory is compactified are discussed in section 2.3. Compactification spaces fulfilling these properties are called Calabi–Yau spaces.

In the bosonic description of heterotic string theory, the 16 extra left-moving degrees of freedom are described by 16 additional real bosonic worldsheet fields that provide the map into the gauge degrees of freedom. Consistency requirements impose that these extra bosonic fields are compactified on a 16-dimensional torus with an underlying even and self-dual lattice. There are only two 16-dimensional lattices which have these properties, namely the Lie algebra root lattice of $E_8 \times E_8$ and the root lattice of Spin(32) together with the spinorial weight lattice. Transformations in the 16-dimensional torus manifest themselves as gauge transformations in the 10D theory. Hence these extra dimensions give rise to the $E_8 \times E_8$ and SO(32) gauge groups of the heterotic string, respectively. This is remarkable for two reasons: First, as we shall discuss in great detail in section 4.2, these two gauge groups are the only ones which allow for an anomaly-free super-Yang–Mills theory coupled to supergravity in ten dimensions. Second, these gauge groups contain all GUT groups like SU(5), SO(10), and even the exceptional GUT groups in the case of $E_8 \times E_8$. The bosonic construction is well-suited for the

discussion of heterotic orbifold models, since it geometrizes the gauge degrees of freedom and allows for a nice description of the orbifold action in terms of shifts in the root lattices.

However, via the process of fermionization, there is also the possibility of combining two fermions into one boson. The two possible heterotic string theories then arise from imposing different boundary conditions for these fermions. This description will be useful in the context of the $\mathcal{N} = (0,2)$ gauged linear sigma model description of heterotic string theory.

2.1.1 Low energy 10D field content

As we have seen, heterotic string theory is a ten-dimensional theory. The observable 4D physics strongly depends on the choice of the compactification manifold used to get from ten to four dimensions. In almost all cases, these spaces are rather complicated and quantities like the metric are not known explicitly. For this reason, one cannot work in full-fledged string theory, but only in its low-energy approximation (i.e. in the limit where the string length $\ell_S^2 = \alpha'$ goes to zero) called heterotic supergravity, which describes $E_8 \times E_8$ or $SO(32)$ super-Yang–Mills theory coupled to supergravity. There is one special class of compactification manifolds, so-called orbifolds, which allow for an exact CFT calculation. Nevertheless, the 10D low-energy theory is a useful starting point since many properties of these compactification spaces are closely related to the (torus reduction of) the 10D theory. For the description of the 10D supergravity theory, we introduce ten left- and right-moving bosonic fields X^M together with the fermionic right-handed SUSY partners ψ^M, $M = 0, \ldots, 9$. In addition, we introduce 16 bosonic fields X^I, $I = 1, \ldots, 16$, which describe the extra left-moving degrees of freedom. We parameterize the worldsheet of the closed strings with (σ_1, σ_2) where σ_1 is the timelike direction. This worldsheet has the topology of an annulus, and we have to specify the boundary conditions for the fields X^I, X^M, and ψ^M:

$$
\begin{aligned}
X^I(\sigma_1, \sigma_2 + 2\pi) &= X^I(\sigma_1, \sigma_2) + P^I, \qquad P \in \Lambda_{E_8 \times E_8} \text{ or } \Lambda_{\text{Spin}(32)}, \\
\psi^M(\sigma_1, \sigma_2 + 2\pi) &= \pm \psi^M(\sigma_1, \sigma_2), \\
X^M(\sigma_1, \sigma_2 + 2\pi) &= X^M(\sigma_1, \sigma_2),
\end{aligned}
\tag{2.1}
$$

The first equation tells us that the strings describing the 16 extra left-moving degrees of freedom only have to close up to a lattice translation of $\Lambda_{E_8 \times E_8}$ or $\Lambda_{\text{Spin}(32)}$ on the 16-torus. If the string closes only under the addition of such a lattice vector P, it winds around the torus. The second equation encodes the freedom of choosing a spin structure on the worldsheet. The plus sign corresponds to the Ramond (R) boundary conditions which give rise to 10D target space fermions and the minus sign corresponds to the Neveu–Schwarz (NS) boundary conditions which give rise to target space bosons.

Since we will be interested in the massless spectrum, it is convenient to work in light-cone gauge where we define $X^{\pm} = X^0 \pm X^9$. The coordinates X^M, $M = 1, \ldots, 8$ then transform in the little group $SO(8)$ of the 10D Lorentz group $SO(1,9)$. The ground state

of the 10D theory is obtained by tensoring the left- and right-moving ground states. We find for their masses

$$\frac{M_L^2}{8} = \frac{P^2}{2} + \widetilde{\mathcal{N}} - 1 \,, \qquad \frac{M_R^2}{8} = \frac{q^2}{2} - \frac{1}{2} \,, \tag{2.2}$$

where P is an element of $\Lambda_{\mathrm{E_8 \times E_8}}$ or $\Lambda_{\mathrm{Spin(32)}}$ as in (2.1) and q is a weight vector of SO(8). Furthermore, $\widetilde{\mathcal{N}}$ denotes oscillator excitations. We denote the ground states of the right-moving sector by $|q\rangle$ and of left-moving sector by $\alpha_{-\widetilde{\mathcal{N}}}|P\rangle$. Imposing $M_R^2 = 0$, we find that $q^2 = 1$, which means that it is either in the vector representation $\mathbf{8}_V$ or the spinor representation $\mathbf{8}_S$ of SO(8), which correspond to the (NS) and (R) sector, respectively. The cospinor representation $\mathbf{8}_C$ is projected out by the GSO projection. From $M_L^2 = 0$, we find that either $P^2 = 2$ and $\widetilde{\mathcal{N}} = 0$ or $P^2 = 0$ and $\widetilde{\mathcal{N}} = 1$. In the first case, P has to be a root vector. By tensoring these right- and left-moving ground states, we obtain the following 10D SUGRA states

- $|q\rangle \otimes \alpha_{-1}^M|0\rangle$: This is the $\mathcal{N} = 1$ SUGRA multiplet containing the graviton g_{MN} together with the gravitino ψ_M, a scalar ϕ called dilaton together with its SUSY partner the dilatino χ, and an antisymmetric 2-form field B_{MN} called Kalb–Ramond field.

- $|q\rangle \otimes \alpha_{-1}^I|0\rangle$: These states correspond to the vector multiplets containing the Cartan generators of $\mathrm{E_8 \times E_8}$ or SO(32).

- $|q\rangle \otimes \quad |P\rangle$: These states give rise to non-Cartan vector multiplets of $\mathrm{E_8 \times E_8}$ or SO(32). Together with the Cartan generators mentioned above, they form the 10D vector multiplet transforming in the adjoint of $\mathrm{E_8 \times E_8}$ or SO(32).

Note that in particular there are no (chiral) matter superfields in 10D $\mathcal{N} = 1$ SUSY. The chiral multiplets of the 4D $\mathcal{N} = 1$ theory arise from the 10D vector multiplets, from which they inherit their behavior under gauge transformations. Their multiplicities are given by the number of zero modes that these fields have in the internal space. We discuss in the next section how to determine these zero modes for a generic CY, and in section 2.4 how to construct them for an orbifold.

2.2 Cohomology

The properties of models for particle physics derived from string theory depend strongly on the choice of the compactification space. As mentioned before, its properties will determine the amount of supersymmetry in 4D. Furthermore, its geometry places constraints on the gauge degrees of freedom, such that the geometry also influences the gauge group and (massless) matter content in 4D. The most useful tool for classifying the geometry and calculating properties like the particle spectrum is (co)homology. For this reason, we will briefly introduce the concept and set our notation. There are different cohomologies that can be used, and we describe how they are connected (see e.g. [26, 27]).

2.2.1 De Rham cohomology

Let us denote the p-forms of some Riemann manifold M by ω_p. They are sections of the pth exterior power of the cotangent bundle of M. The set of p-forms is usually denoted by $\Omega^p(M)$.

Definition (closed and exact forms)   A form $\omega_p \in \Omega^p(M)$ which satisfies $\mathrm{d}\,\omega_p = 0$ is called *closed* and a form that satisfies $\omega_p = \mathrm{d}\,\omega_{p-1}$ for some $(p-1)$-form ω_{p-1} is called *exact*.

Obviously, since the exterior derivative satisfies $\mathrm{d}^2 = 0$, every exact form is closed. It can be shown that the converse is true locally, but not necessarily globally. Cohomology groups are defined to contain closed forms which do not differ by exact forms,

$$H^p_{\mathrm{DR}}(M) = \frac{\text{closed forms } \omega_p}{\text{exact forms } \omega_p} \,. \tag{2.3}$$

This quotient space gives rise to the equivalence relation $\omega_p \sim \omega_p + \mathrm{d}\omega_{p-1}$, i.e. all closed forms that differ by exact forms are in the same cohomology class. To express this fact, we will sometimes say that the forms are equal in cohomology.

Definition (Hodge star)   Given a p-form in a d-dimensional manifold M, one can construct a $(d-p)$-form via the *Hodge star*, whose action on the basis elements $\mathrm{d}x^i$ is defined as

$$*(\mathrm{d}x^{i_1} \wedge \ldots \wedge \mathrm{d}x^{i_p}) = \frac{\sqrt{\det(g)}}{(d-r)!}\, \varepsilon^{i_1 \ldots i_p}{}_{i_{p+1} \ldots i_d}\, \mathrm{d}x^{i_{p+1}} \wedge \ldots \wedge \mathrm{d}x^{i_d} \,, \tag{2.4}$$

where g is the metric. For the sake of clarity we have explicitly written the wedge product, which we usually omit when writing down forms.

Definition (Harmonic forms)   A further important notion that can be defined with the help of the Hodge star are *harmonic forms*. A form ω_p is called harmonic if it is a zero of the Laplacian Δ, i.e. if it satisfies $\Delta\omega_p := (d + *d*)^2 \omega_p = 0$. Using the Hodge decomposition theorem, one can associate one harmonic representative to each cohomology class.

Definition (Homology)   Homology is defined similarly to cohomology, only in this case one takes p-cycles (or p-dimensional submanifolds) instead of p-forms and the exterior derivative d is replaced by the boundary map δ. Let us denote the p-cycles by c_p. One then defines closed cycles as those which do not have a boundary, $\delta c_p = 0$, and exact cycles as those which are the boundary of some higher-dimensional cycle, $c_p = \delta c_{p+1}$. Thus the homology groups are defined as

$$H_p(M) = \frac{\text{closed cycles } c_p}{\text{exact cycles } c_p} \,. \tag{2.5}$$

It is common to denote the dimensions of the cohomology groups by h^p_{DR} and of the homology groups by h_p.

Theorem (Poincaré duality)   As it turns out, the homology and cohomology groups are related via *Poincaré duality*, which provides an isomorphism between the pth cohomology and the $(d-p)^{\text{th}}$ homology group, $H^p(M) \simeq H_{d-p}(M)$. Furthermore, a given p-form ω_p can be integrated naturally over a p-cycle c_p, which, combined with Poincaré duality and Stoke's theorem on a manifold M, yields

$$\int_{c_p} \omega_p = \int_M \text{PD}(c_p) \wedge \omega_p = \int_{c_p \cap \text{PD}(\omega_p)} 1 \,. \tag{2.6}$$

Here, $\text{PD}(\cdot)$ denotes the Poincaré dual. By an abuse of notation, we will in the future denote both the cycle and its Poincaré dual with the same symbol. Poincaré duality will be used frequently to relate $(d-2)$ real-dimensional cycles (so-called divisors) to 2-dimensional forms and to calculate integrals by virtue of (2.6) via counting intersections of hypersurfaces.

2.2.2 Complexes and exact sequences

We want to introduce at this point also the notion of complexes and exact sequences, since it is frequently used in the literature and arises naturally when describing heterotic compactification spaces via gauged linear sigma models.

Definition (Complex)   With a *complex* we denote here a sequence of linear maps f_i between vector bundles $A, B, C, \ldots$,

$$\ldots \to A \xrightarrow{f_1} B \xrightarrow{f_2} C \xrightarrow{f_3} \ldots \tag{2.7}$$

which have the property that the image of a map f_i is contained in the kernel of the next map f_{i+1}, $\text{im}(f_i) \subset \text{ker}(f_{i+1})$.

Definition (Exact sequence)   A sequence of the type (2.7) is called *exact* if the image of a map equals the kernel of the next, $\text{im}(f_i) = \text{ker}(f_{i+1})$. A *short exact sequence* is a sequence with three nontrivial elements, where A injects into B via f_1 and B surjects onto C via f_2. This is sometimes written as

$$A \xhookrightarrow{f} B \xtwoheadrightarrow{g} C \,. \tag{2.8}$$

The fact that the map f is an injection can also be expressed in terms of an exact sequence as $0 \to A \xrightarrow{f} B$, since the image of the first map $0 \to A$ is just zero and hence the kernel of f also contains only zero. In a similar manner, the fact that the map g is surjective can be written as $B \xrightarrow{g} C \to 0$, since the kernel of the map $C \to 0$ is the whole of C and hence the image of g has to be the whole of C as well. Thus an alternative way of writing a short exact sequence is

$$0 \to A \to B \to C \to 0 \,. \tag{2.9}$$

The connection with cohomology becomes clear when we remember that p-forms $\omega_p \in \Omega^p(M)$ are sections of the exterior power of the cotangent bundle of M. Furthermore, we have maps $d := \Omega^p \to \Omega^{p+1}$ that satisfy $d^2 = 0$ (i.e. the image of one map is contained in the kernel of the next, since each exact form is closed); hence they can be used to define a complex, the so-called de Rham complex

$$0 \to \Omega^0(M) \xrightarrow{d} \Omega^1(M) \xrightarrow{d} \Omega^2(M) \xrightarrow{d} \dots . \tag{2.10}$$

If this complex was an exact sequence, each $(p+1)$-form $\omega_{p+1} \in \Omega^{p+1}(M)$ would be the image under d of some p-form $\omega_p \in \Omega^p(M)$, or in other words each closed form would be exact. Since cohomology is defined by quotienting out those forms which are exact, the cohomology would be trivial in this case. In this sense cohomology is a measure for how "inexact" the sequence is, i.e. how many forms are not the image of lower forms.

2.2.3 Dolbeault cohomology

In the cases we will be dealing with, the manifold M will be complex. From now on, when talking about dimensions, we will always be referring to complex dimensions unless explicitly stated otherwise. After specifying a complex structure J on M we can split the tangent bundle TM into two disjoint spaces, $TM = TM^+ \otimes TM^-$, whose vectors have eigenvalues $\pm i$. Likewise, we split the cotangent spaces. (p,q)-forms are now defined as sections of $\wedge^p T^*M^+ \otimes \wedge^q T^*M^-$. This space of sections is usually denoted by $\Omega^{p,q}(M)$. We thus find that $\Omega^n(M) = \bigoplus_{p+q=n} \Omega^{p,q}(M)$. Using this, we decompose the exterior derivative as $d = \partial + \bar{\partial}$, where $\partial : \Omega^{p,q}(M) \to \Omega^{p+1,q}(M)$ and $\bar{\partial} : \Omega^{p,q}(M) \to \Omega^{p,q+1}(M)$, which means that the de Rham cohomology can be decomposed as $H^n_{\mathrm{DR}}(M) = \bigoplus_{p+q=n} H^{p,q}(M)$. We use $\bar{\partial}$ to define $\bar{\partial}$-closed and $\bar{\partial}$-exact forms as in the de Rham case (and likewise for ∂). Both ∂ and $\bar{\partial}$ square to zero. The associated Dolbeault complexes are

$$\begin{aligned} \dots \to \Omega^{p,0}(M) \xrightarrow{\bar{\partial}} \Omega^{p,1}(M) \xrightarrow{\bar{\partial}} \Omega^{p,2}(M) \xrightarrow{\bar{\partial}} \dots , \\ \dots \to \Omega^{0,q}(M) \xrightarrow{\partial} \Omega^{1,q}(M) \xrightarrow{\partial} \Omega^{2,q}(M) \xrightarrow{\partial} \dots . \end{aligned} \tag{2.11}$$

Using this, Dolbeault cohomology is defined via

$$H^{p,q}_{\bar{\partial}}(M) = \frac{\bar{\partial}\text{-closed forms } \omega_{p,q}}{\bar{\partial}\text{-exact forms } \omega_{p,q}} , \tag{2.12}$$

and likewise for $H^{p,q}_{\partial}(M)$. We denote the dimensions of $H^{p,q}_{\bar{\partial}}(M)$ by $h^{p,q}$. They agree with the dimension of $H^{p,q}_{\partial}(M)$. It is common to write down the dimensions $h^{p,q}(M)$ in the so-called Hodge diamond, which reads in d dimensions

$$
\begin{array}{ccccc}
& & h^{0,0} & & \\
& h^{1,0} & & h^{0,1} & \\
\iddots & & \vdots & & \ddots \\
h^{d,0} & \cdots & & \cdots & h^{0,d} \\
\ddots & & \vdots & & \iddots \\
& h^{d,d-1} & & h^{d-1,d} & \\
& & h^{d,d} & &
\end{array}
\qquad (2.13)
$$

Definition (Holomorphic form)   Lastly, we introduce a *holomorphic form* as a $(p, 0)$ form ω that satisfies $\bar{\partial}\omega = 0$. Of course, we can also carry over the notion of homology, the Hodge star, Poincaré duality and so on from the definitions in the de Rham case.

2.2.4 Vector bundle cohomology

Up to now, we have been discussing cohomology for sections of the cotangent bundle (i.e. of forms). However, we need to generalize the concept to arbitrary (gauge) vector bundles V over the compactification manifold M. The dimensions of the cohomology groups count the number of massless particles transforming in some representation of the Lie group. The vector bundle valued extension of Dolbeault cohomology is called Čech cohomology. It is defined rather abstractly in terms of local sections over the intersections of open covers, but the idea is the same as before: one defines a map between the different spaces of sections with the property that the map squares to zero. In this way, one obtains a complex and closed and exact objects. The cohomology groups $H^q(M, V)$ are then again given as the quotient of closed objects by exact objects, or as the kernel divided by the image. Dolbeault's theorem states that $H^q(M, \Omega^{0,p}) \simeq H^{p,q}(M)$, which establishes an isomorphism between Čech and Dolbeault cohomology for the cotangent bundle. Due to this, we will not go into more details about Čech cohomology here and simply think of the Čech cohomology groups in terms of Dolbeault cohomology groups, with e.g. $\bar{\partial}$ acting on $\Omega^{p,q}(M) \otimes V$ via $\bar{\partial} : \Omega^{p,q}(M) \otimes V \to \Omega^{p,q+1}(M) \otimes V$ as before.

Serre duality   In the context of vector bundle cohomology (or more generally sheaf cohomology), *Serre duality* is also very useful. It relates the qth Čech cohomology group of a vector bundle V to the $(d - q)^{\text{th}}$ cohomology of the dual bundle twisted by K,

$$
H^q(M, V) \simeq H^{d-q}(M, (V \otimes K)^*)^* , \qquad (2.14)
$$

where K is the canonical bundle which we will define later.

While counting the dimensions of the various cohomology groups is very involved and exceeds most of the times the available computational power by far, the alternating

sum $\chi = \sum_{i=0}^{d} (-1)^i h^i(M, V)$ of the dimensions of the bundle valued cohomology groups can be calculated without much effort from the Hirzebruch–Riemann–Roch index theorem. From Serre duality on manifolds with $K = 0$ (which are precisely the Calabi–Yau manifolds we are dealing with predominantly), we see that furthermore $h^i(M, V) = h^{d-i}(M, V^*)$.

2.2.5 Topological invariants

The extraction of phenomenological properties of heterotic CY models is closely linked to the characterization of the topological properties of vector bundles. Very important invariants of a vector bundle are the so-called Chern classes. They are defined as the coefficients of the characteristic polynomial $P(\mathcal{V})$ of the curvature Ω of the bundle $\mathcal{V}$:

$$P(\mathcal{V}) := \det\left(\mathbb{1} + \lambda \frac{i\Omega}{2\pi} \right) := \sum_i \lambda^i c_i(\mathcal{V}) \tag{2.15}$$

The curvature Ω is defined using the connection ω via $\Omega = d\omega + [\omega, \omega]$. Since it is a two-form, the Chern class $c_k(\mathcal{V})$ is a $2k$-form.

We are mainly interested in two types of bundles:

- The tangent bundle $\mathcal{V} = TX$ of the compactification manifold X. In this case, the connection is the spin connection and the curvature Ω is the Ricci curvature R.

- A (gauge) vector bundle $\mathcal{V} = V$. In this case, the connection is the gauge connection or gauge field A in the representation corresponding to V, and the curvature is the field strength F.

In particular, the first Chern class is $c_1 = \mathrm{tr}(i\Omega)/(2\pi)$. Using Chern classes, one can define other useful topological invariants like the Chern character, which we will encounter at various points throughout our discussion, and the Todd class:

$$\mathrm{ch}(\mathcal{V}) := \mathrm{tr}\, e^{\frac{i\Omega}{2\pi}} = \dim(\mathcal{V}) + c_1(\mathcal{V}) + \frac{1}{2!}\left[c_1(\mathcal{V})^2 - 2c_2(\mathcal{V}) \right]$$
$$+ \frac{1}{3!}\left[c_1(\mathcal{V})^3 - 3c_1(\mathcal{V})c_2(\mathcal{V}) + 3c_3(\mathcal{V}) \right] + \dots \tag{2.16}$$

$$\mathrm{Td}(\mathcal{V}) := 1 + \frac{1}{2}\left[c_1(\mathcal{V}) \right] + \frac{1}{12}\left[c_1(\mathcal{V})^2 + c_2(\mathcal{V}) \right] + \frac{1}{24}\left[c_1(\mathcal{V})c_2(\mathcal{V}) \right] + \dots . \tag{2.17}$$

Using these quantities, the Hirzebruch–Riemann–Roch index theorem reads

$$\chi(X, \mathcal{V}) := \sum_{i=0}^{d} (-1)^i h^i(X, \mathcal{V}) = \int_X \mathrm{ch}(\mathcal{V})\mathrm{Td}(TX) \,. \tag{2.18}$$

This formula simplifies for the cases of interest to us, in which the compactification manifold X is three-dimensional and has $c_1(TX) = 0$, and the gauge bundle V is either

an SU(N) bundle or a line bundle U(1). In the first case, $c_0(V) = N$, $c_1(V) = 0$ and thus

$$\chi(X, V) = \int_X \frac{1}{2} c_3(V) \,. \tag{2.19}$$

Since the integral over the top Chern class is the Euler number of the bundle, we find that the chiral index is half the Euler number. In the case where V is a line bundle, $c_k = 0$ for $k > 1$ and we find

$$\chi(X, V) = \int_X \frac{1}{12} \left[c_1(V) c_2(TX) + 2 c_1(V)^3 \right] \,. \tag{2.20}$$

2.2.6 Spectrum computation

Let us now explain how to compute the low-energy spectrum given a compactification manifold X (which we assume has $c_1(TX) = 0$) and a vector bundle V valued in the Lie algebra of some Lie group H. The low-energy gauge group G is given by the commutant of H in $E_8 \times E_8$. We will be dealing with the case where V is a rank r bundle which is the sum of r line bundles and thus $H = U(1)^r$. Then, the $E_8 \times E_8$ is branched but the rank is not reduced by the bundle since U(1) commutes with itself. Nevertheless, we will find that these U(1) symmetries are generically massive and thus not present in the 4D spectrum. After determining the gauge group, we have to find the irreducible representations (irreps) and their multiplicities. As explained in (2.1), the 4D matter states arise from the 10D vector multiplet which transforms in the adjoint of $E_8 \times E_8$. Hence we obtain the irreps by branching the **248**'s of $E_8 \times E_8$ into irreps of $G \times H \subset E_8 \times E_8$. Then we can count the multiplicity of each irrep H by using the vector bundle cohomology methods outlined above. In the end, we are interested in the multiplicities of the irreps of G, which is given in terms of the irreps of H under the branching of the **248**. Let us outline this in an example.

Example (Vector bundle with SU(3) structure group)   For the sake of this example we assume again that X is three-dimensional with vanishing first Chern class and a trivial canonical bundle. The gauge group G will be given by the commutant of $H = SU(3)$ in $E_8 \times E_8$, which is $E_6 \times E_8$, since $[E_6 \times SU(3)] \times E_8$ is a maximal subgroup of $E_8 \times E_8$. Since the second E_8 is not involved in the analysis at all, we will suppress it for the rest of the example. The branching of the **248** into irreps of $E_6 \times SU(3)$ is

$$\mathbf{248} \to (\mathbf{78}, \mathbf{1}) \oplus (\mathbf{1}, \mathbf{8}) \oplus (\mathbf{27}, \mathbf{3}) \oplus (\overline{\mathbf{27}}, \overline{\mathbf{3}}) \,. \tag{2.21}$$

The first two terms correspond to the adjoints of E_6 and SU(3), respectively. From the decomposition, we see that the **27** of the 4D gauge group E_6 comes together with the **3** of SU(3). Hence we get the multiplicity of the **27** by calculating the dimension of the cohomology group $H^1(X, V)$. Likewise, the multiplicity of the $\overline{\mathbf{27}}$ is given by the dimension of $H^1(X, \wedge^2 V) \simeq H^i(X, V^*)$, where we used that the two-fold antisymmetrized fundamental irrep of SU(3) is equal to the complex conjugated fundamental $\overline{\mathbf{3}}$.

In cases where it is enough to know the chiral spectrum (i.e. the number of **27** minus the number of **$\overline{27}$**), we can apply the HRR index theorem (2.19). We will return to this example in the next section after we discussed more properties of the compactification space X.

2.3 Calabi–Yau manifolds

In this section we outline the conditions we impose on our string compactification spaces following [16, 19, 28]. As explained before, we want to choose the compactification space to yield low-scale $\mathcal{N} = 1$ SUSY. For the analysis we decompose the 10D target space of string theory into 4D Minkowski space times the internal 6D compactification manifold, $M_{10} = \mathcal{M}_{1,3} \times X_6$. Let us look at the SUSY variations of the 10D $\mathcal{N} = 1$ fermionic SUSY fields, which are the gravitino ψ_M, the dilatino χ, and the gaugino λ (following [28], it is convenient to redefine the fundamental fields by including the dilaton and the dilatino into their definition). Denoting the 10D SUSY parameter with ε, we find

$$\delta\psi_M = 0 \quad \Rightarrow \quad \left(D_M - \frac{1}{4}H_M\right)\varepsilon = 0\,, \tag{2.22a}$$

$$\delta\chi = 0 \quad \Rightarrow \quad \left(\Gamma \cdot \partial\phi + \frac{1}{24}H\right)\varepsilon = 0\,, \tag{2.22b}$$

$$\delta\lambda = 0 \quad \Rightarrow \quad \left(e^{\phi/2}F_{MN}\Gamma^{MN}\right)\varepsilon = 0\,. \tag{2.22c}$$

Here, H_M and H are the three-form field strength of the Kalb–Ramond two-form field B contracted with Γ matrices. As will be discussed in chapter 4, the absence of anomalies requires this field to contain the curvature and gauge connection Chern–Simons three-forms as well. Furthermore, F_{MN} is the gauge field strength. For the further analysis it is convenient to split the 10D spinor ε transforming in the **16** of SO(1,9) into its Minkowski part η transforming in the **2** and its internal part ζ transforming in the **4** of SO(6), $\mathbf{16} \rightarrow (\mathbf{2},\mathbf{4}) + (\overline{\mathbf{2}},\overline{\mathbf{4}})$.

Geometry   Let us first discuss the solutions in the case of a vanishing H field and a constant dilaton ϕ, but point out the relations to the general case as we go along. Imposing the gravitino variations to vanish, one finds that ζ needs to be covariantly constant, $D_M\zeta = 0$. Unbroken SUSY requires a parallelizable spinor which can act as the SUSY generator of the effective 4D theory. A general 6D manifold does not admit such a spinor, since it has in general SO(6) $\simeq$ SU(4) holonomy. As we are interested in $\mathcal{N} = 1$ SUSY, we need one invariant spinor, which means that the manifold has to have reduced holonomy SU(3) $\subset$ SO(6). Using this spinor, one can construct a complex structure by contracting with Γ matrices. From the complex structure, one can define the so-called Hermitian fundamental form J. Since it is Hermitian it is a $(1,1)$-form. If this fundamental form is closed, $\mathrm{d}J = 0$, the manifold is Kähler and the fundamental

form is the Kähler form. It can be shown [28] that the fundamental form satisfies the relation

$$H = \frac{1}{2} \mathrm{i} \, (\bar{\partial} - \partial) J \,. \tag{2.23}$$

Thus in the case $H = 0$, we find that our compactification manifold is Kähler. We note for later that (2.23) implies

$$\mathrm{d} \, H = \mathrm{i} \, \partial \, \bar{\partial} \, J \,. \tag{2.24}$$

As a next step, it can be shown that the SUSY variations (2.22) imply the existence of a globally defined holomorphic 3-form Ω, which is again built out of the spinors and Γ matrices. This 3-form is a representative of the unique equivalence class of $(3,0)$-forms, or in other words $h^{3,0} = 1$. Its norm

$$|\Omega| = \Omega_{ijk} \overline{\Omega}^{ijk} \,, \tag{2.25}$$

where $\overline{\Omega}$ is the complex conjugate of Ω, satisfies $|\Omega| = e^{8\phi}$. In particular, $|\Omega|$ is constant if the dilaton ϕ is. Using (2.22), one finds the relation

$$\mathrm{d}^{\dagger} J + \mathrm{i}(\bar{\partial} - \partial) \ln |\Omega| = 0 \,, \tag{2.26}$$

where $\mathrm{d}^{\dagger}$ is the adjoint of d. Thus in the case of a constant dilaton on a Kähler manifold one finds that the variation of the dilatino vanishes automatically (this is of course also obvious from (2.22b)). In terms of topological data, the $(3,0)$-form Ω transforms as a section of the canonical bundle $K = \wedge^3 T^* X^+$. Hence for Ω to be globally defined, the canonical bundle needs to be trivial. We come back to this in section 3.2.2.

Lastly, (2.22) can be shown to imply that X is Ricci-flat [28], i.e. its Ricci tensor $\mathcal{R}_{mn}$ vanishes. But this statement is equivalent to the holonomy of X actually being SU(3), since the Ricci tensor can be expressed in terms of the U(1) part of the spin connection. Again, this can be phrased in terms of topological data. Using the definition of the first Chern class $c_1 = (2\pi)^{-1} \mathcal{R}_{i\bar{j}} \, \mathrm{d} z^i \mathrm{d} \bar{z}^{\bar{j}}$, we see that the corresponding topological condition reads $c_1 = 0$. Yau's proof of Calabi's conjecture ensures the existence of a unique Ricci-flat Kähler metric for manifolds with SU(3) holonomy. While the condition of Ricci-flatness remains true also in the general case (with the torsion-improved connection), an analog of Yau's proof is still missing for general torsion geometries (see [29–33] for interesting results). Unfortunately, almost all phenomenologically viable models require torsion. It is common to classify torsion in terms of five torsion classes $W_1, \ldots, W_5$ appearing in $\mathrm{d}J$ and $\mathrm{d}\Omega$

$$\begin{aligned} \mathrm{d}J &= -\frac{3}{2} \mathrm{Im}(W_1 \overline{\Omega}) + W_4 \wedge J + W_3 \,, \\ \mathrm{d}\Omega &= -W_1 J \wedge J + W_2 \wedge J + \overline{W}_5 \wedge \Omega \,. \end{aligned} \tag{2.27}$$

As discussed above, in the case with constant dilaton and vanishing H field, J is closed since X is Kähler, and Ω is constant. Hence all torsion classes vanish. The only other

case with torsion which allows for a maximally symmetric (i.e. without domain wall) non-compact space $\mathcal{M}_{1,3}$ is the Strominger system with $W_1 = W_2 = 0$, $W_4 \sim W_5 \sim \mathrm{d}\phi$. Most of the time we will investigate heterotic string theory to lowest order in α', to which we ignore the torsion effects.

Let us collect the (not necessarily independent) properties of CY compactification manifolds: They are Kähler manifolds with vanishing first Chern class, which is equivalent to the existence of a Ricci-flat Kähler metric. At the same time, there is a unique volume $(3,0)$-form Ω, which means that the canonical bundle is trivial. Lastly, the holonomy group is $SU(3)$. These properties fix most of the topological data of a CY manifold. By complex conjugation, we see that $h^{p,q} = h^{q,p}$, and thus only roughly one half of the Hodge diamond can be independent (i.e. the Hodge diamond is symmetric along the vertical axis). Furthermore, using the Hodge star or Serre duality together with complex conjugation, one can show that $h^{i,j} = h^{N-i,N-j}$, which induces a symmetry along the horizontal axis of the Hodge diamond. Since additional $h^{i,0}$ forms on a CY would give rise to more parallelizable spinors and we only have $\mathcal{N} = 1$ SUSY, we find that $h^{k,0} = 0$ for $0 < k < d$. This means that for $d = 3$, only the dimension of two cohomology classes is not determined, namely the one of $h^{1,1} = h^{2,2}$, which corresponds to Kähler deformations, and the one of $h^{1,2} = h^{2,1}$, which corresponds to complex structure deformations. This means that the Euler number is $\chi(X) = 2(h^{1,1} - h^{2,1})$.

Gauge sector   Let us now turn to the gauge sector. For this we have to investigate the SUSY gaugino variations (2.22c).

As alluded to before and explained in chapter 4 in great detail, the geometric sector and the gauge sector are correlated by requiring anomaly freedom, which leads to a modification of the transformation behavior of the B field under gauge and gravitational variations and thus to an inclusion of Chern–Simons terms in the field strength H (cf. also (4.32)),

$$H = \mathrm{d}B + \omega_{3,\mathrm{L}} - \omega_{3,\mathrm{YM}}\,, \tag{2.28}$$

where the Chern–Simons three-forms are expressions in the spin and gauge connection, cf. (4.26). We note that, except for the so-called standard embedding case where the gauge connection and the spin connection are identified, the H field is in general non-vanishing. Thus, from (2.23) we find that J cannot be vanishing either and thus the compactification space cannot be Kähler.

However, the Bianchi identity derived from (2.28) by taking the exterior derivative is not the only condition which we impose on the gauge sector. By looking at the SUSY gaugino variations, one finds two conditions on the gauge flux $\mathcal{F}_{ij}$ of the internal manifold X:

$$\mathcal{F}_{ij} = \mathcal{F}_{\bar{i}\bar{j}} = 0\,, \qquad G^{i\bar{j}}\mathcal{F}_{i\bar{j}} = 0\,. \tag{2.29}$$

This set of equations is called the Hermitian Yang–Mills equations. The first two equations mean that $\mathcal{F}$ has to be a holomorphic $(1,1)$-form. The last equation is much harder to deal with (as the explicit form of the metric is unknown). Fortunately,

Donaldson, Uhlenbeck and Yau provided a set of topological conditions which the gauge flux has to satisfy in order to guarantee the existence of a solution [34, 35], which we call henceforth the DUY equations. These conditions will again be of topological nature, so we need to introduce some notation, following e.g. [36, 37]. For the sake of generality, we assume that the gauge sector is described by an arbitrary vector bundle, which can be written as the sum of subbundles, $V = \bigoplus_i \mathcal{V}_i$. We have to impose that the gauge flux $\mathcal{F}$ associated with the bundle V admits spinors, which means that the first Chern class of the gauge bundle has to be even, $c_1(V) \in H^2(X, 2\mathbb{Z})$. If $c_1(V) = 0$, the gauge bundle will be an SU(N) rather than a U(N) bundle, in analogy with the reduction of the structure group from U(N) to SU(N) in the case of the tangent bundle on Kähler manifolds with vanishing first Chern class. As a next step, it is convenient to introduce the slope of a vector bundle (or more generally of a coherent sheaf).

Definition (Slope)   The *slope* $\mu(V)$ of a coherent sheaf V on a CY threefold X with Kähler form J is defined as

$$\mu(V) = \frac{1}{\text{rk}(V)} \int_X c_1(V) \wedge J \wedge J. \qquad (2.30)$$

A stable vector bundle is a bundle for which the slope of all coherent subsheaves $W \subset V$ with $0 < \text{rk}(W) < \text{rk}(V)$ is strictly smaller than the slope of V. SUSY requires that the slope $\mu(V)$ of the gauge bundle vanishes. In the case we are considering, the bundle V consists of several bundles $\mathcal{V}_i$. This then requires the slope of all subbundles $\mathcal{V}_i$ to be equal (and zero), which is known as poly-stability of the bundle V in the literature. Checking whether or not a given bundle is stable is an incredibly hard task, since the slope has to be compared to all subsheaves. This complication can be circumvented by choosing all bundles $\mathcal{V}_i$ to be line bundles, i.e. vector bundles of rank one. In this case, there are no nontrivial subsheaves and thus this condition is trivially fulfilled. This is the approach we are taking here. The only thing that remains to be checked for the sum of line bundles is that there is a direction in Kähler moduli space along which all slopes vanish simultaneously. This is still a strong restriction on both the vector bundle and the geometry: by wandering around in Kähler moduli space, it can easily happen that one leaves the Kähler cone of the particular geometry under consideration and enters a new one with a different underlying geometry. However, this means that the Bianchi identity conditions derived from (2.28) change as well and the new geometry might be incompatible with the chosen gauge bundle.

Let us finally comment on the spectrum calculation for a given gauge bundle. As mentioned before, the number of particles is counted by the dimension of the bundle valued cohomology groups $h^i(X, V)$. It can be shown [37] that a line bundle $\mathcal{L}$ has $h^0(\mathcal{L}) = 0$ if it has negative slope $\mu(\mathcal{L}) < 0$. By Serre duality on a CY with trivial anticanonical bundle, this implies that $h^3(\mathcal{L}) = 0$ if $\mu(\mathcal{L}) > 0$. We are looking for directions in the Kähler moduli space where $\mu(\mathcal{L}) = 0$. If there are points in moduli space where also $\mu(\mathcal{L}) \gtrless 0$ then $h^0(\mathcal{L}) = h^3(\mathcal{L}) = 0$. The only exception to this is the trivial bundle $\mathcal{O}$, which has vanishing slope everywhere, but we will not include the trivial bundle in the gauge bundle, hence this case will not arise. Thus in these cases only $h^1(\mathcal{L})$ and $h^2(\mathcal{L})$ will be non-vanishing. They will count the number of particles

and antiparticles, respectively. As alluded to before, the computational power is in most cases not sufficient to calculate these cohomology groups separately; the only computationally accessible quantity is the chiral index $\chi(V)$. In chapter 7, we will choose a description of the compactification space which allows for computing these classes explicitly by appealing to a simplified version of the compactification space. In the other cases, we can sometimes disentangle the number of particles and antiparticles by relating the CY manifold X to its singular orbifold limit, where the calculation can be done explicitly, which is explained in detail in chapter 5.2. Using these techniques, we can access models on compactification spaces which have a large number of Kähler moduli and are thus inaccessible to direct computations, since computation costs of the fastest implementation of the calculation still grows roughly exponentially with the size of the Kähler moduli space [38] (more precisely, it grows exponentially with the size of the Stanley Reissner ideal to be defined in section 3.2).

Example (Standard embedding) Let us return to the example already discussed in section 2.2.6, namely the one of a CY threefold in standard embedding. In this case the CY has SU(3) spin and gauge connection. Due to the properties of the Hodge diamond of a CY, their Euler number is $\chi(X) = 2(h^{1,1} - h^{2,1})$. Thus the net number of chiral massless particles obtained from the HRR index theorem (2.19) is

$$\chi(V) = \frac{1}{2} \int_X c_3(V) = \frac{1}{2} \int_X c_3(TX) = \frac{1}{2}\chi(X) = h^{1,1} - h^{2,1} \,. \qquad (2.31)$$

In other words, the number of "families" (i.e. the number of **27**'s) is given by the number of Kähler moduli minus the number of complex structure moduli of the CY.

The same result is of course found from vector bundle cohomology. Take $V = \Omega^{0,1}$. Since the tangent bundle is stable, we find $h^0(X, V) = h^3(X, V) = 0$, and thus $h^1(X, V)$ and $h^2(X, V)$ count the number of particles and antiparticles respectively. By using the isomorphism between Čech and Dolbeault cohomology, we have $h^1(X, V) = h^{1,1}(X, V)$ and $h^2(X, V) = h^{1,2}(X, V)$. We thus obtain $\chi(V) = \sum_{i=0}^d (-1)^i h^i(X, V) = h^{1,1} - h^{1,2}$.

Let us investigate the rest of the Hodge diamond. Under complex conjugation, one finds that $h^{p,q} = h^{q,p}$. By Serre duality we have that $h^{p,q} = h^{3-p,3-q}$. Using this information together with the fact that we have $\mathcal{N} = 1$ SUSY in 4D, we can reconstruct the whole Hodge diamond and verify that $h^{0,0} = h^{3,0} = h^{0,3} = h^{3,3} = 1$, $h^{1,1} = h^{2,2}$, $h^{2,1} = h^{1,2}$, and the rest zero.

2.4 Orbifolds

Orbifolds were first introduced in [20, 21]. The review of the main properties in this section is based on [39, 40]. Good reviews can e.g. be found in [41, 42]. In summary, (toroidal) orbifolds are a special class of CY manifolds constructed from a torus by modding out a discrete symmetry group. This introduces singularities, which are, however, rather mild and unproblematic for the definition of a consistent string theory in this background.
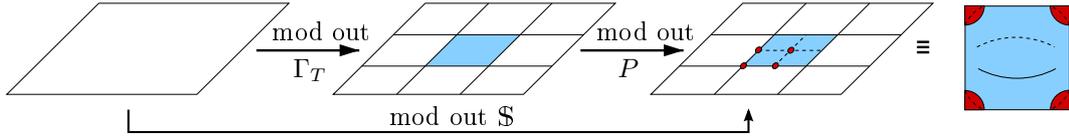
Figure 2.1: Summary of the orbifold construction mechanism in 2D. One starts with $\mathbb{R}^2 \simeq \mathbb{C}$. Dividing by a lattice Λ_T leads to equivalence relations defining a torus. Modding out the point group P then leads to an orbifold. Alternatively, one start with $\mathbb{R}^2 \simeq \mathbb{C}$ and mod out the space group $\mathbb{S}$.

2.4.1 Orbifold constructions

The idea of orbifolds is to start with the simplest conceivable compact space, namely a torus T^6 as the internal compactification manifold. This torus can be described as the quotient space $T^6 = \mathbb{R}^6/\Lambda_T$, where $\Lambda_T = \{n_i e_i \mid n_i \in \mathbb{Z}\} \simeq \mathbb{Z}^6$ is a six-dimensional lattice spanned by lattice vectors e_i, $i = 1, \ldots, 6$. As explained in the previous section, the flat torus allows for more parallelizable spinors and thus the amount of supersymmetry is not reduced upon compactification. This means that all 16 components of the 10D Majorana–Weyl spinor are conserved, which gives rise to $\mathcal{N} = 4$ SUSY in 4D. In order to break the supersymmetry down to $\mathcal{N} = 1$, a discrete symmetry group G is modded out of the underlying toroidal space. The resulting space is called an orbifold $\mathbb{O}$. In the following, we take this discrete symmetry group G to be the discrete cyclic Abelian group $G = \mathbb{Z}_N$ or $G = \mathbb{Z}_M \times \mathbb{Z}_N$ (for a discussion of orbifolds and torus lattices based on non-Abelian discrete symmetries and roto-translations, see [43]).

Point group and space group The symmetry group G is called the *point group*. The semidirect product of the point group G and the torus lattice Λ_T is the so-called *space group* $\mathbb{S} = \Lambda_T \rtimes G$. Its elements are given in terms of an orbifold rotation $\theta_1^{p_1}\theta_2^{p_2}$ and a lattice translation $\lambda = \sum_i n_i e_i$. The group operation $\circ$ acting on two group elements $g, h \in \mathbb{S}$ reads

$$g \circ h = (\theta_1^p \theta_2^q, \, \lambda_1) \circ (\theta_1^r \theta_2^s, \, \lambda_2) = (\theta_1^{p+r} \theta_2^{q+s}, \, \theta_1^p \theta_2^q \lambda_1 + \lambda_2). \tag{2.32}$$

Note the intermixing of the orbifold rotations and the lattice shifts, which shows again that the space group is a semidirect product.

In summary, an orbifold is obtained by either dividing T^6 by the point group G or by dividing $\mathbb{R}^6$ by the space group $\mathbb{S}$, $\mathbb{O} = T^6/G = \mathbb{R}^6/(\Lambda_T \rtimes G)$, which gives rise to the equivalence relation $z \sim \theta_1^p \theta_2^q z + \lambda$. The construction mechanism described above is depicted schematically in figure 2.1 for the two-dimensional case.

Orbifold points $z_f \in \mathbb{O}$ that fulfill

$$g z_f = \theta_1^p \theta_2^q z_f + \lambda \equiv z_f \tag{2.33}$$

are called fixed points. For most orbifolds, there are fixed loci where g acts trivial on an entire two-torus. These fixed loci are called fixed tori or fixed lines.

In order to be able to mod out the symmetry, the complex structure of the underlying torus has to be chosen such that its symmetry is compatible with the discrete group action. This severely restricts the possible torus lattices and leads to a classification of the torus lattices in terms of root lattices of Lie algebras [44, 45]. (See [46] for a discussion of non-Lie lattices obtained from an orbifold GLSM.)

2.4.2 Orbifold conditions

$\mathcal{N} = 1$ **SUSY** The fixed points of the orbifold action lead to a (discrete) nontrivial holonomy which breaks the amount of SUSY that remains in the resulting 4D theory. The condition that has to be imposed on G in order to preserve exactly $\mathcal{N} = 1$ SUSY can be derived from imposing that one spinor of the internal SO(6) holonomy is left invariant. It is convenient to introduce complex coordinates z_i, $i = 1, 2, 3$ for the internal compactification space. The action of G, which we call orbifold twist in the following, can be chosen to act diagonally on the z_i, and can thus be written for $G = \mathbb{Z}_M \times \mathbb{Z}_N$ as

$$
\begin{aligned}
\theta_1(z_1, z_2, z_3) &\to (e^{2\pi i v_1} z_1, \ e^{2\pi i v_2} z_2, e^{2\pi i v_3} z_3), \\
\theta_2(z_1, z_2, z_3) &\to (e^{2\pi i w_1} z_1, \ e^{2\pi i w_2} z_2, e^{2\pi i w_3} z_3).
\end{aligned}
\tag{2.34}
$$

Here, we have associated the action of $\mathbb{Z}_M$ with θ_1 and of $\mathbb{Z}_N$ with θ_2. By definition, $\theta_1^M = 1$ and $\theta_2^N = 1$, hence the v_i and w_i are quantized in units of $1/M$ and $1/N$, respectively. In general, there are also two-tori in which the orbifold action is not the full $\mathbb{Z}_M \times \mathbb{Z}_N$ but only a subgroup $\mathbb{Z}_P$. It is common to collect the orbifold rotations in the twist vectors $v = \{v_1, v_2, v_3\}$ and $w = \{w_1, w_2, w_3\}$. When interested in $\mathbb{Z}_M$ orbifolds, one simply sets $w = 0$.

In order to leave one SO(6) spinor invariant that can generate $\mathcal{N} = 1$ SUSY (or alternatively, in order to embed $\mathbb{Z}_M \times \mathbb{Z}_N$ into SU(3) $\subset$ SO(6)), we need the sum of the v_i to be integer (and likewise for the w_i), since this allows for defining the invariant holomorphic (3,0)-form $\Omega = \mathrm{d}z_1 \wedge \mathrm{d}z_2 \wedge \mathrm{d}z_3$. From imposing that $\mathbb{Z}_N$ or $\mathbb{Z}_M \times \mathbb{Z}_N$ acts crystallographically on the underlying real six-dimensional torus lattice (i.e. G is an automorphism of Λ_T) and leaves exactly $\mathcal{N} = 1$ SUSY in 4D, one finds that the only possible orbifold groups are $\mathbb{Z}_N$ with $N = 3, 4, 6, 7, 8, 12$ or $\mathbb{Z}_M \times \mathbb{Z}_N$ with $N = 2, 3, 4, 6$ and M dividing N. For $\mathbb{Z}_M \times \mathbb{Z}_N$, the twist can be chosen such that it always acts trivially in one torus[1],

$$
v = \frac{1}{M}\{0, 1, -1\}, \quad w = \frac{1}{N}\{1, 0, -1\}.
\tag{2.35}
$$

Of course, the two orbifold actions should act trivially in different tori, as otherwise a whole T^2 is left invariant which leaves more supersymmetry unbroken in the resulting 4D theory. Likewise in the case of $\mathbb{Z}_N$ the orbifold action should not be trivial on any of the z_i.

---

[1]An exception to this is the $\mathbb{Z}_{6-\mathrm{I}}$ and the $\mathbb{Z}_2 \times \mathbb{Z}_6$ orbifold.
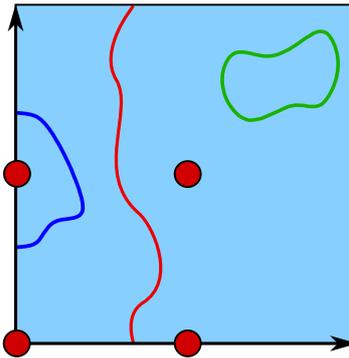
Figure 2.2: Schematic depiction of untwisted strings (green), twisted strings (blue), and winding strings (red) for one torus of the $T^6/(\mathbb{Z}_2 \times \mathbb{Z}_2)$ orbifold. The red dots indicate the fixed points.

Boundary conditions   Heterotic string theory is a theory of closed strings only. Hence the boundary conditions of the bosonic and fermionic worldsheet coordinates z and ψ have to be chosen such that the string closes under the orbifold action. This means that we impose for each $g \in \mathbb{S}$

$$z(\sigma_1, \sigma_2 + 2\pi) \stackrel{!}{=} gz(\sigma_1, \sigma_2) = \theta_1^m \cdot \theta_2^n z(\sigma_1, \sigma_2) + \lambda \,, \qquad (2.36)$$

$$\psi(\sigma_1, \sigma_2 + 2\pi) \stackrel{!}{=} \pm\theta_1^m \theta_2^n \psi(\sigma_1, \sigma_2) \,, \qquad (2.37)$$

where the $\pm$ encodes the (NS) or (R) boundary conditions. We can thus distinguish between three qualitatively different kinds of strings:

- *Untwisted strings*: They are already closed on the covering space.

- *Winding strings*:   They close by winding around the torus.

- *Twisted strings*:   They close only under the orbifold action.

The closed strings are just the ordinary 10D heterotic strings. The winding strings are new if one compactifies string theory on a torus. Since they wind around the torus, they will be massive and hence less relevant for our future discussion. The twisted strings are a novel feature of orbifold compactification. They always close by encircling an orbifold singularity, which means that these twisted strings are located at the orbifold fixed points and cannot be moved away. We will exploit this fact when matching heterotic orbifold theories to their resolution models. The three types of strings are depicted in figure 2.2 for a two-torus of the $\mathbb{Z}_2 \times \mathbb{Z}_2$ orbifold.

Modular invariance   Modular invariance of the string partition function at one-loop level imposes more constraints that the orbifold has to satisfy. First we note that the action of the space group has to be extended to the gauge sector of the heterotic string as well. We choose the so-called shift embedding in which the orbifold twist of

the geometry is accompanied by a shift in the gauge degrees of freedoms, i.e. in the root lattice $\Lambda_{E_8 \times E_8}$ of $E_8 \times E_8$,

$$g = (\theta_1^m \theta_2^n, n_i e_i) \hookrightarrow (\mathbb{1}, V_g), \qquad V_g = m V_{\mathrm{sh},\,1} + n V_{\mathrm{sh},\,2} + \sum_{i=1}^{6} n_i W_i \,. \qquad (2.38)$$

We thus see that both the rotation $\theta_1^m \theta_2^n$ and the orbifold lattice translations $n_i e_i$ lead to a shift in the gauge sector. The shifts associated with the orbifold rotations are called *orbifold shift vectors* $V_{\mathrm{sh},\,1,2}$. The W_i are up to six (discrete) Wilson lines, which can be thought of as a constant gauge background along the six torus directions. Hence a lattice translations by $n_i e_i$ causes a further shift of $n_i W_i$ in the gauge sector. It should be noted that the shift embedding does not reduce the rank of the gauge group, but merely leads to a branching of the primordial $E_8 \times E_8$ into its subgroups.

The first condition we have to impose on the shift vectors and Wilson lines is that they are trivial (i.e. in the root lattice $\Lambda_{E_8 \times E_8}$) if the space group element is trivial,

$$M\,V_{\mathrm{sh},\,1} \in \Lambda_{E_8 \times E_8}\,, \qquad N\,V_{\mathrm{sh},\,2} \in \Lambda_{E_8 \times E_8}\,, \qquad N_i\,W_i \in \Lambda_{E_8 \times E_8}\,. \qquad (2.39)$$

The N_i denote the order of the orbifold action along the ith torus direction. Furthermore, we remark that there are in general less than six independent Wilson lines, since they might not be compatible with the orbifold action (the only orbifold which allows for six Wilson lines is the $\mathbb{Z}_2 \times \mathbb{Z}_2$ orbifold). The second condition we have to impose is derived from modular invariance, which constrains the combination of allowed orbifold twist and lattice shifts via the modular invariance conditions [47]

$$
\begin{aligned}
M(V_{\mathrm{sh},\,1}^2 - v^2) &\equiv 0 \bmod 2\,, & N(V_{\mathrm{sh},\,2}^2 - w^2) &\equiv 0 \bmod 2\,, \\
N(V_{\mathrm{sh},\,1} \cdot V_{\mathrm{sh},\,2} - v \cdot w) &\equiv 0 \bmod 2\,, & N_i(W_i \cdot V_{\mathrm{sh},\,1,2}) &\equiv 0 \bmod 2\,, \\
N_i W_i^2 &\equiv 0 \bmod 2\,, & \gcd[N_i, N_j] W_i W_j &\equiv 0 \bmod 2\,,
\end{aligned}
\qquad (2.40)
$$

where $\gcd[\cdot, \cdot]$ denotes the greatest common divisor.

Spectrum computation   We will be interested in the massless orbifold spectrum. It is convenient to define the local twist v_g associated with a space group element $g = (\theta_1^m \theta_2^n, n_i e_i)$ in analogy with (2.38) as

$$v_g = mv + nw\,. \qquad (2.41)$$

Similarly to (2.2), we find for the masses of left-movers with momentum P and right-movers with momentum q

$$
\begin{aligned}
\frac{M_L^2}{8} &= \frac{(P + V_g)^2}{2} + \widetilde{\mathcal{N}} + \delta c - 1\,, \\
\frac{M_R^2}{8} &= \frac{(q + v_g)^2}{2} + \delta c - \frac{1}{2}\,.
\end{aligned}
\qquad (2.42)
$$

In addition, we have to impose the level matching condition $M_L \overset{!}{=} M_R$. Let us discuss the various contributions to the string masses. From the first term, we find that the momentum is shifted by the local orbifold shift and twist as compared to (2.2). Hence it is convenient to define the shifted momenta $P_{\mathrm{sh}} := P + V_g$ and $q_{\mathrm{sh}} := q + v_g$, respectively. Furthermore, we augment the orbifold twist vectors v, w and the momenta q with a zeroth component, which specifies the action and momenta in the transverse direction of the 4D spacetime in light-cone gauge (this is also sometimes called H momentum in the literature). In this way, the components of the shifted momenta determine the charges under the Cartan generators of the gauge group $E_8 \times E_8$ and the little group $SO(8)$ of the Lorentz group, respectively. Thus these quantities can be used to identify a massless string transforming in a specific representation. The $\widetilde{\mathcal{N}}_i$ are (fractional) quantum numbers corresponding to possible oscillator excitations of the string. The last terms correspond to a shift in the zero point energy arising from normal ordering. The shifts δc are given in terms of the twists by

$$\delta c = \frac{1}{2} \sum_{i=1}^{3} \omega_i (1 - \omega_i) \qquad \text{with} \qquad \omega_i = (v_g)_i \bmod 1 \,, \quad 0 \leq \omega_i < 1 \,. \tag{2.43}$$

Thus in order to find the massless spectrum, we have to find all combinations of shifted momenta P_{sh} and q_{sh} together with possible oscillator excitations $\widetilde{\mathcal{N}}_i$ that fulfill (2.42) with $M_L = M_R = 0$. However, not all states that fulfill the masslessness and level matching condition can actually be found in the 4D massless spectrum. Some states, which are not compatible with the orbifold action, get projected out. States that survive the orbifold projection satisfy

$$P_{\mathrm{sh}} V_h - (q_{\mathrm{sh}} - \widetilde{N} + \widetilde{N}^*) v_h \equiv 0 \bmod 1 \,, \tag{2.44}$$

for all local shifts V_h associated with some space group element $h \in \mathbb{S}$. The $\widetilde{N}^i, \widetilde{N}^{*\,i}$ count the number of (anti-)holomorphic oscillator excitations,

$$\widetilde{\mathcal{N}}^i = a\,\omega_i \widetilde{N}^i + b\,\omega_i^* \widetilde{N}^{*\,i} \,, \qquad a, b \in \mathbb{Z} \,, \tag{2.45}$$

with ω_i as defined in (2.43) and $\omega_i^* = -(v_g)_i \bmod 1$ such that $0 \leq \omega_i^* < 1$. A powerful tool for automated calculation of orbifold spectra is the `orbifolder` [48], which we use for determining the massless orbifold spectra in the following.

Gauge sector   In particular, (2.44) allows for finding the branching of the primordial $E_8 \times E_8$. The gauge bosons live in the untwisted sector and their shifted momenta P_{sh} are the 480 roots of $E_8 \times E_8$. Since the simple roots have length squared 2 and since $\delta c = 0$ in the untwisted sector, we find from (2.42) that $\widetilde{\mathcal{N}} = 0$. Furthermore, (2.42) tells us that $q_{\mathrm{sh}}^2 = 1$. Inserting this into the projection condition (2.44), one finds $P_{\mathrm{sh}} V_h \equiv 0 \bmod 1$. Choosing the space group element h to be a pure rotation or a pure translation in one torus direction, this means that the unbroken gauge group is given by the roots of $E_8 \times E_8$ that have an integral inner product with all orbifold shift vectors and Wilson lines.

R charge   The combination appearing in the brackets on the left-hand side of (2.44) is used to define the R charge of an orbifold state via [49]

$$R^i := q^i_{\rm sh} - \widetilde{N}^i + \widetilde{N}^{*\,i}\,, \tag{2.46}$$

where the index $i = 1, 2, 3$ labels the oscillators in the three two-tori. Defining the R charge in this way has the advantage that the combination (2.46) is invariant under picture changing. Furthermore, the orbifold moduli carry both shifted momenta and oscillator numbers $\widetilde{N}^i, \widetilde{N}^{*\,i}$, and the R charge is precisely the diagonal combination under which the moduli have R charge zero. It is an R charge since bosons and fermions transform differently, which follows from the fact that the right-moving shifted momenta of bosons and fermions are related via

$$q^{\rm f}_{\rm sh} = q_{\rm sh} - \left\{\frac{1}{2}, \frac{1}{2}, \frac{1}{2}, \frac{1}{2}\right\}\,, \tag{2.47}$$

and hence $R^{\rm f}_i = R_i - \frac{1}{2}$.

2.4.3 A note on R charge quantization

There are different naming conventions for the discrete R charges throughout the literature. Hence we would like to clarify how the different namings arise [50]. The discussion is carried out using the example of the $(T^2)^3/\mathbb{Z}_3$ orbifold. This orbifold possesses a discrete $(\mathbb{Z}_3)^3$ rotational symmetry stemming from rotating each torus independently by $\frac{2\pi{\rm i}}{3}$ (note that this is a symmetry of the compactification space but not an orbifold space group element). R charge conservation requires that the charges of a superpotential coupling involving L chiral superfields Φ_α, $W \supset \Phi_1 \cdots \Phi_L$, satisfy[2]

$$\sum_{\alpha=1}^{L} R^i_\alpha \equiv 1 \bmod N_i\,, \quad i = 1, 2, 3\,. \tag{2.48}$$

Here N_i is the order of the orbifold twist in the $i^{\rm th}$ torus. It should be noted that in this convention the superpotential W has R charge 1 and thus θ has R charge $\frac{1}{2}$.

In cases where rotating a sub-torus independently by $\frac{2\pi{\rm i}}{N_i}$ is a symmetry, an orbifold state Φ transforms as

$$\mathcal{R} \,:\, \Phi \to e^{2\pi{\rm i}v\cdot R}\,\Phi \tag{2.49}$$

with $v = \left(0, \frac{1}{N_1}, 0, 0\right)$ and similarly for the other sublattice rotations. Explicitly, this transformation acts in the following way:

- The bosonic R charge (2.46) is quantized in units of $\frac{1}{N_i}$, so under (2.49) bosons get a phase in multiples of $e^{\frac{2\pi{\rm i}}{N_i^2}}$.

---

[2]See [51] for a discussion of this rule in the case of non-prime orbifolds.

- The R charges of the fermions is shifted by $-\frac{1}{2}$, so θ transforms with a phase $e^{\frac{2\pi i}{2N_i}}$, i.e. sublattice rotations act as a $\mathbb{Z}_{2N_i}$ R symmetry.

- Finally, the order of (2.49) acting on the fermions is given by the least common multiple of N_i^2 and $2N_i$.

To summarize, the R transformations form a $\mathbb{Z}_{2N_i^2}$ symmetry, under which the charges of bosons, fermions and θ are of the form $2k$, $2k - N$ and N, respectively, where k is an integer. If N is even, so are all charges, and consequently, only a $\mathbb{Z}_{N_i^2}$ is realized on the fields.

Owing to this pattern, one finds at least 3 different R charge normalizations in the literature:

1. W has charge 1, and the smallest charge quantization is in units of $\frac{1}{2N_i}$. This is inspired by the orbifold R rule (2.48).

2. W has charge 2, and the smallest charge quantization is in units of $\frac{1}{N_i}$, which fits with the usual four-dimensional R charge conventions.

3. W has charge $2N_i$, and the smallest charge quantization is in units of 1.

In our example of the $\mathbb{Z}_3$ orbifold, each two-torus can be rotated independently (i.e. $N_i = 3$). We will be using the second normalization, such that we speak in this case of a $\mathbb{Z}_6^R$ symmetry where fermion charges are quantized in multiples of $\frac{1}{3}$, bosonic ones in multiples of $\frac{2}{3}$, and θ has charge 1. Note that there are states which transform with charge $\frac{1}{9}$ under each $\mathbb{Z}_3$ sublattice rotation. Clearly, this is not a bona fide $\mathbb{Z}_6$ symmetry because applying it six times does not give the identity of the fields, but it fits with the standard R charge normalization from four-dimensional supersymmetry, and the orbifold R charge conservation (2.48) becomes a mod 6 condition. This example will be discussed in detail in chapter 7.

Chapter 3

· ·

ALGEBRAIC GEOMETRY AND TORIC RE-SOLUTIONS

Algebraic geometry [26] is a very powerful mathematical framework which we will be using to describe the geometry of the CY compactification spaces. We will mostly be dealing with toric geometry and introduce two approaches to the topic: one approach which uses fans and toric diagrams and one approach which uses gauged linear sigma models (GLSMs). We will also comment on the connection of the two.

3.1 Divisors and line bundles

In order to access string theory on a generic Calabi–Yau manifold X, one needs to resort to topological quantities. The most important ones will be divisors and their associated line bundles. They are the basic ingredient for the study of other topological data. Since this section is a bit technical, let us state the rough idea first: Divisors are given as the zero locus of some polynomial equation f, which corresponds to a codimension one surface (a hypersurface) S inside a manifold X. The transition functions of this f across different patches of X can then be used to associate a line bundle to a divisor.

In the following, we will denote the set of meromorphic and holomorphic functions on some space X by $\mathcal{M}_X$ and $\mathcal{O}_X$, respectively. The sets of meromorphic and holomorphic functions which are not identically zero are denoted by $\mathcal{M}_X^*$ and $\mathcal{O}_X^*$.

Definition (Divisor)   A *divisor* D of X is a formal integer linear sum of analytic hypersurfaces S_i of X,

$$D = \sum_i a_i S_i \,, \qquad a_i \in \mathbb{Z} \,. \tag{3.1}$$

A divisor for which all $a_i \geq 0$ is called *effective*.

There is another way to define divisors. The definition is given in terms of transition functions between open covers of X. This description is advantageous for associating a line bundle to a divisor. For this, let $\{U_\alpha\}$ be an open cover of X. Choose non-vanishing meromorphic functions $f_\alpha \in \mathcal{M}^*_{U_\alpha}$ such that on the overlap of two covers U_α and U_β the quotient is a non-vanishing holomorphic function, $f_\alpha/f_\beta \in \mathcal{O}^*_{U_\alpha \cap U_\beta}$, which means that $\mathrm{ord}_{S_i}(f_\alpha) = \mathrm{ord}_{S_i}(f_\beta)$. Here, ord_{S_i} denotes the order of the zeros and poles of f along S_i, with $\mathrm{ord}_{S_i}(f)$ negative for poles. We then define a divisor via

$$D = \sum \mathrm{ord}_{S_i}(f_\alpha) S_i \,, \tag{3.2}$$

where we choose α for each S_i s.t. $U_\alpha \cap S_i \neq \varnothing$. Thus a divisor is a global section of $\mathcal{M}^*/\mathcal{O}^*$.

Definition (Principal divisor)   A *principal divisor* (f) is defined via a function $f \in \mathcal{M}$ by

$$(f) = \sum \mathrm{ord}_{S_i}(f) S_i \,. \tag{3.3}$$

Definition (Linear equivalence)   Two divisors D and D' are linear equivalent, $D \sim D'$, if they differ by a principal divisor.

Next, we describe how to assign a holomorphic line bundle to a divisor. A line bundle $\mathcal{L}$ is a vector bundle where the fiber F has dimension one. Let us choose an open cover $\{U_i\}$ of the base B and trivializations

$$\phi_\alpha : \mathcal{L}|_{U_\alpha} \to U_\alpha \times \mathbb{C} \,. \tag{3.4}$$

In terms of the trivializations ϕ_α, the holomorphic transition functions $g_{\alpha\beta} \in \mathcal{O}^*_{U_\alpha \cap U_\beta}$ on the overlap of two open covers $U_\alpha \cap U_\beta$ are given by $g_{\alpha\beta} = \phi_\alpha \circ \phi_\beta^{-1}$. Sections s_α of $\mathcal{L}$ associate points on the base B with points in the fiber $F \simeq \mathbb{C}$. In our case, the base will be some projective space $\mathbb{CP}^d$ and the sections will thus just be homogeneous polynomials of some degree Q in the homogeneous coordinates. This degree is the first Chern class $c_1(\mathcal{L})$ of the bundle. For a line bundle $\mathcal{L}$ with first Chern class Q we will simply write $\mathcal{L} = \mathcal{O}(Q)$ with $\mathcal{O}(0) = \mathcal{O}$.

As we have seen, divisors correspond to (a sum of) hypersurfaces cut out by sections f_α on open patches U_α with transition functions $g_{\alpha\beta}$. We take these transition functions to be the transition function of the associated line bundle. The degree of the sections is the first Chern class of the bundle. The linear equivalences of divisors also have a simple correspondence in terms of line bundles: a principal divisor D is given in terms of a global meromorphic function. Hence all transition functions $g_{\alpha\beta}$ are trivial and thus the bundle itself is trivial.

Example ($\mathbb{CP}^d$)   Let us look at the introduced concepts in the simple case of projective spaces. We denote the $N + 1$ homogeneous coordinates of $\mathbb{CP}^d$ by z_i, $i = 0, \ldots, d$, which are related by the equivalence relation $(z_0, \ldots, z_d) \sim (\lambda z_0, \ldots, \lambda z_d)$, $\lambda \in \mathbb{C}^*$. It is common to define an open cover $\{U_i\}$ of $\mathbb{CP}^d$ via $U_i = \{z_i \neq 0\}$. There

are two important divisors or line bundles in this case: the tautological line bundle and the canonical bundle.

The tautological line bundle is obtained as follows. Take the line bundle $\pi : \mathcal{L} \to \mathbb{CP}^d$ and define the fiber over a point $z := (z_0, \ldots, z_d)$ in the base to be the line through the origin and z in $\mathbb{C}^{d+1}$. The transition functions are $g_{ij} = z_i / z_j$ in $U_i \cap U_j$. The dual (in the sense that the transition functions are inverse) of this line bundle is called the hyperplane bundle. The associated divisors are the hyperplanes $z_i = 0$. Since their defining equations are homogeneous functions of degree one, the hyperplane bundle is denoted by $\mathcal{O}(1)$ (and the dual tautological bundle by $\mathcal{O}(-1)$). Note that a priori all $D_i = \{z_i = 0\}$ and any linear combination of them is given in terms of a homogeneous polynomial of degree 1. Hence all hyperplanes are linearly equivalent. Indeed, $D_i \sim D_j$, since they differ by a global meromorphic function.

The canonical bundle of $\mathbb{CP}^d$ equals the (negative) sum of its basic divisors D_i and is the negative of the first Chern class, $K_{\mathbb{CP}^d} = -\sum_{i=1}^{d+1} D_i$. However, since all are linear equivalent to the hyperplane class, $D_i \sim H$, we find for the canonical bundle $K_{\mathbb{CP}^d} = -(d+1)H$. Hence $\mathbb{CP}^d$ is not Calabi–Yau.

3.2 Toric geometry

There are many good introductions to toric geometry [26, 52, 53] and its application to string theory and resolution of orbifold singularities [39, 54–61]. We will not present a mathematically rigorous treatment, but merely outline the concepts needed for our studies. Nevertheless, this requires the introduction of some mathematical vocabulary. We try to provide enough examples to give a feeling for what the following definitions mean in simple and well-known cases.

Definition (Toric variety)   A *toric variety* X of complex dimension $d = N - m$ is defined as the quotient space

$$X_\Sigma = \left(\mathbb{C}^N - Z(\Sigma) \right) / \left(\mathbb{C}^* \right)^m \tag{3.5}$$

which contains the algebraic torus $(\mathbb{C}^*)^{N-m}$ acting via coordinate-wise multiplication. The exclusion set $Z(\Sigma)$ is a subset of $\mathbb{C}^N$ that is fixed under a continuous subgroup of $(\mathbb{C}^*)^m$ and thus has to be removed for the variety to be smooth up to "mild" singularities. It is generically not unique.

In order to familiarize ourselves with the concept let us look at two simple examples.

Example ($\mathbb{CP}^d$)   Let us return to our example of the projective space. From the equivalence $(z_0, z_1, \ldots, z_d) \sim (\lambda z_0, \lambda z_1, \ldots, \lambda z_d)$ with $\lambda \in \mathbb{C}^*$, we find that the origin $(0, 0, \ldots, 0) \in \mathbb{C}^{N+1}$ is fixed under the multiplication with λ and thus has to be removed. Hence in the notation of (3.5), the toric variety $\mathbb{CP}^d$ is defined as

$$\mathbb{CP}^d = \left(\mathbb{C}^{d+1} - \{(0, 0, \ldots, 0)\} \right) / \left(\mathbb{C}^* \right) \tag{3.6}$$

where the $\mathbb{C}^*$ acts by a simultaneous multiplication of $\lambda \in \mathbb{C}^*$ on all coordinates $z_i \in \mathbb{C}^{d+1}$.

Example (Weighted projective space)   The weighted projective space is similar to the projective space, differing only in the action of $\mathbb{C}^*$ on the coordinates $z_i \in \mathbb{C}^{d+1}$. The corresponding toric variety is

$$\mathbb{CP}^d_{Q_0 Q_1 \ldots Q_d} = \left(\mathbb{C}^{d+1} - \{(0,0,\ldots,0)\} \right) / (\mathbb{C}^*) \tag{3.7}$$

with the $\mathbb{C}^*$ equivalence relation $(z_0, z_1, \ldots, z_d) \sim (\lambda^{Q_0} z_0, \lambda^{Q_1} z_1, \ldots \lambda^{Q_d} z_d)$. We thus recover ordinary projective spaces if we set all $Q_i = 1$.

The generalization to $m > 1$, i.e. to more than one $\mathbb{C}^*$ action, is done by simply introducing a matrix $Q = Q_i^\alpha$ with $i = 0, \ldots, d$ labeling the coordinates and $\alpha = 1, \ldots, m$ labeling the various different $\mathbb{C}^*$ actions.

It is common to encode the toric variety X_Σ using a fan Σ, which is specified by a collection of cones and a lattice $M \cong \mathbb{Z}^N$ as well as $M_\mathbb{R} = M \otimes_\mathbb{Z} \mathbb{R}$ in the following sense:

Definition (Cone)   A *strongly convex rational polyhedral cone* σ of dimension n, or *cone* for short, is spanned by a finite set of vectors $v_i \in M$,

$$\sigma = \left\{ \sum_{i=1}^n c_i v_i \;\middle|\; c_i \in \mathbb{R}^+ \right\} \qquad \Rightarrow \qquad \sigma \subset M_\mathbb{R} \tag{3.8}$$

such that $\sigma \cap (-\sigma) = \varnothing$. The cones of dimension one are called *edges*.

Definition (Fan)   A *fan* Σ is a collection of cones such that each face of a cone in Σ is also a cone in σ and that the intersection of two cones in σ is a face of both cones. A fan is specified by its edges and its choice of the exclusion set.

While this seems a bit abstract at first, the formulation is very useful, since it lends itself to computer-assisted automatization and thus makes it possible to work with even fairly complicated toric varieties. Let us next clarify the correspondence between fans and the toric data introduced in (3.5). The rough idea is as follows: the vectors v_i correspond to coordinates z_i of $\mathbb{C}^N$. The $(\mathbb{C}^*)^m$ actions relate the various coordinates and thus correspond to linear relations among the v_i. Finally, the exclusion set contains those coordinates which correspond to vectors that do not belong to the same cone. We associate a coordinate $z_i \in X_\Sigma$ to each edge $v_i \in M$ subject to the m equivalence relations

$$\sum_{i=1}^N Q_i^\alpha \, v_i = 0, \qquad \alpha = 1, \ldots, m \,. \tag{3.9}$$

This shows that the (transpose of the) vectors v_i span the kernel of the matrix Q defined above.

Using these conventions, we assign a codimension n submanifolds Z_σ of X_Σ to an n-dimensional cone σ spanned by $v_1, \ldots, v_n$ via

$$Z_\sigma = \left\{ z \in X_\Sigma \mid z_{v_1} = z_{v_2} = \ldots = z_{v_n} = 0 \right\}, \tag{3.10}$$

where z_{v_i} is the coordinate $z_i \in X_\Sigma$ associated with v_i. In particular, the edges of the fan correspond to the divisors (i.e. codimension 1 hypersurfaces) in X_Σ. The correspondence is such that

$$\sum_{i=1}^{N} (v_i)_j \, D_i \sim 0, \qquad j = 1, \ldots, d, \tag{3.11}$$

where $(v_i)_j$ denotes the jth component of the vector v_i.

Using the correspondence between the vectors and the coordinates, it is very useful to define the so-called the Stanley–Reissner ideal, which encodes the same information as the exclusion set but is expressed in terms of monomials of the coordinates:

Definition (Stanley–Reissner ideal)   The *Stanley–Reissner ideal* is a square-free monomial ideal containing the monomials associated to the different subsets of the exclusion set $Z(\Sigma)$ of a toric variety X_Σ.

After these definitions let us consider again a simple example:

Example ($\mathbb{CP}^2_{111}$)   Our starting point is the quotient space

$$\mathbb{CP}^2_{111} = \left(\mathbb{C}^3 - \{(0,0,0)\} \right) / \mathbb{C}^*, \qquad (z_1, z_2, z_3) \sim (\lambda z_1, \lambda z_2, \lambda z_3). \tag{3.12}$$

Let us construct the associated toric diagram. First, we have to find the vectors v_i, which means we have to find the kernel of the (1×3) matrix $Q = (1,1,1)$:

$$(\ker(Q))^T = \left\langle \begin{pmatrix} 1 & 0 \\ 0 & 1 \\ -1 & -1 \end{pmatrix} \right\rangle. \tag{3.13}$$

Thus $v_1 = (1,0)$, $v_2 = (0,1)$, $v_3 = (-1,-1)$. These vectors are the edges of the fan Σ which contains the following seven cones:

$$\begin{aligned}
\text{Dimension 0:} \quad & \sigma_0 = \langle (0,0) \rangle, \\
\text{Dimension 1:} \quad & \sigma_1 = \langle (1,0) \rangle, \qquad \sigma_2 = \langle (0,1) \rangle, \qquad \sigma_3 = \langle (-1,-1) \rangle, \\
\text{Dimension 2:} \quad & \sigma_{12} = \langle (1,0), (0,1) \rangle, \qquad \sigma_{13} = \langle (1,0), (-1,-1) \rangle, \\
& \sigma_{23} = \langle (0,1), (-1,-1) \rangle.
\end{aligned}$$

Since there is no three-dimensional cone σ_{123} the exclusion set is given by $Z(\Sigma) = \{z_1 = z_2 = z_3 = 0\}$, as usual for $\mathbb{CP}^N$. The associated toric diagram can be found in figure 3.1.

We can also use the fan to analyze whether a given toric variety is smooth or compact:
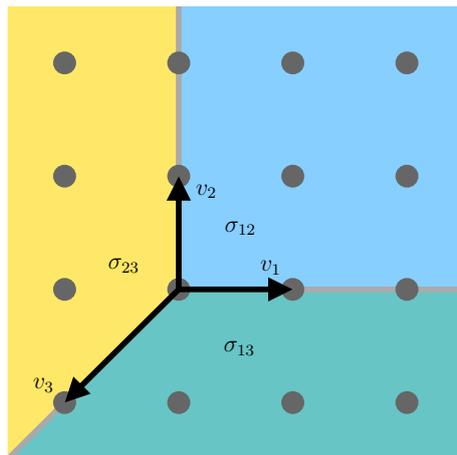
Figure 3.1: Toric diagram of $\mathbb{CP}^2$. The lattice points of M are in gray. Furthermore, the vectors v_i and the two-dimensional cones σ_{ij} are indicated.

Theorem (Smoothness and compactness)   A toric variety is *compact* if the union of all cones σ covers the whole lattice $M_{\mathbb{R}}$. A cone σ is *smooth* if every point in the sublattice $M \cap \sigma$ can be obtained as a linear combination with integer coefficients of the vectors v_i that generate σ. A fan is smooth if all its cones are smooth.

Example ($\mathbb{CP}^2_{111}$)   From figure 3.1 we see that the cones of $\mathbb{CP}^2$ cover the whole lattice $M_{\mathbb{R}} \simeq \mathbb{Z}^2 \otimes \mathbb{R}$ and that all points in $N \cap \sigma$ can be reached. Hence $\mathbb{CP}^2$ is smooth and compact.

3.2.1 Resolution of singularities

Let us now consider examples where the toric variety is no longer smooth. In particular, we want to study $T^d/\mathbb{Z}_N$ or $T^d/(\mathbb{Z}_N \times \mathbb{Z}_M)$ orbifolds. In order to describe the resolution process, we start with local orbifold singularities of the form $\mathbb{C}^d/\mathbb{Z}_N$. We will be interested in the cases $d = 2, 3$. The reason why we start our discussion with the local non-compact resolution rather than the compact one is that there are in fact no compact Calabi–Yau toric varieties. As we shall see in the next section, the anticanonical bundle of a toric variety is simply the sum of the divisors, cf. (3.17). In order for this to be trivial, we need that the sum is linear equivalent to zero (or the trivial bundle $\mathcal{O}$), $\sum D_i \sim 0$. Using (3.11), we see that then one component (which we take to be the last one) of all vectors has to be equal to one, or in other words that the toric fan has to lie in a plane one unit above the origin. Hence this fan does not cover the whole lattice M and thus the corresponding toric variety is non-compact. However, note that this means that we can draw the toric varieties of $\mathbb{C}^2/\mathbb{Z}_N$ and $\mathbb{C}^3/\mathbb{Z}_N$ in one and two dimensions, respectively, by projecting onto the plane above the origin.

Of course our entire discussion up to now has not been in vain, since there is nevertheless a way to obtain compact Calabi–Yaus from toric geometry, by embedding the CY as
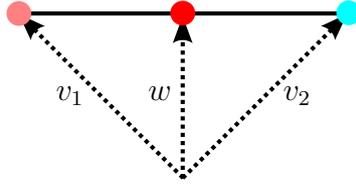
Figure 3.2: Toric diagram of $\mathbb{C}^2/\mathbb{Z}_2$. To make it smooth, we have introduced the new vector w. The triangulation is always unique in two dimensions.

a hypersurface or an intersection of hypersurfaces inside the toric ambient space. This discussion is deferred to the next section.

So let us turn to the non-compact resolution process. We assume we start off with a singular non-compact CY. From the criterion for smoothness it is clear how to resolve the singularities. For a singular fan, there are points in the sublattice $M \cap \sigma$ which cannot be reached by integer linear combinations of the v_i. Hence the solution is to introduce additional vectors w until all points in the sublattice can be reached. We call the divisors corresponding to these newly introduced coordinates exceptional divisors. As long as the newly introduced vectors also all lie in the surface one unit above the origin, the toric variety stays CY. There is also a new $\mathbb{C}^*$ action coming with each newly introduced divisor. This process is known as refining the fan. After refining the fan, it needs to be subdivided which amounts to choosing a specific maximal triangulation or equivalently specifying a new Stanley–Reissner ideal. Let us consider three examples:

Example ($\mathbb{C}^2/\mathbb{Z}_2$)   The associated fan is given in figure 3.2. To illustrate that the fan lies one unit away from the origin, we have drawn here the two dimensions and not projected onto the line in which the fan lies. The fan is spanned by the vectors $v_1 = (-1,1)^T$ and $v_2 = (1,1)^T$ to which we associate the divisors $D_1 = \{z_1 = 0\}$ and $D_2 = \{z_2 = 0\}$, respectively. We call these divisors ordinary divisors. As we can see, there is one lattice point that cannot be reached which is responsible for the $\mathbb{Z}_2$ singularity. We resolve the singularity by introducing a new vector $w = (0,1)^T$ corresponding to the exceptional divisor $E = \{x = 0\}$. The associated $\mathbb{C}^*$ action is given by the charges Q which we obtain from the transpose of the kernel of the matrix (v_1, v_2, w). It is easy to check that $Q = (1, 1, -2)$ and thus $(z_1, z_2, x) \sim (\lambda z_1, \lambda z_2, \lambda^{-2} x)$, which gives rise to the linear equivalence relation $2D_i + E \sim 0$.

Example ($\mathbb{C}^3/\mathbb{Z}_3$)   The toric fan is given in figure 3.3 (again, we have drawn the toric diagram in three dimensions for illustration purposes). The fan is spanned by the vectors $v_1 = (-1,-1,1)^T$, $v_2 = (0,1,1)^T$, $v_3 = (1,0,1)^T$ corresponding to the divisors $D_i = \{z_i = 0\}$. There is one interior lattice point, $(0,0,1)$ which is not an integer linear combination of the v_i and thus causes the singularity. By introducing $w = (0,0,1)^T$ and the associated exceptional divisor $E = \{x = 0\}$ we resolve the singularity. This gives rise to the new scaling relation

$$Q = (1, 1, 1, -3) \,, \tag{3.14}$$

(a) Toric diagram of $\mathbb{C}^3/\mathbb{Z}_3$.   **(b)** Refined toric diagram.   **(c)** Triangulated toric diagram.
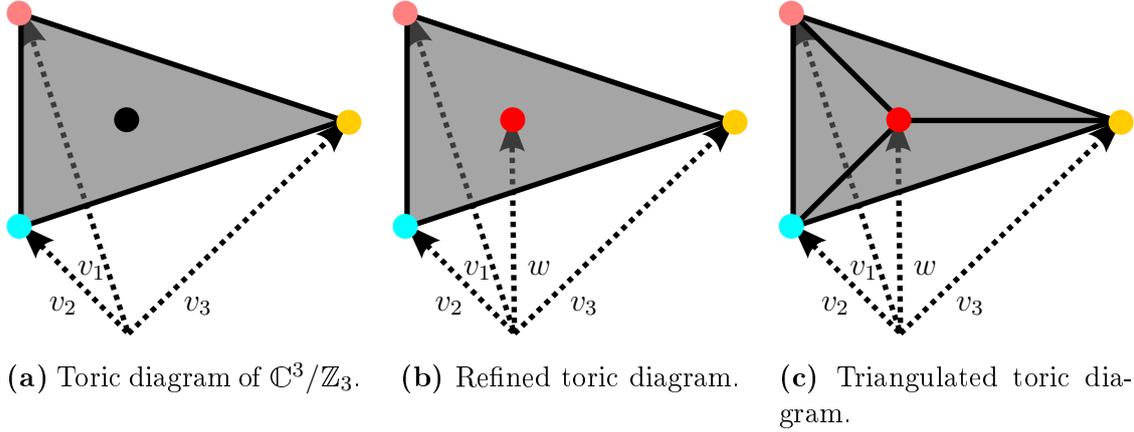
Figure 3.3: Toric diagram of $\mathbb{C}^3/\mathbb{Z}_3$, its subdivision via the inclusion of w, and its triangulation.

i.e. $(z_1, z_2, z_3, x) \sim (\lambda z_1, \lambda z_2, \lambda z_3, \lambda^{-3}x)$. The occurrence of the negative scaling λ^{-3} in front of the exceptional coordinate is generic for $\mathbb{Z}_N$ singularities. We will discuss this point in much more detail when we describe toric geometry in terms of GLSMs.

From this we can read off which sum of divisors correspond to a principal divisor, or in other words which charge combination sums to zero. This gives rise to the linear equivalence relation $3D_i + E \sim 0$. Now we need to subdivide the fan. The choice is unique and we obtain the three cones $\langle D_i D_j E \rangle$, $i \neq j$ over the origin. The fact that the exceptional divisor is completely inside the toric diagram means that the divisor is compact. In fact, by comparing the part of the toric fan centered at E with the fan of $\mathbb{CP}^2$ (figure 3.1), we find that they have the same topology. In other words, the singularity at the origin has been blown up into a whole $\mathbb{CP}^2$. The new Stanley–Reissner ideal is found to contain $z_1 z_2 z_3$.

Example ($\mathbb{C}^3/(\mathbb{Z}_2 \times \mathbb{Z}_2)$)   The associated fan is given in figure 3.4. The fan is spanned by the vectors $v_1 = (2, 0, 1)^T$, $v_2 = (0, 0, 1)^T$, $v_3 = (0, 2, 1)^T$. Note that the fan contains three copies of the fan of $\mathbb{C}^2/\mathbb{Z}_2$. There are three lattice points which cause the singularity: $w_1 = (0, 1, 1)^T$, $w_2 = (1, 1, 1)^T$, and $w_3 = (1, 0, 1)^T$. We introduce these vectors together with the associated exceptional divisors E_1, E_2, and E_3, and the scaling relations encoded in the matrix

$$Q = \begin{pmatrix} 1 & 1 & 0 & 0 & 0 & -2 \\ 1 & 0 & 1 & 0 & -2 & 0 \\ 0 & 1 & 1 & -2 & 0 & 0 \end{pmatrix}. \tag{3.15}$$

Note that in this case all exceptional divisors are on the boundary of the toric diagram which signals that they are non-compact. From the charge matrix we obtain the linear equivalence relations

$$2D_1 + E_2 + E_3 \sim 0, \qquad 2D_2 + E_1 + E_3 \sim 0, \qquad 2D_3 + E_1 + E_2 \sim 0. \tag{3.16}$$

(a) Toric diagram of $\mathbb{C}^3/(\mathbb{Z}_2 \times \mathbb{Z}_2)$.

(b) Refined toric diagram.

(c) One possible triangulation of the toric diagram.
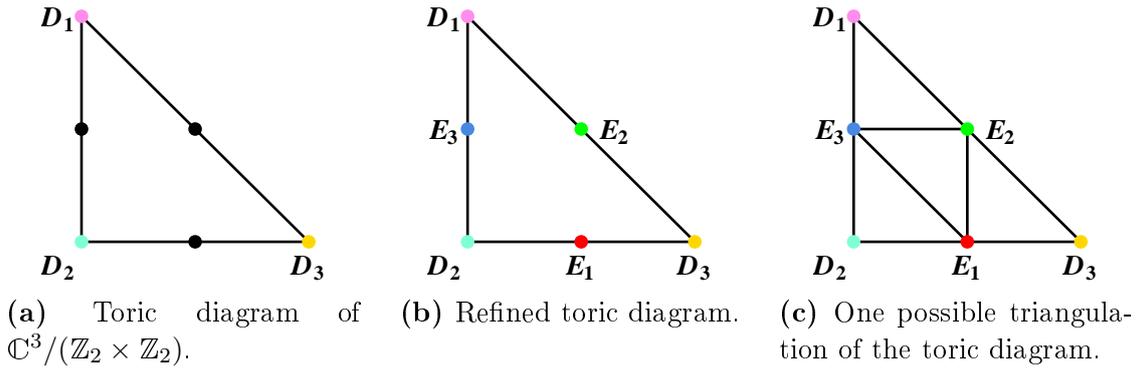
Figure 3.4: Toric diagram of $\mathbb{C}^3/(\mathbb{Z}_2 \times \mathbb{Z}_2)$, its subdivision via the inclusion of new vectors w_i corresponding to the exceptional divisors E_i, and one of its possible triangulations.

(a) Triangulation E_1.

(b) Triangulation E_2.

(c) Triangulation E_3.
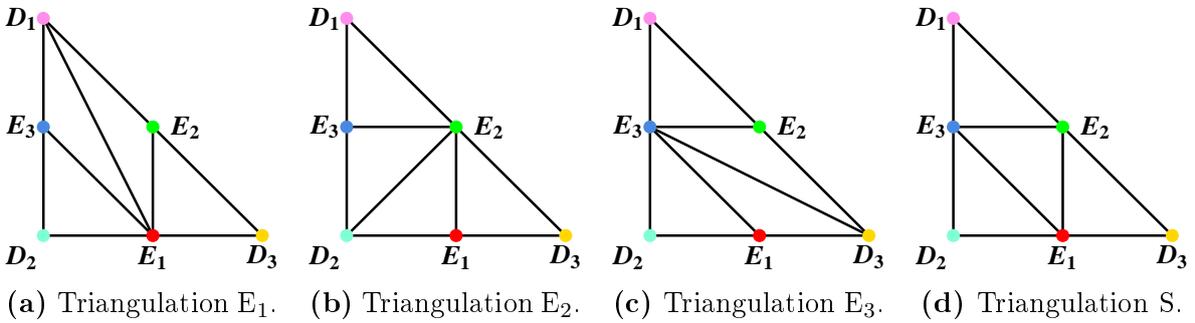
(d) Triangulation S.

Figure 3.5: The four possible triangulations for the toric diagram of $\mathbb{C}^3/(\mathbb{Z}_2 \times \mathbb{Z}_2)$.

This finishes the procedure of refining the fan. Now we need to subdivide it. Here we encounter for the first time a situation where the choice is ambiguous: there are 4 possible choices of triangulations (or equivalently for the Stanley–Reissner ideal) which lead to a maximal refinement. The four possible choices are given in figure 3.5. As we shall see later in section 5.3, the choice of triangulation influences the massless matter spectrum: flopping the curves represented by lines in figure 3.5 makes some states massive while others become massless.

3.2.2 Calabi–Yaus as hypersurfaces in toric varieties

Let us now turn to compact CYs in toric varieties. As mentioned before, this requires to describe them as (intersections of) hypersurfaces, as compact toric varieties themselves are never CY since their canonical bundle is nontrivial. To illustrate this further let us investigate the holomorphic $(d, 0)$ form Ω. Expanding $\Omega = \Omega_U(z_1, \ldots, z_d) \, dz_1 \wedge \ldots \wedge dz_d$ in some patch U, we see that there is a rank 1 bundle (a line bundle) K of $(d, 0)$-forms, of which we have chosen some section $\Omega_U(z_1, \ldots, z_d)$ (actually, for non-smooth varieties this is a sheaf rather than a line bundle). This line bundle is the canonical bundle which we encountered in the case of $\mathbb{CP}^d$ in the example in section 3.1. Using the correspondence between divisors and line bundles, we associate the canonical divisor

K with the canonical bundle. For Ω to be globally defined and non-vanishing on the Calabi–Yau, we need this bundle to be trivial, $\mathcal{O}(K) = \mathcal{O}$. It can be shown that for a toric variety X_Σ

$$K_{X_\Sigma} = -\sum_i D_i \tag{3.17}$$

where the D_i are the divisors associated with the edges of the fan Σ (they could be ordinary or exceptional divisors). In order to obtain a compact Calabi–Yau, we start from a toric variety and take a compact hypersurface within the variety. The hypersurface itself will be given in terms of the vanishing locus of a homogeneous polynomial in the coordinates of the toric variety. The point is to choose this hypersurface X such that the canonical bundle is trivial on X. In this way the hypersurface will be CY even though the ambient space itself is not. In order to know how to choose the polynomial, we have to know how to calculate the canonical bundle or the first Chern class[1] on CY hypersurface. Let us denote the ambient space by A and the CY hypersurface by X. We decompose the tangent space at each point p of X into a direct sum of the tangent and the normal bundle of X:

$$T_{p,A}\big|_X = T_{p,X} \oplus N_{p,X}\,. \tag{3.18}$$

Using short exact sequences introduced in section 2.2, this can be written as

$$0 \to T_X \to T_A\big|_X \to N_X \to 0\,, \tag{3.19}$$

where the vertical bar means restriction to the hypersurface X. This is known as the adjunction formula. It implies for the total Chern class

$$c(T_X) = c(T_A)/c(N_X)\,, \tag{3.20}$$

with $N_X = \mathcal{O}_A(X)|_X$. Using the adjunction formula together with

$$c(\mathcal{L}_1 \oplus \mathcal{L}_2 \oplus \ldots \oplus \mathcal{L}_N) = \prod_{i=1}^N c(\mathcal{L}_i) = \prod_{i=1}^N (1 + c_1(\mathcal{L}_i))\,, \tag{3.21}$$

we can calculate all Chern classes of line bundles from (3.20). To illustrate the procedure we consider an example.

Example (Hypersurface in $\mathbb{CP}^N$)   Hypersurfaces in $\mathbb{CP}^N$ provide a very simple class of examples. As usual, we denote the $N + 1$ coordinates of the ambient space by z_i. As we have already seen, all the coordinates correspond to linear equivalent divisors, which we denote by H with associated line bundle $\mathcal{O}(1)$. In this ambient space, we choose a degree k polynomial P which describes the submanifold X. Since this divisor will be a formal linear combination of the divisors corresponding to the z_i in homology,

---

[1]One has to be careful since there are examples like the Enriques surface where the first Chern class is zero but the canonical bundle is non-vanishing but pure torsion ($K = \mathbb{Z}_2$ for the Enriques). These surfaces thus do not have a non-vanishing volume form and thus we do not call them CY.

X will be linear equivalent to kH. The associated line bundle is hence $\mathcal{O}(k)$. We thus find

$$c(T_X) = c_0(T_X) + c_1(T_X) + \ldots = c(T_A)/c(N_X) = \left[\prod_{i=1}^{N+1}(1+H)\right] / \left[1+kH\right]$$
$$= \left[(1 + (N+1)H + \ldots)\right] \cdot \left[1 - kH + k^2 H^2 - \ldots\right].$$
(3.22)

The first Chern class is a two-form and thus represented by the term linear in H. We obtain $c_1(T_X) = (N+1-k)H$, which means that the first Chern class vanishes precisely for a hypersurface given in terms of a degree $k = N + 1$ polynomial. Thus a simple way to construct compact CY manifolds in d dimensions is to start with $\mathbb{CP}^{d+1}$ and consider a degree $d + 2$ polynomial. For $d = 1$, we obtain the cubic in $\mathbb{CP}^2$, which is a torus. For $d = 2$, we get the quartic in $\mathbb{CP}^3$ which is a K3, and for $d = 3$, we get the (well-known) quintic, which is a CY threefold.

The next question is how to incorporate the notion of submanifolds into toric geometry. In the case of toric resolutions of orbifolds, this can be done in an indirect way via the introduction of inherited divisors and auxiliary polyhedra [55, 56]. The idea is to resolve the orbifold fixed points and fixed tori locally, which are then of the form $\mathbb{C}^3/\mathbb{Z}_N$ and $\mathbb{C}^2/\mathbb{Z}_N$, respectively, using the procedure outlined in 3.2. After the local resolution, the various resolved fixed points are glued into a $T^6/\mathbb{Z}_N$ with the appropriate fixed point structure. This is done by specifying how the local coordinates z_i of $\mathbb{C}^n$ glue together across the different patches, for which we introduce the so-called inherited divisors R_i, where $i = 1, 2, 3$ labels the three tori. Their names stem from the fact that they are inherited from the torus. We take z_i as the torus coordinates and denote the position of the σth fixed point locus in the ith torus by $z_{i,\sigma}^{\text{fixed}}$. This means that the ordinary divisors are placed at the positions $D_{i,\sigma} = \{z_i = z_{i,\sigma}^{\text{fixed}}\}$. Away from the singularity, we define for factorizable orbifolds the inherited divisors via

$$R_i = \{z_i = c \neq z_{i,\sigma}^{\text{fixed}}\}.$$
(3.23)

However, since the ith torus is folded by the orbifold action of the order N_i, the R_i are obtained by taking the union over points which are identified, $R_i = \bigcup_{k=1}^{N_i}\{z_i = \epsilon^k c\}$ with $\epsilon = e^{2\pi i/N_i}$. In the limit $c \to z_{i,\sigma}^{\text{fixed}}$, the R_i thus correspond to N_i copies of $D_{i,\sigma}$, thus $R_i \sim N_i D_{i,\sigma}$. After introducing the exceptional divisors to resolve the singularities, the linear equivalence relations are of the schematic form

$$R_i \sim N_i D_{i,\sigma} + \sum_k E_{k,\sigma},$$
(3.24)

where $i = 1, 2, 3$ labels the three tori, k labels the exceptional divisors, and σ labels the fixed points. As we can see, the linear equivalences relate local resolutions from different fixed points, which reflects the gluing. Note, however, that the whole procedure is done without explicitly mentioning hypersurfaces. We will see in section 3.3 how to write toroidal orbifolds as (complete) intersections in toric ambient spaces and how the hypersurface equations give rise to the inherited divisors used above to describe the

(a) Triangulation E_1. (b) Triangulation E_2. (c) Triangulation E_3. (d) Triangulation S.
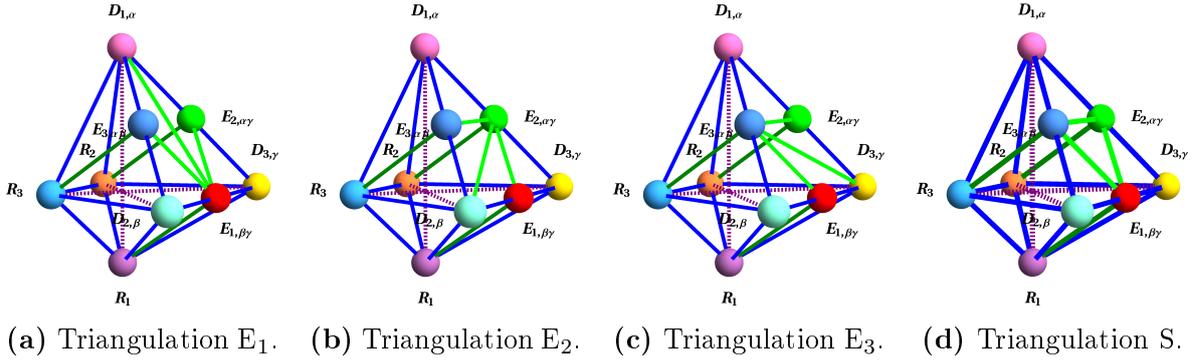
Figure 3.6: The auxiliary polyhedra for the four possible triangulations of $T^6/(\mathbb{Z}_2 \times \mathbb{Z}_2)$.

gluing. Using (3.24), the ordinary divisors can be expressed in terms of the inherited and exceptional divisors, which form a divisor basis.

A further complication arises if there are singularities on the torus that are mapped onto each other on the orbifold via the orbifold action. In this case, one has introduce new divisors which are the sum of the divisors over the equivalent fixed points, and (3.24) is altered accordingly. This complication also does not arise when treating the resolutions within the GLSM framework.

Example ($T^6/\mathbb{Z}_2 \times \mathbb{Z}_2$)   We will not go into the details of the global resolution process, which can be found in [60], but only outline the procedure. First, we introduce a label $i = 1, 2, 3$ for each two-torus and fixed point labels $\alpha, \beta, \gamma = 1, 2, 3, 4$ labeling the fixed point position in the three tori. Furthermore, we introduce a label $k = 1, 2, 3$ which labels the twisted sectors $\theta_1, \theta_2, \theta_1\theta_2$ of the orbifold, respectively. We follow the convention that the kth twisted sector leaves the kth torus fixed. The local resolutions have already been discussed in a previous example, and the corresponding toric diagrams can be found in figure 3.5. Roughly, the vectors corresponding to the inherited divisors R_i are introduced in the opposite direction of those corresponding to the ordinary divisors $D_{i,\sigma}$. The resulting auxiliary polyhedra are given in figure 3.6. Note how the local resolution appears as a face in the polyhedron describing the global gluing. From the polyhedron, we obtain the linear equivalences

$$R_1 \sim 2D_{1,\alpha} + \sum_\gamma E_{2,\alpha\gamma} + \sum_\beta E_{3,\alpha\beta}\,, \quad R_2 \sim 2D_{2,\beta} + \sum_\gamma E_{1,\beta\gamma} + \sum_\alpha E_{3,\alpha\beta}\,,$$
$$R_3 \sim 2D_{3,\gamma} + \sum_\beta E_{1,\beta\gamma} + \sum_\alpha E_{2,\alpha\gamma}\,. \tag{3.25}$$

Using these equations to express the ordinary divisors D in terms of the exceptional divisors E and the inherited divisors R yields a basis of divisors.

3.2.3 Intersection numbers

In the previous sections we have seen how to resolve orbifold singularities, how to find a divisor basis of the resolution space, and how to describe its geometry in terms

Int($S_1S_2S_3$) \ Triangulation	"E_1"	"E_2"	"E_3"	"S"
$E_{1,\beta\gamma}E_{2,\alpha\gamma}E_{3,\alpha\beta}$	0	0	0	1
$E_{1,\beta\gamma}E^2_{2,\alpha\gamma}$, $E_{1,\beta\gamma}E^2_{3,\alpha\beta}$	-2	0	0	-1
$E_{2,\alpha\gamma}E^2_{1,\beta\gamma}$, $E_{2,\alpha\gamma}E^2_{3,\alpha\beta}$	0	-2	0	-1
$E_{3,\alpha\beta}E^2_{1,\beta\gamma}$, $E_{3,\alpha\beta}E^2_{2,\alpha\gamma}$	0	0	-2	-1
$E^3_{1,\beta\gamma}$	0	8	8	4
$E^3_{2,\alpha\gamma}$	8	0	8	4
$E^3_{3,\alpha\beta}$	8	8	0	4
$R_1R_2R_3$	2			
$R_1E^2_{1,\beta\gamma}$, $R_2E^2_{2,\alpha\gamma}$, $R_3E^2_{3,\alpha\beta}$	-2			

Table 3.1: The upper part gives the intersection numbers when using the same triangulation at all 64 fixed points of the $T^6/(\mathbb{Z}_2 \times \mathbb{Z}_2)$ blowup. The lower part gives the triangulation-independent intersection numbers.

of triangulated toric diagrams and patch gluings. This gives us everything we need to determine the last topological piece of information needed for the description of the heterotic supergravity approximation on CY manifolds: the intersection numbers of the divisors. The term intersection numbers can be taken literally when different divisors are involved: it counts the number of points in which d divisors intersect (in homology). However, using linear equivalence relations, one can use the intersection numbers of distinct divisors to also calculate self-intersections of divisors, which have a less straightforward geometric interpretation. In particular, they can be fractional (for non-compact varieties) or negative (for exceptional divisors). Roughly, self-intersections can be thought of as the intersection of a submanifold with its slightly perturbed copy. A negative self-intersection then signals that a divisor cannot be moved. The fractional intersection numbers signal that by taking the local (non-compact) case we are neglecting contributions from the global gluing.

The intersection numbers involving only distinct divisors can be simply read off from the toric diagram. In the non-compact case, the intersection number of all divisors which form a cone together with the origin have intersection number 1. Since the cones depend on the choice of the triangulation, we see that the intersection numbers become a function of the Stanley–Reissner ideal as well. In the compact case, the prescription is similar, only that the intersection number is weighted by the volume of the cone. Let us illustrate this in examples.

Example ($\mathbb{CP}^2$) We have constructed the fan in figure 3.1. We denote the three divisors associated with the v_i by D_i. Since we have three 2-dimensional cones, we find the intersection numbers $D_1D_2 = D_1D_3 = D_2D_3 = 1$. From the linear equivalences, we know that $D_1 \sim D_2 \sim D_3 = H$. Thus we have the intersection ring $H^2 = 1$.

Example ($T^6/(\mathbb{Z}_2 \times \mathbb{Z}_2)$) As alluded to before, in this case the Stanley–Reissner ideal is not unique and hence the intersection numbers depend on the triangulation. Let us carry out the analysis in the case of the symmetric triangulation. We find the

triple intersection numbers $D_{1,\alpha}E_{2,\alpha\gamma}E_{3,\alpha\beta} = 1$. Note that the index α has to be the same on the ordinary and exceptional divisors. This ensures that each local resolution is glued into the correct fixed point. The intersections for $D_2 E_1 E_3$ and $D_3 E_1 E_2$ can be read off in a similar way. For the intersection involving the inherited divisors, we find e.g. $R_1 R_2 R_3 = 2$, where the multiplicity arises from the volume factor in the auxiliary polyhedron. The intersection numbers of the form $D_i D_j R_k$ can be worked out similarly (see [60] for the detailed procedure). Next, one uses the linear equivalence relations (3.25) in order to obtain a divisor basis containing the three inherited divisors R_i and the 48 exceptional divisors $E_{k,\sigma}$. Intersections involving the same divisor multiple times can be calculated by starting from expressions like $R_i D_j D_k$, replacing the ordinary divisors and solving the linear system of equations. While tedious due to the huge amount of equations, this can be done rather easily with the help of a computer. For the cases where the same triangulation is used at all fixed points, we give the intersection numbers in table 3.1 We have now all topological information we need in order to build MSSM-like models on the resolved $T^6/\mathbb{Z}_2 \times \mathbb{Z}_2$ orbifold.

In summary, to collect all geometric data needed for the description of a heterotic string model on a resolved CY orbifold, one proceeds as follows:

- Construct the fan of toric variety under investigation,

- Introduce exceptional divisors and choose the Stanley–Reissner ideal such that the singularities are resolved,

- Introduce the inherited gluing divisors and construct the auxiliary polyhedra,

- Use the vectors of the toric diagram to read off the linear equivalence relations,

- Read off the intersection numbers and calculate the self-intersections using the linear equivalence relations.

Now that we have a basis of divisors, we can construct fundamental objects like Chern classes and Kähler forms by expanding them in terms of a basis of divisors S_i or rather their Poincaré-dual forms. In the case of the Kähler form, we expand

$$J = \sum_{i=1}^{h^{1,1}} d_i S_i \,. \tag{3.26}$$

The scalars d_i are called Kähler moduli. Using the Kähler form, we can define the volume of curves C_i, divisors D_i, and the entire Calabi–Yau X as

$$\mathrm{vol}(C_i) = \int_{C_i} J \,, \qquad \mathrm{vol}(D_i) = \frac{1}{2} \int_{D_i} J^2 \,, \qquad \mathrm{vol}(X) = \frac{1}{6} \int_X J^3 \,. \tag{3.27}$$

These integrals can be evaluated using the intersection numbers and they will lead to linear, quadratic, and cubic terms in the Kähler moduli, respectively. In a sensible theory, these volumes should all be larger than zero, which restricts the relative size of the Kähler moduli. The range of Kähler moduli for which the volumes are positive forms a cone, the so-called Kähler cone. Since the volume depends on the intersection numbers

and thus on the SR ideal, we get different Kähler cones for different triangulation choices. These Kähler cones can be connected via flop transitions: if the volume of some curve becomes negative, this signals that one crossed the boundary between two Kähler cones. So the theory can be made sense of by using a different SR ideal, in which the intersection numbers changed such that for the given Kähler moduli values all volumes are positive again. It is also useful to define the dual of the Kähler cone, the so-called Mori cone. This is the cone of all effective curves, i.e. the cone in which all curves have a non-negative intersection with all divisors. Let us illustrate the flops again using the example of $\mathbb{C}^3/(\mathbb{Z}_2 \times \mathbb{Z}_2)$ (the story does not change when going to the compact case, since the only triangulation dependence comes from the fixed point resolution).

Example $(\mathbb{C}^3/(\mathbb{Z}_2 \times \mathbb{Z}_2))$ The four possible triangulations are given in figure 3.4. Let us discuss for example how to get from triangulation E_1 to triangulation S. In the E_1 triangulation, the divisors D_1 and E_1 intersect in a curve C_{11}. This curve is not present in the S triangulation. Instead, we find a curve C_{23}, corresponding to the intersection $E_2 E_3$. First, we expand the Kähler form as $J = -b_1 E_1 - b_2 E_2 - b_3 E_3$. The minus signs are of course convention, which we choose here in analogy with the compact case, where the volumes of the E_i and of X are positive for $b_i > 0$. Let us look at the curves. In triangulation E_1, we find

$$
\begin{aligned}
\mathrm{vol}(C_{11}) &= \int_{C_{11}} J = \int_X D_1 E_1 J = \int_X -b_1 D_1 E_1 E_1 - b_2 D_1 E_1 E_2 - b_3 D_1 E_1 E_3 \\
&= 1\, b_1 - 1\, b_2 - 1\, b_3 \,, \\
\mathrm{vol}(C_{23}) &= \int_{C_{23}} J = \int_X E_2 E_3 J = \int_X -b_1 E_1 E_2 E_3 - b_2 E_2 E_3 E_2 - b_3 E_2 E_3 E_3 \\
&= 0\, b_1 + 0\, b_2 + 0\, b_3 = 0 \,,
\end{aligned}
\tag{3.28}
$$

where the coefficients are the triple intersection numbers which we read off from the toric diagram and (in the case of self-intersections) calculate from the linear equivalence relations $0 \sim 2D_i + E_j + E_k$ with all indices different. We see that the curve C_{11} has positive volume if $b_1 > b_2 + b_3$ while the curve C_{23} has a vanishing volume (i.e. it does not exist). Thus the Kähler cone for triangulation E_1 is given by $\{b_1, b_2, b_3 \in \mathbb{R}^+ \mid b_1 > b_2 + b_3\}$. Let us see what happens if we make the volume of C_{11} negative by taking $b_i > 0$ but $b_1 < b_2 + b_3$. We can still make sense out of this if we at the same time change from triangulation E_1 to triangulation S. In this triangulation, one finds

$$
\begin{aligned}
\mathrm{vol}(C_{11}) &= \int_{C_{11}} J = \int_X D_1 E_1 J = \int_X -b_1 D_1 E_1 E_1 - b_2 D_1 E_1 E_2 - b_3 D_1 E_1 E_3 \\
&= 0\, b_1 + 0\, b_2 + 0\, b_3 = 0 \,, \\
\mathrm{vol}(C_{23}) &= \int_{C_{23}} J = \int_X E_2 E_3 J = \int_X -b_1 E_1 E_2 E_3 - b_2 E_2 E_3 E_2 - b_3 E_2 E_3 E_3 \\
&= -1\, b_1 + 1\, b_2 + 1\, b_3 \,.
\end{aligned}
\tag{3.29}
$$

So indeed we find that the volume of C_{11} vanishes identically and furthermore that precisely in this case the volume of C_{23} becomes positive. Hence for this choice of the values of the Kähler moduli, we have left the Kähler cone of triangulation E_1 and entered the Kähler cone of triangulation S.

3.3 Gauged linear sigma models

In this section we want to describe an alternative approach to toric geometry via gauged linear sigma models (GLSMs). The approach might seem more "physical", since it reduces the study of algebraic varieties to finding a supersymmetric configuration of two-dimensional SUSY field theories. GLSMs were first introduced by Witten in [62]. For nice reviews on the topic see e.g. [63, 64]. A sigma model is a field theory where the fields correspond to maps from a spacetime into some target space. In the case of heterotic string theory, we consider a sigma model which describes the embedding of the string worldsheet into a ten-dimensional target space (the spacetime). For phenomenological reasons, we require the spacetime to be $M^{1,3} \times X$ where we choose X to be a Calabi–Yau threefold. Furthermore, we require[2] that the worldsheet theory has $\mathcal{N} = (0, 2)$ supersymmetry, which gives rise to an $\mathcal{N} = 1$ theory in four dimensions. The notation $(0, 2)$ means that there are zero left-handed and two right-handed supersymmetries.

In order to define the GLSM, we actually need to specify both the GLSM fields responsible for the geometry and for the gauge sector at the same time, and the two are bound together via anomaly considerations. We will discuss this in depth in chapter 8. At this point, however, we are merely interested in the geometric part since we want to discuss the relation between sigma models and toric geometry. Hence we will not concern ourselves with the description of the gauge bundle at this point and simply choose for the gauge degrees of freedom the so-called standard embedding, which is known to yield a consistent (albeit phenomenologically uninteresting) theory in 4 dimensions. This choice enhances the amount of worldsheet supersymmetry to $\mathcal{N} = (2, 2)$. Hence we will carry out the discussion in terms of $(2, 2)$ GLSM superfields. The reduction of the theory to $(0, 2)$ and the implications are discussed in chapter 8.

3.3.1 Non-linear sigma model

String theory can be described via a non-linear sigma model with the action

$$
\begin{aligned}
S = \frac{1}{4\pi} \int \mathrm{d}^2\sigma \Big[& G_{MN}(z) + B_{MN}(z)]\partial_\sigma z^M \partial_{\bar{\sigma}} z^N + G_{MN}(z)\psi^M D_\sigma \psi^N \\
& + \delta_{IJ}\lambda^I D_{\bar{\sigma}}\lambda^J + \frac{1}{2}R_{MN}^{IJ}\lambda_I \lambda_J \psi^M \psi^N \Big]
\end{aligned}
\tag{3.30}
$$

---

[2]$\mathcal{N} = (0, 1)$ would be enough for a consistent string theory, but we want target space supersymmetry.

with the following field content: $\sigma, \bar{\sigma}$ describe the worldsheet coordinates, $z : \Sigma \to X$ are the maps from the worldsheet into the target space, and ψ and λ are right- and left-handed worldsheet fermions that couple to the pullback of the tangent bundle and the gauge bundle of X, respectively. Furthermore, G_{MN} and B_{MN}, are the metric and the two-form field, $D_\sigma \psi^M = \partial_\sigma \psi^M + [\Gamma_{NP}^M(z) - \frac{1}{2} H_{NP}^M(z)]\partial_\sigma \psi^N \psi^P$ is the covariant derivatives with the torsion connection, $D_{\bar{\sigma}} \lambda^I = \partial_{\bar{\sigma}} \lambda^I - \mathrm{i} A(z)_{MJ}^I \partial_{\bar{\sigma}} z^M \lambda^J$ is the covariant derivative with the gauge connection, and R is the associated curvature.

The problem is that this action can in general not be studied directly since the metric and B field are (unknown) complicated non-linear functions of the maps z. Furthermore, in order to describe string theory, the theory should be conformal, which imposes constraints on the above data (e.g. that the metric is Ricci-flat). So instead of dealing with this complicated non-linear sigma model, we study a non-conformal gauged linear sigma model, which flows under the renormalization group in the IR to a conformal non-linear sigma model describing the associated string theory. The non-linearity arises then from the marginal and relevant terms (in the RG sense) of the GLSM after integrating out the massive fields and taking the conformal limit.

3.3.2 Gauged linear sigma model

Gauged linear sigma models with $\mathcal{N} = (2, 2)$ supersymmetry in two dimensions are best thought of in terms of a dimensional reduction of the well-known $\mathcal{N} = 1$ theory in four dimensions with reduced Lorentz group SO(1,1). We denote the worldsheet variables by (σ_1, σ_2) and the Grassmann superspace variables by $\theta^\pm, \bar{\theta}^\pm$. This facilitates going later from $(2, 2)$ to $(0, 2)$ models: the latter are obtained by dropping the Grassmann variables θ^+ and $\bar{\theta}^+$. There is also a global $\mathrm{U}(1)_L \times \mathrm{U}(1)_R$ symmetry, transforming θ^+ and θ^-, respectively. Furthermore, we will only be discussing Abelian GLSMs with gauge group $\mathrm{U}(1)^m$, and we will label the different $\mathrm{U}(1)$ factors with I. The SUSY derivatives read

$$D_\pm = \frac{\partial}{\partial \theta^\pm} - \mathrm{i}\bar{\theta}\partial_\pm \,, \qquad \overline{D}_\pm = -\frac{\partial}{\partial \bar{\theta}^\pm} + \mathrm{i}\theta\partial_\pm \tag{3.31}$$

with $\partial_\pm = \partial_{\sigma_1} \pm \partial_{\sigma_2}$.

The massless representations we need in order to describe the GLSM are given in terms of the following multiplets:

Chiral multiplet   The chiral multiplet satisfies the chirality constraint $\overline{D}_\pm \Phi = 0$. In components it reads $\Phi = \phi + \theta^+ \psi^+ + \theta^- \psi^- + \theta^+ \theta^- F$. Here, ϕ is a complex scalar, $\psi^\pm$ are left- and right-chiral fermions, and F is an auxiliary scalar field.

Vector multiplet   The vector multiplet in WZ gauge can be expanded as $V = \theta^+ \bar{\theta}^+ a_+ + \theta^- \bar{\theta}^- a_- + \theta^- \bar{\theta}^+ \sigma + \theta^+ \bar{\theta}^- \bar{\sigma} + \text{gauginos} + \theta^2 \bar{\theta}^2 D$. The $a_\pm$ arise from the external part of the 4D gauge field and the complex scalar σ arises from the internal part. D is an auxiliary scalar. The SUSY gauge variation can be written as $V \to V + i(\Lambda - \overline{\Lambda})$ with a chiral superfield Λ.

Twisted chiral multiplet   The twisted chiral multiplet is a feature that can occur in two-dimensional theories due to the reduced Lorentz group and thus does not have a counterpart in four dimensions. It is defined to satisfy $\overline{D}_+\Upsilon = D_-\Upsilon = 0$. These fields are important since the 2D super field strength $\mathcal{F} = \overline{D}_+ D_- V$ is a twisted chiral multiplet built from the component fields of the vector multiplet V.

The action of the $(2,2)$ GLSM consists of four terms

$$S = S_{\text{Kin}} + S_{\text{W}} + S_{\text{Gauge}} + S_{\text{Twisted}}\,. \tag{3.32}$$

The components read

S_{kin}   The kinetic terms for the chiral fields are $S_{\text{kin}} = \int \mathrm{d}^2\sigma \mathrm{d}^4\theta \sum_i \Phi_i e^{2Q_i^I V_I} \overline{\Phi}_i$.

S_{W}   The superpotential terms are $S_{\text{W}} = m \int \mathrm{d}^2\sigma\, \mathrm{d}\theta^+ \mathrm{d}\theta^- W(\Phi) + \text{h.c.}$ Note the mass parameter m in front.

S_{Gauge}   The gauge kinetic terms are $S_{\text{gauge}} = -\sum_I \frac{1}{4e_I^2} \int \mathrm{d}^2\sigma \mathrm{d}^4\theta \overline{\Upsilon}_a \Upsilon_a$. The e_I are the (dimensionful) coupling constants of the Ith U(1).

S_{Twisted}   The twisted superpotential terms are $S_{\text{Twisted}} = \int \mathrm{d}^2\sigma \mathrm{d}\theta^+ \mathrm{d}\overline{\theta}^- \rho^I \Upsilon^I + \text{h.c.}$ The ρ^I are constant FI parameters, $\rho^I = a^I + \mathrm{i}\vartheta^I$. Later, in chapter 8, we make these constants field-dependent and generate in this way a Green–Schwarz mechanism on the worldsheet.

As we can see, the theory is non-conformal due to the appearance of the dimensionful parameters m, e_I in the action. In the conformal limit, these parameters are sent to infinity. We obtain for the potential of the scalar fields Φ, σ

$$U(\phi, \sigma) = \sum_I \frac{1}{2e_I^2} D_I^2 + \sum_i |F|_i^2 + 2\sum_I \overline{\sigma}_I \sigma_I \sum_i Q_i^{I\,2} |\phi_i|^2\,. \tag{3.33}$$

We usually consider the branch with $\sigma = 0$. As in 4D, the D terms receive contributions from S_{Kin} and from the FI parameters in S_{Twisted}, and the F terms come from the superpotential,

$$D^I = \sum_i Q_i^I |\phi|^2 - a^I\,, \qquad F_i^* = \left.\frac{\partial W}{\partial \Phi_i}\right|\,, \tag{3.34}$$

where the vertical bar indicates that the Grassmann variables $\theta^\pm, \overline{\theta}^\pm$ have been set to zero. We want to ensure that the parameters of the scalar potential do not renormalize when flowing to the IR CFT. While this is automatic for the superpotential due to non-renormalization theorems, we find constraints coming from the FI terms: they impose that $\sum_i Q_i^I = 0$ for all U(1)'s $I = 1, \dots, m$. In terms of geometric data, the sum of the charges corresponds to the first Chern class, so this means that $c_1(TX) = c_1(V) = 0$, i.e. the target space is Calabi–Yau and the gauge bundle has structure group SU(N) (as usual in the standard embedding).

3.3.3 Algebraic geometry from GLSMs

Now we have in principle everything we need for the study of algebraic geometry via GLSMs. Let us start by explaining the relation between the two. The fields ϕ_i correspond to the coordinates of $\mathbb{C}^N$, and $\phi_i = 0$ will give rise to divisors D_i. The $(\mathbb{C}^*)^m$ action is generated in two steps: The D terms constrain the absolute value, and the phase constraints comes from the gauge fixing of the $U(1)^m$. Together, this gives rise to a symplectic quotient. Finally, the Stanley–Reissner ideal, which contains those coordinates that cannot be set to zero simultaneously (or equivalently, those divisors which do not intersect), is encoded in the D terms via the relative size of the various FI parameters a_I together with the sign of the charges of the coordinate fields ϕ. The GLSM FI parameters correspond to the Kähler parameters in the target space. Hence their choice fixes a Kähler cone and thus different regimes or "phases" of the theory. The different phases might simply be connected by flop transitions, or there might be more radical transitions, which can even change the dimensionality of the target space and the number of divisors.

We assign $U(1)_L \times U(1)_R$ charges $(2, 2)$ to some chiral superfields Φ while keeping others neutral. The charged ones will be called C_a and the uncharged ones Z_i with scalar components c_a and z_i, respectively. This ensures that the C_a appear (at most) linearly in the superpotential. Furthermore, we choose the $U(1)$ gauge generators such that the C_a have non-positive charges $q_a \leq 0$ and the Z_i have non-negative charges $z_i \geq 0$. In this case, the superpotential can be written as $W = \sum_a C_a P(Z_i)$ where the $P(Z_i)$ are polynomials which are forced to be homogeneous by gauge invariance. We also want the polynomials to be transverse, i.e. the only solution to $P = \mathrm{d}P = 0$ is that all $z_i = 0$. From the D terms we find that $\sum_i Q_i^I |z_i|^2 + \sum_a q_a^I |c_a|^2 = a^I$. Before going into more detail, let us start with an example.

Example ($\mathbb{CP}^N$)   Again, we take $\mathbb{CP}^N$ as a simple example to illustrate the basic ideas. As we have seen, we need $n + 1$ coordinate fields z_i. Since there is only one scaling relation, we need only a single $U(1)$. Furthermore, since all coordinates scale with the same factor λ, all fields have the same charge $Q_i = 1$. These charges are the charges Q_i which we introduced in the previous section as being in the kernel of the transposed matrix of vectors that define the toric fan. Thus generalizations to weighted projective spaces or to spaces with more than one equivalence relations can be done easily: in the former case, one assigns different charges Q_i to the different coordinates, and in the latter case one introduces more than one $U(1)$. The charge assignment gives rise to the D term constraint

$$\sum_i |z_i|^2 - a = 0. \tag{3.35}$$

Obviously this equation only has solutions if $a \geq 0$.[3] Now if $a > 0$, some of the z_i have to have a VEV in order to ensure D flatness. Often, the regime $a > 0$ is called

---

[3]The point $a = 0$ is peculiar, since it allows for all fields to be vanishing. In this case, the scalars σ become important and one enters the Coulomb branch, but we will not go into details of this discussion [62].

the geometric regime, since in this case the target space has a geometric interpretation. The point $z_1 = z_2 = \ldots = z_{N+1} = 0$ has to be excluded, which gives rise to the usual Stanley–Reissner ideal of $\mathbb{CP}^N$. Lastly, let us note that from the fact that all fields have the same charge one can deduce that the corresponding divisors are all linear equivalent.

While being a perfectly valid example for constructing toric spaces via the symplectic quotient, in order to interpret the GLSM as the UV part of a string worldsheet theory we have to ensure that the D terms do not renormalize: the sum of charges is $N + 1$ and not zero, as dictated from the tadpole cancelation condition. Equivalently, the toric space is not Calabi–Yau since it has non-vanishing first Chern class. However, as we already know, no compact toric space is Calabi–Yau. This also fits well with the GLSM. Since all fields have charges of the same sign, we could not write down a gauge invariant superpotential. In order to have the charges sum to zero, we introduce in the above example another field C with charge $Q_0 = -(N + 1)$. The resulting target space has vanishing first Chern class since now the charges sum to zero. At the same time, we can write down a superpotential $W = CP(z_i)$ where $P(z_i)$ is a homogeneous polynomial of degree $N + 1$. We thus find $N + 1$ F terms from the z_i and one F term from C,

$$
\begin{aligned}
F_{z_i} = 0 &\quad\Rightarrow\quad C\partial_{z_i}P(z_i) = 0\,, &\qquad F_c = 0 &\quad\Rightarrow\quad P(z_i) = 0\,, \\
D = 0 &\quad\Rightarrow\quad \sum_i |z_i|^2 - (N+1)|c|^2 = a\,.
\end{aligned}
\tag{3.36}
$$

From the transversality constraint on $P(z_i)$, we see that there are two possibilities for solving the F terms: either all z_i are identically zero and c is arbitrary, or c is identically zero. In the geometric regime $a > 0$, the first possibility violates D flatness, since the FI term can only be canceled by a VEV of one of the z_i fields. In contrast, in the non-geometric regime $a < 0$, the FI term is canceled by giving a VEV $|c|^2 = a/(N+1)$. This is non-geometric since the target space is one point where c has the aforementioned VEV and all z_i are identically zero. In this phase, the U(1) symmetry is not broken completely. A discrete $\mathbb{Z}_{N+1}$ symmetry is left which generates a Landau–Ginzburg (LG) $\mathbb{Z}_{N+1}$ orbifold. This LG orbifold is, however, not the heterotic orbifold which we want to study here. Rather, the $\mathbb{Z}_N$ orbifold actions in our considerations arise as discrete remnants of U(1) symmetries resulting from VEVs of the exceptional divisors used to resolve the orbifold singularity. In particular, these orbifolds are in the geometric regime of the GLSM, and from now on we will not say too much about the LG phase.

So let us return to our discussion of the geometric regime $a > 0$. In this case, c vanishes identically at every point in field space. Such a field does not correspond to a divisor in target space. With $c \equiv 0$, the D term reduces to the previously discussed one, i.e. $\sum_i |z_i|^2 = a$. But on top of that we have from the F term the equation $P(z_i) = 0$. This cuts out a hypersurface of degree $N + 1$ from the toric ambient space. Note that this is precisely the correct order to cancel the anti-canonical bundle in a toric $\mathbb{CP}^N$ ambient space. This of course had to happen since we already know that the target space will be Calabi–Yau due to it having vanishing first Chern class. This hypersurface will be smooth since $P(z_i)$ was chosen transversal, and compact since none of the z_i

can have a VEV larger than a. The FI parameter a becomes the Kähler parameter, which is inherited by the CY submanifold from the ambient space. For CY threefolds, the coefficients in the polynomial (up to $GL(N + 1)$ rotations) correspond to (some of) the complex structure moduli. With this we finish our discussion on how to map hypersurfaces in toric geometry to the GLSM description and vice versa. Let us discuss the resolution process next.

3.3.4 Resolution of singularities in the GLSM

In analogy to the previous chapter, let us discuss how to resolve non-compact spaces first and afterwards see how to patch the different resolutions together. As alluded to before, this can be done rather easily and directly in the GLSM. The idea of local resolutions has already been lined out: a space with quotient singularities can be resolved by introducing new divisors together with linear equivalence relations.

Example ($\mathbb{C}^3/\mathbb{Z}_3$)   In our discussion of local resolutions, we want to start again by investigating the example of $\mathbb{C}^3/\mathbb{Z}_3$, which is toric and non-compact. This means that we should not have hypersurface equations arising from the F terms, which can for example be achieved by introducing no C type fields but only fields that are neutral under $U(1)_L \times U(1)_R$. We start with the three coordinates z_1, z_2, z_3 of $\mathbb{C}^3$ corresponding to the ordinary divisors and one exceptional coordinate x together with one $U(1)$ gauge symmetry such that the overall dimension of the target space is three. We choose the charge assignment $Q(z_1, z_2, z_3, x) = (1, 1, 1, -3)$. As we have seen, this gives rise to the toric fan of figure 3.3. The charges sum to zero, so the underlying space is a non-compact Calabi–Yau. The associated D term reads

$$|z_1|^2 + |z_2|^2 + |z_3|^2 - 3|x|^2 = a \,. \tag{3.37}$$

Let us consider the two regimes $a < 0$ and $a > 0$. In the first case, x has to have a VEV since it is the only field that carries a negative charge needed to cancel the FI term. Hence in this regime the divisor $E = \{x = 0\}$ does not exist. The VEV of x does, however, not break the entire $U(1)$ but leaves an unbroken $\mathbb{Z}_3$ symmetry, which is the orbifold action. In the regime $a > 0$, at least one of the fields z_i has to have a VEV. Thus in this regime the singular point $z_1 = z_2 = z_3 = 0$ is forbidden by the D term. The VEV can be arbitrarily big, since it can be balanced by giving a big VEV to x as well. Thus the space is non-compact. However, in this regime, we have the possibility of setting $x = 0$, which corresponds to the divisor E. On this divisor, the D term (3.37) becomes the D term (3.35) of $\mathbb{CP}^2$. Hence, as explained in the previous chapter on the level of toric diagrams, we have replaced the singular point by a $\mathbb{CP}^2$. The FI parameter a corresponds to the Kähler parameter associated with the blowup cycle E, with $a = 0$ marking the boundary of the Kähler cone. This examples also illustrates that it is possible to continue the theory beyond the boundary of the Kähler cone, although the theory will change: the exceptional divisor is removed completely from the theory and one obtains a $\mathbb{Z}_3$ action.

3.3.5 Calabi–Yaus as hypersurfaces in the GLSM

Finally, we are in a position to discuss the compact resolution of orbifold models from the GLSM perspective. The analysis has been carried out in great detail in [46] for the geometry of most orbifold models. We will not repeat the full analysis here and only outline the techniques we need for our studies later. We start by describing a two-torus as an elliptic curve. Then we tune the complex structure (i.e. the coefficients in the polynomials defining the torus as a hypersurface) to be compatible with the orbifold action. This can be checked via the Weierstrass $\wp$ function and its derivative, which establishes a relation between the coordinate u on a double-periodic lattice $\mathbb{C}/\Lambda_T$ and the elliptic curve by virtue of the Weierstrass differential equation. Although there exist various descriptions of elliptic curves which are all equivalent, the different complex structures needed for toroidal orbifolds of the type $T^2/\mathbb{Z}_N$ make it convenient for us to choose a specific elliptic curve for a specific $\mathbb{Z}_N$ orbifold:

Orbifold action	$\mathbb{Z}_2$	$\mathbb{Z}_3$	$\mathbb{Z}_4$	$\mathbb{Z}_6$
Complex structure	free	$e^{2\pi i/3}$	i	$e^{2\pi i/3}$
Submanifold	$\mathbb{CP}^3_{1111}[2,2]$	$\mathbb{CP}^2_{111}[3]$	$\mathbb{CP}^2_{112}[4]$	$\mathbb{CP}^2_{123}[6]$

Here we introduced the following notation: The subscripts of $\mathbb{CP}^N$ give the charges of the weighted projective space and the number(s) in square bracket the degree of the homogeneous polynomial(s) used to define the hypersurface equation. As we can see, for $\mathbb{Z}_{3,4,6}$, the torus is given as a single hypersurface in some (weighted) projective space while for $\mathbb{Z}_2$ the torus arises as the intersection of two degree two hypersurfaces in $\mathbb{CP}^3$. Let us exemplify the resolution of $T^6/\mathbb{Z}_3$.

Example (Resolution of $T^6/\mathbb{Z}_3$)   We start with three copies of $\mathbb{CP}^2_{111}[3]$ which correspond to T^6. This means that we introduce for each $\mathbb{CP}^2$ labeled by $a = 1, 2, 3$ three coordinates $Z_{a,i}$, one hypersurface constraint field C_a, and one U(1) gauging. The charge assignment is given in the first three lines of table 3.2 (let us ignore the last line for the moment). We want to study the geometric regime where $a_i > 0$ and thus $c_a = 0$. From the F_{C_a} terms, we then obtain the three hypersurface constraints

$$
\begin{aligned}
0 &= z_{1,1}^3 + z_{1,2}^3 + z_{1,3}^3 + \kappa_1 z_{1,1} z_{1,2} z_{1,3}\,, \\
0 &= z_{2,1}^3 + z_{2,2}^3 + z_{2,3}^3 + \kappa_2 z_{2,1} z_{2,2} z_{2,3}\,, \\
0 &= z_{3,1}^3 + z_{3,2}^3 + z_{3,3}^3 + \kappa_3 z_{3,1} z_{3,2} z_{3,3}\,.
\end{aligned}
\tag{3.38}
$$

It can be shown that these are already the most general polynomials of degree 3 since other terms like $z_{1,1} z_{1,2}^2$ can be absorbed via field redefinitions. The κ_i are constants and encode the complex structure τ_i of the tori. Via the Weierstrass map, it can be checked that for $\tau_i = e^{2\pi i/3}$ we get $\kappa_i = 0$. Thus fixing the complex structure such that it is compatible with the $\mathbb{Z}_3$ orbifold action means that we have to drop the last terms.

	$Z_{1,1}$ $Z_{1,2}$ $Z_{1,3}$	$Z_{2,1}$ $Z_{2,2}$ $Z_{2,3}$	$Z_{3,1}$ $Z_{3,2}$ $Z_{3,3}$	X_{111}	C_1 C_2 C_3
$U(1)_{R_1}$	1 1 1	0 0 0	0 0 0	0	-3 0 0
$U(1)_{R_2}$	0 0 0	1 1 1	0 0 0	0	0 -3 0
$U(1)_{R_3}$	0 0 0	0 0 0	1 1 1	0	0 0 -3
$U(1)_{E_{111}}$	1 0 0	1 0 0	1 0 0	-3	0 0 0

Table 3.2: GLSM charge assignment for the minimal resolution of $T^6/\mathbb{Z}_3$.

The three D terms read

$$|z_{1,1}|^2 + |z_{1,2}|^2 + |z_{1,3}|^2 - 3|c_1|^2 = a_1\,,$$
$$|z_{2,1}|^2 + |z_{2,2}|^2 + |z_{2,3}|^2 - 3|c_2|^2 = a_2\,, \qquad (3.39)$$
$$|z_{3,1}|^2 + |z_{3,2}|^2 + |z_{3,3}|^2 - 3|c_3|^2 = a_3\,.$$

In the geometric regime $a_i > 0$ we have $c_i = 0$ from the F terms and hence we can drop them from the D terms. In the LG regime $a_i < 0$ we have $c_i \neq 0$ and the residual $\mathbb{Z}_3$ generates a Landau–Ginzburg $\mathbb{Z}_3$ orbifold. However, as mentioned before, this is not the orbifold we are after. So let us introduce the orbifold action instead using exceptional divisors. This means we introduce new exceptional fields x and new $U(1)$ charges in order to keep the dimensionality fixed. Giving VEVs to the exceptional fields x will remove the corresponding exceptional divisors E and give rise to residual $\mathbb{Z}_3$ actions. All this happens in the geometric regime $a_i > 0$. In $T^6/\mathbb{Z}_3$, there are 27 fixed points. We label the position of the fixed point in the first torus by $\alpha = 1, 2, 3$, in the second torus by β, and in the third torus by γ. Hence we get 27 exceptional divisors $E_{\alpha\beta\gamma} = \{x_{\alpha\beta\gamma} = 0\}$, 27 $U(1)$ gauging $U(1)_{E_{\alpha\beta\gamma}}$, and 27 FI parameters $b_{\alpha\beta\gamma}$ on top of the GLSM data needed to describe the T^6.

It is instructive to proceed step by step and to first introduce one exceptional coordinate, say x_{111}. The GLSM charge assignment for this case is given in the last line of table 3.2. From this, we obtain in the geometric regime $a_i > 0$ the following F terms

$$0 = z_{1,1}^3 x_{111} + z_{1,2}^3 + z_{1,3}^3\,,$$
$$0 = z_{2,1}^3 x_{111} + z_{2,2}^3 + z_{2,3}^3\,, \qquad (3.40)$$
$$0 = z_{3,1}^3 x_{111} + z_{3,2}^3 + z_{3,3}^3\,.$$

Note that they are almost identical to those of the torus (3.38), except for the appearance of x_{111} in front of some monomials which is needed for gauge invariance. Also note that the absence of the $\kappa_i z_{i,1} z_{i,2} z_{i,3}$ term is crucial for the resolution: with the given charge assignment, such a term would not be gauge invariant. The D terms are now

$$|z_{1,1}|^2 + |z_{1,2}|^2 + |z_{1,3}|^2 = a_1\,,$$
$$|z_{2,1}|^2 + |z_{2,2}|^2 + |z_{2,3}|^2 = a_2\,,$$
$$|z_{3,1}|^2 + |z_{3,2}|^2 + |z_{3,3}|^2 = a_3\,, \qquad (3.41)$$
$$-3|x_{111}|^2 + |z_{1,1}|^2 + |z_{2,1}|^2 + |z_{3,1}|^2 = b_{111}\,.$$

In this case, the first three D terms are the same as in (3.39). The last D term is precisely the one from the local non-compact resolution (3.37). There the target space was non-compact since the D terms contain fields of opposite signs, such that an arbitrary large value for the z_i could be canceled by a large VEV of x. In this case, however, the first three D terms prevent the z_i from becoming too large and in this way lead to a compact target space. As before, the geometric orbifold and blowup regime are separated by the value of the Kähler parameter b_{111}. If $b_{111} < 0$, the last D term forces x to get a VEV and thus the $\mathrm{U}(1)_{E_{111}}$ is broken to a $\mathbb{Z}_3$ acting as

$$\theta_{111} : \ (z_{1,1},\, z_{2,1},\, z_{3,1}) \mapsto (e^{2\pi\mathrm{i}/3}z_{1,1},\, e^{2\pi\mathrm{i}/3}z_{2,1},\, e^{2\pi\mathrm{i}/3}z_{3,1}) . \tag{3.42}$$

This $\mathbb{Z}_3$ has fixed points at $z_{1,1} = z_{2,1} = z_{3,1} = 0$. By inserting them into the F term equations (3.40), we find that the equations can be satisfied by choosing $z_{i,2} = -e^{2\pi\mathrm{i}k/3}z_{i,3}$, $k = 0, 1, 2$. We thus obtain a total of $3 \cdot 3 \cdot 3 = 27$ fixed points on the torus, all of which are described by the same zero locus. Note that $x_{111} \neq 0$ in the orbifold phase and thus the exceptional divisor E_{111} does not exist on the orbifold. In the geometric blowup regime $b > 0$, it is possible to set $x_{111} = 0$, corresponding to the divisor E_{111}. In this case, however, the fourth D term forbids setting $z_{1,1} = z_{2,1} = z_{3,1} = 0$, since at least one of these fields has to get a VEV to cancel the FI term, and thus the 27 fixed points have been resolved by the same exceptional divisor E_{111}. This is remarkable, since we have only introduced one exceptional divisor instead of 27 and yet all 27 singularities are resolved. This model corresponds to a resolution of $T^6/\mathbb{Z}_3$ where all 27 exceptional divisors are identical or put differently, where the same exceptional divisor E_{111} is glued into all 27 fixed points to resolve the singularity simultaneously. In particular, we only have one FI or Kähler parameter b_{111} which controls the size of the resolution $\mathbb{CP}^2$ that is glued into the 27 fixed points. The model corresponds to the blowup of an orbifold where all exceptional divisors are identical and thus have the same size and carry the same gauge flux. Nevertheless, the model is smooth. For this reason, we call it the minimal resolution model. This type of model was e.g. also studied in [65]. Albeit being far from the most general case, these minimal resolution models provide a nice class of traceable examples due to their simplicity, which mainly stems from the fact that the Stanley–Reissner ideal is much smaller than in the maximal resolution models. For this reason, we will use a resolution model with three exceptional divisors (instead of 27) for the discussion in chapter 7.

Before moving on and introducing more exceptional divisors, let us discuss the correspondence between the divisors as introduced in section 3.2.2 and the GLSM coordinates: the ordinary divisors $D_{i,\sigma}$ correspond in the GLSM to $\{z_{i,\sigma} = 0\}$. As already mentioned, the exceptional divisors $E_{\alpha\beta\gamma}$ correspond in the GLSM to $\{x_{\alpha\beta\gamma} = 0\}$. Lastly, let us turn to the inherited divisors. Remember that these were divisors inherited from the torus away from the singularity. Using the Weierstrass map to match the flat torus with the elliptic curve description, it can be shown that [46]

$$R_1 = \{k_{1,1}z_{1,1}^3 x_{111} + k_{1,2}z_{1,2}^3 + k_{1,3}z_{1,3}^3 = 0\} \tag{3.43}$$

and likewise for R_2 and R_3. We note that the R_i are basically the F_{C_i} terms (3.40) that cut out the torus. The coefficients $k_{i,\sigma}$ correspond to the positions of the divisors on

	$Z_{1,1}$ $Z_{1,2}$ $Z_{1,3}$	$Z_{2,1}$ $Z_{2,2}$ $Z_{2,3}$	$Z_{3,1}$ $Z_{3,2}$ $Z_{3,3}$	X_{111} X_{211}	C_1 C_2 C_3
$U(1)_{R_1}$	1 1 1	0 0 0	0 0 0	0 0	-3 0 0
$U(1)_{R_2}$	0 0 0	1 1 1	0 0 0	0 0	0 -3 0
$U(1)_{R_3}$	0 0 0	0 0 0	1 1 1	0 0	0 0 -3
$U(1)_{E_{111}}$	1 0 0	1 0 0	1 0 0	-3 0	0 0 0
$U(1)_{E_{211}}$	0 1 0	1 0 0	1 0 0	0 -3	0 0 0

Table 3.3: GLSM charge assignment for a partly singular resolution of $T^6/\mathbb{Z}_3$.

the torus (they can be related to the c's appearing in the definition (3.23)). Thus in the GLSM the "inheritance" of the inherited divisors becomes quite obvious. Furthermore, we see how the three linear equivalent relations involving the same R_i but different divisors $D_{i,\sigma}$ arise, which were used to describe the gluing in the resolution process: The expressions for the R_i have three different terms, each of which has the same charge (the negative of the C_i). Thus each term in the sum will be linearly equivalent to R_i. In this sense, the R_i, which are the "inverse" of the C_i, define the gluing of the fixed points across the torus. Thus the hypersurface construction that proceeds via the introduction of the R_i and the associated auxiliary polyhedra discussed in section 3.2.2 implicitly uses the hypersurface constraints from the C_i, as can be seen from the GLSM.

Let us now consider what happens when we introduce another exceptional divisor, say E_{211}, where the charge assignment is given in table 3.3. This should break the degeneracy which identifies the exceptional divisor of all 27 fixed points. As we can see, in the orbifold phase $a_i > 0$, $b_{111}, b_{211} < 0$ where both x have a VEV, the following two discrete $\mathbb{Z}_3$ remnants of $U(1)_{E_{111}}$ and $U(1)_{E_{211}}$ are left:

$$
\begin{aligned}
\theta_{111} &: (z_{1,1},\, z_{2,1},\, z_{3,1}) \mapsto \left(e^{2\pi i/3} z_{1,1},\, e^{2\pi i/3} z_{2,1},\, e^{2\pi i/3} z_{3,1}\right), \\
\theta_{211} &: (z_{1,2},\, z_{2,1},\, z_{3,1}) \mapsto \left(e^{2\pi i/3} z_{1,2},\, e^{2\pi i/3} z_{2,1},\, e^{2\pi i/3} z_{3,1}\right).
\end{aligned}
\tag{3.44}
$$

Clearly, these actions have fixed points $z_{1,1} = z_{2,1} = z_{3,1} = 0$ and $z_{1,2} = z_{2,1} = z_{3,1} = 0$, respectively. Proceeding as before and substituting them into the F terms, we find that the two zero loci have nine different F term solutions each. Also as before, substituting the fixed points into the D terms shows that in the blowup regime $b_{111}, b_{211} > 0$ the fixed points are forbidden since at least one of the z's has to have a VEV to cancel the FI term. So the degeneracy of 27 is broken into sets of 9. But so far we have only uncovered 18 of the 27 fixed points. To find the last group of 9 fixed points, observe that there is a linear combination of $U(1)$'s, $\widetilde{U}(1) := U(1)_{R_1} + 3U(1)_{R_2} + 3U(1)_{R_3} - U(1)_{E_{111}} - U(1)_{E_{211}}$, which is broken by either VEV of x_{111} or x_{211} to a discrete $\mathbb{Z}_3$ symmetry acting as

$$
\theta_{311} : \; (z_{1,3},\, z_{2,1},\, z_{3,1}) \mapsto \left(e^{2\pi i/3} z_{1,3},\, e^{2\pi i/3} z_{2,1}, e^{2\pi i/3} z_{3,1}\right).
\tag{3.45}
$$

The fixed points of this discrete action are at $z_{1,3} = z_{2,1} = z_{3,1} = 0$. Inserting these fixed points into the F terms, we find the last group of nine fixed points at this zero locus. A surprise awaits us when inserting the fixed point equation into the D terms. Unlike the other cases, there is no D term that forbids setting $z_{1,3} = z_{2,1} = z_{3,1} = 0$. Thus

	$Z_{1,1}\ Z_{1,2}\ Z_{1,3}$	$Z_{2,1}\ Z_{2,2}\ Z_{2,3}$	$Z_{3,1}\ Z_{3,2}\ Z_{3,3}$	$X_{111}\ X_{211}\ X_{311}$	$C_1\ C_2\ C_3$
$U(1)_{R_1}$	1 1 1	0 0 0	0 0 0	0 0 0	-3 0 0
$U(1)_{R_2}$	0 0 0	1 1 1	0 0 0	0 0 0	0 -3 0
$U(1)_{R_3}$	0 0 0	0 0 0	1 1 1	0 0 0	0 0 -3
$U(1)_{E_{111}}$	1 0 0	1 0 0	1 0 0	-3 0 0	0 0 0
$U(1)_{E_{211}}$	0 1 0	1 0 0	1 0 0	0 -3 0	0 0 0
$U(1)_{E_{311}}$	0 0 1	1 0 0	1 0 0	0 0 -3	0 0 0

Table 3.4: GLSM charge assignment for the a (degenerate) smooth resolution of $T^6/\mathbb{Z}_3$.

these fixed points remain unresolved. This means that by introducing more exceptional divisors, we have re-introduced unresolved fixed points!

However, the zero locus $z_{1,3} = z_{2,1} = z_{3,1} = 0$ already guides us to a solution: We simply introduce another exceptional divisor x_{311} together with the associated scaling and the associated FI term, see table 3.4. Precisely when this $b_{311} < 0$, the coordinate x_{311} has to have a VEV and the exceptional scaling $U(1)_{E_{311}}$ is broken to a $\mathbb{Z}_3$ acting as θ_{311} in (3.45). However, this time the D term associated with the FI parameter b_{311} forbids the nine fixed points of θ_{311} when $b_{311} > 0$. Thus by introducing three exceptional divisors we have broken the fixed point degeneracy from one group containing all 27 fixed points into three groups containing 9 fixed points each.

If we go on and introduce further exceptional divisors, we will further break the degeneracy into 9 groups of 3 fixed points each. This description will have all of its fixed points resolved once we have introduced a total of 9 exceptional divisors together with their scalings and FI parameters. When going on further and introducing the tenth exceptional divisor, the degeneracy is broken completely, but only 10 out of 27 fixed points are resolved. Thus in order to obtain a fully resolved model without remnant fixed points, we have to introduce all 27 exceptional divisors. We call this model the maximal resolution model.

Lastly, we have to explain what the meaning of all the induced $\mathbb{Z}_3$ actions $\theta_{\alpha\beta\gamma}$ actually is. In the end, we want to describe a simple $T^6/\mathbb{Z}_3$ orbifold and not a $T^6/(\mathbb{Z}_3)^{27}$ orbifold. First, we notice that not all 27 $\theta_{\alpha\beta\gamma}$ are independent since they can be related by defining linear combinations of charges and by rotating all fields simultaneously in a way similar to what was done in (3.45). Using redefinitions of this type, it can be shown that out of the 27 only four $\mathbb{Z}_3$ actions remain. One of them corresponds to the orbifold action and the other three are used to break the degeneracy of the fixed points from 27 to 9 with the first, to 3 with the second, and to 1 with the the last. All the details of this are worked out in [46], also for the other orbifolds, and we refrain from repeating it here.

## 3.3.6 SR ideal and intersection numbers in the GLSM

After we have recovered the divisors from the toric description in the GLSM language, let us discuss the Stanley–Reissner ideal and the intersection numbers. As we shall see,

the Stanley–Reissner ideal is by far not unique, not even for the $T^6/\mathbb{Z}_3$ as could have been expected from the discussion in section 3.2.1. Instead, there exist a whole variety of geometric, non-geometric, and mixed phases living in different Kähler cones.

We start the discussion in the simple setup of the minimal resolution model. In the example in section 3.2.1, we have seen that intersections like $D_{1,\alpha}D_{2,\beta}D_{3,\gamma}$ never form a cone in the toric blowup and hence are part of the Stanley–Reissner ideal. Indeed, setting $z_{1,1} = z_{2,1} = z_{3,1} = 0$ in (3.41), we see that we cannot solve the fourth D term constraint in the blowup regime $b_{111} > 0$ and thus the intersection number is zero. Likewise, combinations like $D_{1,1}D_{1,2}D_{1,3}$ with all divisors in the same torus, which also do not form a cone after the introduction of the exceptional divisor, are forbidden by the first three D terms. In contrast, it can be checked that $z_{i,1} = z_{j,1} = x_{111} = 0$ is allowed by the D terms. And indeed, these divisors do form a cone. In order to find the intersection numbers, we simply count the number of solutions to the F terms. We obtain three equations of the form $z_{i,2}^3 + z_{i,3}^3 = 0$, each of which has three distinct solution, such that the total intersection number is 27. After introducing all 27 exceptional divisors and thereby breaking the degeneracy completely, we find the intersection number to be 1. Using linear equivalences and the method described above to construct the inherited divisors, all intersections can be calculated.

Note that the discussion is solely based on the D terms. So for example the combination $D_{1,1}D_{1,2}D_{2,1}$ is allowed by the D terms, which set in particular $|z_{1,3}|^2 = a$ in this case. Nevertheless, setting $z_{1,1} = z_{1,2} = 0$, $|z_{1,3}|^2 = a$ does not solve the F terms. In other words, the divisors do intersect in the toric ambient space but not on the CY hypersurface. This illustrates the major complication that is introduced when studying hypersurfaces: one needs to restrict the ambient space data to the hypersurface. This restriction is best formulated via exact sequences. (See (3.19) as an example for the restriction of the tangent bundle; for the restriction of the gauge bundle, we later use the Koszul sequence.)

Let us briefly discuss the various phases. For ease of exposition, we assume that all torus Kähler parameters are of the same size, $a_i = a$. As we already know, the case $a > 0$, $b_{111} < 0$ corresponds to the orbifold phase. The case $a, b_{111} < 0$ corresponds to the Landau–Ginzburg orbifold. Furthermore, we have discussed the blowup case $a \gg b_{111} > 0$. However, a careful analysis shows that one has to be more careful, as this phase is actually subdivided into four phases, out of which only one corresponds to the toric blowup description we are seeking to describe (blowup I). An overview over the various phases is given in figure 3.7. By analyzing all simultaneous solutions to the D terms, we find that for $0 < 3b_{111} < a$, we reproduce the SR ideal associated with the toric fan given in figure 3.3. As we increase the ratio b_{111}/a, we leave the Kähler cone of the resolution and enter new ones, where first (blowup II) the exceptional divisors start to intersect the inherited divisors (thus destroying the local resolution picture of the $\mathbb{Z}_3$ singularity). Upon increasing the ratio further, we enter yet other cones (critical blowup + over-blowup) where we obtain a mixed description, as here the c_i can be vanishing or non-vanishing. Depending on the situation, the dimensionality of the target space jumps between one and three dimensions. Finally, going to a phase where $a < 0$, $b > 0$, we end up in a regime where the c_i cannot vanish and x_{111} vanishes identically
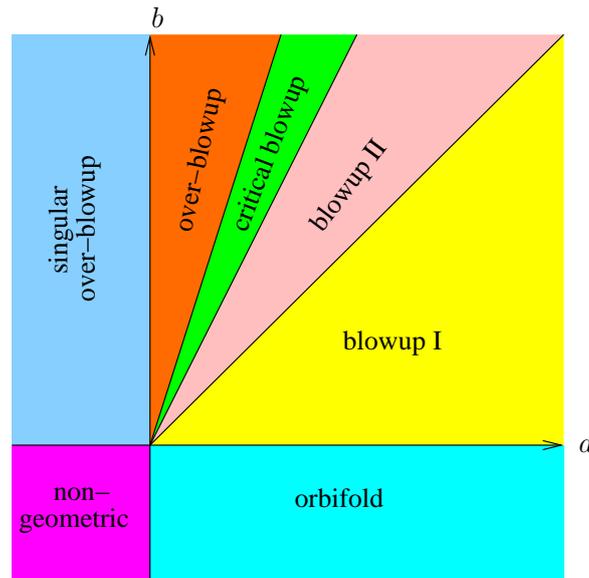
Figure 3.7: Overview over the various GLSM phases that can be obtained from a simplified version of the minimal blowup model of $T^6/\mathbb{Z}_3$.

(singular over-blowup). This corresponds to a mixed phase as well. Situations like this with topology changing hybrid models and exoflop transitions have also been studied in [66–68]. In order to avoid such complications, we usually study regions deep inside the orbifold regime ($a_i \gg 0$, $b_{\alpha\beta\gamma} \ll 0$) or the CY regime ($a_i \gg b_{\alpha\beta\gamma} \gg 0$).

We want to conclude this section by outlining the resolution procedure for toroidal orbifolds in the GLSM framework:

- For each torus T^2, choose the description in terms of an elliptic curve that is best-suited for the orbifold action under consideration.

- Introduce exceptional divisors and $U(1)$ gaugings that generate the orbifold action when the x's get a VEV and that forbid the fixed points when the x's are set to zero. Depending on the intended use, this might be a minimal resolution model, a full resolution model, or even some model that cannot be completely resolved.

- Calculate the SR ideal from the D terms in the Kähler cone of the toric resolution.

- Read off the linear equivalences from the GLSM charges.

- Calculate the intersection numbers form counting the solutions to the F terms and by employing the linear equivalence relations.

Chapter 4

$\cdots\cdots\cdots\cdots\cdots\cdots\cdots\cdots\cdots\cdots\cdots$

ANOMALIES

Anomalies provide an extremely powerful tool for studying string compactifications. This is based on the fact that string theory is, by construction, free of anomalies. Hence, any theory that is derived from it, has to be free of anomalies as well. The mechanism we are invoking for this argumentation is based on the 't Hooft anomaly matching principle [69], which states that the calculation of anomalies is independent of the energy scale at which the calculation is carried out. Thus anomalies are protected quantities that can be used to connect theories which are defined at different scales[1]. As will be discussed in the following, anomalies are characterized in terms of the massless chiral spectrum of a theory. Since the spectrum computation is accessible in both the supergravity approximation and exact string CFT calculations (cf. sections 2.3 and 2.4), anomalies can be computed and compared in both theories.

4.1 Introduction to anomalies

In this section we review anomalies, their computation and the possibility of anomaly cancelation via the Green–Schwarz mechanism [70] in various dimensions. For a review of anomaly cancelation in higher dimensions, see e.g. [16, 27, 71, 72].

Definition (Anomaly)   An anomaly arises from a classical symmetry that is not preserved upon quantization of the theory. While the breakdown of a global symmetry does not necessarily lead to inconsistencies, the breakdown of a gauge theory renders the quantum theory inconsistent.

The reasons for this are the following: local symmetries are characterized by gauge transformations which are necessary for decoupling unphysical degrees of freedom from the theory. If a gauge theory cannot be quantized without anomalies, this means that

---

[1]Having such protected quantities is extremely useful, as can be seen e.g. from the ample usage of BPS states in string theory.

the unphysical states contribute among other things in internal loops which leads to a breakdown of unitarity. On the other hand, global anomalies can be present in a theory since they come from symmetries that are not needed to decouple unphysical states. The probably best-known example of a global anomaly is the chiral QCD anomaly which is needed to explain the decay $\pi^0 \to \gamma\gamma$.

For concreteness, consider a theory in $d = 2\ell$ dimensions with a gauge group which is a product of a non-Abelian group G (where G can contain several factors) and a number of U(1)'s, and a set of chiral fermions Ψ, transforming in a representation $\boldsymbol{r}_\Psi$ of G and with U(1) charges Q^i_Ψ. We will be working with anti-Hermitian gauge connections $A^a_\mu T^a$ where the T^a are the generators of the gauge symmetries in the appropriate representation. Furthermore, we will be working with the spin connection ω^{ab}_μ which is a 1-form taking values in the Lie Algebra of SO(D). We consider the Lagrangian

$$\mathcal{L} = \det(e^a_\mu)\overline{\Psi}\mathrm{i}\gamma^\mu D_\mu\Psi\,, \tag{4.1}$$

where e^a_μ is the vielbein, γ^μ are the gamma matrices and D_μ the gauge and gravity covariant derivative given by

$$D_\mu = \partial_\mu + \frac{1}{8}\omega^{ab}_\mu[\gamma_a, \gamma_b] + A^a_\mu T_a\,. \tag{4.2}$$

4.1.1 Descent equations

Let us consider the effective action $S_{\text{eff}}(e, A, \omega)$ defined by

$$e^{-S_{\text{eff}}(e,A,\omega)} = \int \mathcal{D}\Psi\mathcal{D}\overline{\Psi}e^{-\int \mathrm{d}^d x \mathcal{L}}\,. \tag{4.3}$$

A (possibly combined) gauge and gravitational symmetry transformation δ_{α_1} acts on $S_{\text{eff}}(e, A, \omega)$ as

$$\delta_{\alpha_1}S_{\text{eff}}(e, A, \omega) =: \int I_d(\alpha_1)\,, \tag{4.4}$$

where we have expressed, for reasons that will become apparent soon, the anomalous variation in terms of an integral of a d-form I_d. Let us now act with another symmetry transformation δ_{α_2} and impose the property $[\delta_{\alpha_1}, \delta_{\alpha_2}] = \delta_{[\alpha_1,\alpha_2]}$. We find for the variation of $S_{\text{eff}}(e, A, \omega)$ that

$$\delta_{\alpha_1}\delta_{\alpha_2}S_{\text{eff}}(e, A, \omega) - \delta_{\alpha_2}\delta_{\alpha_1}S_{\text{eff}}(e, A, \omega) = \delta_{[\alpha_1,\alpha_2]}S_{\text{eff}} =: \int I_d(\alpha_1, \alpha_2), \tag{4.5}$$

which is known as the Wess–Zumino consistency condition. Its solution can be characterized elegantly in terms of a (formal) uniquely defined $(d + 2)$-form I_{d+2} which is closed ($\mathrm{d}I_{d+2} = 0$) and invariant under the symmetry variation ($\delta_\alpha I_{d+2} = 0$). It is a polynomial in the traces of field strength $\mathrm{tr}(\mathrm{i}F)^n$ and the curvature $\mathrm{tr}(R)^n$ only. The most general solution for (4.5) can be constructed from I_{d+2}, which is called the

anomaly polynomial, by using the Stora–Zumino descent equations, or just descent equations for short:

$$I_{d+2} = \mathrm{d} I_{d+1}^{(0)}, \qquad\qquad \delta_\alpha I_{d+1}^{(0)} = \mathrm{d} I_d^{(1)}. \qquad\qquad (4.6)$$

For the definition of $I_{d+1}^{(0)}$, we made use of the fact that I_{d+2} is closed and hence locally exact. $I_{d+1}^{(0)}$ is not invariant under symmetry transformations anymore, but the variations are closed again, which allows for the definition of the $(d+1)$-form I_{d+1} as the exterior derivative of the gauge variation of I_d. The $I_{d+1}^{(0)}$ are called Chern–Simons forms. Their gauge variations $I_d^{(1)}$ solve (4.5). The superscripts indicate that the Chern–Simons form is independent and that the anomaly is linear in the symmetry parameter.

We do not present the proof that (4.6) solves (4.5) here, which would take us too much afar. We rather content ourselves with remarking that this can be treated completely rigorously in terms of BRST cohomology where it can be shown that (4.5) implies that anomalies are associated with BRST-closed objects, and trivial anomalies corresponding to the variation of local counterterms are associated with BRST-exact objects. Thus, the solutions are characterized in terms equivalence classes of the BRST cohomology, which is consistent with the descent construction [71].

As we shall discuss now, the formal object I_{d+2} used above to solve the Wess–Zumino condition (4.5) for the anomaly I_d arising from local gauge and Lorentz transformations, can be associated with a chiral anomaly in $d+2$ dimensions.

4.1.2 The chiral anomaly

Our discussion of the chiral anomaly is based on the so-called Fujikawa method [73]. We consider a theory of fermions Ψ coupled to an external gauge field (i.e. a gauge field which is not integrated over in the path integral). As we shall see, the computation reduces to the calculation of the index of the Dirac operator. There is a classically conserved chiral current J^μ associated to the global chiral transformation $\Psi \to e^{i\lambda\gamma_{d+1}}\Psi$ where γ_{d+1} is the generalization of γ_5 to d dimensions, λ is the chiral symmetry gauge parameter, and Ψ is a massless Dirac fermion. In order to study the anomaly, investigate the behavior of this symmetry under quantization.

Note that the variation $\delta_\lambda S_{\mathrm{eff}}$ receives contributions from both the variation of the path integral measure and from the variation of the classical action

$$\delta_\lambda \int \mathrm{d}^d x\, \mathcal{L} = \int \mathrm{d}^d x\, J^\mu \partial_\mu \lambda, \qquad \delta_\lambda(\mathcal{D}\Psi\mathcal{D}\overline{\Psi}) = e^{-2\mathrm{i}\int\lambda\mathcal{A}}. \qquad (4.7)$$

Thus the transformation $\delta_\lambda S_{\mathrm{eff}}$ vanishes if both contributions cancel each other.

The variation of the path integral measure can be calculated by decomposing Ψ and $\overline{\Psi}$ in terms of eigenfunctions of the covariant derivative $\gamma^\mu D_\mu$, introducing a Gaussian

cut-off regularization, and performing the integration over the fermionic zero modes. We do not give the details, but quote the final result:

$$\delta_\lambda S_{\text{eff}}(e, A, \omega) = \int \lambda \langle \partial_\mu J^\mu \rangle \stackrel{!}{=} \int 2\mathrm{i}\lambda \mathcal{A} = \mathrm{ind}(\mathrm{i}\gamma_\mu D^\mu) = \int \mathrm{ch}_{\mathbf{r}_\Psi}(F)\hat{A}(R) \,. \qquad (4.8)$$

Here we have introduced the Dirac genus (or A roof genus) $\hat{A}$, which is defined by

$$\hat{A}(R) = \prod_{i=1}^{n} \frac{x_i^R}{2} \frac{1}{\sinh\left[\frac{x_i^R}{2}\right]} = 1 + \frac{1}{12}\mathrm{tr}R^2 + \dots \,, \qquad (4.9)$$

$$\mathrm{ch}_{\mathbf{r}_\Psi}(F) = \mathrm{tr}_{\mathbf{r}_\Psi} e^{\frac{\mathrm{i}F}{2\pi}} = \dim(\mathrm{G}) + \frac{1}{2\pi}\mathrm{tr}(\mathrm{i}F) + \frac{1}{2}\frac{1}{(2\pi)^2}\mathrm{tr}(\mathrm{i}F)^2 + \dots \,. \qquad (4.10)$$

The x_i^R appearing in the power series of the $\hat{A}$ genus are skew-symmetric eigenvalues of R, which are linked to $\mathrm{tr}R^{2m}$ via $\mathrm{tr}R^{2m} = 2(-1)^m \sum_i x_i^{2m}$. The Chern character ch has already been introduced in (2.16) and is repeated here for convenience. The traces are evaluated in the representation $\mathbf{r}_\Psi$, and appropriate wedge products are understood, as well as the projection onto the d-form part prior to the integration in (4.8).

4.1.3 Gauge and gravitational anomalies

Next, we want to study the gauge variations λ and gravitational variations ε of a massless Weyl fermion ψ:

$$\delta_\lambda \psi = -\lambda_a T^a \psi \,, \qquad \delta_\lambda \overline{\psi} = \lambda_a T^a \overline{\psi} \,, \qquad (4.11\mathrm{a})$$

$$\delta_\varepsilon \psi = -\varepsilon_\mu D^\mu \psi \,, \qquad \delta_\varepsilon \overline{\psi} = \varepsilon_\mu D^\mu \overline{\psi} \,. \qquad (4.11\mathrm{b})$$

We want to evaluate these expressions in a similar way to the one outlined above for the chiral anomaly, i.e. using Fujikawa's method. However, one faces the problem that the anomaly obtained this way does not satisfy the Wess–Zumino consistency condition (4.5), as the Gaussian cut-off introduced above does not preserve the bosonic symmetry. However, (4.5) is strong enough such that we can use Fujikawa's method to derive the leading order contribution of the gauge fields and the spin connection to the anomaly and then fix the subleading parts and the appropriate bosonic normalization factors by imposing (4.5). As alluded to before, the resulting expressions agree with the descent of the associated chiral anomaly in $d + 2$ dimensions.

Since we are studying super-Yang–Mills theories coupled to supergravity, we need to consider the anomaly contribution of spin $\frac{1}{2}$ Weyl fermions as well as the contributions of spin $\frac{3}{2}$ Rarita–Schwinger gravitinos[2]. The total anomaly polynomial is then given as the sum of the two anomaly polynomials, and the anomaly itself can be extracted via

---

[2]In principle self-dual tensor fields contribute to the anomaly as well, but these fields are absent in theories derived from heterotic string theories which are the ones dealt with here.

the descent equations. In general, the contributions of spin $\frac{1}{2}$ and Rarita–Schwinger spin $\frac{3}{2}$ fermions are

$$I_{d+2}^{(1/2)}(R, F) = \pm(2\pi \mathrm{i})^{\frac{d}{2}} \mathrm{ch}_{\mathbf{r}_{\Psi}}(F) \hat{A}(R) \,, \tag{4.12a}$$

$$I_{d+2}^{(3/2)}(R, F) = \pm(2\pi \mathrm{i})^{\frac{d}{2}} \hat{A}(R) \left(1 - \sum_i 2\cosh(x_i^F)\right) \mathrm{ch}_{\mathbf{r}_{\Psi}}(F) \,. \tag{4.12b}$$

The contribution from the Weyl fermions (4.12a) is simply given by the chiral anomaly (4.8). From the contribution of the Rarita–Schwinger spinors we subtract the part $\mathrm{ch}(F)\hat{A}(R)$ of a spin $\frac{1}{2}$ ghost fermion needed for the proper quantization of the spin $\frac{3}{2}$ field [72]. The sign depends on the chirality of the Weyl fermions. In dimensions where one can impose a Majorana–Weyl condition, the anomaly contributions are given by one half of those in (4.12). We will drop the factors of $(2\pi \mathrm{i})^{d/2}$, since they are not relevant in what follows.

4.1.4 Anomalies from Feynman graphs

In the previous part we have seen how to characterize anomalies topologically using index theorems. However, anomalies can also be calculated directly via Feynman diagrams. They arise from chiral massless Weyl fermions (and hence only in even dimensions) at one loop order from $(d/2 + 1)$-sided polygon graphs where the external fields are gauge bosons or gravitons and fermions are running in the loop, and are one-loop exact. The anomaly graphs which are relevant for our analysis characterize 10D, 4D and 2D anomalies and are thus given in terms of hexagon, triangle, and "diangle" (i.e. loop) diagrams, respectively. The diagrams, including a possible Green–Schwarz counterterm to be discussed in section 4.1.6, are given in figure 4.1. Note furthermore that we are dealing with $\mathcal{N} = 1$ supersymmetric theories, such that the information on the chiral fermions is enough to determine the full chiral spectrum (this statement is of course also true for the characterization of anomalies via topological formulas using the Dirac index).

Example (Gauge and gravitational anomalies in 4D)   In four dimensions, we can take all fields to be left-handed. Concentrating on the U(1) anomalies, we can attach either three U(1) gauge fields to the vertices, or one U(1) and two non-Abelian gauge fields or gravitons. Either via direct computation or from the descent equations along the lines outlined before, one finds for the anomalous divergence of the U(1) current J_i,

$$\langle \partial_\mu J_i^\mu \rangle \sim \frac{1}{2} A_{\mathrm{G}^2-\mathrm{U}(1)_i} \mathrm{tr} F\widetilde{F} + \frac{1}{s_{ijk}} A_{\mathrm{U}(1)^3_{ijk}} F_j \widetilde{F}_k + \frac{1}{48} A_{\mathrm{grav}^2-\mathrm{U}(1)} \mathrm{tr} R\widetilde{R} \,. \tag{4.13}$$

Here F, F_i and R are the field strengths of G, $\mathrm{U}(1)_i$ and the Riemann tensor, the tilde denotes the dual (i.e. $\widetilde{F}^{\mu\nu} = \frac{1}{2}\varepsilon^{\mu\nu\rho\sigma} F_{\mu\nu}$), and the traces are taken in the representation in which the chiral Weyl fermions transform. Finally, s_{ijk} is a symmetry factor taking
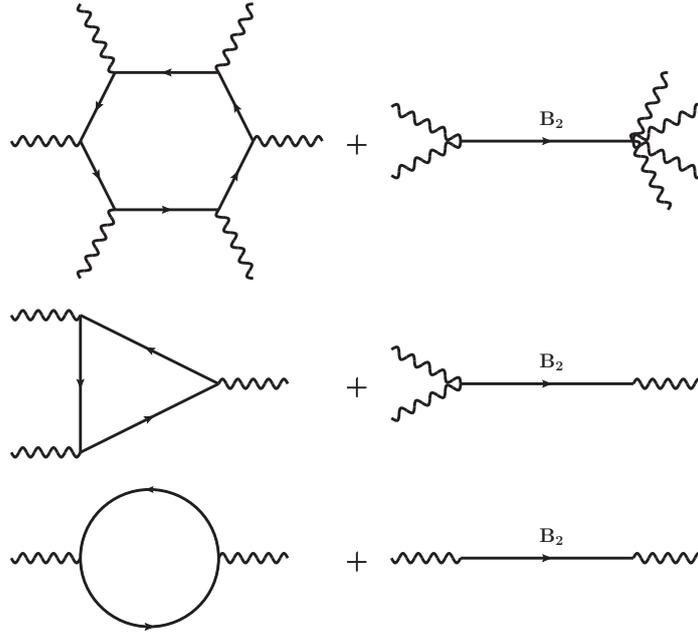
Figure 4.1: Anomalous diagrams and the corresponding Green–Schwarz counterterms for anomalies in 10, 4, and 2 dimensions.

into account permutations of the legs (i.e. for distinct i, j and k, we have $s_{iii} = 3!$, $s_{iij} = 2!$ and $s_{ijk} = 1$). The anomaly coefficients for these cases are given by

$$A_{\mathrm{G}^2-\mathrm{U}(1)} = \sum_{\psi} \ell(\boldsymbol{r}_{\psi}) \, q_{\psi} \,, \quad A_{\mathrm{grav}^2-\mathrm{U}(1)} = \sum_m Q_m \,, \quad A_{\mathrm{U}(1)^3_{ijk}} = \sum_m Q^i_m Q^j_m Q^k_m \,. \quad (4.14)$$

Here the first sum runs over all chiral massless Weyl fermions ψ, and $\ell(\boldsymbol{r}_{\psi})$ is the Dynkin index of $\boldsymbol{r}_{\psi}$. The second and third sums run over all chiral fermions. Since in general the field strengths are non-vanishing, the coefficients A have to vanish in an anomaly-free theory, which poses extremely strong conditions on the possible U(1) charge assignments in chiral theories.

4.1.5 Discrete anomalies

Let us close this section with a short discussion of discrete anomalies. To be more precise, we will be interested in $\mathbb{Z}_N$ anomalies. In principle, they can be be obtained from the expressions for the Abelian anomalies by replacing the charges of the continuous U(1)'s in (4.14) by the discrete $\mathbb{Z}_N$. However, since these charges are only defined modulo N, some subtleties arise [74, 75].

- Let us first consider the $\mathrm{G}^2 - \mathbb{Z}_N$ and $\mathrm{grav}^2 - \mathbb{Z}_N$ anomalies. In a normalization where the Dynkin index $\ell(\mathbf{M}) = \frac{1}{2}$ for the fundamental representation $\mathbf{M}$ of SU(M) and $\ell(\mathbf{M}) = 1$ for the vector representation $\mathbf{M}$ of SO(M), a factor of $\frac{1}{2}$ arises such that the corresponding equations in (4.14) need only be satisfied modulo $\frac{N}{2}$ for an even $\mathbb{Z}_N$ symmetry. If N is odd, the discrete charges of all fields

can be shifted by adding multiples of N such that they are all even, which cancels the factor of $\frac{1}{2}$ and the anomaly coefficients need to vanish modulo N.

- Now consider the discrete anomalies arising from the Abelian anomalies $\mathrm{U}(1)^3_{ijk}$. In contrast to non-Abelian gauge groups, the normalization of the $\mathrm{U}(1)$ charges is (in general) not fixed. This means that replacing one $\mathrm{U}(1)$ with a discrete $\mathbb{Z}_N$ symmetry does not give rise to a meaningful constraint [76]. Furthermore, it can be argued that cubic discrete anomalies are not meaningful either [75]. So the only case in which we actually get constraints from mixed $\mathrm{U}(1)$–$\mathbb{Z}_N$-anomalies is when the $\mathrm{U}(1)$ charge normalization is fixed. This happens e.g. for the hypercharge arising from an $\mathrm{SU}(5)$ GUT.

4.1.6 The Green–Schwarz mechanism and anomaly cancelation

As explained above, if a gauged symmetry is anomalous, the theory is generically inconsistent. However, if the anomalies are reducible, they can be canceled by the Green–Schwarz mechanism [70]. Reducible means that the anomaly polynomial factorizes,

$$I_{d+2} = \sum_{a=1}^{m} X_{k_a} X_{d+2-k_a} \,, \tag{4.15}$$

where each of the factors is by itself closed, gauge invariant and of even degree. The idea of the Green–Schwarz mechanism is to compensate the variation of the effective action by an explicitly non-gauge invariant piece involving fields that transform with a shift. In an effective field theory approach, one may add these fields by hand, while in a "fundamental" approach, such as a string compactification, these fields have to be present from the start.

Concretely, a reducible anomaly of the form (4.15) requires a set of $(k_a - 2)$-form fields C_{k_a-2}, whose gauge transformation is a shift proportional to the descent of X_{k_a},

$$\delta C_{k_a-2} = -\xi X^{(1)}_{k_a-2} \,. \tag{4.16}$$

Here $X^{(1)}_{k_a-2}$ is the descent of the factor X_{k_a} in the anomaly polynomial, and ξ is a free parameter. This transformation implies that the field strength of C_{k_a-2} contains the associated Chern–Simons form,

$$H_{k_a-1} = \mathrm{d}C_{k_a-2} + \xi X^{(0)}_{k_a-1} \,, \tag{4.17}$$

and consequently the Bianchi identity for H_{k_a-1} becomes

$$\mathrm{d}H_{k_a-1} = \xi X_{k_a} \,. \tag{4.18}$$

The anomalous variation of the action is now canceled by the Green–Schwarz action[3]

$$S_{\text{GS}} = \sum_{a=1}^{m} \int \frac{1}{2} H_{k_a-1} \wedge *H_{k_a-1} + \frac{1}{\xi} C_{k_a-2} X_{d+2-k_a} \, . \tag{4.19}$$

Hence, each form field couples to a combination of gauge and gravitational field strengths encoded in X_{d+2-k_a}.

We have phrased the previous discussion in terms of the C_{k_a-2} with $\delta C_{k_a-2} = -\xi X^{(1)}_{k_a-2}$. We could just as well have described the mechanism in terms of the dual forms $\widetilde{C}_{d-k_a}$ by switching the roles of X_{k_a} and X_{d+2-k_a}. At the same time, the shift in (4.17) and the coupling in (4.19) are exchanged. In particular, if we have in an anomaly-free theory a field C_{k_a-2} which shifts under gauge transformations but does not couple to X_{d+2-k_a} and thus does not induce a mass term, the dualized field $\widetilde{C}_{d-k_a}$ will couple but not shift. This is the case in anomaly-free theories when the axion is dualized to the B field.

4.2 Anomalies in 10D heterotic string theory

Next we want to analyze anomalies in low-energy effective theories derived from heterotic string theory, which is $\mathcal{N} = 1$ supergravity coupled to a super-Yang–Mills theory with an (a priori generic) gauge group G. Most of the discussion will focus on perturbative heterotic $E_8 \times E_8$ string theory. However, in the end we will include some comments on anomaly cancelation in heterotic M-theory.

4.2.1 Anomalies in perturbative $E_8 \times E_8$ string theory

The SUGRA multiplet contains the graviton, the left-handed Majorana–Weyl gravitino, a Kalb-Ramond 2-form field B, the dilaton, and the right-handed Majorana–Weyl dilatino. The super-Yang–Mills theory contributes a vector multiplet which contains a gauge field 1-form and the corresponding left-handed Majorana–Weyl gauginos, valued in the adjoint of G. For this field content, the individual contributions are given in (4.12) such that we obtain

$$
\begin{aligned}
I_{12} &= I_{12}^{(3/2)}(\mathfrak{R}) - I_{12}^{(1/2)}(\mathfrak{R}) + I_{12}^{(1/2)}(\mathfrak{R}, \mathfrak{F}) \\
&= -\frac{1}{720} \operatorname{Tr}(i\mathfrak{F})^6 + \frac{1}{1152} \operatorname{Tr}(i\mathfrak{F})^4 \operatorname{tr}\mathfrak{R}^2 - \frac{1}{256} \operatorname{Tr}(i\mathfrak{F})^2 \left[\frac{1}{45} \operatorname{tr}\mathfrak{R}^4 + \frac{1}{36}(\operatorname{tr}\mathfrak{R}^2)^2 \right] \\
&\quad + \frac{\dim(\text{G}) - 496}{64} \left[\frac{1}{5670} \operatorname{tr}\mathfrak{R}^6 + \frac{1}{4320} \operatorname{tr}\mathfrak{R}^2 \operatorname{tr}\mathfrak{R}^4 + \frac{1}{10368}(\operatorname{tr}\mathfrak{R}^2)^3 \right] \\
&\quad + \frac{1}{384} \operatorname{tr}\mathfrak{R}^2 \operatorname{tr}\mathfrak{R}^4 + \frac{1}{1536}(\operatorname{tr}\mathfrak{R}^2)^3 \, .
\end{aligned}
\tag{4.20}
$$

---

[3] There is in principle a third term $\sim X^{(0)}_{k_a-1} X^{(0)}_{d+1-k_a}$, and an ambiguity as one can take any linear combination of the descents of X_{d+2-k_a} and of X_{k_a}. We have made a particular choice here for simplicity.

where we have denoted the 10D Riemann curvature by $\mathfrak{R}$ and the 10D field strength associated with G by $\mathfrak{F}$. Furthermore, the symbol Tr is used for traces in the adjoint, while tr is used for traces in the lowest-dimensional representation. We follow the convention where we call this representation the fundamental representation, even for groups other than SU(N).

Certainly, this I_{12} is non-vanishing for any gauge group G. Thus the only way to get a consistent (i.e. anomaly-free) theory is to employ the Green–Schwarz anomaly cancelation mechanism. However, for this we need the anomaly polynomial (4.20) to factor. Along the lines of (4.15), we make the factorization ansatz $I_{12} = X_4 X_8$. In order to obtain such a factorization, we re-express the adjoint traces Tr of G in terms of fundamental traces tr. In particular, the factorization is only possible if the terms $\mathrm{tr}\,\mathfrak{R}^6$ and $\mathrm{tr}\,(\mathrm{i}\mathfrak{F})^6$ are absent for gauge groups which have a Casimir invariant of that order.

Since SO(10) has an independent sixth order Casimir and I_{12} contains a term proportional to $(\dim(\mathrm{G}) - 496)\mathrm{tr}\,\mathfrak{R}^6$, we find that the dimension of the gauge group has to be 496. The next term we have to worry about is the $\mathrm{Tr}\,(\mathrm{i}\mathfrak{F})^6$ term. In order to factorize this, we write it in terms of tr in the fundamental. Since relating traces in various representations is useful also on other occasions, let us briefly explain how it can be done using Chern characters defined in (4.9) following [77]. First we use that

$$
\begin{aligned}
\mathrm{ch}_{\mathbf{r}_1 \otimes \mathbf{r}_2}(F) &= \mathrm{ch}_{\mathbf{r}_1}(F) \cdot \mathrm{ch}_{\mathbf{r}_2}(F)\,, \\
\mathrm{ch}_{\mathbf{r}_1 \oplus \mathbf{r}_2}(F) &= \mathrm{ch}_{\mathbf{r}_1}(F) + \mathrm{ch}_{\mathbf{r}_2}(F)\,.
\end{aligned}
\tag{4.21}
$$

Next we realize that for the regular Lie algebras one has

$$
\mathrm{SU(N)}:\ \mathrm{Adj} \oplus \mathbb{1} = \mathbf{N} \times \overline{\mathbf{N}}\,, \quad \mathrm{SO(N)}:\ \mathrm{Adj} = [\mathbf{N}]_2\,, \quad \mathrm{SP}(N):\ \mathrm{Adj} = (\mathbf{N})_2\,, \tag{4.22}
$$

where $(\cdot)_k$ and $[\cdot]_k$ denote k-fold symmetrization and anti-symmetrization, respectively, which can be obtained from expanding the generating functions

$$
\sum_{k=1}^{\dim(G)} x^k \mathrm{ch}_{[\mathbf{r}]_k}(F) = \det{}_\mathbf{r}(1 + xe^F) \quad = \exp\left[\sum_{n\geq 1} \frac{(-1)^{n-1}}{n} x^n \mathrm{ch}(nF)\right]\,, \tag{4.23a}
$$

$$
\sum_{k=1}^{\dim(G)} x^k \mathrm{ch}_{(\mathbf{r})_k}(F) = \det{}_\mathbf{r}(1 - xe^F)^{-1} = \exp\left[\sum_{n\geq 1} \frac{1}{n} x^n \mathrm{ch}(nF)\right]\,, \tag{4.23b}
$$

to the kth degree. Using (4.22) to express the adjoint in terms of the fundamental, the following trace decompositions can be calculated from (4.21) and (4.23):

$$
\begin{aligned}
\mathrm{SU(N)}:&\ \mathrm{Tr}(\mathrm{i}\mathfrak{F})^6 = 2N\,\mathrm{tr}(\mathrm{i}\mathfrak{F})^6\,, \\
\mathrm{SO(N)}:&\ \mathrm{Tr}(\mathrm{i}\mathfrak{F})^6 = (N-32)\,\mathrm{tr}(\mathrm{i}\mathfrak{F})^6 + 15\,\mathrm{tr}(\mathrm{i}\mathfrak{F})^4\mathrm{tr}(\mathrm{i}\mathfrak{F})^2\,, \\
\mathrm{SP}(N):&\ \mathrm{Tr}(\mathrm{i}\mathfrak{F})^6 = (N+32)\,\mathrm{tr}(\mathrm{i}\mathfrak{F})^6 + 15\,\mathrm{tr}(\mathrm{i}\mathfrak{F})^4\mathrm{tr}(\mathrm{i}\mathfrak{F})^2\,.
\end{aligned}
\tag{4.24}
$$

We thus find that the $\mathrm{tr}\,(\mathrm{i}\mathfrak{F})^6$ term can only be factorized for G = SO(32), since precisely in this case the nontrivial sixth order Casimir does not contribute. Remarkably, the

dimension of SO(32) is precisely 496, which is necessary for the absence of the $\mathrm{tr}\,\mathfrak{R}^6$. A further possibility is to use groups which do not have a sixth order Casimir invariant like the exceptional Lie groups. Among them, $E_8 \times E_8$ has precisely the correct dimension of 496. We will focus on this theory in the following. Note that for E_8, the fundamental representation is the adjoint, and we shall use the definition $\mathrm{Tr} = 30\,\mathrm{tr}$ in this case. Let us finally remark that replacing one or both E_8's by $U(1)^{248}$ does not work, basically because the $U(1)$'s appear in the transformation of B (which is the descent of the X_4 in our factorization ansatz) but not in the anomaly polynomial [78].

After choosing $E_8 \times E_8$ as a gauge group, the anomaly polynomial (4.20) factorizes as

$$I_{12} = X_8 \cdot X_4 = \left(\frac{1}{8}\mathrm{tr}\,\mathfrak{R}^4 + \frac{1}{32}\left(\mathrm{tr}\,\mathfrak{R}^2\right)^2 - \frac{1}{8}\mathrm{tr}\,\mathfrak{R}^2\,\mathrm{tr}\,(\mathrm{i}\mathfrak{F})^2 + \frac{1}{24}\mathrm{tr}\,(\mathrm{i}\mathfrak{F})^4 - \frac{1}{8}\left(\mathrm{tr}\,(\mathrm{i}\mathfrak{F})^2\right)^2 \right)$$
$$\cdot \left(\mathrm{tr}\,\mathfrak{R}^2 - \mathrm{tr}\,(\mathrm{i}\mathfrak{F}^2) \right) , \tag{4.25}$$

where $\mathfrak{F} = \mathfrak{F}' \oplus \mathfrak{F}''$ is the direct sum of the field strengths in the two E_8's.

Next, we can calculate the 10D anomaly by using the descent equations (4.6) for (4.25). Since X_8 and X_4 are closed, we can descend via $I_{12} = \mathrm{d}I_{11}^{(0)}$. Using the Chern–Simons three-forms

$$\omega_{3,\mathrm{YM}} = \mathrm{tr}\,\mathfrak{A}\mathrm{d}\mathfrak{A} - \frac{2\mathrm{i}}{3}\mathfrak{A}^3 , \qquad \omega_{3,\mathrm{L}} = \mathrm{tr}\,\Omega\mathrm{d}\Omega + \frac{2}{3}\Omega^3 , \tag{4.26}$$

with Ω and $\mathfrak{A}$ the spin[4] and gauge connection, respectively, we find $\mathrm{tr}\,(\mathrm{i}\mathfrak{F})^2 = \mathrm{d}\omega_{3,\mathrm{YM}}$ and $\mathrm{tr}\,\mathfrak{R}^2 = \mathrm{d}\omega_{3,\mathrm{L}}$. We omit the superscripts on the Chern–Simons forms which indicate that they are the first descent of X_4 in order to not clutter up the notation. Thus the first descent is

$$I_{11}^{(0)} = \frac{1}{3}(\omega_{3,\mathrm{L}} - \omega_{3,\mathrm{YM}})X_8 + \frac{2}{3}\left(\mathrm{tr}\,\mathfrak{R}^2 - \mathrm{tr}\,(\mathrm{i}\mathfrak{F})^2\right)X_7^{(0)} + \kappa\,\mathrm{d}\left[(\omega_{3,\mathrm{L}} - \omega_{3,\mathrm{YM}})X_7^{(0)}\right] , \tag{4.27}$$

where the coefficients of the first two terms are fixed by the Wess–Zumino consistency condition (4.5) and we allowed for the addition of an exact term with some arbitrary parameter κ.

To find the second descent, we note that under local gauge and Lorentz transformations

$$\delta_\lambda\,\omega_{3,\mathrm{YM}} = \mathrm{d}(\mathrm{tr}\lambda\,\mathrm{d}\mathfrak{A}) , \qquad \delta_\varepsilon\,\omega_{3,\mathrm{L}} = \mathrm{d}(\mathrm{tr}\,\varepsilon\,\mathrm{d}\Omega) , \tag{4.28}$$

while X_8 is invariant and the variation of $X_7^{(0)}$ is exact, $\delta X_7 = \mathrm{d}X_6^{(1)}$. We thus arrive at the anomaly form

$$I_{10}^{(1)} = \left(\frac{2}{3} + \kappa\right)\left(\mathrm{tr}\,\mathfrak{R}^2 - \mathrm{tr}\,(\mathrm{i}\mathfrak{F})^2\right)X_6^{(1)} + \left(\frac{1}{3} - \kappa\right)(\mathrm{tr}\,\varepsilon\,\mathrm{d}\Omega - \mathrm{tr}\lambda\mathrm{d}\mathfrak{A})\,X_8 . \tag{4.29}$$

---

[4]We usually use the common convention in which both the Chern–Simons three-forms and the spin connection are denoted by ω. To avoid confusion, we use here Ω for the spin connection.

If we take the transformation of the Kalb–Ramond two-form B to be given by

$$\delta B = \operatorname{tr}\lambda\,\mathrm{d}\mathfrak{A} - \operatorname{tr}\varepsilon\,\mathrm{d}\Omega\,, \tag{4.30}$$

the anomaly (4.29) can be canceled by the Green–Schwarz counterterm

$$\Delta S_{\mathrm{eff}} = \int BX_8 - \left(\frac{2}{3} + \kappa\right)(\omega_{3,\mathrm{L}} - \omega_{3,\mathrm{YM}})X_7^{(0)}\,. \tag{4.31}$$

As explained in section 4.1.6, the new transformation law (4.30) leads to a modification of the associated three-form field strength H

$$H = dB + \omega_{3,\mathrm{L}} - \omega_{3,\mathrm{YM}} \tag{4.32}$$

and to a modified Bianchi identity

$$\mathrm{d}H = \operatorname{tr}\mathfrak{R}^2 - \operatorname{tr}(i\mathfrak{F})^2 \quad\Rightarrow\quad 0 = \int_S \mathrm{d}H = \int_S \operatorname{tr}\mathfrak{R}^2 - \operatorname{tr}(i\mathfrak{F})^2 \tag{4.33}$$

for all closed four-cycles S. In other words, $\operatorname{tr}\mathfrak{R}^2 - \operatorname{tr}(i\mathfrak{F})^2$ must be trivial in cohomology. This requirement can again be conveniently expressed in Chern characters, where we find

$$2[\mathrm{ch}_2(\mathfrak{F}) - \mathrm{ch}_2(TX)] = [0]\,, \tag{4.34}$$

where $\mathrm{ch}_2(TX)$ and $\mathrm{ch}_2(\mathfrak{F})$ denote the second Chern characters of the tangent bundle of the compactification manifold and of the gauge bundle, respectively. Here, we use the square brackets to indicate that the equation has to be satisfied in cohomology, i.e. up to the addition of closed forms. Having said this, we will omit them from now on for notational convenience. We would like to mention that the inclusion of $\omega_{3,\mathrm{YM}}$ has also been found in SUSY calculations [11] and string calculations [18, 79].

4.2.2 Anomalies in heterotic M-Theory

In most parts we will be using perturbative heterotic $\mathrm{E}_8 \times \mathrm{E}_8$ string theory. Nevertheless, we would like to briefly mention anomaly cancelation in heterotic M-theory as we will make some reference to it in chapter 8. The discussion will be led using the Hořava–Witten description of heterotic M-Theory [80, 81]. At low energies, the theory is obtained by compactifying 11D supergravity to 10D on the interval $S^1/\mathbb{Z}_2$. There is an E_8 theory attached to the 10D orbifold fixed planes on each end of the interval. This can then be compactified further on some compact manifold X_d, giving rise to lower dimensional heterotic theories on $S^1/\mathbb{Z}_2 \times X_d \times \mathbb{R}^{1,9-d}$.

We can now include new objects called Neveu–Schwarz five (NS5) branes and investigate the consequences for anomaly cancelation in the presence of these objects [82–84]. If we compactify to $\mathcal{N} = 1$ SUGRA in four dimensions on a Calabi–Yau threefold X, we wrap these NS5 branes around the 4D Minkowski spacetime to preserve Lorentz invariance

times a curve $\mathcal{C}_2$ in the internal manifold X. The NS5 branes appear now as magnetic sources in (4.33). They are topological invariants and given by the intersection number of $\mathcal{C}_2$ with a four-cycle S. In order to preserve $\mathcal{N} = 1$ SUSY in 4D, one must only include NS5 branes and no anti-NS5 branes [85], which means that the intersection of $\mathcal{C}_2$ and S should be positive and thus the curve $\mathcal{C}_2$ has to be effective. Furthermore, it is found that NS5 branes and Yang–Mills instantons contribute with the same sign to the irreducible part of the gravitational anomaly [86]. Thus (4.33) is modified to

$$\int_S \operatorname{tr} \mathfrak{R}^2 = \int_S \operatorname{tr} (\mathrm{i}\mathfrak{F})^2 + \sum_i \int_S J_i(\mathcal{C}_{2,i}) \,, \tag{4.35}$$

where we sum over the contribution of the NS5 brane sources J_i wrapped around the effective curves $\mathcal{C}_{2,i}$. Note that, also with the inclusion of NS5 branes, the contribution of the Yang–Mills instantons are bounded from above by the instanton number of the compactification space, which still puts strong constraints on possible choices for the gauge bundle. However, on the worldsheet of the NS5 brane an enhanced gauge symmetry can arise, allowing the presence of gauge groups with rank larger than 16 in the heterotic string as well [87].

4.3 Anomalies in 4D heterotic string theory

For four-dimensional theories, the only way in which the anomaly polynomial can factorize is $I_6 = \sum_a X_2^a X_4^a$, and can thus be canceled by two-forms or scalars (axions). Since in four dimensions, these are dual to each other (in the sense that their field strengths satisfy $*H_3 = H_1$), we can phrase the following discussion in terms of scalars only. The two-form X_2 can only be a field strength of a U(1) gauge group factor, $X_2 = \mathrm{d}A_1$. If such a factor appears, we call the U(1) anomalous. Hence reducible anomalies in four dimensions involve the anomalous U(1) and either two more U(1)'s or a square of a non-Abelian group (including gravity).

If the axion C_0 cancels the anomaly, its field strength (4.17) becomes

$$H_1 = \mathrm{d}C_0 + \xi A_1 \,, \tag{4.36}$$

and the kinetic term for ω_0 leads to a mass term $\sim \xi^2 \, |A_1|^2$. Thus, an anomalous U(1) gets a Stückelberg mass from the Green–Schwarz axion.

For four-dimensional heterotic models, we investigate two cases: Compactifications on orbifolds and on smooth Calabi–Yaus with vector bundles, including orbifold blowups. In the first case, B gives rise to exactly one two-form b_2 in four dimensions, and hence I_6 factorizes into a single product, $I_6 = X_4 X_2$. Furthermore, X_4 is simply given by the second line of (4.25), restricted to four-dimensional forms and the unbroken gauge group.

Upon dualizing b_2 to an axion a, the anomaly is canceled by the coupling $\int a X_4$, so in particular a couples universally to all gauge groups. Note that this coupling arises

in the dualization as a consequence of the gauge transformation properties of b_2, so it is actually independent of the existence of an anomalous U(1) in 4D. This rather manifests itself as a shift of a under the anomalous symmetry. Furthermore, if one E_8 is unbroken, there will be no matter under this E_8 and consequently no mixed anomaly to cancel. Hence the coupling $\int a\, X_4$ cannot produce a gauge variation, and there is no anomalous U(1) in this case.

In the second case, there will generically be many additional axions β_r arising from the reduction of B along internal cohomology two-forms E_r. Their transformation follows from (4.30) by expanding the internal flux and comparing the terms proportional to E_r. Hence these axions will not couple universally to all gauge groups (otherwise one could redefine them by a term proportional to the universal axion). So in this setup, there can be up to 16 anomalous U(1)'s, at most one of which couples universally. Note further that if an axion shifts under a U(1), the gauge boson is massive by its field strength (4.36) even if the U(1) is non-anomalous.

In particular, for a compactification on a Calabi–Yau X with line bundles, the anomaly polynomial can be easily evaluated: Split the gauge fields into internal background flux and four-dimensional fluctuations, $\mathfrak{F} = \mathcal{F} + F$, $\mathfrak{R} = \mathcal{R} + R$. Here we assume that the four-dimensional backgrounds vanish and that there are no massless internal fluctuations. The backgrounds satisfy the Bianchi identity

$$\mathrm{d}H = \mathrm{tr}\mathcal{R}^2 - \mathrm{tr}\,(\mathrm{i}\mathcal{F})^2 = 0 \tag{4.37}$$

Then one can straightforwardly insert this split into the ten-dimensional anomaly polynomial[5] (4.25) and keep the terms cubic in the backgrounds to get

$$I_6 = \frac{1}{(2\pi)^6} \int_X \left[\frac{1}{6}\mathrm{tr}(\mathrm{i}\mathcal{F}'\,\mathrm{i}F')^2 + \frac{1}{4}\left(\mathrm{tr}(\mathrm{i}\mathcal{F}')^2 - \frac{1}{2}\mathrm{tr}\mathcal{R}^2 \right)\mathrm{tr}(\mathrm{i}F')^2 \right.$$
$$\left. - \frac{1}{8}\left(\mathrm{tr}(\mathrm{i}\mathcal{F}')^2 - \frac{5}{12}\mathrm{tr}\mathcal{R}^2 \right)\mathrm{tr}R^2 \right]\mathrm{tr}(\mathrm{i}\mathcal{F}'\,\mathrm{i}F') + (F',\mathcal{F}' \leftrightarrow F'',\mathcal{F}'') \tag{4.38}$$

The three terms per E_8 in (4.38) contribute to the various anomalies as follows:

- $\int_X \mathrm{tr}(\mathrm{i}\mathcal{F}'\,\mathrm{i}F')^2 \cdot \mathrm{tr}(\mathrm{i}\mathcal{F}'\,\mathrm{i}F')$ gives rise to Abelian anomalies only, since $\mathrm{tr}(\mathrm{i}\mathcal{F}'\,\mathrm{i}F')$ vanishes for non-Abelian gauge groups.

- $\int_X \left(\mathrm{tr}(\mathrm{i}\mathcal{F}')^2 - \frac{1}{2}\mathrm{tr}\mathcal{R}^2 \right)\mathrm{tr}(\mathrm{i}F')^2 \cdot \mathrm{tr}(\mathrm{i}\mathcal{F}'\,\mathrm{i}F')$ gives rise to Abelian and mixed Abelian–non-Abelian anomalies, since $\mathrm{tr}(\mathrm{i}\mathcal{F}'\,\mathrm{i}F')$ projects again onto the Abelian part and $\mathrm{tr}(\mathrm{i}F')^2$ can be non-vanishing for both Abelian and non-Abelian gauge group factors.

- $\int_X \left(\mathrm{tr}(\mathrm{i}\mathcal{F}')^2 - \frac{5}{12}\mathrm{tr}\mathcal{R}^2 \right)\mathrm{tr}R^2 \cdot \mathrm{tr}(\mathrm{i}\mathcal{F}'\,\mathrm{i}F')$ gives rise to mixed Abelian–gravitational anomalies.

---

[5]Since there are no purely gravitational anomalies in four dimensions, one can restrict to the gaugino contributions, since the gravitino and dilatino anomalies only involve the Riemann tensor.

So we see that there is some partial anomaly universality: The non-Abelian anomalies coming out of the first E_8 are captured by one anomalous $U(1)$ factor with universal coefficients, and similar for the second E_8. Furthermore, if one E_8 is unbroken, i.e. $\mathcal{F}'' = 0$, the Bianchi identity (4.37) implies that the non-Abelian and gravitational anomalies are captured by the same $U(1)$, and their coefficients are proportional to each other.

Chapter 5

. . . .

MATCHING ORBIFOLD AND CALABI–YAU MODELS

In sections 2.3 and 2.4 we have explained how to describe heterotic string theory on smooth Calabi–Yau and on singular orbifold compactification spaces, respectively. Both approaches have their advantages and drawbacks for describing string theory and for studying heterotic model building, as we shall discuss now. For concreteness, we focus again on heterotic $E_8 \times E_8$ theory, but the results can be applied to heterotic $SO(32)$ in the same way.

Orbifolds Orbifolds are probably the simpler approach. The geometry is much less involved, as they are flat everywhere except for the orbifold fixed points, where curvature singularities occur. Yet, they capture many essential features of string model building and allow for studying many phenomenologically appealing models. Due to the simple description, all necessary quantities (like for example the metric) are known and exact free CFT calculations can in principle be used to calculate all desired quantities like Yukawa couplings, effects that are non-perturbative in α', remnant symmetries, etc. Unfortunately, there are also drawbacks:

- Generically, one $U(1)$ symmetry is Green–Schwarz anomalous.

- There are much more massless states (exotics) than just the field content of the MSSM.

- The rank of the gauge group[1] is much larger that just the MSSM gauge group $SU(3) \times SU(2) \times U(1)_Y$.

All semi-realistic orbifold models that have been constructed up to now suffer from these problems. Let us discuss how to overcome them, starting with the first one. The more precise statement would be that there exists a basis of $U(1)$ generators such

---

[1] In this work we are focusing on orbifolds with shift embeddings, where the rank of the primordial $E_8 \times E_8$ gauge group is not reduced.

that at most one $U(1)$ is anomalous. This anomaly is canceled by the Green–Schwarz mechanism discussed in section 4.1.6. Since all possible anomalies are canceled by one axion a, usually called the universal axion, the axionic couplings all have to be related, i.e. they fulfill [49, 88]

$$\frac{1}{6|T_i|^2}\operatorname{tr}Q_i^3 = \frac{1}{2|T_j|^2}\operatorname{tr}Q_j^2 Q_i = \operatorname{tr}\ell Q_i = \frac{1}{24}\operatorname{tr}Q_i\,, \quad i, j = 1, \ldots, \#U(1)\text{'s} \qquad (5.1)$$

where the four terms come from the pure Abelian, mixed Abelian, mixed Abelian–non-Abelian and mixed Abelian–gravitational anomalies respectively. $T_i = a^I H_I$ is the generator of the ith $U(1)$ embedded in $E_8 \times E_8$ and ℓ is the Dynkin index of the non-Abelian gauge group representation. We define $|T|^2$ as $|T|^2 = \sum_{I=1}^{16} a_I^2$. The trace is running over all massless states in the theory. There exists a basis in which (5.1) is non-vanishing for only one $U(1)$. However, in this case a constant Fayet–Iliopoulos D term is induced which is proportional to $\operatorname{tr}Q$. Since we want to preserve $\mathcal{N} = 1$ SUSY in our models, this means that this induced FI term has to be canceled by giving VEVs to orbifold states such that overall D flatness is ensured. Of course these VEVs also have side-effects. One has to choose them carefully to ensure that F terms are not generated. However, since the superpotential can in principle be computed from the underlying CFT, this can be checked for.

Note that introducing VEVs for some of the orbifold fields, which is necessitated by the first drawback listed above, also helps in overcoming the other problems. By choosing the VEVs appropriately, one can decouple exotic states by making them heavy in a Higgs-like mechanism and at the same time reduce the rank of the remnant gauge group. In this way, many phenomenologically semi-realistic orbifold models have been constructed [40, 89, 90]. However, the VEVs of the twisted orbifold fields backreact on the geometry and cause a resolution of the orbifold singularity, leading to a Calabi–Yau in which the singularity has been smoothed out. Those models are referred to as blowups.

Calabi–Yau models   The advantage of the Calabi–Yau models is that they appear to correspond to the more generic case in the sense that orbifold models require fixing (some of) the complex structure parameters to a specific value and freezing the Kähler moduli of the fixed points. In a general Calabi–Yau construction, the value of the moduli are a priori not fixed. As a matter of fact, stabilization of all moduli in general heterotic models is an open problem. The drawback of the Calabi–Yau models is that many quantities like e.g. the metric are unknown. Thus there is no CFT description of these models and one has to resort to the heterotic supergravity approximation and use topological quantities like intersection numbers in order to calculate interesting properties such as the massless matter spectrum or Yukawa couplings. Concerning the drawbacks of the orbifold mentioned above, let us note that in Calabi–Yau models with line bundles there are generically many Green–Schwarz anomalous $U(1)$'s (in fact the number is equal to the rank of the gauge bundle) and also many exotics. Thus, finding a semi-realistic vacuum VEV configuration in orbifolds compares to finding a semi-realistic gauge sector in Calabi–Yaus. Up to now, there is no fully systematic way of constructing such models and they are found purely by trial and error.
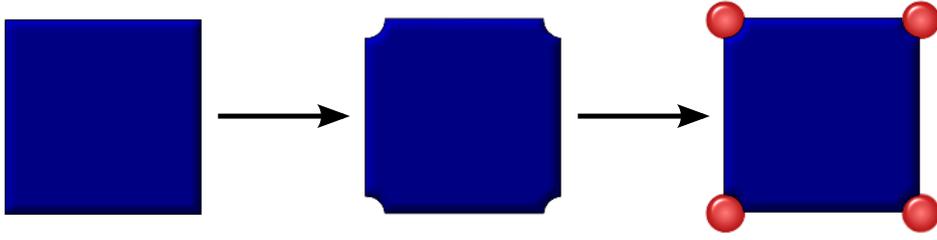
Figure 5.1: Schematic description of the resolution procedure: the singular points are cut out and replaced by smooth compact hypersurfaces.

For the reasons outlined above, it is desirable to be able to do calculations in both regimes since neither captures all physics by itself. This requires matching the two theories, which will be discussed in the remainder of this chapter. In the first section we discuss the general idea of the matching, which is done on the level of the compactification geometry, the gauge sector, the spectrum, the consistency conditions, and the anomalies. In section 5.2, we apply this general discussion to the concrete example of the $\mathbb{Z}_7$ orbifold where we match the entire massless spectrum and the anomalies. In section 5.3, we provide an example how flop transitions can change the chiral massless spectrum, which can lead to complications in the matching procedure. Since there are no flops in the $\mathbb{Z}_7$ resolution, we carry out the analysis for the $T^6/(\mathbb{Z}_2 \times \mathbb{Z}_2)$ orbifold.

5.1 Matching the theories

Matching the geometry

As explained in section 2.4, the orbifold geometry is specified in terms of an orbifold twist vector together with an underlying compatible torus lattice. On the Calabi–Yau, the geometry is described in terms of divisors and their intersection properties. In order to connect the two compactification spaces, we find a crepant resolution of the orbifold singularities. For the orbifolds under investigation, such a resolution always exists. The tools necessary to describe the resolution procedure were introduced in chapter 3. The idea behind the resolution is to cut out the orbifold singularity and replace it by a smooth hypersurface, the so-called exceptional or blowup divisor, as illustrated pictorially in figure 5.1. The orbifold limit is reproduced by blowing down the exceptional divisor again such that the singularity reoccurs. As outlined in section 3.3.4, this corresponds in the GLSM to choosing the Kähler parameters b_i controlling the size of the blowup divisor to be $b_i \ll 0$.

Matching the gauge flux

The orbifold gauge sector is specified in terms of an orbifold shift vector and Wilson lines. The local shift at each orbifold fixed point is given as a sum of orbifold shifts and Wilson lines, which corresponds to the background flux at this fixed point, where

it has delta-function support. Furthermore, the flux is different in different twisted sectors, and it varies between fixed points of the same twisted sector if Wilson lines are switched on.

The gauge sector on a CY is specified in terms of a gauge bundle which describes the embedding of the gauge flux into the primordial $E_8 \times E_8$ along each divisor. From what we have said above, the orbifold regime is reproduced by shrinking the exceptional divisors, which we denote collectively by E_r in the following. By wrapping the gauge flux on these divisors only, it is ensured that the flux becomes concentrated at the orbifold fixed points in blowdown. In particular, there should be no flux on the torus underlying the orbifold construction, which means that the gauge flux should not wrap the inherited divisors R_i.

This motivates the expansion of the CY background gauge flux $\mathcal{F}$ in terms of the exceptional divisors and of the local orbifold shifts V_g, which are a combination of orbifold shift vectors V_{sh}, Wilson lines W_i, and $E_8 \times E_8$ lattice vectors, see (2.38):

$$\mathcal{F} = E_r V_I^r H^I \,. \tag{5.2}$$

The V_I^r are the so-called line bundle vectors and the H^I are the Cartan generators of $E_8 \times E_8$. We take the Cartan generators only since we are interested in cases where the gauge bundle is a sum of line bundles. The primary advantage of this is that it avoids many complications present for non-Abelian bundles arising from bundle stability. Note that the matrix V_I^r can be read in two ways, depending on whether it is preferable to think of it as an expansion in the exceptional divisors or in the Cartan generators: reading it row-wise (i.e. as an expansion in the E_r), it specifies the gauge flux at each divisor E_r. This will be advantageous when comparing the CY and the orbifold input data, since on the orbifold, it is more natural to think of the flux as different shifts in the $E_8 \times E_8$ lattice at the various fixed points. Reading it column-wise (i.e. as an expansion in the H^I), it specifies how the flux embeds into the 16 Cartan generators of $E_8 \times E_8$ across the various fixed points. This makes the connection to the line bundles much clearer, since each H^I corresponds to a U(1) and thus each column to (the first Chern class of) one line bundle, where the entries describe the transformation properties of the bundle in the chosen divisor basis. We will use this point of view in the GLSM, where the GLSM charges of the fields that specify the gauge bundle correspond to the first Chern class of the line bundle. Note that the local orbifold shifts are fractional and hence the entries of V_I^r are fractional as well. In the GLSM, we normalize all U(1) charges such that they are integer. Of course this choice does not influence the physical results.

Despite these similarities, the orbifold flux is different from the flux on the Calabi–Yau. The former is discrete and thus does not reduce the rank of the gauge group or induce masses for Abelian gauge factors. The latter breaks the $E_8 \times E_8$ gauge group to the commutant with the structure group of the gauge bundle and thus reduces the rank for non-Abelian bundles. For Abelian bundles, the $E_8 \times E_8$ is branched into the corresponding U(1) factors times the remnant gauge group, and the U(1)'s become generically Green–Schwarz massive.

Matching the blowup modes

The key to reconciling this difference (and others to be discussed next) lies in the identification of twisted orbifold fields that get a VEV on the orbifold and blowup modes of the CY via a field redefinition. As explained before, orbifold fields can be identified via their shifted momenta P_{sh}^I, which are a combination of the local orbifold shift and $\mathrm{E}_8 \times \mathrm{E}_8$ lattice vectors. We choose the shifted momenta of the blowup modes to be line bundle vector V_r^I. Since the VEVs of the orbifold twisted states backreact on the geometry, and the sizes of the VEVs characterize the departure from the orbifold point, we relate them to the Kähler parameters b_r that measure the volume of the blowup cycles E_r. The real Kähler parameters b_r form together with the axions β_r a complex scalar $t_r = b_r + \mathrm{i}\beta_r$, which is the lowest component of a chiral $\mathcal{N} = 1$ multiplet T_r in 4D. The complex combination of the CY Kähler parameters and axions appears in the complexified Kähler form $\mathcal{J}$,

$$\mathcal{J} = J + \mathrm{i}B \,, \quad J = \sum_i a_i R_i - \sum_r b_r E_r \,, \quad B = \sum_i \alpha_i R_i - \sum_r \beta_r E_r \,. \tag{5.3}$$

Let us explain the occurring quantities. We first note that both the Kähler form J and the Kalb–Ramond two-form B are $(1,1)$-forms. Hence they can be expanded in a basis of $(1,1)$-forms, which we take to be the duals of the divisor basis given by the inherited divisors R_i and the exceptional blowup divisors E_r. The relative sign of the Kähler parameters in J has been chosen such that the Kähler cone of the blowup CY is given by $a_i \gg b_r > 0$, as was already discussed in the examples in chapter 3. Being axions, the β_r transform with a shift proportional to the line bundle vectors V_I^r under an Abelian gauge transformation with gauge parameter λ_I, while the α_i are chosen to transform trivially,

$$\alpha_i \to \alpha_i \,, \qquad \beta_r \to \beta_r + \lambda_I V_r^I \,. \tag{5.4}$$

Using this, the map between the VEV of orbifold state $\Phi_r^{\mathrm{BU\text{-}Mode}}$ generating the blowup and the complexified Kähler modulus t_r reads [39, 91]

$$\langle \Phi_r^{\mathrm{BU\text{-}Mode}} \rangle = e^{t_r} = e^{b_r + \mathrm{i}\beta_r} \,. \tag{5.5}$$

As we will discuss in the following using the example of the $\mathbb{Z}_7$ orbifold [61], this leads to the same gauge group in the smooth CY model with line bundle flux and in the orbifold model with VEVed twisted states: The U(1) symmetries which are in the structure group of the bundle appear to have an anomalous 4D spectrum. The anomaly is canceled via a Green–Schwarz mechanism involving the axions β_r, which gives a Stückelberg mass to the U(1) gauge bosons. From the orbifold point of view, the field that gets a VEV breaks the gauge group it is charged under via the Higgs mechanism. While this works out perfectly in all fine prints, the behavior of the Kähler modulus seems to be incorrect. The volume of the exceptional divisors is defined as $\mathrm{vol}(E_r) = \frac{1}{2} \int_X J^2 E_r$, which is proportional to b_r for compact exceptional divisors in our divisor basis. In particular, the volumes of all exceptional divisors vanish in the limit $b_r \to 0$. Indeed, we know that $b_r = 0$ marks a boundary of the Kähler cone. However,

the VEV of the blowup mode (5.5) vanishes in the limit $b_r \to -\infty$. This looks startling, but was explained in [92]. There it is shown that the apparent mismatch is resolved by changing the algebraic measure used to calculate the divisor volume via (3.27) to the sigma model measure, where the volume of the exceptional divisor goes to zero for $b_r \to 0$. In any case, the SUGRA description is expected to break down as soon as the b_r gets of the order of the string scale.

Matching the consistency conditions

Neither the gauge flux on the orbifold nor the gauge flux on the Calabi–Yau can be chosen at will; both have to satisfy stringent consistency requirement. Let us discuss them in the following and point out the correspondence between the conditions in the different regimes.

BIs and modular invariances   On the orbifold, there are conditions linking the orbifold twist, which is responsible for the orbifold geometry, with the orbifold shifts and lattice vectors, which are responsible for the orbifold gauge sector. These conditions are the modular invariance conditions (2.40) and assure anomaly freedom of the orbifold spectrum via the Green–Schwarz mechanism. On the Calabi–Yau, we have the Bianchi identities (4.33) that relate the curvature and the field strengths, or equivalently the second Chern characters of the gauge and the tangent bundle. As discussed in chapter 4, satisfying the Bianchi identities ensures that the 4D anomalies are canceled à la Green–Schwarz. Hence, they seem to be the counterpart of the modular invariance conditions. Indeed, we will uncover their relation in chapter 8 from the GLSM point of view.

Flux quantization   The shift vectors and Wilson lines on the orbifold have to be properly quantized, as described in (2.39). Likewise, the internal gauge flux $\mathcal{F}$ should be chosen such that it is integral when integrated over any closed curve. These conditions are linked, since according to (5.2), the gauge flux is expanded in terms of orbifold shifts and Wilson lines. In [60], it was shown that the flux quantization condition on the orbifold and on the CY are equivalent for the $\mathbb{Z}_2 \times \mathbb{Z}_2$ orbifold.

D flatness and DUY   The VEVs of the orbifold states have to be chosen such that the field space remains D flat. A convenient way of finding D flat directions is outlined in [93, 94]. One proceeds by defining so-called holomorphic invariant monomials (HIMs) which parameterize D flat directions. They are defined to be gauge invariant monomials of the form $\prod_r \Phi_r^{n_r}$ with positive integers n_i. The HIM is gauge invariant if $\sum_r Q_r n_r = 0$ where Q_r is the charge of the orbifold field Φ_r. To make contact with the D flatness condition, we parameterize $|\Phi_r|^2 = n_r |\psi|^2$ and obtain for D flatness

$$D_I = |\psi|^2 \sum_r Q_I^r n_r \overset{!}{=} 0 \,. \tag{5.6}$$

This shows that the n_r have to be in the kernel of the charge matrix Q_r^I, which is equivalent to the HIM being gauge invariant. Thus a field Φ_r can take a VEV if it appears in the ideal generated from the monomial basis of the HIMs.

On the CY, we have the DUY equations at zero slope (2.30),

$$\int_X J^2 \mathcal{F} = \sum_r \int_X J^2 E_r V_I^r H^I = 2 \sum_r \text{vol}(E_r) V_I^r H^I \overset{!}{=} 0 \,. \tag{5.7}$$

These are 16 equations for the 16 Cartan generators of $E_8 \times E_8$. The bundle V corresponding to $\mathcal{F}$ is automatically stable since it is a sum of line bundles and hence there are no destabilizing subsheaves. Since the volume of all divisors is positive, we see that the zero slope DUY equation on the smooth CY is equivalent to solving the D flatness constraint on the orbifold: the V_I^r are set equal to the shifted orbifold momenta which specify the Cartan charges of the orbifold blowup modes that get a VEV, $V_I^r = Q_I^r$, and hence the equations (5.6) and (5.7) are equivalent with $n_r \sim \text{vol}(E_r)$. Note that while the equations are simple linear equations in the volume, they can be more complicated functions of the Kähler parameters, which is due to the fact that the exceptional divisors intersect other exceptional divisors as well as inherited divisors. However, since we do not discuss the issue of moduli stabilization here, we content ourselves with showing that a solution exists. Hence it is enough to solve the linear equations in the volumes deep inside the CY Kähler cone. Existence of a solution can be checked easily and rather efficiently using Gröbner basis techniques.

F flatness and DUY   The final condition we have to impose on the orbifold states that get a VEV is F flatness. This is more complicated since it involves knowledge of the entire superpotential. While the superpotential can in principle be calculated to all orders on the orbifold using CFT techniques, this becomes increasingly difficult with growing number of fields involved in the couplings. The counterpart on the CY is also somewhat elusive. The condition that remains to be satisfied is the Hermitian Yang–Mills equation (2.29) which imposes that the gauge flux $\mathcal{F}$ is a holomorphic $(1, 1)$-form. However, this is satisfied by construction since we expanded $\mathcal{F}$ in the E_r, which are holomorphic $(1, 1)$-forms. As we shall see in the next part when matching the massless spectra of the two theories, the supergravity approximation on the smooth CY side does not really account for couplings that are non-perturbative in α' (i.e. couplings at different fixed points which are exponentially suppressed by $e^{-a/\alpha'}$ where a is the Kähler parameter that measures the separation of the fixed points) in the orbifold superpotential. In fact exceptional divisors from different fixed points do not intersect each other at all. Thus F flatness could be spoiled in the heterotic SUGRA approximation by VEVs of multiple fields that are at the same fixed point. But in the line bundle blowup, always only one field per fixed point gets a VEV. In this sense, F flatness is satisfied automatically. As a final remark, we note that exceptional divisors that arise from resolving fixed tori might intersect other fixed tori or fixed point resolution divisors. In these cases, it could be expected that F flatness constrains the choices of which fields can get a VEV. Nonetheless, the exceptional resolution divisors are $(1, 1)$-forms as well and thus $\mathcal{F}$ will be a $(1, 1)$-form. However, in the case where exceptional divisors intersect, the Bianchi identities put constraints on the V_I^r. Whether these constraints are equivalent to F flatness on the orbifold we do not know.

Matching the massless matter

After the discussion on how to match the gauge sector, let us turn to the matching of the matter spectra. The massless matter spectrum on orbifolds can be obtained by finding all shifted momenta that satisfy the mass condition (2.42) with $M = 0$ and subsequently restricting to those states which survive the orbifold projections. The massless spectrum in blowup can be calculated by branching the adjoint with respect to the gauge bundle and calculating the corresponding bundle-valued cohomology groups. However, this calculation is rather involved and grows exponentially in computation complexity with the size of the Stanley–Reissner ideal in toric constructions. Since typical orbifold models have $h^{1,1} = O(40)$ and thus a big Stanley–Reissner ideal, this by far exceeds the calculational power of modern PCs. We thus have to resort to the Hirzebruch–Riemann–Roch index theorem (2.18) which, however, only contains information about the chiral spectrum. As we shall see, the fact that we have an underlying orbifold theory to which the blowup model can be matched, together with a local version of the index theorems, nevertheless allows to infer the exact massless spectrum. Thus the match of heterotic orbifold models with their blowup Calabi–Yaus offers a window for studying semi-realistic models for geometries with large $h^{1,1}$ which would be inaccessible otherwise.

Before going on, let us briefly explain how we calculate the spectrum using the HRR theorem. For each E_8, we start with the 240 root vectors $\lambda_a^I \in E_8$, $I = 1, \ldots, 8$, $a = 1, \ldots, 240$, since both the 4D adjoints and the 4D chiral matter arise from the 10D vector multiplet. The adjoints of the 4D gauge groups are given by those root vectors which are orthogonal to one of the line bundle flux vectors, $\lambda_a^I V_I^r = 0$ for all r. In this way we obtain the generators of the adjoint of the remaining gauge group G, which is the non-Abelian part of the commutant of the structure group H with $E_8 \times E_8$ (the Abelian part is generically Green–Schwarz massive). For calculating the chiral spectrum, we take those $E_8 \times E_8$ roots that are not perpendicular to $\mathcal{F}$ and classify them according to the representations they form under the remaining gauge group G. For each highest weight, we then evaluate its multiplicity (i.e. the number of 4D zero modes) via the HRR theorem (2.20) with $\mathcal{V} = V_I^r \lambda^I$. In this sense, the blowup spectrum is given in terms of the $E_8 \times E_8$ root vectors.

Thus when matching the massless matter spectrum on the orbifold with the blowup spectrum, we encounter several differences:

- On the orbifold, states are characterized by their shifted momenta which has fractional entries while in blowup the states are characterized by $E_8 \times E_8$ lattice vectors.

- On the orbifold, states can be charged under both E_8's while in blowup each state is charged under one E_8 only.

- On the orbifold, there is at most one anomalous U(1) while in blowup there are generically as many as the rank of the gauge bundle which we take to be a sum of line bundles.

Again, these differences can be overcome by connecting orbifold states $\Phi_{r,i}^{\mathrm{Orb}}$ to states Φ_i^{CY} in blowup via field redefinitions [39, 91]

$$\Phi_{r,i}^{\mathrm{Orb}} = e^{f^i(t_r)}\Phi_i^{\mathrm{CY}}\,. \tag{5.8}$$

Here, r labels the fixed points and i enumerates the number of fields at a particular fixed point r. The function $f(t_r)$ is linear in the complexified Kähler moduli $t_r = b_r + \mathrm{i}\beta_r$. Since the β_r shift under gauge transformations, the charges on the orbifold equal the charges in blowup plus the sum of the charges of the redefined blowup modes as specified by $f(t_r)$. In the simplest cases when $f(b_r) = b_r + \mathrm{i}\beta_r$, this means that the charges of the orbifold fields are redefined with the charges of the blowup modes at each fixed point r. The function $f(t_r)$ has to be chosen such that the redefined charges in blowup correspond to the $\mathrm{E}_8 \times \mathrm{E}_8$ root vectors. In many cases, this choice is unique. We will provide an example and explain how to deal with non-unique field redefinition possibilities in the example of the $\mathbb{Z}_7$ orbifold. A further complication that can arise is that the charges are such that more than one orbifold state is redefined to the same $\mathrm{E}_8 \times \mathrm{E}_8$ lattice vector. In this case, evaluating the HRR gives the number of orbifold states that are redefined to the same $\mathrm{E}_8 \times \mathrm{E}_8$ vector. However, the HRR only gives information about the net number of chiral states. Hence, if two orbifold states of opposite chirality are redefined to the same $\mathrm{E}_8 \times \mathrm{E}_8$ vector, their contribution to the HRR multiplicity cancels out and the states are not seen. Thus in particular a net multiplicity of zero can either mean that no orbifold state is redefined to this particular $\mathrm{E}_8 \times \mathrm{E}_8$ root vector in blowup or that orbifold states of different chiralities are redefined to this $\mathrm{E}_8 \times \mathrm{E}_8$ vector. Again, we shall see this explicitly in an example. Note that by knowing how each orbifold state is redefined, we can compare with the HRR multiplicity and thus find the states of both chiralities even though we cannot calculate the dimensions of the cohomology groups separately. This is a nice example where the connection to the orbifold allows for carrying out a computation which is too costly on the CY.

Generically, some of the orbifold states become massive in blowup via a Higgs mechanism involving the blowup modes. In particular a trilinear coupling in the orbifold superpotential of the form $\Phi_r^{\mathrm{BU\text{-}Mode}}\Phi_{r,i}^{\mathrm{Orb}}\Phi_{r,j}^{\mathrm{Orb}}$ lifts a linear combination of $\Phi_{r,i}^{\mathrm{Orb}}$ and $\Phi_{r,j}^{\mathrm{Orb}}$. These states will be missing in the massless spectrum in blowup. However, as explained before, the blowup is only sensitive to perturbative effects and thus non-perturbative trilinear couplings which involve states at different fixed points remain in the massless spectrum in blowup and are counted by the HRR index theorem even though they have a (highly suppressed) instantonic mass from the orbifold perspective. A further intriguing result is that the massless matter spectrum can jump between different triangulations in blowup. Such a behavior is to be expected: as explained in section 3.2.3, a flop transition corresponds to a change of the Kähler cone, which means that the SR ideal and the intersection numbers are changed as well. But the spectrum calculation depends on these geometric properties (in the case of the HRR theorem, the dependence on the intersection numbers can be seen to come in from evaluating the integral, and in the case of vector bundle cohomology, the change can be seen to come in from the SR ideal which is used to calculate the Čech cohomology). Using the

field redefinitions, this behavior is beautifully reproduced by their dependence on the Kähler parameters: if the VEV of the blowup mode is large in one triangulation, the corresponding orbifold state is seen as massive. If it is small after the geometric flop transition, the mass term gets exponentially suppressed and the state appears in the massless blowup spectrum. Since in the $\mathbb{Z}_7$ this effect cannot be seen since there are no flop transitions in the geometric regime of the blowup, we illustrate this effect in section 5.3 using the $\mathbb{Z}_2 \times \mathbb{Z}_2$ orbifold [60], which allows for flop transitions in abundance.

Matching the anomalies

Matching the massless matter spectrum deals with the Kähler parameters and hence with the real part of the blowup modes. Matching the anomalies, in contrast, deals with the axions and hence the imaginary part or the phase of the blowup modes. We want to match the 4D anomaly on the orbifold with VEVs and field redefinitions on the one hand to the blowup on the other hand. For this we make the ansatz [91, 95]

$$I_{\text{Orb}}^{\text{uni}} + I_{\text{Orb}}^{\text{red}} = I_{\text{CY}}^{\text{uni}} + I_{\text{CY}}^{\text{non}} . \tag{5.9}$$

Here, $I_{\text{Orb}}^{\text{uni}}$ is the 4D orbifold anomaly polynomial which contains (at most) one anomalous $U(1)$ factor. With $I_{\text{Orb}}^{\text{red}}$, we take into account that we redefined the $U(1)$ charges in blowup by subtracting the charges of the blowup modes and that the VEVs of the blowup modes have changed the massless spectrum by Higgsing some states. On the CY side, we have the $I_{\text{CY}}^{\text{uni}}$ which accounts for the anomaly canceling contribution of the universal axion b_2. Finally, $I_{\text{CY}}^{\text{non}}$ is the contribution of the non-universal axions β_r coming from the phases of the blowup modes. Since they come from the redefinitions in (5.8), their contribution to the anomaly cancelation should correspond to the contribution of the redefinition part $I_{\text{Orb}}^{\text{red}}$ on the orbifold. As we shall see now in the example of the $\mathbb{Z}_7$ orbifold, this is indeed the case.

5.2 Example: Matching the $\mathbb{Z}_7$ orbifold to its blowup model

Let us illustrate the matching techniques outlined above for the case of the $\mathbb{Z}_7$ orbifold. The model is very well-suited for studying the match between the orbifold and the blowup regime. The reason is that there are no ambiguities that could lead to problems when matching the two theories. The possible ambiguities that could and indeed do occur for other (non-prime) orbifolds are the presence of discrete torsion on the orbifold side and the choice of the triangulation on the blowup side, which we discuss now in turn. See [96] for a discussion of the match in a geometry where these subtleties need to be partially taken into account.

## Possible ambiguities in the matching procedure

Let us start with the ambiguity due to discrete torsion on the orbifold [97, 98], which can change the orbifold matter content. In [47], discrete torsion phases were related to the addition of $E_8 \times E_8$ lattice vectors to the orbifold shift vector and Wilson lines. In this way, discrete torsion modifies the orbifold projection condition while leaving the shifted momenta P_{sh} invariant. This means that the set of states fulfilling the orbifold mass conditions (2.42) is not changed. The whole change of the spectrum is attributed to the orbifold projection conditions. However, when choosing the line bundle vectors on the blowup side, there is no known obstruction like the orbifold projection conditions. Hence it is in principle possible to choose bundle vectors that correspond to orbifold states that are projected out. Thus it could be that such blowup models can be matched to orbifold models with discrete torsion where the respective state is not projected out. However, the precise correspondence of discrete torsion on the blowup side remains elusive.

Next, we want to turn to flop transitions. Recall that flop transitions correspond to different choices of the SR ideal. In the GLSM, the SR ideal is obtained by calculating the possible solutions to the D term constraints. Whether there exist solutions or not depends on the relative size of the GLSM FI terms b_r, which in turn are linked to the Kähler parameters b_r in blowup, as explained in section 3.2.3 (this is why we use the same name for both objects, although there are again issues concerning the different choices of measures for the volumes). But we know that the size of the Kähler parameters b_r is given by the VEV of the blowup mode. However, in the orbifold limit all these VEVs go to zero and their information on the relative size seems to be not well-defined (the orbifold point is at the tip of the Kähler cone where all triangulations meet). However, the spectrum calculation strongly depends on the SR ideal. In other words, the massless blowup spectrum can change across the various triangulations [60], as further explained in section 5.3. On the blowup side, the bundle vectors are related to the (relative size of the) Kähler parameters via the DUY equations (2.30). These, in turn, correspond to the D flatness constraints on the orbifold side. Hence the different triangulations correspond to different choices of D flat directions. The jump in the spectrum between the different triangulations is accounted for by checking which orbifold states become light/massive by matching the orbifold and blowup states via the field redefinitions.

5.2.1 Matching the geometry

Orbifold geometry The requirement to have a $\mathbb{Z}_7$ symmetry puts strong constraints on the torus lattice underlying the orbifold. The only possibility is the non-factorizable root lattice of SU(7). In particular, all complex structure moduli are completely fixed and hence $h^{2,1} = 0$.[2] This behavior also occurs in the $\mathbb{Z}_3$ orbifold, which is the only

---

[2] We expect interesting consequences for the mirror of such models.
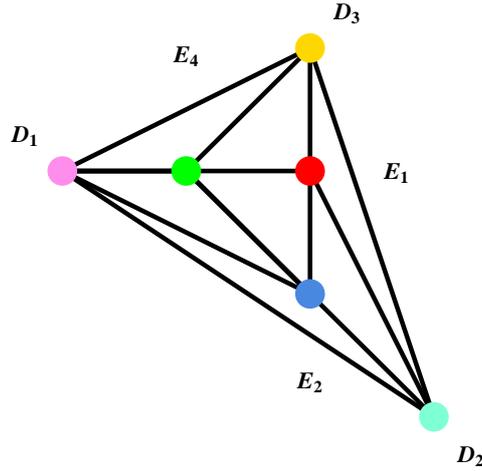
Figure 5.2: Toric diagram for the resolution of $\mathbb{C}^3/\mathbb{Z}_7$.

other orbifold whose orbifold action is prime. Denoting the six lattice vectors of T^6 by e_a, the $\mathbb{Z}_7$ symmetry acts via

$$e_a \to e_{a+1} \, , \quad a = 1, \dots, 5 \, , \qquad e_6 \to -\sum_{a=1}^{6} e_a \, . \qquad (5.10)$$

Expressed in terms of three complex coordinates z_i, the $\mathbb{Z}_7$ action reads

$$\theta : (z_1, \, z_2, \, z_3) \to (\xi z_1, \, \xi^2 z_2, \, \xi^4 z_3) \qquad \text{with} \qquad \xi = e^{2\pi i/7} \, . \qquad (5.11)$$

The fixed point positions of the orbifold are given by the weights of the anti-symmetric fundamental representations, so altogether there are seven of them. Locally each of these singularities looks like $\mathbb{C}^3/\mathbb{Z}_7$.

In this example we consider the $\mathbb{Z}_7$ orbifold model of [99], which has a semi-realistic gauge group and allows for three chiral families. However, the hypercharge generator is not embeddable into an intermediate $SU(5)$ GUT and hence the model is not expected to yield gauge coupling unification on this level. In any case, as we shall see in chapter 6, the resolution of the model does not allow for an unbroken hypercharge. The shift vector and the Wilson line of the model are

$$V = \frac{1}{7} \, (0, 0, -1, -1, -1, 5, -2, 6) \, (-1, -1, 0, 0, 0, 0, 0, 0) \, ,$$
$$W = \frac{1}{7} \, (-1, -1, -1, -1, -1, -10, 2, -9) \, (4, 3, -3, 0, 0, 0, 0, 0) \, . \qquad (5.12)$$

They break the primordial $E_8 \times E_8$ to $SU(3) \times SU(2) \times SO(10) \times U(1)^8$. The summary of the charged massless orbifold spectrum in terms of the non-Abelian irreducible representations (irreps) is

irrep	$(\mathbf{3}, \mathbf{2}, \mathbf{1})$	$(\mathbf{3}, \mathbf{1}, \mathbf{1})$	$(\overline{\mathbf{3}}, \mathbf{1}, \mathbf{1})$	$(\mathbf{1}, \mathbf{2}, \mathbf{1})$	$(\mathbf{1}, \mathbf{1}, \mathbf{10})$	$(\mathbf{1}, \mathbf{1}, \mathbf{1})$
multiplicity	3	12	18	21	1	133

Blowup geometry   We start with the local resolution of the $\mathbb{Z}_7$ singularity. The toric diagram for the local resolution is given in figure 5.2. The resolution requires the introduction of three exceptional divisors whose intersection numbers are

$$E_1^3 = E_2^3 = E_4^3 = 8\,, \qquad\qquad E_1 E_2^2 = E_2 E_4^2 = E_4 E_1^2 = 0\,,$$
$$E_1^2 E_2 = E_2^2 E_4 = E_4^2 E_1 = -2\,, \qquad\qquad E_1 E_2 E_4 = 1\,. \tag{5.13}$$

 As a next step we want to describe the resolution of the full $T^6/\mathbb{Z}_7$ [55]. The global description of the resolution is rather complicated. However, since the resolution of singularities happens just locally, we can figure out the topological properties by hand. For this, we start with the orbifold and cut out small open sets around the seven fixed points. Then we replace them by the resolved local singularities which we constructed above. Therefore, we now have seven sets of three exceptional divisors, $E_{k,\sigma}$, $\sigma = 1, \ldots, 7$ which do not intersect when they are located at formerly different fixed points, $E_{k,\sigma} E_{l,\rho} = 0$ if $\sigma \neq \rho$. In addition we get three inherited divisors R_i. However, since they neither appear in the characteristic classes of the resolution nor in the expansion of the gauge flux, they are not of importance for the following discussion.

5.2.2 Matching the blowup modes

For this, we use the observation [39, 60] that some of the Bianchi identities enforce that the line bundle vectors are chosen from the orbifold shifted momenta corresponding to massless twisted states without oscillators. Scanning over the shifted momenta of all these states, we select one (arbitrary) set of bundle vectors such that they fulfill the Bianchi identities, the DUY equations, and are singlets under the non-Abelian gauge groups. While the first two choices are mandatory for a well-defined model, the third choice is done for convenience. Leaving the non-Abelian gauge groups unbroken simplifies the matching since we do not have to consider the branching of the non-Abelian gauge groups induced by the Higgs mechanism arising from VEVing the blowup states. Let us look at the Bianchi identities (4.34) for the case where the vector bundle V is a sum of line bundles, $V = \oplus \mathcal{L}_i$. We find for the second Chern character $\mathrm{ch}_2(V) = \frac{1}{2}(c_1(V) - 2c_2(V))$. Using that the total Chern class of a vector bundle which is a sum of line bundles satisfies $c(\oplus \mathcal{L}_i) = \prod_i (1 + c_1(\mathcal{L}_i))$, we find $\mathrm{ch}_2(V) = \frac{1}{2} \sum_i c_1(\mathcal{L}_i)^2$. For the second Chern character of the compactification CY we find simply $\mathrm{ch}_2(TX) = -c_2(TX)$. With this, the Bianchi identities can be written as

$$0 = \mathrm{tr}\mathcal{R}^2 - \mathrm{tr}(\mathrm{i}\mathcal{F})^2 = 2(\mathrm{ch}_2(V) - \mathrm{ch}_2(TX)) = \sum_{r,s} \sum_I V_r^I V_s^I E_r E_s + 2c_2(TX)\,. \tag{5.14}$$

5.2.3 Matching the spectra

For matching the massless states, we use that the states on the orbifold and in blowup are connected via field redefinitions (5.8). There are various kinds of field redefinitions that can be employed encoded in the $f(t_r)$ in (5.8). Since on the orbifold we only have

fixed points that become arbitrarily widely separated in the SUGRA blowup limit (the intersection between exceptional divisors at different fixed points vanishes identically in the Kähler cone of the blowup), we require that orbifold fields that live at a certain fixed point σ are only redefined with the charges of the blowup modes that reside at the same fixed point. However, since in blowup we lose the information which twisted sector an orbifold state corresponds to, we allow for the inclusion of blowup modes coming from different twisted sectors θ^k. From this we find that the following charge redefinitions are realized:

$$Q^{\text{Orb}}_{k,\sigma} \mapsto Q^{\text{CY}}_{k,\sigma} = Q^{\text{Orb}}_{k,\sigma} - V_{k,\sigma} \,, \tag{5.15a}$$

$$Q^{\text{Orb}}_{k,\sigma} \mapsto Q^{\text{CY}}_{k,\sigma} = Q^{\text{Orb}}_{k,\sigma} + V_{l,\sigma} + V_{m,\sigma} \,, \quad k \neq l \neq m \neq k \,, \tag{5.15b}$$

$$\begin{aligned}
Q^{\text{Orb}}_{1,\sigma} &\mapsto Q^{\text{CY}}_{1,\sigma} = Q^{\text{Orb}}_{1,\sigma} + V_{1,\sigma} - V_{2,\sigma} \,, \\
Q^{\text{Orb}}_{2,\sigma} &\mapsto Q^{\text{CY}}_{2,\sigma} = Q^{\text{Orb}}_{2,\sigma} + V_{2,\sigma} - V_{4,\sigma} \,, \\
Q^{\text{Orb}}_{4,\sigma} &\mapsto Q^{\text{CY}}_{4,\sigma} = Q^{\text{Orb}}_{4,\sigma} - V_{1,\sigma} + V_{4,\sigma} \,,
\end{aligned} \tag{5.15c}$$

$$\begin{aligned}
Q^{\text{Orb}}_{1,\sigma} &\mapsto Q^{\text{CY}}_{1,\sigma} = Q^{\text{Orb}}_{1,\sigma} + V_{1,\sigma} + V_{2,\sigma} - V_{4,\sigma} \,, \\
Q^{\text{Orb}}_{2,\sigma} &\mapsto Q^{\text{CY}}_{2,\sigma} = Q^{\text{Orb}}_{2,\sigma} - V_{1,\sigma} + V_{2,\sigma} + V_{4,\sigma} \,, \\
Q^{\text{Orb}}_{4,\sigma} &\mapsto Q^{\text{CY}}_{4,\sigma} = Q^{\text{Orb}}_{4,\sigma} + V_{1,\sigma} - V_{2,\sigma} + V_{4,\sigma} \,.
\end{aligned} \tag{5.15d}$$

Massless states   In order to illustrate the methods for matching the spectra explained above, let us look at examples for the redefinition. We included some orbifold states together with their redefinition and the corresponding $E_8 \times E_8$ root in blowup in table 5.2. The full spectrum where the match is performed for all orbifold states can be found in [61]. In the match, we will use again that the resolution is an entirely local process. This means that the HRR index theorem can be split up and applied to each of the seven local resolutions of $\mathbb{C}^3/\mathbb{Z}_7$ individually. In this way, we can compare the spectra easily and even extract information on vector-like pairs in blowup which could not be seen by the HRR index theorem applied to the whole compact $T^6/\mathbb{Z}_7$, as we discuss now.

First we explain how to read table 5.2. In the first column, we assign a unique label (e.g. Q_1) to each orbifold state; for the blowup counterpart we give the irrep under which the states transform. The second column identifies the twisted sector θ^k from which the state emerges. The local multiplicity columns give the multiplicity of the states at the fixed points 1-7. In blowup, they are evaluated via the local HRR theorem and on the orbifold by solving the mass conditions. The total multiplicity is the sum of the local multiplicities as obtained from the global HRR operator. Since this sees only chiral states, the total blowup multiplicity is at the same time the sum of the multiplicities of the orbifold states that are redefined to the same blowup $E_8 \times E_8$ vector. The next column gives the shifted momenta for the orbifold states and the $E_8 \times E_8$ root for the blowup states. Finally, the last column gives the field redefinition that was used to match the orbifold state to its blowup counterpart.

State	Sector	Local multiplicity							tot	$E_8 \times E_8$ root / P_{sh}	Redef
		1	2	3	4	5	6	7			
$(\mathbf{3},\mathbf{2},\mathbf{1})$	–	$\frac{1}{7}$	$\frac{1}{7}$	$\frac{1}{7}$	$\frac{1}{7}$	$\frac{1}{7}$	$\frac{1}{7}$	$\frac{1}{7}$	1	$(1,0,0,0,-1,0,0,0)(0,0,0,0,0,0,0,0)$	–
Q_1	untw.	$\frac{1}{7}$	$\frac{1}{7}$	$\frac{1}{7}$	$\frac{1}{7}$	$\frac{1}{7}$	$\frac{1}{7}$	$\frac{1}{7}$	1	$(1,0,0,0,-1,0,0,0)(0,0,0,0,0,0,0,0)$	none
$(\mathbf{3},\mathbf{2},\mathbf{1})$	–	1	$-\frac{1}{7}$	$-\frac{1}{7}$	$\frac{1}{7}$	$-\frac{1}{7}$	$\frac{1}{7}$	$\frac{1}{7}$	1	$(\frac{1}{2},-\frac{1}{2},\frac{1}{2},\frac{1}{2},-\frac{1}{2},\frac{1}{2},-\frac{1}{2},-\frac{1}{2})(0,0,0,0,0,0,0,0)$	–
Q_2	2	1	0	0	0	0	0	0	1	$\frac{1}{14}(7,-7,3,3,-11,-1,-1,3)(-4,-4,0,0,0,0,0,0)$	(5.15a)
$(\mathbf{3},\mathbf{2},\mathbf{1})$	–	1	$-\frac{1}{7}$	$-\frac{1}{7}$	$\frac{1}{7}$	$-\frac{1}{7}$	$\frac{1}{7}$	$\frac{1}{7}$	1	$(\frac{1}{2},-\frac{1}{2},\frac{1}{2},\frac{1}{2},-\frac{1}{2},\frac{1}{2},\frac{1}{2},-\frac{1}{2})(0,0,0,0,0,0,0,0)$	–
Q_3	1	1	0	0	0	0	0	0	1	$\frac{1}{14}(7,-7,5,5,-9,3,3,5)(-2,-2,0,0,0,0,0,0)$	(5.15a)
$(\mathbf{3},\mathbf{1},\mathbf{1})$	–	$-\frac{1}{7}$	$\frac{1}{7}$	$-\frac{1}{7}$	$\frac{1}{7}$	$\frac{1}{7}$	1	$-\frac{1}{7}$	1	$(0,0,0,0,-1,0,1,0)(0,0,0,0,0,0,0,0)$	–
t_6	4	0	0	0	0	0	1	0	1	$\frac{1}{14}(-5,-5,1,1,-13,-3,1,3)(-2,0,3,0,0,0,0,0)$	(5.15a)
$(\overline{\mathbf{3}},\mathbf{1},\mathbf{1})$	–	$\frac{1}{7}$	$\frac{1}{7}$	$-\frac{1}{7}$	$\frac{1}{7}$	$-\frac{1}{7}$	$-\frac{1}{7}$	-1	-1	$(\frac{1}{2},\frac{1}{2},-\frac{1}{2},\frac{1}{2},-\frac{1}{2},\frac{1}{2},\frac{1}{2},\frac{1}{2})(0,0,0,0,0,0,0,0)$	–
$\overline{t}_7$	4	0	0	0	0	0	0	-1	-1	$\frac{1}{14}(1,1,-7,-7,7,1,3,1)(2,10,-2,0,0,0,0,0)$	(5.15a)
$(\mathbf{3},\mathbf{1},\mathbf{1})$	–	$\frac{1}{7}$	$-\frac{1}{7}$	$\frac{1}{7}$	$\frac{1}{7}$	1	$-\frac{8}{7}$	$-\frac{1}{7}$	0	$(0,0,0,0,-1,0,0,-1)(0,0,0,0,0,0,0,0)$	–
t_5	4	0	0	0	0	1	0	0	1	$\frac{1}{7}(-2,-2,1,1,-6,0,3,-1)(-3,2,1,0,0,0,0,0)$	(5.15a)
t_{12}	1	0	0	0	0	1	0	0	1	$\frac{1}{7}(3,3,2,2,-5,0,-1,-2)(1,-3,2,0,0,0,0,0)$	(5.15a)
$\overline{t}_{11}$	2	0	0	0	0	-1	0	0	-1	$\frac{1}{7}(-1,-1,4,-3,-3,0,-2,-4)(2,1,-3,0,0,0,0,0)$	(5.15b)
$\overline{t}_{18}$	1	0	0	0	0	0	-1	0	-1	$\frac{1}{14}(-3,-3,9,-5,-5,1,-5,-1)(10,0,-2,0,0,0,0,0)$	(5.15c)
$(\mathbf{1},\mathbf{1},\mathbf{1})$	–	$\frac{13}{7}$	$-\frac{1}{7}$	$-\frac{13}{7}$	$\frac{13}{7}$	$\frac{1}{7}$	$\frac{1}{7}$	1	3	$(0,0,0,0,0,1,0,-1)(0,0,0,0,0,0,0,0)$	–
s_{25}	4	0	0	0	1	0	0	0	1	$\frac{1}{14}(-3,-3,3,3,3,-3,-3,-7)(4,-6,-2,0,0,0,0,0)$	(5.15a)
s_{26}	4	0	0	0	1	0	0	0	1	$\frac{1}{14}(-3,-3,3,3,3,-3,-3,-7)(4,-6,-2,0,0,0,0,0)$	(5.15a)
									...		
$(\mathbf{1},\mathbf{1},\mathbf{1})$	–	$\frac{13}{7}$	$-\frac{1}{7}$	$-\frac{13}{7}$	$\frac{13}{7}$	$\frac{1}{7}$	$\frac{1}{7}$	1	3	$(0,0,0,0,0,1,0,-1)(0,0,0,0,0,0,0,0)$	–
s_{70}	2	0	0	0	1	0	0	0	1	$\frac{1}{7}(1,1,-1,-1,-1,6,1,0)(1,2,3,0,0,0,0,0)$	(5.15a)
									...		
$(\mathbf{1},\mathbf{1},\mathbf{1})$	–	$\frac{6}{7}$	$-\frac{1}{7}$	-1	$\frac{15}{7}$	$\frac{1}{7}$	$\frac{13}{7}$	$\frac{1}{7}$	4	$(0,0,0,0,0,0,1,-1)(0,0,0,0,0,0,0,0)$	–
s_{111}	1	0	0	0	1	0	0	0	1	$\frac{1}{14}(1,1,-1,-1,-1,-1,1,-7)(-6,2,-4,0,0,0,0,0)$	(5.15a)
s_{113}	1	0	0	0	1	0	0	0	1	$\frac{1}{14}(1,1,-1,-1,-1,-1,1,-7)(-6,2,-4,0,0,0,0,0)$	(5.15a)
									...		
$(\mathbf{1},\mathbf{1},\mathbf{1})$	–	$\frac{13}{7}$	$-\frac{1}{7}$	$-\frac{13}{7}$	$\frac{13}{7}$	$\frac{1}{7}$	$\frac{1}{7}$	1	3	$(0,0,0,0,0,1,0,-1)(0,0,0,0,0,0,0,0)$	–
s_{112}	1	0	0	0	-1	0	0	0	-1	$\frac{1}{14}(1,1,-1,-1,-1,-1,1,-7)(-6,2,-4,0,0,0,0,0)$	(5.15b)
									...		

Table 5.2: Excerpt of the match of orbifold states with their blowup counterparts [61].

Let us begin with the 3 quark doublets $(\mathbf{3},\mathbf{2},\mathbf{1})$. The first field Q_1 lives in the untwisted sector. Hence it does not need to be redefined. Applying the local HRR theorem to the (non-compact) resolution of $\mathbb{C}^3/\mathbb{Z}_7$, we get a multiplicity of 1/7 at each fixed point. The fact that a fractional multiplicity appears is linked to the fact that $\mathbb{C}^3/\mathbb{Z}_7$ is non-compact. The "real" multiplicity is given by summing over the contribution from the various local patches and they are always found to be integer as it should be. In fact, the fractional multiplicities are rather nice: they tell us that the field Q_1 lives to 1/7 at each of the 7 fixed points, i.e. the field is democratically smeared out over all fixed points, as one would expect for an untwisted field. The fields Q_2 and Q_3 both live at the first orbifold fixed point. Both are redefined to a unique root vector via (5.15a) at the first fixed point (and of the second respectively first twisted sector). By looking at the local multiplicity operator, we see a multiplicity of one at the first fixed point. Hence the local multiplicity operator exactly sees the orbifold state. At the other fixed points, we see fractional multiplicities of $\pm 1/7$, which however sum to zero and thus the overall multiplicity is one. These fractional non-existing states can be interpreted as those untwisted states which were projected out on the orbifold. As long as they sum to zero, we will ignore them in the following. If they do not sum to zero but to one, they indicate an untwisted sector field, as seen for the field Q_1.

For the triplets $(\mathbf{3},\mathbf{1},\mathbf{1})$ there are states that transform in the fundamental $\mathbf{3}$ as well as in the anti-fundamental $\overline{\mathbf{3}}$. It suffices to investigate the triplet weights since the anti-triplets weights correspond to their negatives. Thus, a positive multiplicity indicates

a triplet state whereas a negative multiplicity indicates an anti-triplet state. As an example for this, we look at the states $\bar{t}_7$ and t_6 which transform in the $(\overline{\mathbf{3}}, \mathbf{1}, \mathbf{1})$ and $(\mathbf{3}, \mathbf{1}, \mathbf{1})$. Their overall multiplicity is -1 and 1, and the local multiplicity operator reveals that these states live at fixed points 7 and 6, respectively. This is again readily confirmed from the orbifold spectrum.

Something conceptually new happens for the orbifold states t_5, t_{12}, $\bar{t}_{11}$, and $\bar{t}_{18}$. Although these four states are redefined to the same root the total multiplicity is zero. This happens because the HRR index can only count the net number of states which is $2 - 2 = 0$. However, the local HRR index gives some insight into what is happening. The three states t_5, t_{12}, $\bar{t}_{11}$ all live at fixed point 5 on the orbifold. As there are two left-chiral and one right-chiral state the local multiplicity is 1. For the one right-chiral state $\bar{t}_{18}$, there is a local multiplicity of -1 at fixed point 6. Hence the overall multiplicity is zero. The multiplicities of all other states can be worked out in a similar manner.

Higgsed states   Vector-like states can acquire a mass in the blowup procedure from trilinear Yukawa couplings. On the orbifold, these couplings can be calculated using CFT techniques. This leads to a set of selection rules which can be used to check which couplings are allowed. The selection rules on the $\mathbb{Z}_7$ orbifold arise from requiring gauge invariance, compatibility with the space group, and conservation of H momentum. Conservation of R charge will be discussed below. Gauge invariance simply amounts to the requirement that the sum of the left-moving shifted momenta of the strings involved in the coupling is zero.

The space group selection rule requires that the product of the constructing space group elements of the states involved in the Yukawa coupling must be the identity element $(\mathbb{1}, 0)$. For trilinear couplings this states that the allowed couplings are of the form

$$(k = 1, \sigma_1) \circ (k = 2, \sigma_2) \circ (k = 4, \sigma_4), \qquad \text{with} \qquad \sigma_1 + 2\sigma_2 + 4\sigma_4 = 0 \bmod 7. \tag{5.16}$$

If the coupling involves states which reside all at the same fixed point $(\sigma_1 = \sigma_2 = \sigma_4)$, the space group selection rule is trivially fulfilled. However, there also exist solutions to (5.16) for states coming from three different fixed points. Since these couplings arise from worldsheet instantons [100, 101], they are suppressed by a factor of the form $e^{-\frac{a_i}{\alpha'}}$ where a_i are the moduli which govern the sizes of the CY or of the lattice underlying the orbifold. As it turns out, in our case H momentum is conserved for the trilinear couplings if the space group selection rule is fulfilled.

The conservation rule of the R charge defined in (2.46) reads

$$\sum_\zeta R_\zeta^i = 1, \tag{5.17}$$

where ζ runs over the three states involved in the Yukawa coupling. Equation (5.17) is trivially fulfilled for states without oscillators if the space group rules are. However, in a compact orbifold this symmetry will be broken down to a subgroup by the torus lattice. Therefore the formerly forbidden couplings are expected to be suppressed by the size of the lattice. If the lattice is factorizable, the remaining symmetry is the discrete

rotation of the three two-tori. In this case the selection rule needs only be satisfied up to multiples of the order of the orbifold group. For the non-factorizable $SU(7)$ lattice of the $\mathbb{Z}_7$ orbifold, we checked that the symmetry is broken completely except for the $\mathbb{Z}_7$ itself, so (5.17) should not be imposed on the orbifold.

The SUGRA theory on the blowup side is, however, only valid in the large volume limit. In particular, we expect that the R charge selection rule (5.17), which is broken by the orbifold lattice, is still a valid symmetry in the large volume limit. We therefore expect the states which are supposed to get a mass via such suppressed couplings on the orbifold, to appear as massless states in the multiplicity operator in blowup. By comparing the spectra we indeed find that the index theorem sees massless states for which the orbifold theory predicts non-local mass terms or mass terms which do not satisfy (5.17). To illustrate the absence of both types of mass terms in blowup we look at suitable examples.

As an example for mass terms not satisfying (5.17) consider the singlet states s_{25}, s_{26}, s_{70}, s_{111}, s_{112} and s_{113}, see table 5.2. These states are all oscillator states which explains their degeneracy and which makes them sensitive to a possible R symmetry. Together with the blowup modes s_{68} and s_{27}, there are the following orbifold trilinear superpotential couplings when imposing only gauge and space group invariance and the H momentum rule:

$$
\begin{pmatrix} s_{111} & s_{112} & s_{113} \end{pmatrix} \begin{pmatrix} a_{11}s_{68} & a_{12}s_{68} & a_{13}s_{27} \\ a_{21}s_{68} & a_{22}s_{68} & a_{23}s_{27} \\ a_{31}s_{68} & a_{32}s_{68} & a_{33}s_{27} \end{pmatrix} \begin{pmatrix} s_{25} \\ s_{26} \\ s_{70} \end{pmatrix} , \tag{5.18}
$$

where the a_{ij} are coefficients which are naively of order one. Now when one gives a VEV to the blowup modes s_{68} and s_{27}, these couplings give rise to a rank three mass matrix and thus one would expect all 6 singlets to become massive and disappear from the chiral spectrum in blowup. However, when we look at the roots to which these singlets can be redefined, the local HRR index reveals that there are four states at the resolved fixed point where the singlets in question were localized. Therefore four of these singlets must stay massless in the heterotic supergravity limit $\alpha' \to 0$. This means that the above mass matrix has to have only rank one, such that just one pair of singlets is decoupled. One could explain this by assuming that all coefficients a_{ij} are equal, but this assumption is a priori not justified and would lead to mixing of the fields during redefinition. It is probably more sensible to argue that the local HRR index sees states only in the large volume limit where the R symmetry (5.17) is exact. Imposing R symmetry here would set all coefficients to zero except for a_{21} and a_{23} and therefore naturally explain the rank one mass matrix at this place.

The local R charge selection rule (5.17) is only relevant for oscillator states, as states satisfying the space group selection rule have $\sum_\zeta q^i_{\text{sh},\zeta} = 1$ and hence (5.17) is fulfilled for states without oscillators. Interestingly, the states which have oscillators often allow for more than one possible redefinition (5.15). Imposing (5.17) in conjunction with consistency of the local blowup spectra singles out a unique field redefinition. Using these redefinitions, we were finally able to establish a perfect match between the

anomalies on the orbifold and in blowup, which we take as a strong cross-check that the above discussion is valid.

To illustrate the presence of the instantonic non-local mass terms, we investigate the triplet states t_5, t_{12}, $\bar{t}_{11}$, and $\bar{t}_{18}$ encountered above. From the employed redefinitions we find

$$t_5^{\mathrm{CY}}\bar{t}_{11}^{\mathrm{CY}} = t_5^{\mathrm{Orb}}\bar{t}_{11}^{\mathrm{Orb}}e^{-b_{4,5}+b_{1,5}+b_{4,5}} = t_5^{\mathrm{Orb}}\bar{t}_{11}^{\mathrm{Orb}}e^{b_{1,5}} \,, \tag{5.19a}$$

$$t_{12}^{\mathrm{CY}}\bar{t}_{11}^{\mathrm{CY}} = t_{12}^{\mathrm{Orb}}\bar{t}_{11}^{\mathrm{Orb}}e^{-b_{1,5}+b_{1,5}+b_{4,5}} = t_{12}^{\mathrm{Orb}}\bar{t}_{11}^{\mathrm{Orb}}e^{b_{4,5}} \,. \tag{5.19b}$$

The coupling of t_5 and t_{12} with $\bar{t}_{18}$ is non-local as the states reside at different fixed points. Hence this coupling is not captured by the multiplicity operator. The redefinitions clearly show that in blowup where $b_{k,\sigma} \gg 1$, the couplings (5.19) provide a mass term which vanishes in the blowdown limit $b_{k,\sigma} \ll 1$ in units of α'. This means that from the blowup perspective a linear combination of t_5 and t_{12} pairs up with $\bar{t}_{11}$ and lifts the exotic state from the massless particle spectrum in blowup. This behavior is also confirmed from the orbifold perspective. The appearance of $b_{1,5}$ (5.19a) shows that t_5 from the θ^4 sector and $\bar{t}_{11}$ from the θ^2 sector couple to the blowup mode from the θ sector as dictated by the space group selection rule. Likewise, for the second mass term (5.19b) we find a coupling between t_{12} from the θ sector, $\bar{t}_{11}$ from the θ^2 sector, and the blowup mode from the θ^4 sector as indicated by $b_{4,5}$.

5.2.4 Matching the anomalies

For comparing the anomalies, it is advantageous to split the contributions to the overall anomaly on the orbifold and the CY according to (5.9). It is also useful to express the various anomaly polynomial contribution in terms of their constituent two- and four-forms,

$$I_{\mathrm{Orb}}^{\mathrm{uni}} + I_{\mathrm{Orb}}^{\mathrm{red}} = I_{\mathrm{CY}}^{\mathrm{uni}} + I_{\mathrm{CY}}^{\mathrm{non}} \,,$$
$$F_{\mathrm{Orb}}X_4^{\mathrm{Orb}} + \sum_r V_I^r F^I X_{4,\,\mathrm{Orb}}^{r,\,\mathrm{red}} = X_{2,\,\mathrm{CY}}^{\mathrm{uni}}X_{4,\,\mathrm{CY}}^{\mathrm{uni}} + \sum_r X_{2,\,\mathrm{CY}}^{r,\,\mathrm{non}}X_{4,\,\mathrm{CY}}^{r,\,\mathrm{non}} \,. \tag{5.20}$$

In writing (5.20), we have made use of the fact that the change in the anomaly arising from field redefinitions is induced by the charges of the blowup modes. The charges are given in terms of their shifted momenta, which in turn equal the line bundle vectors V_I^r. The form X_4^{Orb} on the left hand side will be computed by explicitly constructing the one anomalous U(1) contribution, and the form $X_{4,\,\mathrm{Orb}}^{r,\,\mathrm{red}}$ from constructing the orbifold anomaly polynomial after taking into account the redefinition of charges and the decoupling of states due to the VEVs given to the blowup modes. The forms X on the right hand side are shorthand expressions for the forms that arise from (4.25) when splitting the forms X_M into forms $X_{a,\mu}$ where μ are 4D spacetime indices and a are 6D internal indices and subsequently integrating out the internal manifold $\mathcal{M}$ (here we

deviate from our standard notation in which the compactification manifold is called X to avoid confusion with the anomaly forms X),

$$X_{2,\mathrm{CY}}^{\mathrm{uni}} := \int_{\mathcal{M}} X_{6,2}\,, \quad X_{4,\mathrm{CY}}^{\mathrm{uni}} := X_{0,4}\,, \quad E_r X_{2,\mathrm{CY}}^{r,\,\mathrm{non}} := \frac{1}{6}\mathrm{tr}(\mathrm{i}\mathcal{F}\mathrm{i}F)\,, \quad X_{4,\mathrm{CY}}^{r,\,\mathrm{non}} := \int_{\mathcal{M}} X_{4,4} E_r$$

They are computable from the intersection numbers on the compactification manifold $\mathcal{M}$, the Bianchi identities, and the internal gauge flux $\mathcal{F}$. Using the descent equations, we find for the Green–Schwarz counterterm

$$a_{\mathrm{Orb}}^{\mathrm{uni}} X_{4,\mathrm{Orb}}^{\mathrm{uni}} + \sum_i \tau_i X_{i,\mathrm{Orb}}^{4,\mathrm{red}} = a_{\mathrm{CY}}^{\mathrm{uni}} X_{4,\mathrm{CY}}^{\mathrm{uni}} + \sum_r \beta_r X_{4,\mathrm{CY}}^{r,\mathrm{non}} \tag{5.21}$$

Let us now discuss the four contributions to the anomalies on both sides in the following. After that, we show how the left hand side and the right hand side combine to match the complete anomaly across both theories.

Universal orbifold anomaly $I_{\mathrm{Orb}}^{\mathrm{uni}}$

On the orbifold, we can choose a basis of $\mathrm{U}(1)$ charges such that there is single anomalous $\mathrm{U}(1)_A$ symmetry and the other seven $\mathrm{U}(1)$'s are perpendicular to it. With this anomalous $\mathrm{U}(1)_A$ generator, the anomaly polynomial on the orbifold is

$$I_{\mathrm{Orb}}^{\mathrm{uni}} = 6F_1 \left(\mathrm{tr}(\mathrm{i}F_{\mathrm{SU}(2)})^2 + \mathrm{tr}(\mathrm{i}F_{\mathrm{SU}(3)})^2 + \mathrm{tr}(\mathrm{i}F_{\mathrm{SO}(10)})^2 - \mathrm{tr}R^2 + \kappa^{IJ} \sum_{I,J} F_I F_J \right)\,, \tag{5.22}$$

where the indices I, J label the eight $\mathrm{U}(1)$ factors on the orbifold. The numerical factors κ^{IJ} are not given explicitly because they are not relevant in further discussions. The factor of six could be absorbed by changing the normalization of the anomalous $\mathrm{U}(1)$ generator T_A. However, we prefer not to do so, as otherwise we find this factor of six in all field redefinitions in the next section.

Anomaly from field redefinition $I_{\mathrm{Orb}}^{\mathrm{red}}$

This part of the orbifold anomaly polynomial takes into account that there is a field redefinition between the states on the orbifold and in blowup which induces a change of the $\mathrm{U}(1)$ charges and accounts for the decoupling of Higgsed orbifold states. We calculate this change by splitting up $I_{\mathrm{Orb}}^{\mathrm{red}}$ into contributions from the three types of anomalies, $I_{\mathrm{Orb}}^{\mathrm{red}} = I_{\mathrm{G}}^{\mathrm{red}} + I_{\mathrm{grav}}^{\mathrm{red}} + I_{\mathrm{pure}}^{\mathrm{red}}$, which we will now compute.

$\mathrm{U}(1) \times \mathrm{G}^2$ anomaly redefinition   In order to compute the redefinition of the $\mathrm{U}(1) \times \mathrm{G}^2$ anomaly polynomial we need to consider the change of $\mathrm{tr}\,Q_I$ when going from the orbifold to blowup, where the trace is taken over the fields charged under the non-Abelian group. Let us denote the $\mathrm{U}(1)$ charges on the orbifold by Q_I^γ, where

γ runs over all orbifold states and I labels the the U(1) generators. Likewise, we denote the U(1) charges in blowup by $Q_I'^\gamma$. Furthermore, it is convenient to introduce $\Delta_I^\gamma = Q_I^\gamma - Q_I'^\gamma$, which labels the difference between the charges in the two theories. According to (5.8), the charges Q_I^γ and $Q_I'^\gamma$ differ by $f^\gamma(V_I^r)$ where V_I^r is the line bundle vector, or equivalently, the shifted momentum of the blowup mode at fixed point r, and the function f is given in terms of the redefinitions (5.15).

The sum of the charges in blowup $\mathrm{tr}\,(Q_I)_{\mathrm{BU}} = \sum_\alpha Q_I'^\alpha$ runs over the states α that remain massless after giving VEVs to the blowup modes. Hence, in order to recover the trace on the orbifold prior to having assigned VEVs, we also have to include a sum over the states that gain a mass in blowup, which we label by β. We thus obtain

$$
\begin{aligned}
\mathrm{tr}(Q_I') &= \sum_\alpha Q_I^\alpha - \sum_\alpha \Delta_I^\alpha = \sum_\alpha Q_I^\alpha - \sum_\alpha \Delta_I^\alpha + \sum_\beta Q_I^\beta - \sum_\beta \Delta_I^\beta - \sum_\beta Q_I'^\beta \\
&= \mathrm{tr}(Q_I)_{\mathrm{Orb}} - \sum_{\gamma=\alpha,\beta} \Delta_I^\gamma - \sum_\beta Q_I'^\beta,
\end{aligned}
\tag{5.23}
$$

where we added a zero in the first step and rearranged the terms in the second step. Note that the last sum $\sum_\beta Q_I'^\beta$ which sums over all fields that became massive in blowup vanishes identically: all massive states are vector-like with respect to their charges, so the sum always contains pairs of opposite charges. Leaving out this last term, the contribution to the 4d anomaly polynomial and the redefinition part read

$$
\begin{aligned}
I_{\mathrm{G}} &= F^I \mathrm{tr}(\mathrm{i}F_{\mathrm{G}})^2 \sum_\alpha Q_I'^\alpha, \\
I_{\mathrm{G}}^{\mathrm{red}} &\sim \sum_{\mathrm{G},I} \left(-\sum_\gamma \Delta_I^\gamma \right) F^I \mathrm{tr}(\mathrm{i}F_{\mathrm{G}})^2 \sim \sum_{\mathrm{G},I} c_I^{\mathrm{G}} F^I \mathrm{tr}(\mathrm{i}F_{\mathrm{G}})^2.
\end{aligned}
\tag{5.24}
$$

In the sums G runs over SU(2), SU(3) and SO(10). When evaluating the sum and comparing with the orbifold result, we obtain a perfect match of all $\mathrm{U}(1)\times\mathrm{G}^2$ anomalies of both theories, where the anomaly coefficients c_I^{G} of (5.24) have been calculated in a specific choice of U(1) basis [61].

U(1) × grav² anomaly redefinition   For the $\mathrm{U}(1) \times \mathrm{grav}^2$ anomaly one has to include all the massless fields in the trace. This means that, in contrast to the $\mathrm{U}(1)\times\mathrm{G}^2$ anomalies, one also has to add the contribution coming from the Abelian blowup mode charges V_I^r. The contribution to the 4D anomaly polynomial and the redefinition part is then given by

$$
\begin{aligned}
I_{\mathrm{grav}} &\sim F^I \mathrm{tr}R^2 \, \mathrm{tr}(Q_I') = F^I \mathrm{tr}R^2 \sum_\alpha Q_I'^\alpha \\
&= F^I \mathrm{tr}R^2 \left(\sum_\alpha Q_I^\alpha - \sum_\alpha \Delta_I^\alpha + \sum_\beta Q_I^\beta - \sum_\beta \Delta_I^\beta - \sum_\beta Q_I'^\beta \right), \\
I_{\mathrm{grav}}^{\mathrm{red}} &\sim \left(-\sum_{\gamma=\alpha,\beta} \Delta_I^\gamma - \sum_r V_I^r \right) F^I \mathrm{tr}R^2 \sim c_I^{\mathrm{grav}} F^I \mathrm{tr}R^2,
\end{aligned}
\tag{5.25}
$$

where we again added the contributions from the massive fields and used $\sum_\beta Q_I'^\beta = 0$. The index γ contains both α for massless and β for massive fields. We find again a perfect match between the blowup polynomial and the redefined one, supporting the field redefinition ansatz of (5.15).

Pure U(1) anomaly redefinition   A similar procedure can be applied to the pure U(1) anomalies and in this case the field redefinitions change the polynomial via

$$
\begin{aligned}
I_{\text{pure}} &\sim \frac{1}{3!} \sum_{I,J,K} F^I F^J F^K \sum_\alpha Q_I'^\alpha Q_J'^\alpha Q_K'^\alpha \\
&= \frac{1}{3!} \sum_{I,J,K} F^I F^J F^K \left(\sum_\alpha Q_I^\alpha Q_J^\alpha Q_K^\alpha + \sum_a q_I^a q_J^a q_K^a + \sum_\beta Q_I^\beta Q_J^\beta Q_K^\beta \right) + I_{\text{pure}}^{\text{red}} \\
&= \frac{1}{3!} \sum_{I,J,K} F^I F^J F^K \text{tr}(Q_I Q_J Q_K)_{\text{Orb}} + I_{\text{pure}}^{\text{red}} \,,
\end{aligned}
\tag{5.26}
$$

$$
I_{\text{pure}}^{\text{red}} \sim \frac{1}{3!} \sum_{I,J,K} F^I F^J F^K \left(\sum_{\gamma=\alpha,\beta} (-3\Delta_I^\gamma Q_J^\gamma Q_K^\gamma + 3\Delta_I^\gamma \Delta_J^\gamma Q_K^\gamma - \sum_{\gamma=\alpha,\beta} \Delta_I^\gamma \Delta_J^\gamma \Delta_K^\gamma \right.
$$
$$
\left. - \sum_a q_I^a q_J^a q_K^a - \sum_\beta Q_I'^\beta Q_J'^\beta Q_K'^\beta \right) = c_{IJK}^{\text{pure}} F^I F^J F^K \,.
$$

The factor $1/3!$ takes care of the permutation symmetries of the sum indices as in (4.13). The anomalies match again perfectly assuming the mass term structure explained above.

Universal blowup anomaly $I_{\text{CY}}^{\text{uni}}$

The universal anomaly in blowup is given by

$$
\begin{aligned}
I_{\text{CY}}^{\text{uni}} &= \int_{\mathcal{M}} X_2^{\text{uni}} X_4^{\text{uni}} = -\frac{1}{12} \int_{\mathcal{M}} \left(\text{tr}R^2 - \text{tr}(\mathrm{i}F^2) \right) \\
&\left(\text{tr}(\mathrm{i}\mathcal{F}'\mathrm{i}F') \text{tr}(\mathrm{i}\mathcal{F}')^2 - \frac{1}{2} \text{tr}(\mathrm{i}\mathcal{F}')^2 \text{tr}(\mathrm{i}\mathcal{F}''\mathrm{i}F'') - \frac{1}{4} \text{tr}(\mathrm{i}\mathcal{F}'\mathrm{i}F') \text{tr}\mathcal{R}^2 +' \leftrightarrow'' \right) \,.
\end{aligned}
\tag{5.27}
$$

Using the intersection numbers and the expansion of the internal flux $\mathcal{F}$, we obtain

$$
I_{\text{CY}}^{\text{uni}} = \frac{1}{2} \left(\text{tr}R^2 - \text{tr}(\mathrm{i}F)^2 \right) \cdot \left(g_I F^I \right) \,,
\tag{5.28}
$$

with anomaly coefficients g_I.

Non-universal local anomalies $I_{\text{CY}}^{\text{non}}$

Lastly, we have the non-universal axions β_r to cancel the other U(1) anomalies. Their contributions are given by

$$
I_{\text{CY}}^{\text{non}} = \int_{\mathcal{M}} X_2^r X_4^r \,.
\tag{5.29}
$$

This expression is evaluated by using the Bianchi identities to express $\mathrm{tr}\mathcal{R}^2$ in terms of $\mathrm{tr}(\mathrm{i}\mathcal{F})^2$ as

$$\int_{E_r} \mathrm{tr}\mathcal{R}^2 = \int_{E_r} \mathrm{tr}(\mathrm{i}\mathcal{F})^2 = \int_{\mathcal{M}} V_{r_1}^I V_{r_2}^I E_{r_1} E_{r_2} E_r \,. \tag{5.30}$$

The integration in (5.29) is performed by using the intersection numbers. We obtain

$$\begin{aligned}
I_{\mathrm{CY}}^{\mathrm{non}} = &\frac{1}{2} h_I^{\mathrm{G}} F^I \left(\mathrm{tr}(\mathrm{i}F)_{\mathrm{SO}(10)}^2 - \mathrm{tr}(\mathrm{i}F)_{\mathrm{SU}(2)}^2 - \mathrm{tr}(\mathrm{i}F)_{\mathrm{SU}(3)}^2 \right) + h_{IJK}^{\mathrm{pure}} F^I F^J F^K \\
&+ \frac{1}{12}(h_I^{\mathrm{grav}} F_I) \mathrm{tr}R^2 \,,
\end{aligned} \tag{5.31}$$

where we have denoted the coefficients corresponding to the mixed $\mathrm{U}(1)_I \times \mathrm{G}^2$ anomalies with h_I^{G}, those corresponding to the pure $\mathrm{U}(1)_I \times \mathrm{U}(1)_J \times \mathrm{U}(1)_K$ anomalies with h_{IJK}^{pure}, and those corresponding to the mixed $\mathrm{U}(1)_I \times \mathrm{grav}^2$ anomalies with h_I^{grav}. The numerical values for all the coefficients evaluated in some choice of $\mathrm{U}(1)$ basis can be found in [61]. This concludes the calculation of the four contributions to the anomalies in (5.9).

Relation among the axions

From the above results for $I_{\mathrm{Orb}}^{\mathrm{uni}}$, $I_{\mathrm{Orb}}^{\mathrm{red}}$, $I_{\mathrm{CY}}^{\mathrm{uni}}$, and $I_{\mathrm{CY}}^{\mathrm{non}}$, we can now establish the relation between the single orbifold axion a^{Orb} (which is the dual to the 4D Kalb–Ramond two-form b_2), the axions in blowup, and the blowup modes using the descent equations (5.21). We need to make an ansatz to factorize $I_{\mathrm{Orb}}^{\mathrm{red}}$ which is compatible with this interpretation. A given factorization $I_{\mathrm{Orb}}^{\mathrm{red}} = \sum_r Q_I^r F_I X_{4,\mathrm{Orb}}^{r,\mathrm{red}}$ is canceled via the counterterm $\sum_i \tau_i X_{4,\mathrm{Orb}}^{i,\mathrm{red}}$. The indices i and r run over the same set (k,σ), so we use only r. Considering $X_{4,\mathrm{Orb}}^{\mathrm{uni}} = -6 X_{4,\mathrm{CY}}^{\mathrm{uni}}$ we make the following ansatz for relating the various axions

$$\beta_r = d_r \tau_r \,, \qquad a_{\mathrm{CY}}^{\mathrm{uni}} = -6 a_{\mathrm{Orb}}^{\mathrm{uni}} + \sum_r c_r \tau_r \,. \tag{5.32}$$

Here, the c_r and d_r are coefficients in the linear combinations and the factor of -6 arises due to the normalization choice of the $\mathrm{U}(1)$ generators. Substituting this ansatz into (5.21), the four-form involved in the factorization is expressed as

$$X_{4,\mathrm{Orb}}^{r,\mathrm{red}} = c_r X_{4,\mathrm{CY}}^{\mathrm{uni}} + d_r X_{4,\mathrm{CY}}^{r,\mathrm{non}} \,. \tag{5.33}$$

Substituting this last expression into $I_{\mathrm{Orb}}^{\mathrm{red}}$ in (5.20) yields

$$I_{\mathrm{Orb}}^{\mathrm{red}} = \sum_r Q_I^r F_I \left(c_r X_{4,\mathrm{CY}}^{\mathrm{uni}} + d_r X_{4,\mathrm{CY}}^{r,\mathrm{non}} \right) \,. \tag{5.34}$$

Looking at the whole anomaly polynomial (5.20), we impose equality of each factor on the left hand side and on the right hand side. As there are 8 anomalous $\mathrm{U}(1)$s, we obtain 152 equations in total, where 8 equations arise from the 8 $\mathrm{U}(1) \times \mathrm{grav}^2$ anomalies,

U sector		θ_1-sector	θ_2-sector	θ_3-sector
$(\mathbf{27},\mathbf{1})_{(-2,-2)}$	$(\overline{\mathbf{27}},\mathbf{1})_{(2,2)}$	$16(\overline{\mathbf{27}},\mathbf{1})_{(2,0)}$	$16(\overline{\mathbf{27}},\mathbf{1})_{(-1,1)}$	$16(\overline{\mathbf{27}},\mathbf{1})_{(-1,-1)}$
$(\mathbf{27},\mathbf{1})_{(-2,2)}$	$(\overline{\mathbf{27}},\mathbf{1})_{(2,-2)}$	$16(\mathbf{1},\mathbf{1})_{(-6,0)}$	$16(\mathbf{1},\mathbf{1})_{(3,-3)}$	$16(\mathbf{1},\mathbf{1})_{(3,3)}$
$(\mathbf{27},\mathbf{1})_{(4,0)}$	$(\overline{\mathbf{27}},\mathbf{1})_{(-4,0)}$	$32(\mathbf{1},\mathbf{1})_{0,2}$	$32(\mathbf{1},\mathbf{1})_{(3,1)}$	$32(\mathbf{1},\mathbf{1})_{(3,-1)}$
$(\mathbf{1},\mathbf{1})_{(6,-2)}$	$(\mathbf{1},\mathbf{1})_{(-6,2)}$	$32(\mathbf{1},\mathbf{1})_{(0,-2)}$	$32(\mathbf{1},\mathbf{1})_{(-3,-1)}$	$32(\mathbf{1},\mathbf{1})_{(-3,1)}$
$(\mathbf{1},\mathbf{1})_{(6,2)}$	$(\mathbf{1},\mathbf{1})_{(-6,-2)}$			
$(\mathbf{1},\mathbf{1})_{(0,4)}$	$(\mathbf{1},\mathbf{1})_{(0,-4)}$			

Table 5.3: The massless spectrum of the $\mathbb{Z}_2 \times \mathbb{Z}_2$ standard embedding orbifold model with gauge group $E_6 \times U(1)^2 \times E_8$.

$8 \cdot 3 = 24$ equations arise from the mixed $U(1) \times G^2$ anomalies, and $8 + 8 \cdot 7 + 8 \cdot 7 \cdot 6/3! = 120$ equations arise from the pure $U(1)$ anomalies. At first sight, this system seems highly over-constrained, as we only have $2 \cdot 21 = 42$ coefficients c_r, d_r. However, only 29 out of the 152 equations are independent. In particular, we find that part of the solution is $d_r = -1/6$ for all r. The factor of 6 arises again due to our normalization convention. From (5.32) we thus see that axions τ_r coming from field redefinitions are indeed the same as the non-universal axions β_r, which are responsible for canceling the non-universal anomalies in blowup. This result allows us to interpret the blowup modes as non-universal axions in a compact resolution of the $\mathbb{Z}_7$ orbifold.

However, choosing a common value for all c_r or grouping them by fixed points or by sectors turns out to be impossible. This implies that the universal axion in blowup is a mixture of the unique orbifold axion and the blowup modes.

5.3 Multiplicities and flop transitions

Here we demonstrate how the multiplicity changes when going through flop transitions and how this can be interpreted in terms of the field redefinitions. For our demonstration, we choose a line bundle blowup of the $\mathbb{Z}_2 \times \mathbb{Z}_2$ orbifold in standard embedding. This orbifold allows for a huge number of flop transitions. We study a simultaneous flop at all resolution points for ease of exposition and since the effect is most pronounced in this case.

Let us start with the orbifold model, which is specified by the shifts

$$V_1 = \left(0, \frac{1}{2}, -\frac{1}{2}, 0^5\right)\left(0^8\right) \quad \text{and} \quad V_2 = \left(-\frac{1}{2}, 0, \frac{1}{2}, 0^5\right)\left(0^8\right) \tag{5.35}$$

and vanishing Wilson lines $W_i = 0$. The resulting 4D model has an $E_6 \times U(1)^2 \times E_8$ gauge group and the charged matter spectrum consists of $3(\mathbf{27},\mathbf{1}) + 51(\overline{\mathbf{27}},\mathbf{1})$ and 246 singlets (charged under $U(1)^2$), cf. table 5.3.

In order to study the flop in blowup we have to choose bundle vectors that satisfy the consistency requirements in both Kähler cones simultaneously. Choosing the bundle vectors

$$
\begin{aligned}
V_{1,\beta\gamma} &= \left(\ 0, -\frac{1}{2}, -\frac{1}{2}, 1, 0, 0, 0, 0\right)\left(0, 0, 0, 0, 0, 0, 0, 0\right), \\
V_{2,\alpha\gamma} &= \left(-\frac{1}{2}, 0 - \frac{1}{2}, 0, 1, 0, 0, 0\right)\left(0, 0, 0, 0, 0, 0, 0, 0\right), \\
V_{3,\alpha\beta} &= \left(-\frac{1}{2}, -\frac{1}{2}, 0, 0, 0, 1, 0, 0\right)\left(0, 0, 0, 0, 0, 0, 0, 0\right),
\end{aligned}
\tag{5.36}
$$

the Bianchi identities are fulfilled in any triangulation. However, the DUY equations force the volume of all divisors to zero. Hence we are precisely at the tip of the Kähler cone where all four triangulations meet. The blowup modes are chosen in three different directions inside $\overline{\mathbf{27}}$ of E_6 which induces a gauge symmetry breaking

$$
E_6 \times U(1)^2 \ \longrightarrow \ SO(10) \times U(1)^3 \ \longrightarrow \ SU(5) \times U(1)^4 \ \longrightarrow \ SU(3) \times SU(2) \times U(1)^5 \,.
$$

Since we chose the same blowup mode in each fixed plane of a given twisted sector, the discussion is the same for all 64 local resolutions. Thus, we may drop the fixed point labels α, β and γ. The U(1)'s are chosen such that the charge vectors of the blowup modes are $Q(\Phi_1^{\text{BU-Mode}}) = (10, 0, 0, 0, 0)$, $Q(\Phi_2^{\text{BU-Mode}}) = (0, 10, 0, 0, 0)$, and $Q(\Phi_3^{\text{BU-Mode}}) = (0, 0, 10, 0, 0)$. In this way the axions corresponding to the blowup modes have no effect in anomaly cancelation for the last two U(1) factors. As can be checked by directly inspecting the anomaly polynomial along the lines of the last section, these U(1)'s are anomaly-free. This is also clear from the fact that the bundle has only rank 3, thus there can be at most three anomalous U(1) factors.

In table 5.4 we list an excerpt of the twisted spectrum of the standard embedding model after branching it in representations of $SU(3) \times SU(2)$ using the U(1) basis introduced above, and we match it with the spectra obtained in the resolutions E_1 and S. Since the untwisted sector is completely non-chiral, we do not consider it further in our analysis.

Example: the $(1, 2)$ case

For illustrating the effect of extra states appearing between the flop transitions, we discuss here the SU(2) doublets d_i listed in table 5.4. We focus in particular on the states named d_1 and d_2. The multiplicities of the orbifold states and of the states appearing in each of the four triangulations of the 64 $\mathbb{Z}_2 \times \mathbb{Z}_2$ fixed points are shown in table 5.4. The spectra are matched with the field redefinitions

$$
d_i^{\text{CY}} = e^{b_r + \mathrm{i}\beta_r} d_i^{\text{Orb}}, \quad i = 1, \ldots, 6, \qquad d_7^{\text{CY}} = e^{-(b_r + \mathrm{i}\beta_r)} d_7^{\text{Orb}} \,.
\tag{5.37}
$$

Table 5.4 indicates that the orbifold and resolution multiplicities of the states d_1 and d_2 are identical, except for resolution E_2, where the multiplicity is -48 rather then 16. The negative multiplicity means that in that resolution one does not see the d_1 and d_2 states, but rather their charge conjugates which we call $\underline{d}_1$ and $\underline{d}_2$. In order

State	Orbifold multiplicity			Resolution multiplicity				U(1) charges
	θ_1	θ_2	θ_3	E$_1$	E$_2$	E$_3$	S	
d_1	16	0	0	16	-48	16	16	(7,-5, 3, 1, 2)
d_2	0	0	16	16	-48	16	16	(3,-5, 7,-1,-2)
d_3	0	16	0	16	16	-48	16	(3, 7,-5,-2,-1)
d_4	16	0	0	16	16	-48	16	(7, 3,-5, 2, 1)
d_5	0	0	16	-48	16	16	16	(-5, 3, 7, 1,-1)
d_6	0	16	0	-48	16	16	16	(-5, 7, 3,-1, 1)
d_7	16	16	16	-80	-80	-80	-80	(-5,-5,-5, 0, 0)
ϕ_1	16	0	0	1$^{\text{st}}$ blowup mode				(10, 0, 0, 0, 0)
ϕ_2	0	16	0	2$^{\text{nd}}$ blowup mode				(0,10, 0, 0, 0)
ϕ_3	0	0	16	3$^{\text{rd}}$ blowup mode				(0, 0,10, 0, 0)

Table 5.4: Excerpt of orbifold and resolution multiplicities of the states in the standard embedding (but in non-standard blowup) of the $T^6/(\mathbb{Z}_2 \times \mathbb{Z}_2)$ orbifold. We list the doublets d_i transforming as $(\mathbf{1}, \mathbf{2})$ and the blowup modes ϕ_r For the orbifold multiplicities we indicate the twisted sector θ_i to which they belong.

to explain this we first consider the (lowest order) superpotential terms for d_1 and d_2 that can be written from the orbifold perspective, namely $W = d_1^{\text{Orb}} d_2^{\text{Orb}} \Phi_2^{\text{BU-Mode}}$. This term indicates that all states get a mass term in blowup. From the blowup perspective the corresponding superpotential can be obtained after field redefinition, and reads $W = d_1^{\text{CY}} d_2^{\text{CY}} e^{b_1+b_3-b_2}$. We observe that in all triangulations but E$_2$ the conditions on the blowup moduli are such that we can interpret this superpotential term as an instantonic mass term. Thus, d_1^{CY} and d_2^{CY} have the same multiplicity in the orbifold point and in resolution, since they are massless modes in a perturbative expansion of the theory, receiving instantonic mass corrections which are not counted by the HRR index. When we pass to triangulation E$_2$ from any other triangulation, the twisted moduli fulfill the condition $b_2 > b_1 + b_3$ and the $d_1^{\text{CY}} d_2^{\text{CY}}$ mass term cannot be thought of as an instantonic correction to a well-defined perturbative theory anymore.

In other words, the supergravity construction fails as soon as b_2 is not smaller than $b_1 + b_3$, and we lose control over the "perturbative" computation of the spectrum: the non-perturbative corrections take over, and a new "perturbative" computation comes at hand, i.e. the supergravity construction made in resolution E$_2$, where the states d_1^{CY} and d_2^{CY} indeed disappear from the spectrum. This argument holds in the very same way for the pairs d_3, d_4 and d_5, d_6, disappearing in resolution E$_1$ and E$_3$, respectively. For the d_7 states the orbifold mass term is such that it cannot be seen as an instantonic correction to a perturbatively massless set of states in any of the triangulations: in supergravity, independently of the resolution type, these states have a large mass and are removed from the massless spectrum.

Let us investigate the underlined states next. Their fate is somewhat dual to that of the non-underlined states. Consider the $\underline{d}_1$ and $\underline{d}_2$ states in triangulation E_2. It is reasonable to assume that their superpotential is

$$W = \underline{d}_1^{\mathrm{CY}} \underline{d}_2^{\mathrm{CY}} e^{b_1 + b_3 - b_2} \tag{5.38}$$

and these states are present as massless states with instantonic mass terms only if the moduli are chosen such that we are in triangulation E_2. In all the other cases the instantonic correction grows, a perturbative perspective is non-tenable, and the underlined states drop from the massless spectrum.

Chapter 6

. . . .

Non-Anomalous Hypercharge Models

In this chapter we discuss how to construct heterotic MSSM-like orbifold models that can be related to their blown-up CY counterparts. On the orbifold, around 200 MSSM-like models have been constructed within the so-called mini-landscape, which is based on the $\mathbb{Z}_{6-\mathrm{II}}$ orbifold [90, 102]. The authors proceed by starting with an orbifold shift vector that breaks the visible sector to E_6 or SO(10). Then Wilson lines are introduced that break the gauge group further down to the Standard Model gauge group. One selection criterion that was imposed is that the hypercharge generator embeds into the GUT group SU(5). After taking into account the running of the coupling constants, this leads to the experimentally observed Weinberg angle at the weak scale given that the GUT scale is around 10^{16} GeV (this requirement has been relaxed in [103] and some additional models were found). However, this prevents us from obtaining a phenomenologically viable model in complete blowup [39, 104]. By construction, the mini-landscape orbifold models have fixed points at which all states are charged under the hypercharge. This happens precisely at those fixed points where the SU(5) is broken to the Standard Model gauge group. If one now wants to consider a full blowup of these theories with line bundles, one has to give a VEV to one state per fixed point that generates the blowup as explained in chapter 5 and hence hypercharge is broken. This can also be seen in the blowup picture: As in (5.2), we expand our gauge flux in terms of exceptional divisors E_r and line bundle vectors V_I^r which are the shifted momenta of the twisted orbifold states located at the fixed point that is resolved by E_r. Since some of the orbifold states are charged under the hypercharge, there will be some internal flux in the hypercharge direction. However, looking at (4.38), we see that the anomaly polynomial I_6 is proportional to the term $\mathrm{tr}(\mathrm{i}\mathcal{F}'\mathrm{i}F')$. Hence the anomaly polynomial is generically non-vanishing and the hypercharge is Green–Schwarz anomalous. Another way of seeing that this gauge flux leads to a

Green–Schwarz anomalous and thus massive hypercharge is by looking directly at the kinetic term of the H field [39, 50] arising from (4.19)

$$\int_X H \wedge *_6 H = (M^2)^{IJ} A_\mu^I A^{\mu J} + \dots, \tag{6.1}$$

where $*_6$ denotes the six-dimensional Hodge star and the mass matrix (M^2) is given by

$$(M^2)^{IJ} = V_r^I V_s^J \int_X E_r \wedge *_6 E_s. \tag{6.2}$$

Using [105]

$$*_6 E_s = \frac{3}{4} \frac{\text{vol}(E_s)}{\text{vol}(X)} J \wedge J - \frac{1}{2} E_s \wedge J \tag{6.3}$$

we can rewrite this as

$$(M^2)^{IJ} = \int_X \left[\frac{3}{4} V_s^J \frac{\text{vol}(E_s)}{\text{vol}(X)} V_r^I E_r \wedge J \wedge J \right] - \int_X \left[\frac{1}{2} V_r^I V_s^J E_r \wedge E_s \wedge J \right]. \tag{6.4}$$

The first integral vanishes due to the DUY equation and thus the mass matrix is given by the second term. In particular choosing $I = J$ in the hypercharge direction, the prefactor is non-zero, and, as can be checked from the intersection numbers, the integral is non-zero as well. In fact, this argument is stronger than the argument using the anomaly polynomial. As we shall see in chapter 7, even non-anomalous U(1)'s can get a Stückelberg mass from this kinetic term if the axions shift under a gauge transformation involving the gauge field A appearing in the Chern–Simons form in H.

From the orbifold point of view this result is not surprising at all: blowing up a fixed point corresponds to giving a VEV to some twisted field. If this carries nontrivial hypercharge, the corresponding generator will be Higgsed and the symmetry is broken. This is why on the orbifold the GUT breaking is done via Wilson lines, which embed as a shift into $E_8 \times E_8$ and lead to a rank-preserving gauge group breaking. Thus the GUT group breaking mechanism used on the orbifold resembles a breaking with an adjoint Higgs field while the GUT group breaking mechanism used in blowup resembles a breaking with a Higgs field that transforms in the **10** of SU(5).

There are several ways of avoiding the problem of a massive hypercharge U(1). The probably most obvious way out is to not blow up those fixed points which induce a flux in the hypercharge direction. While this is a theoretical possibility, the resulting compactification space will be a mixture of a smooth CY where the fixed points are blown up and an orbifold theory at the unresolved fixed points. So it is expected that neither the orbifold nor the supergravity approximation are valid descriptions of the global theory. However, one could hope that GLSMs can provide adequate descriptions of such compactification spaces, since there the orbifold and CY phase are just choices of the FI parameters. This is explored further in section 6.1.

Another possible way out is to choose a different construction mechanism. One way would be to construct a model in which another "hypercharge flux" is switched on in the second E_8 but in the same cohomology class as the first one [106, 107] such that one linear combination is eaten and the other combination stays massless. However, this changes the normalization of the hypercharge generator since it does not originate from a single SU(5) GUT group and thus spoils gauge coupling unification.

Building on the fact that from the orbifold perspective blowing up is the same as giving VEVs to (non-adjoint) matter fields, another possibility is to consider other GUT groups which allow for breaking to the Standard Model gauge group using (antisymmetrized) fundamental matter representations as Higgs fields such as Pati–Salam or flipped SU(5). However, for these models the GUT group is not a single gauge group as in the SU(5) GUT case but rather a product of gauge groups, and hence they are not unifying the gauge couplings and matter representations as nicely as SU(5) or SO(10).

The third possibility, which is the one we want to pursue further in section 6.2, is to construct a gauge bundle that breaks the primordial $E_8 \times E_8$ such that an SU(5) appears which serves as the GUT group. This SU(5) is then broken further with a discrete Wilson line. However, this Wilson line needs to be supported by a nontrivial cycle which in turn requires the compactification manifold to be non-simply connected.

6.1 Orbifolds in partial blowup

As we have seen in section 3.3.5, it is possible to construct GLSM theories which cannot resolve some of the orbifold singularities. These models could provide an interesting way of describing such geometries. Let us look at one example.

6.1.1 Example: $\mathbb{Z}_{6-II}$ orbifold geometry

We describe here only the partially resolved geometry and not the gauge part of the orbifold model. The $\mathbb{Z}_{6-II}$ orbifold twist vector[1] reads $v = \frac{1}{6}(1, 2, -3)$ and hence it acts by a 60 degree rotation on the first complex coordinate, by a 120 degree rotation on the second coordinate and by an inversion on the last complex coordinate. For the case where $T^6 = (T^2)^3$ factorizes, this fixes the complex structure such that the torus lattices correspond to the Lie algebra root lattices of $G_2 \times SU(3) \times (SU(2))^2$. (Alternatively, one could use the root lattice of SU(3) in the first torus, see e.g. [46].) This orbifold action has 12 $\mathbb{Z}_6$ fixed points: the only fixed point locus in the first T^2 is the origin, while there are three and four fixed points under the orbifold action θ in the second and third torus, respectively. In the higher twisted sectors, we encounter fixed tori. in the θ^2 sector, $2v = \frac{1}{3}(1, 2, 0)$ the third torus is fixed and the orbifold is effectively a $(T^2)^2/\mathbb{Z}_3 \times T^2$ orbifold which has six fixed tori: two $\mathbb{Z}_3$ fixed loci are in the first torus (one of which is the $\mathbb{Z}_6$ fixed point which is of course also fixed under

---

[1]There are two different possibilities for an order 6 twist. The other possibility $v = \frac{1}{6}(1, 1, -2)$ gives the $\mathbb{Z}_{6-I}$ orbifold.

the $\mathbb{Z}_3$ action, and the other one is a fixed locus that is not fixed under $\mathbb{Z}_6$) and three fixed loci in the second torus. The third torus is left invariant by the orbifold action. A similar statement holds for the θ^4 sector. In the θ^3 sector, the orbifold action reads $3v = \frac{1}{2}(1, 0, -1)$ and the orbifold is effectively a $(T^2)^2/\mathbb{Z}_2 \times T^2$ with 8 fixed tori: there are two $\mathbb{Z}_2$ fixed loci in the first torus (one of which is again the $\mathbb{Z}_6$ fixed locus and the other one is new) and four $\mathbb{Z}_2$ fixed loci in the third torus, while the second one is invariant. Lastly, the fifth twisted sector looks again like the first and needs not be resolved separately [39].

6.1.2 Example: $\mathbb{Z}_{6-\mathrm{II}}$ GLSM resolution

Following the procedure of section 3.3.5, let us start by describing the minimal resolution of the $\mathbb{Z}_{6-\mathrm{II}}$ before extending this to the partially resolved model [46].

Minimal resolution   To describe the blowup, we start by choosing three elliptic curves describing the $(T^2)^3$. We take $\mathbb{CP}^2_{123}[6]$ for the first, $\mathbb{CP}^2_{111}[3]$ for the second, and $\mathbb{CP}^3_{1111}[2, 2]$ for the third T^2 and in addition fix the complex structure parameter for the first two elliptic curves to be compatible with the orbifold action. For the description of the elliptic curves, we introduce three chiral multiplets $Z_{1,\alpha}$, three chiral multiplets $Z_{2,\beta}$ and four chiral multiplets $Z_{3,\gamma}$, where we followed the usual convention where the first index $i = 1, 2, 3$ specifies the torus and the greek indices $\alpha, \beta = 1, 2, 3$, $\gamma = 1, 2, 3, 4$ specifies the fixed point in the torus. On top of this, we need four chiral-Fermi superfields C_1, C_2, C_3, C_3' whose F terms enforce the four hypersurface conditions for the elliptic curves. Furthermore, we introduce the three U(1) gaugings $\mathrm{U}(1)_{R_1}, \mathrm{U}(1)_{R_2}, \mathrm{U}(1)_{R_3}$ for the three $\mathbb{CP}$ factors. Next we introduce the exceptional coordinates such that their VEV generates the orbifold action and that, when set to zero, the geometry is smooth since the fixed points and fixed tori are removed by virtue of the D terms and the SR ideal derived from them. In contrast to the example of the minimal resolution of the $\mathbb{Z}_3$ orbifold discussed in section 3.3.5, the $\mathbb{Z}_{6-\mathrm{II}}$ cannot be resolved with one exceptional divisor only. For the minimal resolution of the fixed points of $\mathbb{Z}_6$, we need four exceptional coordinates $X_{1,111}, X_{2,11}, X_{3,11}, X_{4,11}$ together with their U(1) scalings. Here we follow the convention where the first index $k = 1, 2, 3, 4$ on the exceptional coordinate labels the twisted sector θ^k and the last three or two greek indices label the fixed point and fixed torus positions in $(T^2)^3$, respectively. For the minimal resolution of the pure $\mathbb{Z}_3$ fixed points (pure meaning those $\mathbb{Z}_3$ fixed points that are not fixed under $\mathbb{Z}_6$ as well) we need two exceptional divisors $X_{2,21}$ and $X_{4,21}$ and their two scalings. Lastly, for the pure $\mathbb{Z}_2$ fixed points, one exceptional divisor $X_{3,31}$ together with its scaling is sufficient. The fields and their charges under the U(1) gaugings are summarized in table 6.1.

In order to check that this model reproduces the expected fixed points and fixed tori in the orbifold regime, we investigate the factorization of the F terms. In the orbifold regime we have $c_a = 0$ and all x fields have non-vanishing VEVs. Consequently, the

	$\mathcal{Z}_{1,i}$	$\mathcal{Z}_{2,j}$	$\mathcal{Z}_{3,k}$	$\mathcal{C}_1$	$\mathcal{C}_2$	$\mathcal{C}_3$	$\mathcal{C}_3'$	$\mathcal{X}_{1,111}$	$\mathcal{X}_{2,i'1}$	$\mathcal{X}_{3,i''1}$	$\mathcal{X}_{4,i'1}$
R_1	i	0	0	-6	0	0	0	0	0	0	0
R_2	0	1	0	0	-3	0	0	0	0	0	0
R_3	0	0	1	0	0	-2	-2	0	0	0	0
$E_{1,111}$	δ_{1i}	$2\,\delta_{1j}$	$3\,\delta_{1k}$	0	0	0	0	-6	0	0	0
$E_{2,\alpha'1}$	$\delta_{\alpha'i}$	$2\,\delta_{1j}$	0	0	0	0	0	0	$-3\,\delta_{\alpha'i'}$	0	0
$E_{3,\alpha''1}$	$\delta_{\alpha''i}$	0	δ_{1k}	0	0	0	0	0	0	$-2\,\delta_{\alpha''i''}$	0
$E_{4,\alpha'1}$	$2\,\delta_{\alpha'i}$	δ_{1j}	0	0	0	0	0	0	0	0	$-3\,\delta_{\alpha'i'}$

Table 6.1: U(1) charge assignment for the minimal GLSM resolution of the $T^6/\mathbb{Z}_{6-\mathrm{II}}$ orbifold. The indices i', α' take values 1 or 2 and the indices i'', α'' take values 1 or 3.

relevant F terms are

$$z_{1,1}^6\, x_{1,111} x_{2,11}^2 x_{3,11}^3 x_{4,11}^4 + z_{1,2}^3\, x_{2,21} x_{4,21}^2 + z_{1,3}^2\, x_{3,31} = 0\,, \tag{6.5a}$$

$$z_{2,1}^3\, x_{1,111} x_{2,11}^2 x_{2,21}^2 x_{4,11} x_{4,21} + z_{2,2}^3 + z_{2,3}^3 = 0\,, \tag{6.5b}$$

$$\kappa\, z_{3,1}^2\, x_{111} x_{3,11} x_{3,31} + z_{3,2}^2 + z_{3,3}^2 = 0\,, \tag{6.5c}$$

$$z_{3,1}^2\, x_{111} x_{3,11} x_{3,31} + z_{3,2}^2 + z_{3,4}^2 = 0\,. \tag{6.5d}$$

The $\mathbb{Z}_6$ fixed points are located at $z_{1,1} = z_{2,1} = z_{3,1} = 0$. Here the F term (6.5a) of the first torus does not factorize. The F term (6.5b) of the second torus factorizes into three parts as in the minimal $\mathbb{Z}_3$ torus case. Likewise, the F terms for the third torus (6.5c) − (6.5d) factorize such that they have four solutions $z_{3,2} = \pm z_{3,3} = \pm z_{3,4}$. Hence, in total we find $1 \cdot 3 \cdot 4 = 12$ $\mathbb{Z}_6$ fixed points as expected.

Under the θ^2 (or θ^4) action the last torus is fixed. The fixed tori are at $z_{1,i'} = z_{2,1} = 0$. For $i' = 1$ the discussion is parallel to the one of the $\mathbb{Z}_6$ given above: The F term solution in the first torus is unique, while in the second torus the F terms factorize into three parts, yielding three solutions. For $i' = 2$ the result is the same: the F term of the first torus does not factorize and the F term in the second torus yields three solutions. Hence we find $3 + 3 = 6$ fixed tori in the second and fourth twisted sectors.

The last independent sector is the θ^3 sector, which leaves the second torus fixed. The fixed tori of this action are at $z_{1,i''} = z_{3,1} = 0$. Again, the F term of the first torus does not factorize for $i'' = 1, 3$ and the F terms in the third torus have 4 solutions each, resulting in a total of $4 + 4 = 8$ $\mathbb{Z}_2$ fixed tori. Hence, by combining these results we have recovered all fixed points/tori of the $\mathbb{Z}_{6-\mathrm{II}}$ orbifold.

Finally, we confirm that all singularities are indeed resolved in our minimal model in the blowup regime. We analyze the D term constraints

$$\sum_i i|z_{1,i}|^2 - 6\,|c_1|^2 = a_1\,, \qquad\qquad \sum_j |z_{2,j}|^2 - 3\,|c_2|^2 = a_2$$

$$\sum_k |z_{3,k}|^2 - 2\,|c_1|^2 - 2\,|c_2|^2 = a_3\,, \tag{6.6a}$$

$$|z_{1,1}|^2 + 2\,|z_{2,1}|^2 + 3\,|z_{3,1}|^2 - 6\,|x_{1,111}|^2 = b_{1,111}\,, \tag{6.6b}$$

$$|z_{1,i'}|^2 + 2\,|z_{2,1}|^2 - 3\,|x_{2,i'1}|^2 = b_{2,i'1}\,, \qquad i' = 1,2\,, \tag{6.6c}$$

$$|z_{1,i''}|^2 + |z_{3,1}|^2 - 2\,|x_{3,i''1}|^2 = b_{3,i''1}\,, \qquad i'' = 1,3\,, \tag{6.6d}$$

$$2\,|z_{1,i'}|^2 + |z_{2,1}|^2 - 3\,|x_{4,i'1}|^2 = b_{4,i'1}\,, \qquad i' = 1,2\,, \tag{6.6e}$$

in the regime where all $a_a, b_{r,ijk} > 0$, but the $b_{r,ijk}$ are taken to be parametrically smaller than the a_a. From the second D term (6.6b) we immediately conclude that the 12 $\mathbb{Z}_6$ fixed points $z_{11} = z_{21} = z_{31} = 0$ are removed and replaced by $x_{111} = 0$. Similarly, (6.6c) and (6.6e) forbid the six θ^2 and θ^4 fixed tori, and (6.6d) forbids the eight θ^3 fixed tori. This way, all fixed points/tori are removed in the blowup regime.

Partial resolution   In order to obtain a corresponding partially resolvable GLSM, we introduce the fields $x_{1,111}, x_{2,\alpha'j}, x_{3,\alpha''1}, x_{3,\alpha''2}, x_{4,\alpha'j}$. The fields $x_{2,\alpha'j}$ and $x_{4,\alpha'j}$ only serve to get a fully resolvable model in the $\mathbb{Z}_3$ sectors θ^2 and θ^4. Hence we concentrate on the effect of the four fields $x_{3,\alpha''1}$ and $x_{3,\alpha''2}$. The VEVs of these fields induce the discrete actions

$$\begin{aligned}
\theta_{1,1} &: (z_{1,1}, z_{3,1}) \mapsto (-z_{1,1}, -z_{3,1})\,, & \theta_{1,2} &: (z_{1,1}, z_{3,2}) \mapsto (-z_{1,1}, -z_{3,2})\,, \\
\theta_{3,1} &: (z_{1,3}, z_{3,1}) \mapsto (-z_{1,3}, -z_{3,1})\,, & \theta_{3,2} &: (z_{1,3}, z_{3,2}) \mapsto (-z_{1,3}, -z_{3,2})\,.
\end{aligned} \tag{6.7}$$

Now, the story is similar to the $\mathbb{Z}_3$ case studied in section 3.3.5. The above actions have four fixed points at $z_{1,\alpha''} = z_{3,\rho} = 0$, $\alpha'' = 1,3$, $\rho = 1,2$. We can define two new linear combinations $\widetilde{\mathrm{U}}(1)_1$ and $\widetilde{\mathrm{U}}(1)_2$, generated by the GLSM charges

$$\begin{aligned}
\widetilde{\mathrm{U}}(1)_1 &:= \mathrm{U}(1)_{R_3} - \mathrm{U}(1)_{E_{3,11}} - \mathrm{U}(1)_{E_{3,12}}\,, \\
\widetilde{\mathrm{U}}(1)_2 &:= \mathrm{U}(1)_{R_3} - \mathrm{U}(1)_{E_{3,31}} - \mathrm{U}(1)_{E_{3,32}}\,.
\end{aligned} \tag{6.8}$$

Their D term constraints are

$$-2|z_{1,1}|^2 + |z_{3,3}|^2 + |z_{3,4}|^2 + 2\,|x_{3,11}|^2 + 2\,|x_{3,12}|^2 = a_3 - b_{3,11} - b_{3,12}\,, \tag{6.9a}$$

$$-2|z_{1,3}|^2 + |z_{3,3}|^2 + |z_{3,4}|^2 + 2\,|x_{3,31}|^2 + 2\,|x_{3,32}|^2 = a_3 - b_{3,31} - b_{3,32}\,. \tag{6.9b}$$

This shows that the 4 fixed tori at $z_{1\alpha''} = z_{3\rho} = 0$, $\alpha'' = 1,3$, $\rho = 3,4$ are present in the orbifold or the blowup regime for any value of the a's and b's and thus cannot be resolved (there may exist solutions in other phases beyond the blowup regime not studied here).

6.2 Non-simply connected orbifold and resolution models

Since non-simply connected CY manifolds cannot be obtained directly from toric geometry, the idea is to start from a model on a simply connected compactification space $\widetilde{X}$ from which we can mod out a discrete $\mathbb{Z}_N$ symmetry. Crucially, this symmetry acts

freely, i.e. without introducing fixed points in the theory, which makes it fundamen-
tally different from the orbifold $\mathbb{Z}_N$ actions which do introduce fixed points. For the
symmetry to act freely, it cannot consist of pure twists, since the origin is always fixed
under a twist. Hence the possibilities which can be used are shifts or shifts combined
with rotations (roto-translations). After modding out the freely acting $\mathbb{Z}_N$ from the
original compactification manifold $\widetilde{X}$, we obtain a new manifold $X = \widetilde{X}/\mathbb{Z}_N$ whose
fundamental group is given by $\pi_1(X) = \mathbb{Z}_N$. This can be used to support a discrete
Wilson line W. The compactification manifold itself stays CY, in particular $h^{1,0} = 0$.
If chosen correctly, the Wilson line can break the SU(5) GUT group, project out the
Higgs triplets, and leave the hypercharge massless. The reason why the hypercharge
does not acquire a mass is that the Wilson line is flat, $c_1(W) = 0$. Hence there does
not appear any flux in $\mathcal{F}$ in the hypercharge direction even though W is embedded in
the hypercharge. Since we start with a model on $\widetilde{X}$ and mod out the freely acting sym-
metry by hand, we have to make sure that also the gauge sector (i.e. the gauge bundle
$\widetilde{V}$) on $\widetilde{X}$ is compatible with the $\mathbb{Z}_N$ action. This leads to the notion of equivariant
structure (see e.g. [37, 108, 109]).

Equivariant structure   We will take each line bundle $\widetilde{\mathcal{L}} \in \widetilde{V}$ to be compatible with
the freely acting involution. Note that the bundle $\widetilde{\mathcal{L}}$ comes with a projection π to the
space $\widetilde{X}$. For the bundle to be well-defined on the quotient space, we need to be able
to lift the freely acting symmetry to the bundle. This means that acting with any
element $g \in \mathbb{Z}_N$, $g : \widetilde{X} \to \widetilde{X}$ there has to be a bundle morphism ϕ_g, $\phi_g : \widetilde{\mathcal{L}} \to \widetilde{\mathcal{L}}$, which
commutes with the bundle projection π and covers the action of g in the base. This is
sometimes phrased by saying that the diagram

$$
\begin{array}{ccc}
\widetilde{\mathcal{L}} & \xrightarrow{\phi_g} & \widetilde{\mathcal{L}} \\
\pi \downarrow & \circlearrowleft & \downarrow \pi \\
\widetilde{X} & \xrightarrow{g} & \widetilde{X}
\end{array}
\tag{6.10}
$$

commutes. Furthermore, we have to impose the cocycle condition $\phi_g \circ \phi_h = \phi_{gh}$. Such
a lifting of the group action is know as an *equivariant structure.*

Modding out the equivariant structure also changes the number of massless states.
It can be shown that for a group G of cardinality $|G|$, the chiral index is given by
$\chi(X, V) = \chi(\widetilde{X}, \widetilde{V})/|G|$. On the level of cohomology, the group G introduces a grad-
ing of the Čech cohomologies, which simply means that we split the $H^i(X, V)$ into
$H^i(X, V, R)$ according to the representation R of G under which the bundle trans-
forms. For the case we are considering, $G = \mathbb{Z}_2$, and the cohomology splits into a piece
that is even and a piece that is odd under the $\mathbb{Z}_2$. Since the multiplicity is reduced by
a factor of $|G| = 2$ when going from $\widetilde{X}$ to X, we have to start with a model with six
SM families.

6.3 Examples for models on non-simply connected compactification spaces

6.3.1 The $\mathbb{Z}_2 \times \mathbb{Z}_2 \times \mathbb{Z}_{2,\text{free}}$ orbifold

Let us begin with the discussion of the underlying orbifold model based on [40]. We start with considering the factorizable case where $T^6 = (T^2)^3$. For this orbifold, the complex structure parameters of the underlying three tori are not fixed and we denote them with τ_i, $i = 1, 2, 3$. Hence the lattice of the ith two-torus is spanned by the lattice vectors $e_{2i-1} = 1$ and $e_{2i} = \tau_i$, which leads to the equivalence relations $z_i \sim z_i + 1 \sim z_i + \tau_i$ where the z_i are the three complex torus coordinates.

There are two orbifold rotations θ_1 and θ_2 with twist vectors $v = \frac{1}{2}(0, 1, -1)$ and $w = \frac{1}{2}(1, 0, -1)$. It is useful to define $\theta_3 := \theta_1 \theta_2$ with twist vector $v_3 = \frac{1}{2}(1, -1, 0)$. In this convention, the ith torus is fixed under θ_i. The other two tori have four $\mathbb{Z}_2$ fixed loci each, such that each twisted sector has 16 fixed tori, which amounts to 48 fixed tori in total. As usual, we label them by a latin index $k = 1, 2, 3$ specifying the twisted sector and two greek indices $\rho, \sigma = 1, 2, 3, 4$ specifying the 16 fixed loci. Up to now, this is a regular $\mathbb{Z}_2 \times \mathbb{Z}_2$ orbifold model. Next we perform a scan over the two orbifold shift vectors V_1, V_2 and the six Wilson lines W_a that result in six chiral families plus Higgses and vector-like exotics that can be decoupled via singlet VEVs. The labeling of the Wilson lines is such that W_a is in the direction of e_a on the T^6.

Now we introduce the $\mathbb{Z}_{2,\text{free}}$ involution. It acts via a simultaneous shift in the three e_{2i} directions by half a lattice vector,

$$\theta_{\text{free}} : (z_1, \, z_2, \, z_3) \mapsto \left(z_1 + \frac{\tau_1}{2}, \, z_2 + \frac{\tau_2}{2}, \, z_3 + \frac{\tau_3}{2}\right). \tag{6.11}$$

Under this shift, the fixed tori located at the origin are mapped to those at $\frac{\tau_i}{2}$, and those at $\frac{1}{2}$ are mapped to those at $\frac{1}{2} + \frac{\tau_i}{2}$. Hence on the orbifold half the fixed points and thus half the twisted matter content are identified under the freely acting symmetry. However, this means that the three Wilson lines W_{2i} in the τ_i directions have to be set equal. We thus have at this level four Wilson lines, the three in the e_{2i-1}-direction of the three tori and one that is the same in all e_{2i} directions. From the action (6.11), we find that the Wilson line W associated with the freely acting element satisfies

$$W = \frac{1}{2}\left(W_2 + W_4 + W_6\right) = \frac{3}{2}W_2, \tag{6.12}$$

which means that it is an order four Wilson line. From modular invariance of the string partition function, we find that [60]

$$2\left[\left(k_1\,V_1 + k_2\,V_2 + n_a\,W_a\right)^2 - \left(k_1\,v + k_2\,w\right)^2\right] \equiv 0 \bmod 2 \quad \forall\, k_i, n_a \in \{0, 1\}, \tag{6.13a}$$

$$4\left(n_a\,W_a + n_0\,W\right)^2 \equiv 0 \bmod 2 \quad \forall\, n_0, n_a \in \{0, 1\}. \tag{6.13b}$$

While the first set of modular invariance conditions (6.13a) leads to the orbifold modular invariance conditions (2.40), the second set (6.13b) has not been discussed before.

On top of allowing for a complete resolution with unbroken hypercharge, this orbifold construction has further phenomenologically very appealing features. As was shown in [110, 111], it allows for avoiding GUT scale threshold corrections to the gauge couplings and therefore leads to precision gauge coupling unification. Furthermore, the freedom in the gauge sector is big enough to get the MSSM gauge group without using all Wilson lines. We can thus leave e.g. W_1 switched off. As a result, the local shifts and thus the local gauge groups and matter spectra at the fixed points that usually differ by the addition of W_1 are now identical. This means that for each MSSM family that resides at such a fixed point there will be a copy at the other. These two (light) families form doublets under the discrete group D_4 which is unaffected by modding out the freely acting symmetry. Note that in the θ_1-sector, there are no fixed loci in the first torus and hence there is no such degeneracy of fixed tori in this twisted sector. Hence by taking the third (heavy) family from this sector it will be a D_4 singlet. The D_4 symmetry is known to be phenomenologically attractive as it can ameliorate supersymmetric flavor problems [112]. In this respect the structure of the model is very similar to the $\mathbb{Z}_{6-\mathrm{II}}$ models discussed in [113–115].

6.3.2 Resolution of the $\mathbb{Z}_2 \times \mathbb{Z}_2 \times \mathbb{Z}_{2,\mathsf{free}}$ orbifold

The blowup of the orbifold geometry was discussed in [60] and we will not go into full detail here. For the blowup, we also proceed in two steps: we first resolve the space $\widetilde{X}$ and subsequently mod out the freely acting involution.

Toric resolutions and intersection numbers   The procedure how to resolve the $\mathbb{Z}_2 \times \mathbb{Z}_2$ singularities was explained in section 3.2.2. To recapitulate, we introduce three inherited divisors R_i, $i = 1, 2, 3$ that descend from the torus, $3 \cdot 4$ ordinary divisors $D_{i,\rho}$ parameterizing the coordinates around the fixed points and $3 \cdot 16 = 48$ resolution divisors $E_{k,\rho\sigma}$ to resolve the 48 fixed tori. Using the toric diagram or equivalently the GLSM gaugings, we find the following linear equivalence relations:

$$
\begin{aligned}
2D_{1,\alpha} &\sim R_1 - \sum_{\gamma} E_{2,\alpha\gamma} - \sum_{\beta} E_{3,\alpha\beta}\,, \\
2D_{2,\beta} &\sim R_2 - \sum_{\gamma} E_{1,\beta\gamma} - \sum_{\alpha} E_{3,\alpha\beta}\,, \\
2D_{3,\gamma} &\sim R_3 - \sum_{\beta} E_{1,\beta\gamma} - \sum_{\alpha} E_{2,\alpha\gamma}\,.
\end{aligned}
\tag{6.14}
$$

These linear equivalences are used to eliminate the $D_{i,\rho}$ and to obtain the divisor basis $R_i, E_{k,\rho\sigma}$. As a next step, we read off the intersection numbers from the auxiliary polyhedra or we calculate them from the GLSM F terms. The result depends on the choice of the SR ideal. Choosing the same SR ideal and thus the same triangulation

at all fixed points, we obtain the intersection numbers listed in table 3.1. This gives us what we need to proceed to the next step, namely the investigation of the gauge sector.

Gauge flux   Using the matching techniques outlined in chapter 5, we construct the corresponding bundle vectors and solve the BIs and the (loop-corrected) DUY equations [116] for a specific choice of the SR ideal (i.e. using triangulation E_1 given in figure 3.5 at all fixed tori). In principle we have to choose 51 different line bundle vectors. However, in order to match the orbifold construction, we only want flux on the exceptional divisors and not on the inherited divisors, hence this number reduces to 48. Furthermore, out of the six possible Wilson lines, one Wilson line W_1 is trivial and three are equal, $W_2 = W_4 = W_6$. As explained above, $W_1 = 0$ leads to the same shifted momenta and matter content at those fixed points which differ only by this Wilson line. Similarly, the second condition also leads to the same matter content at those fixed points which are later identified under the freely acting involution. For example the shifted momenta of the twisted states at the fixed points $(\theta_1; 0)$ are given by $P_{\rm sh} = P + V_1$. Likewise, the shifted momenta at the fixed points $(\theta_1; \frac{1}{2}\tau_2 + \frac{1}{2}\tau_3)$ read $P + V_1 + W_4 + W_6 = P + V_1 + 2W_4 \equiv P + V_1$. We make a simplified ansatz in these cases and choose those orbifold states which have exactly the same shifted momenta (i.e. the same choice of the $E_8 \times E_8$ root vector P) as blowup modes. This leads to an ansatz for the gauge flux including only 16 line bundle vectors instead of 48:

$$V_{i,22} = V_{i,11}\,, \quad V_{i,21} = V_{i,12}\,, \quad V_{i,24} = V_{i,13}\,, \quad V_{i,23} = V_{i,14}\,, \tag{6.15a}$$

$$V_{i,42} = V_{i,31}\,, \quad V_{i,41} = V_{i,32}\,, \quad V_{i,44} = V_{i,33}\,, \quad V_{i,43} = V_{i,34}\,, \qquad i = 1,2,3, \tag{6.15b}$$

$$V_{j,3\rho} = V_{j,1\rho}\,, \quad V_{j,4\rho} = V_{j,2\rho}\,, \quad j = 2,3; \quad \rho = 1,\dots,4\,, \tag{6.15c}$$

As the objective here is not to obtain a full classification, but rather to find at least some solutions, we do not mind that this ansatz is far from generic.

Next, we use the observation [39, 60] that some of the Bianchi identities enforce that the line bundle vectors are chosen from the orbifold shifted momenta corresponding to massless twisted states without oscillators: From the orbifold mass formula (2.42) we find that for the $\mathbb{Z}_2 \times \mathbb{Z}_2$ orbifold these states satisfy $P_{\rm sh}^2 = \frac{3}{2}$. This matches with the Bianchi identities (4.37) when integrated over the inherited divisors R_i, which yield $V_r^2 = \frac{3}{2}$. Inserting these assumptions into the Bianchi identities, the complete system of equations simplifies tremendously:

$$(V_{1,11}+V_{1,12}+V_{1,31}+V_{1,32})\cdot V_{2,11} = 1\,, \quad (V_{1,11}+V_{1,12}+V_{1,31}+V_{1,32})\cdot V_{2,12} = 1\,, \tag{6.16a}$$

$$(V_{1,13}+V_{1,14}+V_{1,33}+V_{1,34})\cdot V_{2,13} = 1\,, \quad (V_{1,13}+V_{1,14}+V_{1,33}+V_{1,34})\cdot V_{2,14} = 1\,, \tag{6.16b}$$

$$(V_{1,11}+V_{1,12}+V_{1,13}+V_{1,14})\cdot V_{3,11} = 1\,, \quad (V_{1,11}+V_{1,12}+V_{1,13}+V_{1,14})\cdot V_{3,12} = 1\,, \tag{6.16c}$$

$$(V_{1,31}+V_{1,32}+V_{1,33}+V_{1,34})\cdot V_{3,13} = 1\,, \quad (V_{1,31}+V_{1,32}+V_{1,33}+V_{1,34})\cdot V_{3,14} = 1\,. \tag{6.16d}$$

In particular, instead of 48 Diophantine equations involving scalar products of different bundle vectors, only eight of them remain.

On top of this set of equations we impose the zero slope DUY equations (2.30), or rather their one-loop corrected version [116],

$$\frac{1}{2} \int_X J \wedge J \wedge \mathcal{F} = \xi_{1L} = \frac{e^{2\phi}}{16\pi} \int_X \frac{1}{(2\pi)^3} \left[\left(\mathrm{tr}(\mathrm{i}\mathcal{F}')^2 - \frac{1}{2}\mathrm{tr}\mathcal{R}^2 \right) \mathcal{F}' + (\mathcal{F}' \to \mathcal{F}'') \right] . \tag{6.17}$$

Spectrum   Since $\widetilde{X}$ has $h^{1,1} = 51$, a direct computation of the various cohomology groups is again beyond our computational power, so we have to rely on the calculation of the chiral index for the equivariant bundle as explained above. Matching the massless spectrum by checking which orbifold superpotential terms occur is not so easy for this orbifold, since there are subtleties concerning various choices of discrete torsion on the orbifold and various choices of triangulations in blowup, cf. section 5.3. An example VEV configuration that leads to three MSSM families (plus some exotics) after using the freely acting Wilson line can be found in [60].

Chapter 7

....

ANOMALIES AND R SYMMETRIES

On orbifolds, it has been shown that R symmetries play an important role for phenomenology. Imposing anomaly universality on the orbifold, there is a unique $\mathbb{Z}_4$ R symmetry that can forbid the Higgs μ-term and is compatible with SO(10) GUT charge assignment [117]. In [118], the authors identified such a $\mathbb{Z}_4$ R symmetry for the orbifold constructions introduced in section 6.2. The $\mathbb{Z}_2 \times \mathbb{Z}_2$ orbifold seems particularly fruitful for such a symmetry, since following the discussion in section 2.4, a $\mathbb{Z}_N$ orbifold plane gives rise to a $\mathbb{Z}_{2N}$ R symmetry. As we have seen in section 4.3, on a generic (smooth) CY anomaly universality is not given anymore since there are $h^{1,1}$ axions (the partners of the Kähler parameters) that cancel anomalies and do not exhibit a universal coupling. In fact, their coupling is determined in terms of the background gauge flux $\mathcal{F}$. Since this appears in the gauge kinetic function [119], the axionic couplings with respect to the GUT group have to be approximately universal or balanced by GUT threshold corrections in order not to spoil gauge coupling unification.

In any case, based on the fact that the R symmetries are powerful symmetries on the orbifold, it is interesting to see what happens to them in blowup. In this chapter, we study this question from the GLSM point of view using a toy model, namely the blowup of the $\mathbb{Z}_3$ orbifold in standard embedding with line bundle vectors. At the same time, this example is illustrative with regards to other aspects discussed here as well. First, it is an example where we employ a GLSM resolution where not all $h^{1,1}$ Kähler parameters are independent. Hence we can investigate the cohomology groups of the model independently although its full resolution has a huge SR ideal. Second, due to its simplicity, it provides a traceable example for a model where a non-anomalous symmetry becomes massive in blowup. Finally, it provides an example where we employ equivariant cohomology to check whether a given symmetry is an R symmetry.

7.1 Orbifold and resolution model

The model we are considering is based on the $T^6/\mathbb{Z}_3$ orbifold in $\mathrm{E}_8 \times \mathrm{E}_8$ heterotic string theory in standard embedding. This means that the orbifold twist and shift shift vector

are given by

$$v = \frac{1}{3}(1, 1, -2), \qquad V = \frac{1}{3}\left(1, 1, -2, 0^5\right)\left(0^8\right) \tag{7.1}$$

and all Wilson lines are switched off. The shift breaks the primordial gauge group to $E_6 \times SU(3) \times E_8$. In particular, there is no anomalous $U(1)$. The orbifold action θ on the three two-tori with complex coordinates z_i has 27 fixed points. The massless chiral spectrum is given by

$$3\left(\mathbf{27}, \overline{\mathbf{3}}, \mathbf{1}\right) + 27\left[\left(\mathbf{27}, \mathbf{1}, \mathbf{1}\right) + 3\left(\mathbf{1}, \mathbf{3}, \mathbf{1}\right)\right]. \tag{7.2}$$

To perform the blowup, we follow the by now familiar procedure: First, we replace the fixed points of the orbifold by 27 exceptional divisors $E_{\alpha\beta\gamma} \equiv E_r$, where $\alpha, \beta, \gamma = 1\ldots 3$ label the fixed points on the three tori and $r = 1\ldots 27$. This resolves the geometry. Then, we introduce an internal Abelian $(1,1)$ gauge flux $\mathcal{F} = E_r V_r^I H_I$ which has support at the exceptional divisors only. The line bundle vectors are identified with the shifted momenta of the orbifold blowup modes. In our case they read

$$V_1 = \frac{1}{3}\left(\begin{array}{cccc} 2, & 2, & 2, & 0, 0^4\end{array}\right)\left(0^8\right), \tag{7.3a}$$

$$V_2 = \frac{1}{3}\left(-1, -1, -1, \quad 3, 0^4\right)\left(0^8\right), \tag{7.3b}$$

$$V_3 = \frac{1}{3}\left(-1, -1, -1, -3, 0^4\right)\left(0^8\right). \tag{7.3c}$$

We assign V_1 to the first k fixed points, V_2 to the next p fixed points and V_3 to the remaining $q = 27 - k - p$ ones. They are chosen such that the flux quantization condition, the Bianchi identities and the DUY equations are satisfied. Since the bundle vectors are given by shifted momenta of the twisted states $(\mathbf{27}, \mathbf{1}, \mathbf{1})$, the flux quantization condition $3V_r^I \in \Lambda_{E_8 \times E_8}$ is automatically fulfilled. The Bianchi identities $V_r^2 = \frac{4}{3}$ are solved by choosing the blowup modes to correspond to the massless twisted orbifold states without oscillators. For the DUY equations, we expand the Kähler form $J = a_i R_i - b_r E_r$, where the Kähler cone is given by $a \gg b > 0$. By construction, the DUY equations can be fulfilled for all configurations (k, p, q) with arbitrarily large exceptional divisor volumes. They can be written as

$$\sum_{r=1}^{k} \text{vol}(E_r) \cdot V_1 + \sum_{r=k+1}^{k+p} \text{vol}(E_r) \cdot V_2 + \sum_{r=k+p+1}^{k+p+q} \text{vol}(E_r) \cdot V_3 = 0. \tag{7.4}$$

Since in our model the bundle vectors add up to zero, this simplifies to the condition

$$\sum_{r=1}^{k} \text{vol}(E_r) = \sum_{r=k+1}^{k+p} \text{vol}(E_r) = \sum_{r=k+p+1}^{k+p+q} \text{vol}(E_r). \tag{7.5}$$

Each of the bundle vectors in (7.3) breaks E_6 to a differently embedded $SO(10) \times U(1)$,

but only two breakings are independent. We are thus left with the gauge group

$$G = SO(8) \times U(1)_A \times U(1)_B \times SU(3) \times E_8 \,. \tag{7.6}$$

The two U(1) factors are taken to be generated by

$$T_A = \left(2, 2, 2, 0, 0^4\right)\left(0^8\right) \,, \qquad T_B = \left(0, 0, 0, 2, 0^4\right)\left(0^8\right) \,. \tag{7.7}$$

Using this normalization, all charges are integer. The U(1) generators are related to the bundle vectors (7.3) via

$$V_1 = \frac{1}{3} T_A \,, \quad V_2 = -\frac{1}{6} T_A + \frac{1}{2} T_B \,, \quad V_3 = -\frac{1}{6} T_A - \frac{1}{2} T_B \,. \tag{7.8}$$

The induced decomposition of the **27** (via $SO(10) \times U(1)$) is

$$
\begin{aligned}
\mathbf{27} &\longrightarrow \mathbf{16}_1 + \mathbf{10}_{-2} + \mathbf{1}_4 \\
&\longrightarrow (\mathbf{8}_\mathrm{s})_{1,-1} + (\mathbf{8}_\mathrm{c})_{1,1} + (\mathbf{8}_\mathrm{v})_{-2,0} + \mathbf{1}_{-2,-2} + \mathbf{1}_{-2,2} + \mathbf{1}_{4,0} \,.
\end{aligned}
\tag{7.9}
$$

This illustrates nicely the correspondence between the Higgsing of the gauge group by assigning VEVs to twisted orbifold states and the breaking of the gauge group on the CY side. The three bundle vectors (7.3) on the CY correspond to a VEV of the three singlets in (7.9) on the orbifold side. The massless chiral spectrum depends on the distribution (k, p, q) of the bundle vectors over the 27 fixed points. The untwisted sector and the twisted $(\mathbf{1}, \mathbf{3})$'s in the orbifold spectrum (7.2) always contribute $72 \cdot (\mathbf{1}, \mathbf{3})$ and $9 \cdot (\mathbf{8}, \mathbf{3})$, while some of the twisted $\mathbf{8}$'s get massive or vector-like. As a result, we get

$$(p - q) \cdot (\mathbf{8}_\mathrm{v}, \mathbf{1}) + (k - q) \cdot (\mathbf{8}_\mathrm{s}, \mathbf{1}) + (k - p) \cdot (\mathbf{8}_\mathrm{c}, \mathbf{1}) \,. \tag{7.10}$$

Furthermore, as discussed previously, the U(1) charges of the states from the twisted sector are shifted by the charges of the blowup modes at the respective fixed point according to the field redefinitions

$$\Phi_r^{\mathrm{BU\text{-}Mode}} = e^{b_r + i\beta_r} \,, \qquad \Phi_i^{\mathrm{CY}} = e^{-(b_r + i\beta_r)} \, \Phi_{r,i}^{\mathrm{Orb}} \,. \tag{7.11}$$

where b_r are the Kähler moduli of the rth blowup cycle dual to E_r, and β_r are the localized axions.

7.1.1 Example for anomaly-free but massive U(1) symmetry

Using this blowup model, let us provide an example where a U(1) symmetry is non-anomalous and yet massive. For this we have to calculate the anomaly polynomial in blowup which is done in the same way as in section 5.2. Here, the expression is much simpler since there are only two U(1) symmetries in blowup instead of eight. As a cross-check, we also matched the blowup anomalies to those on the orbifold, but we will not go into the details, since the match has already been performed in all fine prints

in section 5.2. The resulting 4D anomaly polynomial in blowup reads

$$
\begin{aligned}
I_6 \sim{} & F_A^3 \cdot \left(\frac{k-6}{12}\right) + F_A F_B^2 \cdot \left(\frac{k-18}{4}\right) \\
& + F_A \left[\operatorname{tr}(\mathrm{i}F_{\mathrm{SU}(3)})^2 + \operatorname{tr}(\mathrm{i}F_{\mathrm{SO}(8)})^2 - \frac{7}{12}\operatorname{tr}R^2\right] \cdot \left(\frac{k-9}{2}\right) \\
& + F_B \left[\frac{1}{8}F_B^2 + \frac{1}{48}F_A^2 + \operatorname{tr}(\mathrm{i}F_{\mathrm{SU}(3)})^2 + \operatorname{tr}(\mathrm{i}F_{\mathrm{SO}(8)})^2 - \frac{7}{12}\operatorname{tr}R^2\right] \cdot \left(\frac{p-q}{2}\right) .
\end{aligned}
\tag{7.12}
$$

From this it is evident that $\mathrm{U}(1)_B$ is non-anomalous if $p = q$, that the cubic $\mathrm{U}(1)_A$ anomaly vanishes for $k = 6$, and that the mixed $\mathrm{U}(1)_A$–non-Abelian anomalies vanish for $k = 9$. In particular, there is no configuration where $\mathrm{U}(1)_A$ is anomaly-free.

Although $\mathrm{U}(1)_B$ is non-anomalous in some bundle configurations, both $\mathrm{U}(1)$'s are always massive. This is due to the fact that the axion associated with $\mathrm{U}(1)_B$ always feels a shift proportional to the gauge parameter and hence the associated gauge boson gets a Stückelberg mass. This can also be seen directly by investigating the mass matrix for the 4d gauge bosons discussed at the beginning of chapter 6,

$$
\left(M^2\right)^{IJ} = V_r^I V_s^J \cdot \int_X E_r \wedge *_6 E_s .
\tag{7.13}
$$

This takes the form

$$
\left(M^2\right)^{IJ} = \frac{9}{2} V_r^I V_s^J \delta_{rst} b_t = \frac{1}{2}
\begin{pmatrix}
m_1 & m_1 & m_1 & m_2 \\
m_1 & m_1 & m_1 & m_2 \\
m_1 & m_1 & m_1 & m_2 \\
m_2 & m_2 & m_2 & m_3
\end{pmatrix} ,
\tag{7.14}
$$

and $\left(M^2\right)^{IJ} = 0$ for $I, J > 4$. The entries m_i are given by

$$
\begin{aligned}
m_1 &= 4\sum_{r=1}^{k} b_r + \sum_{r=k+1}^{k+p} b_r + \sum_{r=k+p+1}^{27} b_r , \qquad m_2 = -3\sum_{r=k+1}^{k+p} b_r + 3\sum_{r=k+p+1}^{27} b_r , \\
m_3 &= 9\sum_{r=k+1}^{k+p} b_r + 9\sum_{r=k+p+1}^{27} b_r ,
\end{aligned}
\tag{7.15}
$$

which means that $\left(M^2\right)^{IJ}$ always has rank two in the blowup phase.

7.2 Remnant discrete symmetries

7.2.1 Non-R symmetries

Since the blowup is generated from twisted orbifold fields that get a VEV, discrete symmetries can arise from remnants of the $\mathrm{U}(1)$ gauge groups under which the blowup fields were charged.

In the family of models at hand, the discrete non-R symmetries are the ones left over from the two broken U(1)'s. One finds from the branching of the **27** of E_6 in (7.9) that the bundle vectors (7.3) correspond to the blowup modes

$$(\mathbf{1}, \mathbf{1})_{4,0}, \quad (\mathbf{1}, \mathbf{1})_{-2,-2}, \quad (\mathbf{1}, \mathbf{1})_{-2,2}. \tag{7.16}$$

When these get a VEV, a $\mathbb{Z}_2 \times \mathbb{Z}_2$ subgroup survives. It is easy to check that both $\mathbb{Z}_2$ factors are non-anomalous.

7.2.2 R symmetries

The discussion of remnant R symmetries is more involved. R symmetries are those transformations that do not commute with supersymmetry, which in superspace language means that the Grassmann coordinate θ transforms nontrivially. Since there is only one such coordinate in 4D $\mathcal{N} = 1$ supersymmetry, there can be at most a single U(1) or $\mathbb{Z}_N$ R symmetry: If there are several such symmetries, they can be redefined such that only one of them transforms θ, while the others act as usual non-R symmetries. The normalization is commonly chosen such that θ transforms with charge 1, which implies that the superpotential W has charge 2. This convention only fixes the charges of the fields up to an admixture of non-R symmetries that leave θ invariant. Furthermore, a $\mathbb{Z}_2$ R symmetry can be turned into a non-R symmetry by a combination with a sign reversal on the fermions, so $\mathbb{Z}_2$ symmetries do not lead to true R symmetries.

In the following, we begin with reviewing R symmetries from the orbifold point of view. After that, we discuss them from the Calabi–Yau perspective.

R symmetries on the orbifold

R symmetries on the $(T^2)^3/\mathbb{Z}_3$ orbifold have already been discussed in section 2.4.3, so let us only briefly repeat the result. The orbifold possesses a discrete $(\mathbb{Z}_3)^3$ rotational symmetry stemming from rotating each torus independently by $\frac{2\pi i}{3}$. We call this symmetry a $\mathbb{Z}_6^R$ symmetry where fermion charges are quantized in multiples of $\frac{1}{3}$, bosonic ones in multiples of $\frac{2}{3}$, and θ has charge 1. Note that in particular the twisted states Φ corresponding to the **27** of E_6 have $R = \frac{1}{3}(0, 1, 1, 1)$ and thus transform with charge $\frac{1}{9}$ under each $\mathbb{Z}_3$ sublattice rotation.

To find unbroken R symmetries after switching on VEVs to generate the blowup, we seek combinations of the three sublattice rotations $\mathcal{R}_i$ and the two U(1) generators $T_{A,B}$ which leave the blowup modes invariant,

$$\mathbf{1}_{q_A,q_B} \longrightarrow (\mathcal{R}_1)^r (\mathcal{R}_2)^s (\mathcal{R}_3)^t (T_A)^{q^A} (T_B)^{q^B} \mathbf{1}_{q_A,q_B} = \mathbf{1}_{q_A,q_B}, \tag{7.17}$$

for $(q_A, q_B) = (4, 0)$, $(-2, 2)$ and $(-2, -2)$. This implies that $r + s + t \equiv 0 \mod 3$, i.e. only a trivial $\mathbb{Z}_2$ R symmetry remains. Note that by combining with discrete non-R $\mathbb{Z}_N$ symmetries, higher $\mathbb{Z}_N$ R symmetries (with $N > 3$) can be obtained. For the examples

presented here, the discrete non-R symmetries are $\mathbb{Z}_2 \times \mathbb{Z}_2$, such that in this case no R symmetry enhancement by mixing in other symmetries is possible. Hence for the models at hand it is expected that no nontrivial R symmetry will be left after blowing up.

R symmetries from the blowup perspective

Next, we investigate how to reproduce this from the perspective of the resolution space. One way to uncover discrete R symmetries on the resolution Calabi–Yau manifolds is to look at the GLSM realization. For the sake of clarity, we focus on the $(k, p, q) = (9, 9, 9)$ model, where the blowup can be described with just three exceptional coordinates. However, using the results from [46], the analysis can be repeated for more general configurations and for other orbifolds in the same fashion.

This GLSM has already been discussed at the end of section 3.3.5, so again we only repeat the defining equations here for convenience. We obtain the F term equations for the c_i

$$0 = z_{1,1}^3 x_{111} + z_{1,2}^3 x_{211} + z_{1,3}^3 x_{311} \,, \tag{7.18a}$$

$$0 = z_{2,1}^3 x_{111} x_{211} x_{311} + z_{2,2}^3 + z_{2,3}^3 \,, \tag{7.18b}$$

$$0 = z_{3,1}^3 x_{111} x_{211} x_{311} + z_{3,2}^3 + z_{3,3}^3 \,, \tag{7.18c}$$

specifying the complete intersection, and the D term equations

$$|z_{1,\alpha}|^2 + |z_{2,1}|^2 + |z_{3,1}|^2 - 3|x_{\alpha11}|^2 = b_{\alpha11} \,, \qquad \alpha \in \{1, 2, 3\} \,, \tag{7.19a}$$

$$\sum_{\rho=1}^{3} |z_{i,\rho}|^2 = a_i \,, \qquad i \in \{1, 2, 3\} \,, \tag{7.19b}$$

specifying the geometric phase (the VEVs of the c_i have already been set to zero). The $z_{i,\rho}$ correspond to the inherited divisors, where $i = 1, 2, 3$ labels the torus and $\rho = 1, 2, 3$ labels the fixed point. The three coordinates $x_{\alpha11}$ label the three exceptional divisors where each resolves 9 of the 27 orbifold fixed points. Finally, the FI parameters a_i and $b_{\alpha11}$ are related to the sizes of the tori and the exceptional divisors, respectively. We have chosen a phase where $a_i \gg 0$ and $a_i \gg b_{\alpha11}$. For $b_{\alpha11} \gg 0$, one uncovers the blowup regime, while $b_{\alpha11} \to -\infty$ yields the orbifold regime.

To find R symmetries in this picture, we have to find holomorphic automorphisms of the ambient space which leave (7.18) and (7.19) invariant, and under which the holomorphic $(3, 0)$-form Ω transforms nontrivially [108, 120]. This is true because Ω is related to the four-dimensional SUSY generators via the internal spinor ζ by $\Omega_{ijk} = \zeta^T \Gamma_{ijk} \zeta$, where Γ_{ijk} is a product of 3 gamma matrices.[1] Ω can acquire at most a phase $\gamma = e^{2\pi i\alpha}$, $\alpha \in \mathbb{R}$, i.e. $\Omega \mapsto \gamma\Omega$. This means that $\zeta \to \pm\gamma^{\frac{1}{2}}\zeta$ and thus the superpotential W transforms as $W \to \gamma W$, i.e. like Ω. On the orbifold, the twisted $\mathbf{27}^3$ coupling is allowed, so the $\mathbf{27}$ of E_6 has to transform with a phase which is an integer multiple of $\gamma^{\frac{1}{3}}$.

---

[1]Alternatively, this can be seen from the Gukov–Vafa–Witten [121] superpotential $W = \int \Omega \wedge H$.

Representation	Bundles
$(\mathbf{1}, \mathbf{3})$	$\mathcal{O}(0,0,0,4,-2,-2) \oplus \mathcal{O}(0,0,0,-2,4,-2) \oplus \mathcal{O}(0,0,0,-2,-2,4)$
$(\mathbf{8}, \mathbf{3})_{\mathrm{v,s,c}}$	$\mathcal{O}(0,0,0,2,-1,-1), \mathcal{O}(0,0,0,-1,2,-1), \mathcal{O}(0,0,0,-1,-1,2)$
$(\mathbf{8}, \mathbf{1})_{\mathrm{v,s,c}}$	$\mathcal{O}(0,0,0,0,-3,3), \mathcal{O}(0,0,0,-3,0,3), \mathcal{O}(0,0,0,-3,3,0)$

Table 7.1: The bundles whose cohomology groups determine the chiral spectrum of the $T^6/\mathbb{Z}_3$ blowup. The number of left-chiral representations in each case is given by $h^1(V) - h^2(V)$.

In our case, we find that the F and D term constraints are invariant under the $\mathbb{Z}_3$ transformations (note that not all of these symmetries are independent, since some can be related using the GLSM U(1) charges):

$$z_{i,\alpha} \to e^{\frac{2\pi i}{3} \cdot k_{i\alpha}} z_{i,\alpha}, \qquad i, \alpha = 1, 2, 3. \tag{7.20}$$

Furthermore, there is the $\mathbb{Z}_3$ symmetry

$$(x_{111}, x_{211}, x_{311}) \to e^{\frac{2\pi i}{3} \cdot k}(x_{111}, x_{211}, x_{311}). \tag{7.21}$$

It should be noted that the presence of these symmetries is inherited from the symmetries of the orbifold. In other words, the polynomials in (7.18) are not the most general ones in $(\mathbb{CP}^2[3])^3$ but have been chosen to be compatible with the orbifold action. In particular, the complex structure of the elliptic curves has been frozen at $\tau = e^{\frac{2\pi i}{3}}$, so that we are already at a special sublocus of the whole moduli space which exhibits enhanced symmetries. At even more special points in moduli space, there appear certain symmetries under coordinate exchange: When $a_2 = a_3$, there is a symmetry

$$z_{2,\alpha} \leftrightarrow z_{3,\alpha}, \quad \alpha = 1, 2, 3. \tag{7.22}$$

When $b_1 = b_2 = b_3$, we find an S_3 permutation symmetry acting on

$$\{(z_{1,1}, x_{111}), (z_{1,2}, x_{211}), (z_{1,3}, x_{311})\}. \tag{7.23}$$

We can interpret these as exchanges of exceptional or inherited divisors, which are symmetries whenever the corresponding volumes, given by the Kähler parameters a_i and b_α, are equal. Focusing on the $\mathbb{Z}_3$ symmetries, we find combinations such that $\Omega \to e^{\frac{2\pi i}{3}}\Omega$. Thus $\gamma = e^{\frac{2\pi i}{3}}$ and the $\mathbf{27}$ of E_6 transforms with $e^{\frac{2\pi i}{9}}$, which reproduces the quantization in multiples of $\frac{1}{9}$ on the orbifold under sublattice rotations.

So far, we have used the GLSM merely as a book-keeping device to realize the geometry of the blowup space, but it contains more information. In particular, from the preceding discussion it seems that the $\mathbb{Z}_3$ symmetries (7.21) cannot be broken in the GLSM, since the $z_{i,\alpha}$ appear only cubed or as absolute values. This seems puzzling, since the R symmetries are generically broken from the orbifold point of view. On the other hand, from the GLSM point of view the $\mathbb{Z}_3$ symmetries are merely accidental symmetries, and we would expect them to be broken by quantum effects. However, up to now we have not incorporated the gauge bundle into the GLSM description. To make contact to the

Charges	Λ^a	Λ^4	Λ^I	N_{ab}	N_4^a	N^{a4}	N_{aI}	N_a^I	N_{4I}	N_4^I
E_{111}	2	0	0	-4	2	2	-2	-2	0	0
E_{211}	-1	3	0	2	-4	2	1	1	-3	-3
E_{311}	-1	-3	0	2	2	-4	1	1	3	3

(a) Charges of the chiral-Fermi fields and of the polynomials arising as kinetic deformations.

Polynomial	Some contributing monomials
N_{ab}	$x_1^2\left(z_{21}\bar{z}_{22}\right)^2, \left(\bar{z}_{11}^2 z_{12}z_{13}\right)^2, x_1\bar{x}_2\bar{x}_3\bar{z}_{21}z_{22}$
$N_{a,I},\ N_a^I$	$x_2 x_3 z_{21}^2 \bar{z}_{22}^2, z_{11}^2\bar{z}_{12}\bar{z}_{13}, \bar{x}_1\bar{z}_{21}\bar{z}_{22}$
$N_{4I},\ N_4^I$	$\bar{x}_2 x_3, z_{12}^3\bar{z}_{13}^3, x_1\bar{x}_3^2 z_{21}^3\bar{z}_{22}^3$

(b) Some monomials contributing to the chiral massless spectrum.

Table 7.2: Charges of the chiral-Fermi multiplets Λ and the deformation coefficients N and some of the contributing monomials. The monomials for N_4^a and N^{a4} can be obtained from N_{ab} by permutations of indices.

blowup model, we consider the bundle $V = \mathcal{O}(0,0,0,2,-1,-1)^3 \oplus \mathcal{O}(0,0,0,0,3,-3)$ in analogy to the blowup modes (7.3). The chiral spectrum is then given by the bundle cohomology groups listed in table 7.1. Using `cohomCalg` [38, 122] we can calculate the chiral spectrum of the $(9,9,9)$ model,

$$24\,(\mathbf{1},\mathbf{3})_{4,0} + 24\,(\mathbf{1},\mathbf{3})_{-2,-2} + 24\,(\mathbf{1},\mathbf{3})_{-2,2} + 3\,(\mathbf{8}_{\mathrm{v}},\mathbf{3})_{-1,1} + 3\,(\mathbf{8}_{\mathrm{s}},\mathbf{3})_{-1,-1} + 3\,(\mathbf{8}_{\mathrm{c}},\mathbf{3})_{2,0}$$

which is consistent with the orbifold picture.

The transformation of the states under the discrete symmetries can be calculated along the lines discussed chapter 6 using equivariant bundle cohomology. Fortunately, `cohomCalg` also provides an implementation for this. Starting from the symmetries (7.20) and (7.21), which are given in terms of their actions on the GLSM coordinates, we have to determine how they act on the respective cohomologies of our bundle restricted to the Calabi–Yau submanifold. As in the case of the chiral spectrum, this is done by relating the gauge bundle of the ambient space to the gauge bundle on the Calabi–Yau via the Koszul resolution. The transformation of the matter states, which are determined by polynomials in the homogeneous coordinates of the ambient space, is then given in terms of the action of the symmetry on the gauge bundle.[2]

While this should work in principle, there are unfortunately many subtleties concerning anomalies in (2,0) GLSMs as discussed in chapter 8. In particular, there are GLSM anomalies for which their counterpart on the orbifold or the CY is elusive. Also the charge assignment used for this manifold leads to GLSM anomalies. For this reason, we want to resort to the non-compact $\mathbb{C}^3/\mathbb{Z}_3$ orbifold, where a consistent connection between the orbifold and the GLSM bundle description is known [123]. The bundle is described by chiral-Fermi multiplets $\Lambda^{\hat{I}}$, $\hat{I} = 1, \ldots, 16$, which correspond to the Cartan

---

[2]If the bundle is not globally generated, one can twist it by an equivariant ample line bundle and check the transformation for the twisted bundle.

subalgebra of $E_8 \times E_8$. The $\Lambda^{\hat{I}}$ are charged under the exceptional symmetries $U(1)_{E_{\alpha 11}}$, with charges given by the line bundle vectors (7.3) corresponding to the orbifold shifted momenta. Now the coordinates show up when determining the charged spectrum [123]: The massless target space modes $\phi_{4d}(x^{\mu})$ appear as deformations of the GLSM kinetic terms for the $\Lambda^{\hat{I}}$ as

$$\int D^2 \theta^+ \phi_{4d} N_{\hat{I}}^{\hat{j}}(z_{i\alpha}, x_{\alpha 11}) \Lambda^{\hat{I}} \overline{\Lambda}_{\hat{j}} + \phi'_{4d} N_{\hat{I}\hat{j}}(z_{i\alpha}, x_{\alpha 11}) \Lambda^{\hat{I}} \Lambda^{\hat{j}} + \text{h.c.} \qquad (7.24)$$

Here the $N^{\hat{I}\hat{j}}$ and $N_{\hat{I}}^{\hat{j}}$ denote polynomials in the coordinate fields which are chosen such that the expression is gauge invariant. Note that this is a Kähler potential term, so the N's need not be holomorphic.

While locally at each fixed point the gauge group is $SU(3) \times SO(10) \times U(1) \times E_8$, the global model in the end has the gauge group $SU(3) \times SO(8) \times U(1)^2 \times E_8$. With regard to this, we split the index $\hat{I}$ into $\hat{I} = (a, 4, I, \tilde{J})$ with $a = 1, 2, 3$, $I = 5, \ldots, 8$. Furthermore, $\tilde{J}$ corresponds to the second E_8 which is unbroken and hence omitted in the following discussion. The gauge fields are determined by the neutral deformations N_a^b and N_4^4 for $SU(3) \times U(1)^2$, and by N_I^J and N_{IJ} for $SO(8)$. We can also read off the charged spectrum from the coefficients: N_{ab}, N_4^a and N^{a4} correspond to $(\mathbf{1}, \overline{\mathbf{3}})$ and $(\mathbf{1}, \mathbf{3})$, N_{aI} and N_a^I correspond to $(\mathbf{8}, \overline{\mathbf{3}})$, and N_{4I} and N_4^I correspond to $(\mathbf{8}, \mathbf{1})$. The relevant charges of the bundle and the resulting polynomial charges are summarized in table 7.2(a). Some of the contributing monomials are given in table 7.2(b). Note that the charges of the N's reproduce some of the line bundle charges of table 7.1, but not all of them: The missing ones correspond to spinorial roots of E_8 which are not captured in the outlined procedure. Generically, the presence of the N's in (7.24) breaks at least some of the discussed $\mathbb{Z}_3$ symmetries. However, a more thorough understanding of these deformations is needed, e.g. as to which monomials actually contribute in a given phase: Depending on the Kähler parameters, certain coordinates may or may not vanish, and this will play a role in determining the appearing operators, and hence the symmetry breaking. In particular, we should expect R symmetries to reappear in the orbifold limit $b_{\alpha 11} \to -\infty$. However, understanding which deformations of the kinetic terms in the GLSM contribute in the end to the 4D spectrum is currently work in progress.

Chapter 8

. . . .

CANCELATION OF ANOMALIES IN (0,2) GLSMs

In general, the $(0, 2)$ GLSM models are far less understood than their (2,2) extensions. However, theories with $\mathcal{N} = 1$ SUSY in four dimensions stem usually from $(0, 2)$ theories, so one naturally has to deal with them for considering many phenomenologically interesting models. Since the (0,2) GLSM includes chiral fermions on the worldsheet, the U(1) gaugings of the GLSM can become anomalous. In this chapter we discuss these anomalies and introduce a novel mechanism that gives rise to a Green–Schwarz like anomaly cancelation mechanism on the worldsheet [124], which was discussed independently by Quigley and Sethi [125]. The key idea is to make the FI terms appearing in the GLSM field-dependent. This will induce an axionic coupling which can provide an anomaly cancelation mechanism. The cancelation mechanism on the worldsheet corresponds to geometries with torsion or NS5 branes. The backreaction of the FI term on the geometry stems from the fact that in $(0, 2)$ models the topological term is paired with the D term, in contrast to 4D theories, where it is paired with the gauge coupling. In [126, 127] it was shown how such field-dependent FI terms can arise rather naturally from integrating out fields in GLSM constructions. Before this, the only concrete attempts to arrive at a microscopic heterotic string description have been undertaken in [128–130]. Their observation that these torsion geometries can be described by non-invariant FI terms has been the starting point for our investigation.

As explained in chapter 4, the presence of NS5 branes modifies the Bianchi identities and thus the anomaly cancelation in target space. In fact, most of the heterotic MSSM constructions on smooth CYs satisfy the BIs only when NS5 branes are present [131–135]. In order to ensure that there are indeed NS5 branes (and not anti-NS5 branes which would break all supersymmetries [85]), $\mathrm{ch}_2(V) - \mathrm{ch}_2(TX)$ has to be an effective class. The heterotic string by itself is not able to give a microscopic description of these NS5 branes, since they are non-perturbative objects. However, one might hope that it is possible to quantize the heterotic string in the presence of these heterotic solitons. In [136] this was attempted in the specific case of a resolved conifold.

In our study of the worldsheet Green–Schwarz mechanism, we start with introducing the $(0, 2)$ GLSM as a reduction of the $(2, 2)$ GLSM in section 8.1 and discuss its properties in section 8.2. In section 8.3, we then introduce the field-dependent FI terms giving rise to the axions that cancel the GLSM anomalies. Finally in section 8.4, we present examples for the anomalies, their cancelation, and the consequences for the geometry.

8.1 Reduction from (2,2) to (0,2) GLSMs

A good way of reducing the $(2,2)$ theory to the $(0,2)$ theory is by dropping the $\theta^+, \overline{\theta}^+$ dependence of the $(2,2)$ superfields given in section 3.3.2. This means that the $(2, 2)$ chiral multiplet $\Phi_{(2,2)}$ decomposes into a $(0,2)$ chiral multiplet $\mathcal{Z}_{(0,2)}$ and a chiral-Fermi multiplet $\mathcal{C}_{(0,2)}$, $\Phi_{(2,2)} = \mathcal{Z}_{(0,2)} + \theta^+ \mathcal{C}_{(0,2)}$. These in turn posses an expansion in the remaining θ^- superspace coordinate as $\mathcal{Z}_{(0,2)} = \phi + \theta^- \psi^-$ and $\mathcal{C}_{(0,2)} = \psi^+ + \theta^- \widetilde{F}$. Hence the chiral-Fermi superfields contain the auxiliary components $\widetilde{F}$. On-shell, the chirality of the fermions is linked to whether they are left- or right-movers. In our convention, the fermions in the chiral-Fermi multiplet are left-movers and the fermions in the chiral multiplet are right-movers. In contrast, the chirality of the bosonic components is not fixed. When counting the bosonic and fermionic degrees of freedom, one has to bear in mind that they have to be counted separately for left- and right-movers in $(0,2)$ GLSMs. In particular, since SUSY only acts on the right-movers, the left-moving degrees of freedom need not match.

The $(2, 2)$ vector multiplet $V_{(2,2)}$ is decomposed into a $(0, 2)$ gauge multiplet $(V_{(0,2)}, A_{(0,2)})$ and a Fermi-gauge multiplet Σ, $V_{(2,2)} = A_{0,2} + \theta^+ \Sigma + \overline{\theta}^+ \overline{\Sigma} + \theta^+ \overline{\theta}^+ V_{(0,2)}$. From the expansion in section 3.3.2, the components of these $(0, 2)$ fields in Wess–Zumino gauge are found to be

$$A_{0,2} = \theta^- \overline{\theta}^- a_{\overline{\sigma}}, \quad V_{(0,2)} = a_\sigma + \theta^- \overline{\chi}^+ + \overline{\theta}^- \chi^+ + \theta^- \overline{\theta}^- \widetilde{D}, \quad \Sigma = \theta^- \sigma + \theta^- \overline{\theta}^- \chi^-.$$

Note that we renamed the component fields as compared to the $(2,2)$ model in oder to avoid confusion with other occurring quantities and to stick with the standard notation. Furthermore, we drop the $(0, 2)$ indices since we will be dealing exclusively with $(0, 2)$ fields from now on.

8.2 (0,2) GLSMs

We start by introducing the field content of a generic $(0, 2)$ GLSM to set our notations and conventions. (For details on $(0, 2)$ GLSM see e.g. [62, 63, 137].) The complete field content is summarized in table 8.1. As explained above, a $(0, 2)$ GLSM contains a set of chiral superfields $\mathcal{Z}^i$ and chiral-Fermi multiplets $\mathcal{C}^\alpha$. We find it convenient to name them differently according to their R charges. As we shall see below, the R charge determines whether a field contributes to the superpotential of the geometry or

| superfield | | gauge | R | dim. | components |
type	notation	charge	charge		
chiral	Z^a	$(q_I)^a$	0	0	(z^a, ψ^a)
chiral-Fermi	Λ^α	$(Q_I)^\alpha$	0	$\frac{1}{2}$	$(\lambda^\alpha, \widetilde{F}^\alpha)$
chiral	Φ^m	$(q_I)^m$	1	0	(c^m, ψ^m)
chiral-Fermi	Γ^μ	$(Q_I)^\mu$	1	$\frac{1}{2}$	$(\gamma^\mu, \widetilde{F}^\mu)$
gauge	$(V;A)^I$	0	$(0;1)$	$(0;2)$	$(a^I_{\bar\sigma}, \chi^I, \widetilde{D}^I; a^I_\sigma)$

Table 8.1: The superfield content of a gauged linear sigma model and their charge assignments.

to the superpotential of the bundle. We split the chiral fields $\mathcal{Z}$ by calling those that correspond to the geometry Z^a and those that correspond to the bundle Φ^m. Likewise we split the chiral-Fermi fields and call those corresponding to the geometry Γ^μ and those corresponding to the bundle Λ^α.

In general, the superfields can be charged under bosonic gauge transformations

$$\mathcal{Z}^a \to e^{(q_I)^a \Theta^I} \mathcal{Z}^a \,, \qquad \mathcal{C}^\alpha \to e^{(Q_I)^\alpha \Theta^I} \mathcal{C}^\alpha \,, \tag{8.1}$$

with chiral superfield parameters Θ^I. Furthermore, a GLSM can be equipped with a number of fermionic gaugings

$$\delta_\Xi \mathcal{C}^\alpha = M^\alpha{}_i(\mathcal{Z}^a) \, \Xi^i \,, \tag{8.2}$$

with neutral chiral-Fermi parameters Ξ_i which act only on the chiral-Fermi superfields $\mathcal{C}^\alpha$.

For the gauge superfields we can write down an FI term

$$W_{\mathrm{FI}} = \frac{1}{2\pi} \, \rho_J(Z^a) \, F^J \,, \tag{8.3}$$

with the super gauge field strength F^J satisfying $D_+ F^J| = -(\widetilde{D}^J + \mathrm{i}\, f^J_{\sigma\bar\sigma})/2$. Here, $\widetilde{D}^J$ is the auxiliary component of the gauge multiplet and $f^J_{\sigma\bar\sigma}$ is the Abelian worldsheet gauge field strength, $f^J_{\sigma\bar\sigma} = \partial_\sigma a^J_{\bar\sigma} - \partial_{\bar\sigma} a^J_\sigma$ with associated two-form $f^J_2 = f^J_{\sigma\bar\sigma} \mathrm{d}\sigma \mathrm{d}\bar\sigma$. The underlying worldsheet gauge field one-form is $a^I_1 = a^I_\sigma \mathrm{d}\sigma + a^I_{\bar\sigma} \mathrm{d}\bar\sigma$. We furthermore use the notation $\sigma = (\sigma^1 + \sigma^2)/2$, $\bar\sigma = (\sigma^1 - \sigma^2)/2$ such that $\partial = \partial_1 + \partial_2$ and $\bar\partial = \partial_1 - \bar\partial_2$. The parameters $b_J = \mathrm{Re}(\rho_J)$ can be interpreted as Kähler parameters of the resulting target space geometry and the $\beta_J = \mathrm{Im}(\rho_J)$ as the corresponding axions [62].

In addition, the superfields Z^a and Λ^α may be subject to various holomorphic constraints

$$P_\mu(Z^a) = 0 \,, \qquad N_{m\alpha}(Z^a) \Lambda^\alpha = 0 \,. \tag{8.4}$$

These constraints are encoded in the superpotentials

$$W_{\text{geom}} = \Gamma^\mu P_\mu(Z^a), \qquad W_{\text{bundle}} = \Phi^m N_{m\alpha}(Z^a) \Lambda^\alpha. \tag{8.5}$$

Note that the chiral-Fermi superfields Γ^μ and the chiral superfields Φ^m can only appear linearly in the superpotential due to their R charge assignment. The holomorphic functions $P_\mu(Z^a)$ and $N_{m\alpha}(Z^a)$ are subject to the requirement that the superpotential is gauge invariant under both bosonic and fermionic gaugings. This implies that in general also the Γ^μ transform under the fermionic gauge transformations,

$$\delta_\Xi \Gamma^\mu = \Phi^m M_{mi}{}^\mu(Z^a) \Xi^i, \tag{8.6}$$

such that

$$\Phi^m M_{mi}{}^\mu(Z^a) P_\mu(Z^a) + \Phi^m N_{m\alpha}(Z^a) M^\alpha{}_i(Z^a) = 0. \tag{8.7}$$

The two sets of equations in (8.4) are the $(0, 2)$ analog of the hypersurface constraints (3.34) we met in the $(2, 2)$ model. However, crucially for the $(0, 2)$ models, the gauge bundle can be different from the tangent bundle as indicated by the split in (8.5), and thus we obtain two independent equations describing them. Let us start with the $\widetilde{F}$ terms. We get contributions from the auxiliary components $\widetilde{F}^\alpha$ of Λ^α and $\widetilde{F}^\mu$ of Γ^μ, respectively. The former $\widetilde{F}$ terms $\widetilde{F}^*_\alpha = c^m N_{m\alpha}(Z) = 0$ that originate from W_{bundle} are automatically satisfied in the geometric regime where the c^m do not get a VEV. The latter $\widetilde{F}$ terms $\widetilde{F}^*_\mu = P_\mu(Z^a) = 0$ define an intersection of hypersurfaces in the toric space spanned by the Z^a.

In order to analyze the gauge bundle, we check which left-moving fermions of the chiral-Fermi multiplets remain as massless degrees of freedom. There are two ways in which the degrees of freedom could be reduced: the left-moving fermions could either be gauged away (they pair up and become massive via the Fermi gauge covariant kinetic terms with coefficient matrix M) via (8.2) or they could pair up with right-moving fermions and become massive. Thus the bundle degrees of freedom are given by those λ^α which remain massless (i.e. they are in the kernel of $N_{m\alpha}(Z)$) and which cannot be gauged away with fermionic gaugings satisfying (8.7). To express this, it is convenient to define a complex of vector bundles [62]

$$0 \longrightarrow \mathcal{O}^{N_\Sigma} \overset{M}{\longrightarrow} \bigoplus_\alpha \mathcal{O}(Q^\alpha) \overset{N}{\longrightarrow} \bigoplus_m \mathcal{O}(-q_m) \longrightarrow 0, \tag{8.8}$$

where N_Σ denotes the number of fermionic gaugings. The vector bundle then satisfies $V = \ker(N)/\text{im}(M)$, i.e. it is given by the cohomology of this complex. If the complex is exact, all massless gauge degrees of freedom can be gauged away and the vector bundle is trivial. To make the bundle V appear explicitly in the complex (8.8), we can split it in two short exact sequences by introducing an auxiliary sheaf $\mathcal{V}$:

$$\begin{aligned} 0 &\longrightarrow \mathcal{O}^{N_\Sigma} \overset{M}{\longrightarrow} \bigoplus_\alpha \mathcal{O}(Q_\alpha) \longrightarrow \mathcal{V} \longrightarrow 0, \\ 0 &\longrightarrow V \longrightarrow \mathcal{V} \longrightarrow \bigoplus_m \mathcal{O}(-q_m) \longrightarrow 0. \end{aligned} \tag{8.9}$$

In case there are no fermionic gaugings (i.e. $N_\Sigma = 0$), all we have to worry about are the potential mass terms and thus we get

$$0 \longrightarrow V \longrightarrow \bigoplus_\alpha \mathcal{O}(Q^\alpha) \xrightarrow{N} \bigoplus_m \mathcal{O}(-q_m) \longrightarrow 0 \,, \tag{8.10}$$

If we furthermore do not include any fields Φ_m (or if their charge assignment is incompatible with the term appearing in the bundle superpotential), all bundle fermions remain massless and we obtain the case where the gauge bundle splits into a sum of line bundles, $V \simeq \oplus_\alpha \mathcal{O}(Q_\alpha)$. Thus in this case we obtain the situation which we have been studying up to now, where the charge vectors Q_α^I correspond to the first Chern class of the gauge line bundles. These can be related to the bundle vectors V_r^I in the usual way, as for example done in section 7.2. However, one has to be careful, since the index I appears in different contexts in the two examples. Both times it is used as a label the U(1) groups. However, in the GLSM the U(1) gaugings are introduced together with the exceptional divisors to maintain the overall dimensionality of the target space; the chiral-Fermi superfields, each of which corresponds to a massless degree of freedom, are labeled by α. Hence the index I on the GLSM corresponds to the index r in SUGRA, and the index α on the GLSM corresponds to the index I in SUGRA.

We see that the $(0,2)$ GLSM induces a split in the roles of the left- and right-moving fermions: The fields Z^a and Γ^μ determine the geometry (their fermionic components are sections of the tangent bundle of the target space manifold), while the fields Φ^m and Λ^α determine the gauge sector (their fermionic components are sections of the gauge bundle). From this we find the following correspondence between the U(1) charges of the GLSM and the topological quantities of the target space

$$\sum_\mu Q_I^\mu - \sum_a q_I^a \Leftrightarrow c_1(TX)\,, \qquad \sum_\alpha Q_I^\alpha - \sum_m q_I^m \Leftrightarrow c_1(V)\,. \tag{8.11}$$

In particular, this reproduces the known result that the first Chern class of the tangent bundle vanishes if the order of the hypersurface equations equals the sum of the weights of the coordinates z^a. For the first Chern class of the gauge bundle we have to impose that it vanishes modulo 2, as discussed in section 2.3, which means that the corresponding sum of the charges has to be even.

At this point we would like to mention another subtlety that can occur in $(0,2)$ GLSMs but not in their $(2,2)$ counterparts. Since the charges of the left- and right-movers can be chosen independently, the sum of the scalar charges is in general non-zero. As discussed in [63], this leads to a logarithmic divergence for the Kähler parameters, since their beta-function is proportional to the sum of the scalar charges. Thus the geometry either flows to a point or blows up indefinitely in the IR. Curiously, this can be fixed by introducing a pair of spectators S, Ω where S is a chiral and Ω a chiral-Fermi superfield. By choosing their charges such that the charges of S equals the negative of all bosonic charges and the charges of Ω equals the sum of all bosonic charges, the scalar charges sum to zero but the fields do not alter the anomaly equations to be discussed below. Furthermore, this allows for a new superpotential term $W_{\text{spec}} = S\Omega$. The $\widetilde{F}$ term of Ω

immediately sets S to zero, such that the degrees of freedom of both the geometry and the bundle remains unchanged by their inclusion (hence their name spectators).

8.3 Worldsheet Green–Schwarz mechanism

8.3.1 Gauge anomalies on the worldsheet

In two dimensions the fermions of the chiral and the chiral-Fermi superfields can give rise to anomalies. They give contributions with opposite signs as their fermions are right- and left-moving, respectively.

For our discussion of the anomalies we denote the scalar gauge parameters that are part of the lowest components of the chiral superfield gauge parameters Θ^I with α^I. The structure of the gauge anomalies is encoded in the descent equations (4.6)

$$I_4 = \mathrm{d}I_3^{(0)}\,, \qquad \delta_\alpha I_3^{(0)} = \mathrm{d}I_2^{(1)}\,, \tag{8.12}$$

which can be rewritten using the Chern character as

$$I_4 = \mathrm{ch}_2(f_2) := \frac{1}{2}\,\mathrm{tr}\Big(\frac{f_2}{2\pi}\Big)^2 = \frac{1}{2}\sum_{I,J}\mathcal{A}_{IJ}\frac{f_2^I}{2\pi}\frac{f_2^J}{2\pi}\,. \tag{8.13}$$

As we mentioned in chapter 4 the descent equations do not determine the form of the mixed anomalies completely, which will be discussed in a moment. The trace tr over the full charged spectrum on the worldsheet determines the anomaly coefficients

$$\mathcal{A}_{IJ} := Q_I \cdot Q_J - q_I \cdot q_J\,, \tag{8.14}$$

in terms of the inner products

$$Q_I \cdot Q_J := \sum_\alpha (Q_I)^\alpha (Q_J)^\alpha + \sum_\mu (Q_I)^\mu (Q_J)^\mu\,, \tag{8.15a}$$

$$q_I \cdot q_J := \sum_a (q_I)^a (q_J)^a + \sum_m (q_I)^m (q_J)^m\,, \tag{8.15b}$$

that involve sums over all chiral and chiral-Fermi superfields, respectively. The corresponding Feynman graph is given in figure 4.1.

We encode the resulting anomalous variation of the effective action S_{eff} in the anomalous superpotential W_{anom},

$$\delta_\Theta S_{\mathrm{eff}} = \int \mathrm{d}^2\sigma \mathrm{d}\theta^- \, W_{\mathrm{anom}}(\Theta) + \mathrm{h.c.}\,, \qquad W_{\mathrm{anom}}(\Theta) = \frac{1}{4\pi}\sum_{I,J}\mathcal{A}_{IJ}\,\Theta^I F^J\,. \tag{8.16}$$

Shifting mixed anomalies around

Even though the pure anomalies $(I = J)$ are uniquely determined by the descent equations (8.12), this is not the case for the mixed anomalies $(I \neq J)$. The crucial point is that for mixed U(1) anomalies the Chern–Simons three-form

$$I_{3,\,\mathrm{mix}}^{(0)} = \frac{1}{(2\pi)^2} \sum_{I<J} \mathcal{A}_{IJ} \left[\left(1 - c_{IJ}\right) a_1^I f_2^J + c_{IJ}\, a_1^J f_2^I \right], \tag{8.17}$$

and consequently the anomalies

$$I_{2,\,\mathrm{mix}}^{(1)} = \frac{1}{(2\pi)^2} \sum_{I<J} \mathcal{A}_{IJ} \left[\left(1 - c_{IJ}\right) \alpha^I f_2^J + c_{IJ}\, \alpha^J f_2^I \right] \tag{8.18}$$

are determined only up to some unknown constants c_{IJ}. Here we have assumed that we have specified some ordering of the gauge indices, denoted by $I < J$. The appearance of these undetermined constants can be traced back to the regularization dependence in the computation of the gauge anomalies. Moreover, by using counterterms proportional to $\int a_1^I a_1^J$ we can modify these coefficients at will, since the variations read

$$\delta_\alpha \int a_1^I a_1^J = \int \left(\mathrm{d}\alpha^I a_1^J - \mathrm{d}\alpha^J a_1^I \right) = - \int \left(\alpha^I f_2^J - \alpha^J f_2^I \right). \tag{8.19}$$

The choice $c_{IJ} = 1/2$ treats all mixed anomalies symmetrically.

As the interaction $\int a_1^I a_1^J$ can be supersymmetrized to $\int \mathrm{d}^2\sigma \mathrm{d}^2\theta^- \left(V^I A^J - V^J A^I \right)$, the anomalous superpotential

$$W_{\mathrm{anom}}(\Theta) = \frac{1}{2\pi} \left(\frac{1}{2} \sum_I \mathcal{A}_{II}\, \Theta^I F^I + \sum_{I<J} \mathcal{A}_{IJ} \left[\left(1 - c_{IJ}\right) \Theta^I F^J + c_{IJ}\, \Theta^J F^I \right] \right), \quad (8.20)$$

is also only determined up to the coefficients c_{IJ} for $I \neq J$. That is in (8.16) we made the specific choice $c_{IJ} = 1/2$.

8.3.2 Non-invariant Fayet–Iliopoulos terms

Adams et al. noted that gauge anomalies on the worldsheet can be canceled by involving a Green–Schwarz like mechanism on the worldsheet [128, 130, 138]. We first describe this mechanism in general and comment on its concrete realization later.

As noted above, the object to consider for the 2D GS mechanism is the FI superpotential (8.3). Let us assume that under a gauge transformation the FI parameters ρ_I are not invariant, but rather transform as

$$\rho_J \to \rho_J + \mathcal{T}_{IJ}\, \Theta^I, \tag{8.21}$$

where $\mathcal{T}_{IJ}$ are some constants. These constants are in general not symmetric under the interchange of the gauge indices I and J. (A single ρ_J may be charged under various U(1) gauge symmetries simultaneously.) Consequently, the FI superpotential transforms as

$$W_{\mathrm{FI}} \to W_{\mathrm{FI}} + \frac{1}{2\pi} \sum_I \mathcal{T}_{II}\, \Theta^I\, F^I + \frac{1}{2\pi} \sum_{I<J} \left(\mathcal{T}_{IJ}\, \Theta^I\, F^J + \mathcal{T}_{JI}\, \Theta^J\, F^I \right). \qquad (8.22)$$

These transformations can be used to cancel the anomalous variation of the effective action encoded in the anomalous superpotential (8.20), i.e. $\delta_\Theta S_{\mathrm{eff}} - \delta_\Theta S_{\mathrm{FI}} = 0$. The conditions to cancel the pure and mixed gauge anomalies read:

$$\text{Pure anomalies:} \quad \mathcal{T}_{II} = \frac{1}{2}\left(Q_I \cdot Q_I - q_I \cdot q_I \right), \qquad\qquad I = J, \qquad (8.23a)$$

$$\text{Mixed anomalies:} \quad \mathcal{T}_{IJ} = (1 - c_{IJ})\left(Q_I \cdot Q_J - q_I \cdot q_J \right), \qquad I < J, \qquad (8.23b)$$

$$\mathcal{T}_{JI} = c_{IJ}\left(Q_I \cdot Q_J - q_I \cdot q_J \right), \qquad\qquad I > J. \qquad (8.23c)$$

We have again included the freedom to shift mixed anomalies around by making specific choices for the coefficients c_{IJ}. As observed above, the GS coefficients $\mathcal{T}_{IJ}$ are often not symmetric and hence we need the c_{IJ} in order to have more flexibility in canceling the anomalies.

Gauge vortex instantons

Under many circumstances the GS coefficients $\mathcal{T}_{IJ}$ are subject to stringent quantization conditions which can be easily incompatible with the anomaly conditions (8.23). To see how the quantization conditions on the GS coefficients $\mathcal{T}_{IJ}$ arise, we first recall some basic facts concerning gauge instantons in two dimensions [138, 139]. The BPS equations read

$$\left(\partial_\sigma + \mathrm{i} \sum_I (q_I)^a\, a_{\mathrm{E}\,1}^I \right) z^a = 0, \qquad -f_{\mathrm{E}\,01}^I = \widetilde{D}^I = \sum_a (q_I)^a\, |z^a|^2 - b^I, \qquad (8.24)$$

in the Euclidean theory obtained after the Wick rotation $\sigma^1 = -i\sigma^0$, which leads to $f_{\sigma\bar\sigma}^I = -\mathrm{i} f_{\mathrm{E}\,01}^I$. For a one-instanton solution the phase of z^b winds nontrivially around a single point on the worldsheet (say $\sigma = 0$) where the norm of the scalar z^a vanishes. Using polar coordinates $\sigma(\rho,\theta) = \rho \exp(\mathrm{i}\theta)$ on the Euclidean worldsheet we have asymptotically for large ρ [139]

$$z^b(\rho,\theta) \sim \sqrt{\frac{b^J}{(q_J)^a}}\, e^{\mathrm{i}\theta} + \dots, \qquad (q_J)^b a_{\mathrm{E}\,1}^J(\rho,\theta) \sim \frac{\mathrm{d}\theta}{\rho} + \dots, \qquad (8.25)$$

where the ellipses denote exponentially suppressed corrections, and $z^b(0) = a_{\mathrm{E}\,1}^J(0) = 0$. The worldsheet gauge flux is then quantized as

$$\sum_J (q_J)^b \int \frac{f_{\mathrm{E}\,2}^J}{2\pi} = 1, \qquad (8.26)$$

where $f_{\mathrm{E}\,2}^J = f_{\mathrm{E}\,01}^J \, \mathrm{d}\sigma^0 \mathrm{d}\sigma^1$. Consequently, for a set of $U(1)$ gauge multiplets we need to investigate nontrivial vortex solutions supported by all the charged chiral multiplets that only exist for specific values of the parameters b^I. In particular, when certain chiral superfields are charged under a multitude of $U(1)$ gauge symmetries, reading off the precise quantization of their gauge fluxes is rather involved. But if a chiral superfield is charged under a single $U(1)$ with charge q, it induces a quantization of the gauge flux in units of $1/q$. Hence a rough rule of thumb is that the charge with the largest absolute value sets the flux quantization unit.

Logarithmic Fayet–Iliopoulos terms

With this in mind, we return to the quantization conditions of the coefficients $\mathcal{T}_{IJ}$. We give an explicit construction of $\rho_J(Z)$ in the FI action (8.3) that transforms as specified in (8.22). Given that the chiral multiplets Z^a generically transform with chiral superfield phases as described in (8.1), we can obtain ρ_J that transform as shifts under gauge transformations. By taking

$$W_{\log \mathrm{FI}} = \frac{1}{2\pi} \rho_J(Z) F^J \,, \qquad \rho_J(Z) = \rho_J^0 + T_{XJ} \ln R^X(Z) \,, \tag{8.27}$$

we obtain the GS coefficients

$$\mathcal{T}_{IJ} = r_I^X \, T_{XJ} \,. \tag{8.28}$$

Here ρ_J^0 are constants and $R^X(Z)$ are homogeneous polynomials with $U(1)$ charges r_I^X.

The simplest choice for this would be to take $R^X(Z)$ equal to one of the chiral superfields Z^a, i.e. $r_I^X = q_I^a$. In this case the exponentiated Euclidean action $\exp(-S_{\mathrm{FI}})$ is generically not invariant under a trivial phase redefinition $z^a \to e^{2\pi \mathrm{i}} z^a$. As

$$\int \mathrm{d}^2\sigma \mathrm{d}\theta^- \, W_{\mathrm{FI}} + \mathrm{h.c.} \supset -\mathrm{i}\, T_{aJ} \int \mathrm{Im}(\ln z^a) \, \frac{f_{\mathrm{E}\,2}^J}{2\pi} \,, \tag{8.29}$$

$e^{-S_{\mathrm{FI}}} \to e^{-S_{\mathrm{FI}}} \, \exp\left(2\pi \mathrm{i}\, T_{aJ} \int \frac{f_{\mathrm{E}\,2}^J}{2\pi}\right)$ under such a trivial phase redefinition, and we obtain the quantization conditions

$$T_{aJ} \int \frac{f_{\mathrm{E}\,2}^J}{2\pi} \in \mathbb{Z} \,. \tag{8.30}$$

Assuming that the chiral superfields with the largest absolute value of $U(1)$ charges are each charged under a single $U(1)$ only, this condition implies $T_{aJ} \in q_J \, \mathbb{Z}$, in terms of the largest charges q_J.

Similar quantization conditions arise for more general logarithmic FI terms (8.27) with other homogeneous polynomials $R^X(Z)$. In this case the quantization condition involves the degree of this polynomial. For any choice the precise units of quantization of T_{XJ} depend on the chosen $U(1)$ charge normalization. However, whether the anomaly

conditions (8.23) can be solved in the presence of these quantization conditions or not is of course independent of the normalization.

Linear Fayet–Iliopoulos terms

In [128, 130, 138] a non-singular covariant FI term which is linear in a chiral superfield Y has been presented,

$$W_{\text{linear FI}} = \frac{1}{2\pi}\, m\, Y\, F \,. \tag{8.31}$$

If this superfield transforms with a shift $Y \to Y + n\,\Theta$ under a gauge transformation with parameter Θ, we can use it to cancel some pure and mixed worldsheet gauge anomalies. In this case the anomaly coefficient read $\mathcal{T} = mn$. The standard quadratic kinetic action has to be extended to

$$S_{\text{kin}} = \frac{R^2}{4} \int \mathrm{d}^2\sigma \mathrm{d}^2\theta^- \left(Y + \overline{Y} + n\,V\right)\left(\mathrm{i}\partial Y - \mathrm{i}\overline{\partial}\overline{Y} - n\,A\right) , \tag{8.32}$$

to preserve gauge invariance. In order to ensure that the target space is compact, $y = Y|$ has to be the complex coordinate on a flat torus

$$y \sim y + 1 \,, \qquad y \sim y + \tau \,, \tag{8.33}$$

where $\tau = \tau_1 + \mathrm{i}\tau_2$ defines the complex structure of this torus. Its radius R has been scaled out in front of the kinetic term. On an arbitrary instanton background, the resulting action containing the terms

$$S_{\text{kin}} + S_{\text{F}} \subset \int \mathrm{d}^2\sigma \left[\left(\frac{m}{2\pi} - \frac{n\,R^2}{2}\right)\mathrm{Re}(y)\,\widetilde{D} + \left(\frac{m}{2\pi} + \frac{n\,R^2}{2}\right)\mathrm{Im}(y)\,f_{\sigma\bar{\sigma}}\right] , \tag{8.34}$$

violates these torus periodicities, unless

$$\pi\,R^2 = \frac{m}{n} \,, \qquad \frac{1}{\pi}\,m\,\tau_2 \int \frac{f_{\text{E}\,2}}{2\pi} \in \mathbb{Z} \,. \tag{8.35}$$

Now, in order to cancel the anomalies m is fixed. This in turn leads to a quantization of the complex structure τ_2 and the radius R of this torus. The authors of [128, 130, 138] use this to construct a GLSM realization of the torsional geometries [32, 140–142].

8.3.3 Non-Kähler torsion geometry

The inclusion of a non-constant FI term (8.3) leads to a target space geometry which is no longer Kähler [128]. To see this we use that the field strengths f_2 correspond to the pullback of ambient space divisors to the worldsheet, $\frac{f_2^I}{2\pi} = Z^*(D^I)$. The pullback of the complexified target space Kähler form $\mathcal{J} = \sum_I \rho_I(z)D_I = \sum_I (b_I(z) + \mathrm{i}\beta_I(z))D^I$ is thus $\sum_I \rho_I F^I$. Hence, the coefficients $\beta_I(z)$ can be interpreted as axions with a nontrivial

background over the target space geometry. Given that the axions $\beta_I(z) = \text{Im}(\rho_I(z))$ transform with shifts under the worldsheet gauge transformations (8.21), the three-form field strength H of B has to be modified to

$$H = \big(\text{d}\beta_J + r_I^X T_{XJ} A_1^I\big) F^J \,, \tag{8.36}$$

in order to be globally well-defined, where the pullback of A_1^I is a_1^I after imposing the equations of motion. This is the GLSM realization of the effect discussed in [143, 144]: The anomalies in transformations of the worldsheet fermions induce the target space GS mechanism. From (8.36), we see that the three-form H is nontrivial but torsion. Hence, we know from section 2.3 that the fundamental two-form J is not closed and the resulting target space is non-Kähler. For this reason such GLSMs are sometimes called torsion GLSMs (TLSMs).

NS5 branes

When the worldsheet FI term becomes singular a more drastic modification of the target space geometry arises: NS5 branes appear. As discussed in (4.35), this leads to a modification of the Bianchi identities for the H field:

$$\text{d}H = \text{tr}(\mathcal{R})^2 - \text{tr}(\text{i}\mathcal{F})^2 - X_4 = 2\left(\text{ch}_2(V) - \text{ch}_2(TX)\right) - X_4 \,, \tag{8.37}$$

where $\mathcal{R}$ and $\mathcal{F}$ are the target space curvature and gauge field strengths, respectively, and X_4 corresponds to the sum of the NS5 brane source terms. When β_I can become singular, $\text{d}(\text{d}\beta_I) \neq 0$, there is an additional contribution $X_4 = \text{d}(\text{d}\beta_J)F^J$. As X_4 measures the failure of $\text{tr}\mathcal{R}^2 - \text{tr}(\text{i}\mathcal{F})^2$ being exact, it signals the presence of NS5 branes [87, 145]. Even though the perturbative heterotic worldsheet theory is incapable of describing the microscopic dynamics of NS5 branes, it feels their effects.

Another way of seeing the correspondence is by comparing the Bianchi identities with NS5 branes (8.37) with the modified anomaly conditions (8.23) using $\frac{f_2^I}{2\pi} = Z^*(D^I)$. More precisely [63, 128, 138], from (8.13) we find that $I_4 \sim \text{ch}_2(V) - \text{ch}_2(TX)$. This is also plausible following similar arguments that lead to (8.11), which we illustrate in the example in section 8.4.1. Thus I_4 corresponds to the Bianchi identities (without NS5 branes) in ambient space,

$$
\begin{aligned}
I_4 &= \frac{1}{2} \sum_{I,J} \mathcal{A}_{IJ} \frac{f_2^I}{2\pi} \frac{f_2^J}{2\pi} = \sum_{I,J} (Q_I \cdot Q_J - q_I \cdot q_J) \frac{f_2^I}{2\pi} \frac{f_2^J}{2\pi} \\
&= \sum_{I,J} \left(\sum_\mu Q_I^\mu Q_J^\mu - \sum_a q_I^a q_J^a - \sum_m q_I^m q_J^m + \sum_\alpha Q_I^\alpha Q_J^\alpha \right) \frac{f_2^I}{2\pi} \frac{f_2^J}{2\pi} \\
&= Z^* \left(\qquad \text{tr}\mathcal{R}^2 \qquad - \qquad \text{tr}(\text{i}\mathcal{F})^2 \qquad \right) .
\end{aligned}
\tag{8.38}
$$

Upon including the worldsheet GS mechanism (8.23), the anomaly coefficients $\mathcal{A}_{IJ}$ are corrected by the shifts $\mathcal{T}_{IJ}$, which modifies the anomaly polynomial to

$$I_4 = \frac{1}{2}\left(\sum_{I,J}\mathcal{A}_{IJ} - 2\mathcal{T}_{IJ}\right)\frac{f_2^I}{2\pi}\frac{f_2^J}{2\pi} \quad \Leftrightarrow \quad \mathrm{tr}\mathcal{R}^2 - \mathrm{tr}(\mathrm{i}\mathcal{F})^2 - X_4\,. \qquad (8.39)$$

This correspondence is a correspondence in ambient space and not on the hypersurface, which leads to curious effects discussed below. Note that the NS5 branes contribute with the same sign as a gauge instanton.

Before we discuss this further, let us look for example at a logarithmic FI term (8.27) with $\rho_J(Z) = \rho_J^0 + T_{aJ}\ln Z^a$. We find

$$\beta_J = T_{Ja}\ln\left(\frac{z^a}{\bar{z}_a}\right),\quad \mathrm{d}\beta_J = T_{Ja}\left(\frac{\mathrm{d}z^a}{z^a} - \frac{\mathrm{d}\bar{z}_a}{\bar{z}_a}\right),\quad \mathrm{d}(\mathrm{d}\beta_J) = 2\pi\,T_{Ja}\,\delta^2(z^a)\,\mathrm{d}\bar{z}_a\mathrm{d}z^a\,. \quad (8.40)$$

Since the internal profile of the axion β_J is the two-form f_2^J, it follows that the NS5 brane is located at the intersection of the divisor $D_a := \{z^a = 0\}$ with the Poincaré dual of f_2^J. If $R^X(\Psi)$ is a polynomial rather than a monomial of a single superfield, one can interpret its coefficients as NS5 brane position moduli. However, since we only know the class of the divisor dual to f_2^J but not the representative, the precise hypersurface it corresponds to is left unspecified. In particular when this class has more than one representative, the exact locus of the NS5 brane is not determined.

In the light of this interpretation that logarithmic FI terms signal NS5 branes in the system, the coefficients T_{XJ} can be viewed as counting the number of NS5 branes. The quantization condition (8.30) for a logarithm of a single chiral superfield precisely shows that the T_{aJ} are integer provided all worldsheet gauge instantons are supported by scalars of unit charge. However, often there are additional chiral superfields in the GLSM that have larger charges than the minimal one. Hence, unless there is a reason why they cannot induce gauge instantons, T_{aJ} is quantized in units of the largest charges. In the NS5 brane interpretation this corresponds to the presence of a set of NS5 branes. In the examples discussed below we return to this issue in a concrete setting in order to understand the potential consequences.

NS5 brane backreaction

So far the analysis of the resulting geometry of the GLSM has been performed without considering possible geometric backreactions. We now consider this important effect: In the presence of the logarithmic FI term (8.27) the naive worldsheet $\widetilde{D}$ term gets corrected to

$$(q_I)_a\,|z_a|^2 + (q_I)_m\,|z_m|^2 - \frac{1}{2\pi}(b_I^0 + T_{XI}\ln|R^X(z^a)|) = 0\,. \qquad (8.41)$$

In particular, when $R^X(Z^a) = Z^a$, this implies that it is not possible anymore to set $z^a = 0$. This means that the corresponding divisor $D_a := \{z^a = 0\}$ no longer exists:

The infinitely thin NS5 brane is replaced by a nontrivial modification of the target space geometry near the position where this brane used to be. However, there might be a linear equivalent divisor $D_b := \{z^b = 0\} \sim D_a$. Hence the logarithmic FI term might remove an ambient space coordinate without removing the actual target space divisor on the hypersurface.

8.3.4 Orbifold modular invariance conditions

The inclusion of the field-dependent FI terms can be linked to the basic consistency conditions of a $\mathbb{Z}_N$ orbifold theory, namely the modular invariance conditions

$$N\left(V_r^2 - v_r^2\right) = 0 \bmod 2\,, \tag{8.42}$$

for the local orbifold shifts V_r and twist v_r, where r labels the different orbifold fixed points. Note that these are not strict but only mod conditions. From the first set of conditions in (8.23) we see that the GS mechanism on the worldsheet can give rise to mod conditions. As discussed in chapter 3, the resolution of a $\mathbb{Z}_N$ fixed point requires the introduction of an exceptional GLSM field X and a corresponding exceptional U(1) gauging under which X carries charge N. Furthermore, the D terms are such that in the orbifold regime the scalar component x of X has to have a VEV and thus never exists in the orbifold regime. Hence it is an ideal candidate to put under the logarithm for inducing anomaly cancelation. The quantization condition (8.30) from the gauge vortex instantons shows that the anomalies have to be multiples of $1/N$. Hence by multiplying the pure anomaly cancelation conditions by a factor N they have the same structure as the modular invariance conditions (8.42). Note especially how the factor of $1/2$ in (8.23a) gives rise to the 0 mod 2 condition in the modular invariances.

8.4 Examples

8.4.1 Worldsheet, ambient space, and target space anomalies

Here we would first like to illustrate in examples the relation between the anomaly four-form I_4 in the GLSM and the four-form $\mathrm{d}H$ in target space. As we argued above, the field strengths f_I correspond to pullbacks of ambient space divisors D_I. Hence we will find that the coefficients $\mathcal{A}_{IJ}$ appearing in I_4 appear also in $\mathrm{d}H = \mathcal{A}_{IJ}D_I D_J$. Thus the GLSM anomalies measure the non-integrated Bianchi identities.

Example (Cubic in $\mathbb{CP}^2$) The probably simplest example is the torus. It does not really matter which description we choose and how we fix the complex structure (unless it becomes singular), so we choose the $\mathbb{CP}^2[3]$ with unfixed complex structure. Since we are discussing (0,2) models, we have to specify the gauge sector separately. We take it to be completely trivial (i.e. a flat gauge background), which yields a valid

free CFT describing string theory. We thus look at the charge assignment

	Z_1	Z_2	Z_3	Γ	Λ_α	Φ_m	S	Ω
U(1)	1	1	1	-3	0	–	-3	3

In the first four columns we list the fields Z_a and Γ that give rise to the geometry. The next columns containing Λ_α with trivial charges and no fields Φ_m were included to illustrate that the gauge sector is trivial. The last two columns contain the spectator pair which are introduced to yield vanishing bosonic charges. As discussed, the $\widetilde{F}$ term of Ω sets $s = 0$ for any value of the Kähler parameter b associated with the U(1) gauging. The $\widetilde{F}$ term of Γ leads to the cubic equation

$$z_1^3 + z_2^3 + z_3^3 + \kappa z_1 z_2 z_3 = 0 \tag{8.43}$$

with the complex structure encoded in κ. The $\widetilde{D}$ term is found to be

$$|z_1|^2 + |z_2|^2 + |z_3|^2 = b \,, \tag{8.44}$$

where we have already set $s = 0$. The Kähler cone is thus given by $b \geq 0$. Since all GLSM coordinate fields Z_a have the same charges, their corresponding divisors $D_a = \{z_a = 0\}$ are linear equivalent in target space, $D_1 \sim D_2 \sim D_3 \sim D$. They are codimension one in target space, which has dimension one itself, i.e. they are points. Since their intersection $D_a D_b$ would correspond to codimension two objects, they vanish. Alternatively, this can be seen by setting e.g. $z_1 = z_2 = 0$. For $b > 0$ this means that $z_3 \neq 0$, but this violates the $\widetilde{F}$ term constraint (8.43).

Let us next study the gauge sector. The monad describing the gauge bundle V degenerates to

$$0 \longrightarrow V \longrightarrow \mathcal{O}(0) \longrightarrow 0 \,, \tag{8.45}$$

i.e. $V \simeq \mathcal{O}$.

After reviewing the model let us calculate the anomalies. On the GLSM we only have the $U(1)^2$ anomaly, for which we find

$$\mathcal{A}_{II} = Q_I^2 - q_I^2 = 3^2 - 1^2 - 1^2 - 1^2 = 6 \,. \tag{8.46}$$

Hence we see that the GLSM corresponding to a seemingly fine theory has an anomaly. In target space, this is an anomaly which is not part of the hypersurface as we shall see now. As we know, a torus has $c_1(TX) = 0$ since it is flat (or since it is a CY onefold), and $c_2(TX) = 0$ identically for dimensional reasons (since it is impossible to build a nontrivial two-form on a one-dimensional space). Likewise since the gauge bundle is trivial as well, $c_1(V) = c_2(V) = 0$. Let us nevertheless go ahead and calculate

the formal expansion of the total Chern class of the torus up to second order via the adjunction formula (3.19)

$$
\begin{aligned}
c(TX) &= c_0(TX) + c_1(TX) + c_2(TX) + \ldots \\
&= (1 + D_1)(1 + D_2)(1 + D_3)/(1 + D_1 + D_2 + D_3) \\
&= (1 + D)^3/(1 + 3D) = 1 + (3 - 3)D + (3^2 - 3 - 3)D^2 + \ldots = 1 + 3D^2 + \ldots
\end{aligned}
$$

We thus find for the non-integrated Bianchi identity

$$
\mathrm{d}H = \mathrm{tr}\mathcal{R}^2 - \mathrm{tr}\mathcal{F}^2 = 2(\mathrm{ch}_2(V) - \mathrm{ch}_2(TX)) = c_2(TX) = 6D^2 \,. \tag{8.47}
$$

As promised, this corresponds precisely to the anomaly form I_4 of the GLSM,

$$
I_4 = \frac{1}{2} \sum_{I,J} \mathcal{A}_{IJ} \frac{f_2^I}{2\pi} \frac{f_2^J}{2\pi} \,. \tag{8.48}
$$

This anomaly is nonzero, while $\mathrm{d}H$ is zero on the torus since $D^2 = 0$. However, prior to imposing the $\widetilde{F}$ term (8.43), $D^2 \neq 0$: indeed, setting e.g. $z_1 = z_2 = 0$ is a valid surface in $\mathbb{CP}^2$. This is to say the divisor D has non-vanishing self-intersection, but this happens away from the hypersurface. It is precisely in this sense that the GLSM anomaly measures the ambient space anomaly rather than the target space anomaly, which is somehow clear since we have not used the $\widetilde{F}$ terms in calculating the anomaly I_4. The physical meaning of this is still under investigation. As we have seen in section 3.3.6, the target space can have a complicated shape, with various components flopping inside and outside the geometry, depending on the Kähler cone under investigation. Thus the vanishing of the GLSM anomalies ensures that the target space anomalies are absent in all Kähler cones. However, in our example the only Kähler cone is $b \geq 0$. Nevertheless, the GLSM anomalies are non-zero. Note that they can be canceled using a logarithmic FI term of the form $3\ln(\sum_a \kappa_a |z_a|)$.

Example ($\mathbb{CP}^7[2,2,2,2]$)   Both of our next examples deal with the CY threefold $\mathbb{CP}^7[2,2,2,2]$ which is obtained as a complete intersection of four degree-two hypersurfaces in the seven dimensional projective space $\mathbb{CP}^7$.
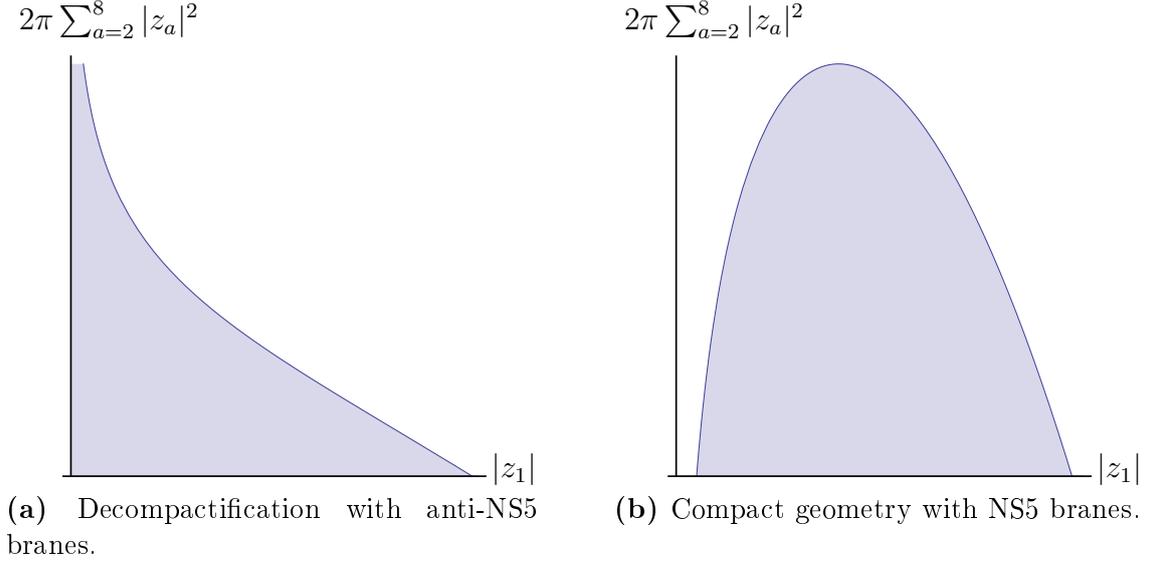
We first consider a stable[1] $SU(6)$ gauge bundle on this geometry. The GLSM describing this model has the following charge assignment:

$$
\begin{array}{|c||c|c|c|c|}
\hline
\text{superfield} & Z_{a=1,\ldots,8} & \Gamma_{\mu=1,\ldots,4} & \Lambda_{\alpha=1,\ldots 8} & \Phi_{m=1,2} \\
\hline
\text{gauge charge} & 1 & -2 & 1 & -4 \\
\hline
\end{array} \tag{8.49}
$$

The geometry and the gauge bundle are encoded in the superpotentials

$$
W_{\mathrm{geom}} = \Gamma^\mu \, P_\mu(Z_a) \,, \qquad W_{\mathrm{bundle}} = \Phi^m \, N_{m\alpha}(Z_a) \, \Lambda^\alpha \,, \tag{8.50}
$$

---

[1] We thank James Gray for helping checking.

(a) Decompactification with anti-NS5 branes.

(b) Compact geometry with NS5 branes.

Figure 8.1: Plot of the valid range of $|z_1|$ in the example of $\mathbb{CP}^7[2,2,2,2]$ with logarithmic terms inducing anti-NS5 or NS5 branes. The former lead to a decompactification of the previously compact geometry.

where $P_\mu(Z_a)$ and $N_{m\alpha}(Z_a)$ are generic polynomials of degree two and three, respectively. Since the first Chern class cancels, the space is CY. All divisors $D_a = \{z_a = 0\}$ are linear equivalent, as can be seen from their charges. The naive $\widetilde{D}$ term reads

$$\sum_{a=1}^{8} |z_a|^2 - 4 \sum_{m=1}^{2} |c_m|^2 = b \, , \tag{8.51}$$

and we want to discuss the geometric regime $b > 0$. The bundle is given by

$$0 \longrightarrow V \longrightarrow \mathcal{O}(1)^8 \longrightarrow \mathcal{O}(4)^2 \longrightarrow 0 \, , \tag{8.52}$$

We can write down the following logarithmic FI term

$$W_{\log \text{ FI}} = \frac{1}{2\pi} \Big(b + T \ln \Big[\sum_a \kappa_a Z_a \Big] \Big) F \, . \tag{8.53}$$

The FI parameter T needs to be quantized. The most stringent conditions come from the instantons involving the scalars with the largest absolute value of the U(1) charge, which are the c_m. Consequently, condition (8.30) implies that $T \in 4\mathbb{Z}$ for this model. With the charge assignment given in (8.49) the worldsheet GS anomaly cancelation condition

$$T = \mathcal{T} = \frac{1}{2} \Big(8 \cdot (1)^2 + 4 \cdot (-2)^2 - 8 \cdot (1)^2 - 2 \cdot (-4)^2 \Big) = -8 \, , \tag{8.54}$$

is compatible with this quantization condition with negative T, which indicates that there are anti-NS5 branes in the system. In the presence of the logarithmic FI term (8.53), the $\widetilde{D}$ term constraint reads

$$\sum_{a=1}^{8} |z_a|^2 - 4\sum_{m=1}^{2} |c_m|^2 - \frac{1}{2\pi}(b - |T|\ln|z_1|) = 0\,, \tag{8.55}$$

where we have assumed that only Z_1 is involved in the logarithmic FI term, i.e. $\kappa_a = \delta_{1a}$ in (8.53). Furthermore, we have made explicit that $T = -|T|$ is negative. In the geometric regime where $|c_m| = 0$, the $\widetilde{D}$ term potential leads to the constraint

$$\sum_{a=2}^{8} |z_a|^2 = \frac{1}{2\pi}(b - 8\ln|z_1|) - |z_1|^2\,. \tag{8.56}$$

This equation has far-reaching consequences for the geometry: Even though the original CY is compact, the geometry described by the model with $T < 0$ is not. While it is not possible to solve the transcendental equation for $|z_1|$, we can discuss its key features. In the cases where $|z_1|$ is large, we can neglect the log term and the geometry looks as usual. However, by taking $|z_1|$ closer and closer to zero, we can neglect the term $|z_1|^2$ and the logarithm completely dominates the right-hand-side, allowing the z_a on the left-hand-side to become arbitrary large. We may take this effect as evidence that the system contains anti-NS5 branes. In figure 8.1(a) we have plotted $|z_1|$ versus the rest $\sum_{a=2}^{8} |z_a|^2$ with b set to a fixed value and $|c_a| = 0$. As we can see, for $|z_1| \to 0$, the other $|z_a|$ can grow indefinitely. For larger values of b, the decompactification occurs for $|z_1|$ closer to zero.

It is also possible to construct a vector bundle for this CICY which leads to NS5 branes instead of anti-branes. This model has the GLSM charge assignment:

superfield	$Z_{a=1,\dots,8}$	$\Gamma_{\mu=1,\dots,4}$	$\Lambda_{\alpha=1,\dots4}$	$\Phi_{m=1,2}$
gauge charge	1	-2	1	-2

$$\tag{8.57}$$

Therefore this GLSM describes an $SU(2)$ bundle

$$0 \longrightarrow V \longrightarrow \mathcal{O}(1)^4 \longrightarrow \mathcal{O}(2)^2 \longrightarrow 0\,, \tag{8.58}$$

In this case we find for the anomaly:

$$T = \mathcal{T} = \frac{1}{2}\Big(4\cdot(1)^2 + 4\cdot(-2)^2 - 8\cdot(1)^2 - 2\cdot(-2)^2\Big) = 2\,, \tag{8.59}$$

which is positive and hence indicates that NS5 branes are present. Moreover, since now the largest absolute value of a chiral superfield charge is 2, the quantization condition is met in the minimal possible way.

The $\widetilde{D}$ term potential constraint reads with $|c_a| = 0$

$$\sum_{a=2}^{8} |z_a|^2 = \frac{1}{2\pi}(b + 2 \ln |z_1|) - |z_1|^2 \,, \tag{8.60}$$

where we have again assumed that only Z_1 is involved in the logarithmic FI term (8.53).
Hence we are able to keep the model compact in the presence of gauge anomalies, since
$T = 2$ is positive. We have again plotted this case in figure 8.1(b) for fixed b. For larger
values of b, $|z_1|$ can come closer to zero.

Finally, since in this setting the Bianchi identity defines an effective class,

$$2 \left(\mathrm{ch}_2(V) - \mathrm{ch}_2(TX) \right) = \mathrm{tr}\mathcal{R}^2 - \mathrm{tr}(\mathrm{i}\mathcal{F})^2 = 2X_4 \,, \tag{8.61}$$

we interpret the resulting geometry as having NS5 branes wrapping an effective curve
in the class X_4. This illustrates the aforementioned meaning of the coefficients κ_a in
the polynomial under the logarithm in (8.53): they can be interpreted as NS5 brane
position moduli. The choice of $\kappa_1 = 1, \kappa_{a \neq 1} = 0$ positions the NS5 brane onto a curve
which is contained in D_1. As we observed in general, since from this equation we cannot
infer its exact representative, the position of the NS5 brane is not completely fixed.

Example ($\mathbb{CP}^1 \times \mathbb{CP}^3[2, 4]$)   The clear interpretation that negative FI terms lead
to a decompactification is lost when we include more than one U(1) gauging, as we
illustrate here. The underlying geometry is taken to be a CY threefold given by a
hypersurface in $\mathbb{CP}^1 \times \mathbb{CP}^3$. The charge assignment for this example reads

superfield	$Z_{1,1}$	$Z_{1,2}$	$Z_{2,1}$	$Z_{2,2}$	$Z_{2,3}$	$Z_{2,4}$	Γ	Λ_1	Λ_2	Φ
U(1)$_1$	1	1	0	0	0	0	-2	3	1	$-$
U(1)$_2$	0	0	1	1	1	1	-4	-3	-1	$-$

$$\tag{8.62}$$

We have omitted the spectators. Let us analyze the geometry. Since the sum of charges
of the $Z_{i,a}$ is the negative of the charge of Γ for both U(1)'s the first Chern class vanishes.
We have six coordinate fields with two scalings and one hypersurface constraint, which
means that the target space will be a CY threefold. From the charge assignment, we find
that the divisors $D_{1,r} = \{z_{1,r} = 0\}$ with $r = 1, 2$ are linearly equivalent, $D_{1,1} \sim D_{1,2}$.
We thus only work with one divisor which we call D_1. Likewise, all four divisors $D_{2,r}$
are linearly equivalent, and we work with a divisor D_2. By investigating the $\widetilde{F}$ term,
we find that the nonvanishing triple intersection numbers are $D_1 D_2^2 = 4, D_2^3 = 2$. The
two $\widetilde{D}$ term constraints

$$\begin{aligned}
|z_{1,1}|^2 + |z_{1,2}|^2 &= b_1 \,, \\
|z_{2,1}|^2 + |z_{2,2}|^2 + |z_{2,3}|^2 + |z_{2,4}|^2 &= b_2 \,,
\end{aligned} \tag{8.63}$$

give rise to the SR ideal $SR = \{Z_{1,1}Z_{1,2}, Z_{2,1}Z_{2,2}Z_{2,3}Z_{2,4}\}$. The Kähler cone is given by $b_1 \geq 0, b_2 \geq 0$, since the left-hand-side of the $\widetilde{D}$ terms is always positive. The manifold has $h^{1,1} = 2$, $h^{2,1} = 86$ and thus $\chi = -168$. For the bundle we have

$$0 \longrightarrow V \longrightarrow \mathcal{O}(3,-3) \oplus \mathcal{O}(1,-1) \longrightarrow 0\,, \tag{8.64}$$

i.e. V is a sum of two line bundles which are chosen such that the DUY equations can be satisfied. Using the adjunction formula, we obtain for the Chern class of the tangent bundle

$$c(TX) = (1 + D_1)^2(1 + D_2)^4/(1 + 2D_1 + 4D_2) = 1 + 0 + (D_1^2 + 8D_1D_2 + 6D_2^2) + \ldots$$

We thus find for the Chern characters

$$\begin{aligned}
\mathrm{ch}_2(TX) &= -c_2(TX) = -(D_1^2 + 8D_1D_2 + 6D_2^2)\,, \\
\mathrm{ch}_2(V) &= \frac{1}{2}c_1(V)^2 = 5D_1^2 + 5D_2^2 - 10D_1D_2\,,
\end{aligned} \tag{8.65}$$

where we used for the Chern character of V that it is a sum of line bundles. For $\mathrm{d}H$ we find

$$\begin{aligned}
\mathrm{d}H &= \mathrm{tr}\mathcal{R}^2 - \mathrm{tr}\mathcal{F}^2 - X_4 = -2(\mathrm{ch}_2(TX) - \mathrm{ch}_2(V)) - X_4 \\
&= 2c_2(TX) + c_1^2(V) - X_4 = 12D_1^2 - 4D_1D_2 + 22D_2^2 - X_4\,.
\end{aligned} \tag{8.66}$$

Thus the curve X_4 is given by $12D_1^2 - 4D_1D_2 + 22D_2^2$. By inserting the intersection numbers we check that it is effective. Let us compare the expression to the anomaly matrix $\mathcal{A}_{IJ}$,

$$\mathcal{A}_{IJ} = \begin{pmatrix} 12 & -2 \\ -2 & 22 \end{pmatrix}\,. \tag{8.67}$$

We find again that the coefficients of the divisors $D_I D_J$ in $\mathrm{d}H$ match the entries of the WS anomaly matrix $\mathcal{A}_{IJ}$ after taking into account that $\mathcal{A}_{IJ}$ is symmetric and thus the entries on the off-diagonal have to be one half of the coefficients $D_I D_J$ in the expansion of $\mathrm{d}H$. Note that both signs appear in the anomaly matrix.

Let us see what happens when we include logarithmic FI terms to cancel the anomaly. We take as an example $b_J(z) = b_J + T_{1J}\ln R^1(Z) + T_{2J}\ln R^2(Z)$ and choose for simplicity $R^1(Z) = Z_{1,1}$ and $R^2(Z) = Z_{2,1}$. With this the charges of the polynomials are $r_I^1 = (1,0)$ and $r_I^2 = (0,1)$. In order to cancel the anomaly, we have to choose the T_{XJ} such that $\frac{1}{2}\mathcal{A}_{IJ} = \mathcal{T}_{IJ} = r_I^X T_{XJ}$, which means $T_{1J} = (6,-1), T_{2J} = (-1,11)$. Since the largest scalar U(1) charge is 1, this is compatible with the charge quantization condition. The new $\widetilde{D}$ terms constraints read

$$\begin{aligned}
|z_{1,1}|^2 + |z_{1,2}|^2 &= \frac{1}{2\pi}(b_1 + 6\ln|z_{1,1}| - \ln|z_{2,1}|)\,, \\
|z_{2,1}|^2 + |z_{2,2}|^2 + |z_{2,3}|^2 + |z_{2,4}|^2 &= \frac{1}{2\pi}(b_2 - \ln|z_{1,1}| + 11\ln|z_{2,1}|)\,.
\end{aligned} \tag{8.68}$$

Naively, it looks as if by taking $z_{2,1} \to 0$, the right-hand-side of the first $\widetilde{D}$ term grows arbitrarily large and thus the left-hand-side is unbounded which means that $z_{1,r}$ can become arbitrarily large and the target space decompactifies. Note, however, that there is also a term $\ln |z_{2,1}|$ in the second $\widetilde{D}$ term. To facilitate the discussion, we take a linear combination of the two terms to obtain

$$11 \sum_{r=1}^{2} |z_{1,r}|^2 + \sum_{r=1}^{4} |z_{2,r}|^2 = \frac{1}{2\pi} \left(11 b_1 + b_2 + 65 \ln |z_{1,1}|\right),$$

$$\sum_{r=1}^{2} |z_{1,r}|^2 + 6 \sum_{r=1}^{4} |z_{2,r}|^2 = \frac{1}{2\pi} \left(b_1 + 6 b_2 + 65 \ln |z_{2,1}|\right). \tag{8.69}$$

Hence, by looking at the combined system, we find that taking $|z_{1,1}| \to 0$ or $|z_{2,1}| \to 0$ does not lead to a decompactification of the target space. Furthermore, the SR ideal now depends on a combination of b_1 and b_2, which means we have to re-evaluate which divisors can be set to zero simultaneously for which value of the b's, which can become involved rather fast.

Chapter 9

. . . .

Conclusion and Outlook

We have studied the use of anomalies as a tool for transferring results in heterotic string theory across different regions in which the theory can be studied. The ultimate idea behind this approach is to study string theory on heterotic orbifolds where an exact CFT description is available and to use anomalies for establishing a connection to other regions in string moduli space, in particular the smooth blowup Calabi–Yau region. We have provided several examples where anomalies helped inferring information from the underlying string theory in regimes where otherwise only approximations to the theory are accessible.

One important result was the explicit construction of orbifold models that can provide phenomenologically viable models in blowup in chapter 6. We have shown that an anomaly-free U(1) that can act as a hypercharge generator requires the use of discrete non-local Wilson lines on the orbifold. We were the first to construct such a full-fledged orbifold model with a nontrivial fundamental group that has many phenomenologically appealing features [40]. It is among the heterotic string models which closest resemble the MSSM to date. By analyzing the underlying CFT, we derived a previously unknown consistency requirement which has to be imposed on the Wilson line supported by the nontrivial fundamental group [60].

As another important result we developed a gauged linear sigma model description for the underlying compactification spaces. For this we first had to work out in detail how to describe orbifolds and their resolution within the GLSM framework. The procedure and the underlying technique were introduced in chapter 3 using examples that are relevant in other parts of the discussion as well. The full analysis including many orbifolds can be found in [46]. With the GLSM description, many different phases of the theory can be studied, including non-geometric and hybrid phases that cannot be accessed otherwise. Furthermore, it allows for analyzing intermediate orbifold resolutions, which proved to open up avenues in two new directions. First, they enable a description of partial orbifold resolutions. Such geometries could serve as compactification manifolds for orbifolds that cannot be blown up completely without breaking the hypercharge. Second, they can be used for studying geometries with a big number

of Kähler parameters. These models are problematic to handle otherwise since they exceed the available computational power rather quickly.

We also provided explicit examples of how orbifold theories can be matched to their blowup counterparts in chapter 5. This match includes both a match of the massless matter spectrum and a match of the anomalies in both regimes starting from a quasi-realistic orbifold model [61]. We presented a careful analysis of how quantities on the orbifold can be related to quantities in blowup. In particular, this analysis revealed limitations in the analysis of the blowup model. It was shown that orbifold states which get an instantonic mass term during the blowup procedure are counted as exactly massless states by the Hirzebruch–Riemann–Roch index theorem. Furthermore, we showed how information on discrete R symmetries are lost during the blowup procedure. Using the developed matching techniques, both discrepancies could be attributed to the large volume limit which one is forced to take in order to arrive at a valid heterotic supergravity approximation employed in blowup.

Since discrete R symmetries play an important role in heterotic orbifold model building, finding a discrepancy between the two regimes sparked interest in a different way of studying such symmetries as discussed in chapter 7. This was done by making use of GLSM descriptions we have developed for these geometries [50]. We outlined how discrete symmetries can be studied in the GLSM, how R and non-R symmetries can be told apart and suggested a way of computing the charges of the massless matter spectrum by making use of the polynomial representation of the cohomology groups corresponding to massless matter states.

Finally, in chapter 8, we implemented a novel anomaly cancelation procedure on the worldsheet [124]. For this we introduced field-dependent worldsheet FI parameters which contain the logarithm of some chiral GLSM fields. This has fascinating and far-reaching consequences. We argued that these new theories can be used for describing geometries with torsion. Having a description for these types of geometries is of utmost importance since basically all phenomenologically interesting heterotic string models constructed to date are based on non-standard embedded theories which require torsion. Furthermore, these logarithmic terms mimic the behavior of NS5 or anti-NS5 branes, which are also frequently used in heterotic model building on smooth CY geometries.

While we developed a sound understanding for the use of anomalies in matching and comparing the theories in different regimes of the moduli space, many open questions remain. First, we require a better understanding of the precise connection between the calculation of the spectrum as deformations of the kinetic terms of the GLSM fields in order to understand observed phenomena like the jumping of the multiplicity of massless states across different Kähler cones or the exact calculation of the graded target space cohomology in the presence of discrete symmetry groups. Furthermore, the variety of phases arising from the GLSM resolution developed here is still largely unexplored. It would be interesting to investigate the new phases and see what their phenomenological consequences are. The same holds true for the torsional geometries which can be constructed via the logarithmic worldsheet FI terms. A more complete study of their properties, also with regard to their implications for target space supersymmetry, would be very interesting. These questions are left for future investigation.

LIST OF FIGURES

LIST OF TABLES

Bibliography

[1] F. Englert and R. Brout "Broken Symmetry and the Mass of Gauge Vector Mesons," *Phys.Rev.Lett.* **13** (1964) 321–323.

[2] P. W. Higgs "Broken symmetries, massless particles and gauge fields," *Phys.Lett.* **12** (1964) 132–133.

[3] **ATLAS Collaboration** Collaboration G. Aad *et al.* "Observation of a new particle in the search for the Standard Model Higgs boson with the ATLAS detector at the LHC," *Phys.Lett.* **B716** (2012) 1–29 [1207.7214].

[4] **CMS Collaboration** Collaboration S. Chatrchyan *et al.* "Observation of a new boson with mass near 125 GeV in pp collisions at sqrt(s) = 7 and 8 TeV," [1303.4571].

[5] **Supernova Cosmology Project** Collaboration S. Perlmutter *et al.* "Measurements of Omega and Lambda from 42 high redshift supernovae," *Astrophys.J.* **517** (1999) 565–586 [astro-ph/9812133].

[6] **Super-Kamiokande Collaboration** Collaboration Y. Fukuda *et al.* "Evidence for oscillation of atmospheric neutrinos," *Phys.Rev.Lett.* **81** (1998) 1562–1567 [hep-ex/9807003].

[7] H. P. Nilles "Supersymmetry, Supergravity and Particle Physics," *Phys.Rept.* **110** (1984) 1–162.

[8] R. Haag, J. T. Lopuszanski, and M. Sohnius "All Possible Generators of Supersymmetries of the s Matrix," *Nucl.Phys.* **B88** (1975) 257.

[9] J. Wess and B. Zumino "Supergauge Transformations in Four-Dimensions," *Nucl.Phys.* **B70** (1974) 39–50.

[10] D. Z. Freedman, P. van Nieuwenhuizen, and S. Ferrara "Progress Toward a Theory of Supergravity," *Phys.Rev.* **D13** (1976) 3214–3218.

[11] E. Bergshoeff, M. de Roo, B. de Wit, and P. van Nieuwenhuizen "Ten-Dimensional Maxwell-Einstein Supergravity, Its Currents, and the Issue of Its Auxiliary Fields," *Nucl.Phys.* **B195** (1982) 97–136.

[12] R. D. Peccei and H. R. Quinn "Cp conservation in the presence of pseudoparticles," *Phys. Rev. Lett.* **38** (Jun, 1977) 1440–1443.

[13] H. Georgi and S. L. Glashow "Unity of All Elementary Particle Forces," *Phys. Rev. Lett.* **32** (1974) 438–441.

[14] J. Schechter and J. Valle "Neutrino Masses in SU(2) x U(1) Theories," *Phys.Rev.* **D22** (1980) 2227.

[15] M. Green, J. Schwarz, and E. Witten *Superstring theory vol. 1: Introduction.* Cambridge, Uk: Univ. Pr. 469 P. (Cambridge Monographs On Mathematical Physics) 1987.

[16] M. B. Green, J. H. Schwarz, and E. Witten *Superstring theory vol. 2: Loop amplitudes, anomalies and phenomenology.* Cambridge, Uk: Univ. Pr. 596 P. (Cambridge Monographs On Mathematical Physics) 1987.

[17] J. Polchinski *String theory vol. 1: An introduction to the bosonic string.* Cambridge, Uk: Univ. Pr. 402 P. (Cambridge Monographs On Mathematical Physics) 1998.

[18] J. Polchinski *String theory vol. 2: Superstring theory and beyond.* Cambridge, Uk: Univ. Pr. 531 P. (Cambridge Monographs On Mathematical Physics) 1998.

[19] P. Candelas, G. T. Horowitz, A. Strominger, and E. Witten "Vacuum Configurations for Superstrings," *Nucl. Phys.* **B258** (1985) 46–74.

[20] L. J. Dixon, J. A. Harvey, C. Vafa, and E. Witten "Strings on orbifolds," *Nucl. Phys.* **B261** (1985) 678–686.

[21] L. J. Dixon, J. A. Harvey, C. Vafa, and E. Witten "Strings on orbifolds. 2," *Nucl. Phys.* **B274** (1986) 285–314.

[22] L. E. Ibanez, H. P. Nilles, and F. Quevedo "Orbifolds and Wilson Lines," *Phys. Lett.* **B187** (1987) 25–32.

[23] D. J. Gross, J. A. Harvey, E. J. Martinec, and R. Rohm "The Heterotic String," *Phys. Rev. Lett.* **54** (1985) 502–505.

[24] D. J. Gross, J. A. Harvey, E. J. Martinec, and R. Rohm "Heterotic String Theory. 1. The Free Heterotic String," *Nucl. Phys.* **B256** (1985) 253.

[25] D. J. Gross, J. A. Harvey, E. J. Martinec, and R. Rohm "Heterotic string theory. 2. The interacting heterotic string," *Nucl. Phys.* **B267** (1986) 75.

[26] P. A. Griffiths and J. Harris *Principles of algebraic geometry.* Wiley New York [u.a.] 1994.

[27] M. Nakahara *Geometry, topology and physics.* Taylor and Francis second ed. 2003.

[28] A. Strominger "Superstrings with Torsion," *Nucl. Phys.* **B274** (1986) 253.

[29] K. Becker, M. Becker, K. Dasgupta, and P. S. Green "Compactifications of heterotic theory on nonKahler complex manifolds. 1.," *JHEP* **0304** (2003) 007 [hep-th/0301161].

[30] K. Becker, M. Becker, P. S. Green, K. Dasgupta, and E. Sharpe "Compactifications of heterotic strings on nonKahler complex manifolds. 2.," *Nucl.Phys.* **B678** (2004) 19–100 [hep-th/0310058].

[31] K. Becker, M. Becker, J.-X. Fu, L.-S. Tseng, and S.-T. Yau "Anomaly cancellation and smooth non-Kahler solutions in heterotic string theory," *Nucl.Phys.* **B751** (2006) 108–128 [hep-th/0604137].

[32] M. Becker, L.-S. Tseng, and S.-T. Yau "New Heterotic Non-Kahler Geometries," *Adv.Theor.Math.Phys.* **13** (2009) 1815–1845 [0807.0827].

[33] K. Becker and S. Sethi "Torsional Heterotic Geometries," *Nucl.Phys.* **B820** (2009) 1–31 [0903.3769].

[34] S. Donalson "Anti-self-dual Yang–Mills connections over complex algebraic surfaces and stable vector bundles," *Proc. Londan Math. Soc.* **50** (1985) 1–26.

[35] K. Uhlenbeck and S. Yau "On the existence of Hermitian-Yang-Mills connections in stable vector bundles," *Commun. Pure Appl. Math.* **39** (1986) 257–293.

[36] R. Blumenhagen, G. Honecker, and T. Weigand "Loop-corrected compactifications of the heterotic string with line bundles," *JHEP* **0506** (2005) 020 [hep-th/0504232].

[37] L. B. Anderson, J. Gray, A. Lukas, and E. Palti "Heterotic Line Bundle Standard Models," *JHEP* **1206** (2012) 113 [1202.1757].

[38] R. Blumenhagen, B. Jurke, T. Rahn, and H. Roschy "Cohomology of Line Bundles: A Computational Algorithm," *J.Math.Phys.* **51** (2010) 103525 [1003.5217].

[39] S. Groot Nibbelink, J. Held, F. Ruehle, M. Trapletti, and P. K. Vaudrevange "Heterotic Z(6-II) MSSM Orbifolds in Blowup," *JHEP* **0903** (2009) 005 [0901.3059].

[40] M. Blaszczyk, S. Nibbelink Groot, M. Ratz, F. Ruehle, M. Trapletti, *et al.* "A Z2xZ2 standard model," *Phys.Lett.* **B683** (2010) 340–348 [0911.4905].

[41] D. Bailin and A. Love "Orbifold compactifications of string theory," *Phys.Rept.* **315** (1999) 285–408.

[42] P. K. Vaudrevange "Grand Unification in the Heterotic Brane World," [0812.3503].

[43] M. Fischer, M. Ratz, J. Torrado, and P. K. Vaudrevange "Classification of symmetric toroidal orbifolds," *JHEP* **1301** (2013) 084 [1209.3906].

[44] J. Erler and A. Klemm "Comment on the generation number in orbifold compactifications," *Commun. Math. Phys.* **153** (1993) 579–604 [hep-th/9207111].

[45] L. E. Ibanez and A. M. Uranga *String theory and particle physics: An introduction to string phenomenology.* Cambridge University Press 2012.

[46] M. Blaszczyk, S. Groot Nibbelink, and F. Ruehle "Gauged Linear Sigma Models for toroidal orbifold resolutions," *JHEP* **1205** (2012) 053 [1111.5852].

[47] F. Ploger, S. Ramos-Sanchez, M. Ratz, and P. K. S. Vaudrevange "Mirage Torsion," *JHEP* **04** (2007) 063 [hep-th/0702176].

[48] H. P. Nilles, S. Ramos-Sanchez, P. K. Vaudrevange, and A. Wingerter "The Orbifolder: A Tool to study the Low Energy Effective Theory of Heterotic Orbifolds," *Comput.Phys.Commun.* **183** (2012) 1363–1380 [1110.5229].

[49] T. Kobayashi, S. Raby, and R.-J. Zhang "Searching for realistic 4d string models with a Pati-Salam symmetry: Orbifold grand unified theories from heterotic string compactification on a Z(6) orbifold," *Nucl. Phys.* **B704** (2005) 3–55 [hep-ph/0409098].

[50] C. Ludeling, F. Ruehle, and C. Wieck "Non-Universal Anomalies in Heterotic String Constructions," *Phys.Rev.* **D85** (2012) 106010 [1203.5789].

[51] N. G. C. Bizet, T. Kobayashi, D. K. M. Pena, S. L. Parameswaran, M. Schmitz, *et al.* "R-charge Conservation and More in Factorizable and Non-Factorizable Orbifolds," [1301.2322].

[52] W. Fulton *Introduction to toric varieties.* Annals of mathematics studies ; 131, The William H. Roever lectures in geometry. Princeton Univ. Pr. 1997.

[53] D. Cox, J. Little, and H. Schenck "Toric varieties," *Graduate studies in mathematics. American Mathematical Society* (2011).

[54] P. S. Aspinwall "Resolution of orbifold singularities in string theory," [hep-th/9403123].

[55] D. Lüst, S. Reffert, E. Scheidegger, and S. Stieberger "Resolved toroidal orbifolds and their orientifolds," *Adv. Theor. Math. Phys.* **12** (2008) 67–183 [hep-th/0609014].

[56] S. Reffert "Toroidal Orbifolds: Resolutions, Orientifolds and Applications in String Phenomenology," [hep-th/0609040].

[57] S. Groot Nibbelink, M. Trapletti, and M. Walter "Resolutions of Cn/Zn Orbifolds, their U(1) Bundles, and Applications to String Model Building," *JHEP* **03** (2007) 035 [hep-th/0701227].

[58] S. Groot Nibbelink, T.-W. Ha, and M. Trapletti "Toric Resolutions of Heterotic Orbifolds," *Phys. Rev.* **D77** (2008) 026002 [0707.1597].

[59] S. Nibbelink Groot "Blowups of Heterotic Orbifolds using Toric Geometry," [0708.1875].

[60] M. Blaszczyk, S. Groot Nibbelink, F. Ruehle, M. Trapletti, and P. K. Vaudrevange "Heterotic MSSM on a Resolved Orbifold," *JHEP* **1009** (2010) 065 [1007.0203].

[61] M. Blaszczyk, N. G. Cabo Bizet, H. P. Nilles, and F. Ruehle "A perfect match of MSSM-like orbifold and resolution models via anomalies," *JHEP* **1110** (2011) 117 [1108.0667].

[62] E. Witten "Phases of N = 2 theories in two dimensions," *Nucl. Phys.* **B403** (1993) 159–222 [hep-th/9301042].

[63] J. Distler "Notes on (0,2) superconformal field theories," [hep-th/9502012].

[64] J. McOrist "The Revival of (0,2) Linear Sigma Models," *Int.J.Mod.Phys.* **A26** (2011) 1–41 [1010.4667].

[65] P. S. Aspinwall and M. R. Plesser "Elusive Worldsheet Instantons in Heterotic String Compactifications," [1106.2998].

[66] P. S. Aspinwall, B. R. Greene, and D. R. Morrison "The Monomial divisor mirror map," [alg-geom/9309007].

[67] P. S. Aspinwall "The Breakdown of topology at small scales," *JHEP* **0407** (2004) 021 [hep-th/0312188].

[68] P. S. Aspinwall "Probing Geometry with Stability Conditions," [0905.3137].

[69] G. 't Hooft (ed.), C. Itzykson (ed.), A. Jaffe (ed.), H. Lehmann (ed.), P. Mitter (ed.), *et al.* "Recent Developments in Gauge Theories," *NATO Adv.Study Inst.Ser.B Phys.* **59** (1980) 1–438.

[70] M. B. Green and J. H. Schwarz "Anomaly Cancellation in Supersymmetric D=10 Gauge Theory and Superstring Theory," *Phys. Lett.* **B149** (1984) 117–122.

[71] C. A. Scrucca and M. Serone "Anomalies in field theories with extra dimensions," *Int.J.Mod.Phys.* **A19** (2004) 2579–2642 [hep-th/0403163].

[72] L. Alvarez-Gaume and P. H. Ginsparg "The Structure of Gauge and Gravitational Anomalies," *Annals Phys.* **161** (1985) 423.

[73] K. Fujikawa "Path integral for gauge theories with fermions," *Phys. Rev.* **D21** (1980) 2848.

[74] T. Araki, T. Kobayashi, J. Kubo, S. Ramos-Sanchez, M. Ratz, *et al.* "(Non-)Abelian discrete anomalies," *Nucl.Phys.* **B805** (2008) 124–147 [0805.0207].

[75] T. Banks and M. Dine "Note on discrete gauge anomalies," *Phys.Rev.* **D45** (1992) 1424–1427 [hep-th/9109045].

[76] L. E. Ibanez and G. G. Ross "Discrete gauge symmetry anomalies," *Phys.Lett.* **B260** (1991) 291–295.

[77] T. van Ritbergen, A. N. Schellekens, and J. A. M. Vermaseren "Group theory factors for feynman diagrams," *Int. J. Mod. Phys.* **A14** (1999) 41–96 [hep-ph/9802376].

[78] A. Adams, O. DeWolfe, and W. Taylor "String universality in ten dimensions," *Phys.Rev.Lett.* **105** (2010) 071601 [1006.1352].

[79] W. Lerche, B. Nilsson, A. Schellekens, and N. Warner "ANOMALY CANCELLING TERMS FROM THE ELLIPTIC GENUS," *Nucl.Phys.* **B299** (1988) 91.

[80] P. Horava and E. Witten "Heterotic and type i string dynamics from eleven dimensions," *Nucl. Phys.* **B460** (1996) 506–524 [hep-th/9510209].

[81] P. Horava and E. Witten "Eleven-dimensional supergravity on a manifold with boundary," *Nucl. Phys.* **B475** (1996) 94–114 [hep-th/9603142].

[82] E. Witten "Strong Coupling Expansion Of Calabi-Yau Compactification," *Nucl. Phys.* **B471** (1996) 135–158 [hep-th/9602070].

[83] A. Lukas, B. A. Ovrut, and D. Waldram "Nonstandard embedding and five-branes in heterotic M theory," *Phys.Rev.* **D59** (1999) 106005 [hep-th/9808101].

[84] A. Lukas and K. S. Stelle "Heterotic anomaly cancellation in five dimensions," *JHEP* **01** (2000) 010 [hep-th/9911156].

[85] K. Becker, M. Becker, and A. Strominger "Five-branes, membranes and nonperturbative string theory," *Nucl.Phys.* **B456** (1995) 130–152 [hep-th/9507158].

[86] M. J. Duff, R. Minasian, and E. Witten "Evidence for Heterotic/Heterotic Duality," *Nucl. Phys.* **B465** (1996) 413–438 [hep-th/9601036].

[87] E. Witten "Small instantons in string theory," *Nucl.Phys.* **B460** (1996) 541–559 [hep-th/9511030].

[88] J. A. Casas, E. K. Katehou, and C. Munoz "U(1) Charges in Orbifolds: Anomaly Cancellation and Phenomenological Consequences," *Nucl. Phys.* **B317** (1989) 171.

[89] H. P. Nilles, S. Ramos-Sanchez, M. Ratz, and P. K. S. Vaudrevange "From strings to the MSSM," *Eur. Phys. J.* **C59** (2009) 249–267 [0806.3905].

[90] O. Lebedev, H. P. Nilles, S. Ramos-Sanchez, M. Ratz, and P. K. S. Vaudrevange "Heterotic mini-landscape (II): completing the search for MSSM vacua in a Z_6 orbifold," *Phys. Lett.* **B668** (2008) 331–335 [0807.4384].

[91] S. Groot Nibbelink, H. P. Nilles, and M. Trapletti "Multiple anomalous U(1)s in heterotic blow-ups," *Phys. Lett.* **B652** (2007) 124–127 [hep-th/0703211].

[92] P. S. Aspinwall, B. R. Greene, and D. R. Morrison "Measuring small distances in N=2 sigma models," *Nucl. Phys.* **B420** (1994) 184–242 [hep-th/9311042].

[93] F. Buccella, J. P. Derendinger, S. Ferrara, and C. A. Savoy "Patterns of Symmetry Breaking in Supersymmetric Gauge Theories," *Phys. Lett.* **B115** (1982) 375.

[94] G. Cleaver, M. Cvetic, J. R. Espinosa, L. L. Everett, and P. Langacker "Classification of flat directions in perturbative heterotic superstring vacua with anomalous U(1)," *Nucl. Phys.* **B525** (1998) 3–26 [hep-th/9711178].

[95] S. Groot Nibbelink, D. Klevers, F. Ploger, M. Trapletti, and P. K. S. Vaudrevange "Compact heterotic orbifolds in blow-up," *JHEP* **04** (2008) 060 [0802.2809].

[96] N. G. C. Bizet and H. P. Nilles "Heterotic Mini-landscape in blow-up,"
      [1302.1989].

[97] C. Vafa "Modular Invariance and Discrete Torsion on Orbifolds," *Nucl. Phys.*
      B273 (1986) 592.

[98] C. Vafa and E. Witten "On orbifolds with discrete torsion," *J. Geom. Phys.* **15**
      (1995) 189–214 [hep-th/9409188].

[99] J. A. Casas, A. de la Macorra, M. Mondragon, and C. Munoz "Z(7) phenomenol-
      ogy," *Phys. Lett.* **B247** (1990) 50–56.

[100] L. J. Dixon, D. Friedan, E. J. Martinec, and S. H. Shenker "The Conformal Field
      Theory of Orbifolds," *Nucl. Phys.* **B282** (1987) 13–73.

[101] S. Hamidi and C. Vafa "Interactions on Orbifolds," *Nucl. Phys.* **B279** (1987) 465.

[102] O. Lebedev *et al.* "A mini-landscape of exact MSSM spectra in heterotic orb-
      ifolds," *Phys. Lett.* **B645** (2007) 88–94 [hep-th/0611095].

[103] S. Raby and A. Wingerter "Can String Theory Predict the Weinberg Angle?,"
      Phys. Rev. **D76** (2007) 086006 [0706.0217].

[104] W. Buchmuller, J. Louis, J. Schmidt, and R. Valandro "Voisin-Borcea Manifolds
      and Heterotic Orbifold Models," *JHEP* **1210** (2012) 114 [1208.0704].

[105] A. Strominger "Yukawa Couplings in Superstring Compactification," *Phys. Rev.
      Lett.* **55** (1985) 2547.

[106] E. Witten "New issues in manifolds of SU(3) holonomy," *Nucl. Phys.* **B268** (1986)
      79.

[107] R. Donagi and M. Wijnholt "Model Building with F-Theory,"
      Adv.Theor.Math.Phys. **15** (2011) 1237–1318 [0802.2969].

[108] E. Witten "Symmetry Breaking Patterns in Superstring Models," *Nucl. Phys.*
      B258 (1985) 75.

[109] R. Blumenhagen, B. Jurke, and T. Rahn "Computational Tools for Cohomology
      of Toric Varieties," *Adv.High Energy Phys.* **2011** (2011) 152749 [1104.1187].

[110] A. Hebecker and M. Trapletti "Gauge unification in highly anisotropic string
      compactifications," *Nucl. Phys.* **B713** (2005) 173–203 [hep-th/0411131].

[111] G. Ross "Wilson line breaking and gauge coupling unification,"
      [hep-ph/0411057].

[112] P. Ko, T. Kobayashi, J.-h. Park, and S. Raby "String-derived D4 flavor symmetry
      and phenomenological implications," *Phys. Rev.* **D76** (2007) 035005 [0704.2807].

[113] W. Buchmüller, K. Hamaguchi, O. Lebedev, and M. Ratz "Supersymmetric
      Standard Model from the heterotic string," *Phys. Rev. Lett.* **96** (2006) 121602
      [hep-ph/0511035].

[114] O. Lebedev *et al.* "Low energy supersymmetry from the heterotic landscape," *Phys. Rev. Lett.* **98** (2007) 181602 [`hep-th/0611203`].

[115] O. Lebedev *et al.* "The Heterotic Road to the MSSM with R parity," *Phys. Rev.* **D77** (2008) 046013 [`0708.2691`].

[116] R. Blumenhagen, G. Honecker, and T. Weigand "Loop-corrected compactifications of the heterotic string with line bundles," *JHEP* **06** (2005) 020 [`hep-th/0504232`].

[117] H. M. Lee *et al.* "A unique Z_4^R symmetry for the MSSM," *Phys. Lett.* **B694** (2011) 491–495 [`1009.0905`].

[118] R. Kappl, B. Petersen, S. Raby, M. Ratz, R. Schieren, *et al.* "String-Derived MSSM Vacua with Residual R Symmetries," *Nucl.Phys.* **B847** (2011) 325–349 [`1012.4574`].

[119] M.-C. Chen, M. Ratz, C. Staudt, and P. K. Vaudrevange "The mu Term and Neutrino Masses," *Nucl.Phys.* **B866** (2013) 157–176 [`1206.5375`].

[120] A. Strominger and E. Witten "New Manifolds for Superstring Compactification," *Commun.Math.Phys.* **101** (1985) 341.

[121] S. Gukov, C. Vafa, and E. Witten "CFT's from Calabi-Yau four folds," *Nucl.Phys.* **B584** (2000) 69–108 [`hep-th/9906070`].

[122] "`cohomCalg` package." Download link 2010. High-performance line bundle cohomology computation based on [38]. http://wwwth.mppmu.mpg.de/members/blumenha/cohomcalg.

[123] S. Groot Nibbelink "Heterotic orbifold resolutions as (2,0) gauged linear sigma models," *Fortsch.Phys.* **59** (2011) 454–493 [`1012.3350`].

[124] M. Blaszczyk, S. Groot Nibbelink, and F. Ruehle "Green-Schwarz Mechanism in Heterotic (2,0) Gauged Linear Sigma Models: Torsion and NS5 Branes," *JHEP* **1108** (2011) 083 [`1107.0320`].

[125] C. Quigley and S. Sethi "Linear Sigma Models with Torsion," *JHEP* **1111** (2011) 034 [`1107.0714`].

[126] C. Quigley, S. Sethi, and M. Stern "Novel Branches of (0,2) Theories," *JHEP* **1209** (2012) 064 [`1206.3228`].

[127] A. Adams, E. Dyer, and J. Lee "GLSMs for non-Kahler Geometries," *JHEP* **1301** (2013) 044 [`1206.5815`].

[128] A. Adams, M. Ernebjerg, and J. M. Lapan "Linear models for flux vacua," *Adv. Theor. Math. Phys.* **12** (2008) 817–851 [`hep-th/0611084`].

[129] A. Adams and D. Guarrera "Heterotic Flux Vacua from Hybrid Linear Models," [`0902.4440`].

[130] A. Adams and J. M. Lapan "Computing the Spectrum of a Heterotic Flux Vacuum," *JHEP* **1103** (2011) 045 [`0908.4294`].

[131] G. Aldazabal, A. Font, L. E. Ibanez, and A. Uranga "New branches of string compactifications and their F theory duals," *Nucl.Phys.* **B492** (1997) 119–151 [hep-th/9607121].

[132] R. Donagi, A. Lukas, B. A. Ovrut, and D. Waldram "Non-perturbative vacua and particle physics in m-theory," *JHEP* **05** (1999) 018 [hep-th/9811168].

[133] R. Blumenhagen, G. Honecker, and T. Weigand "Non-Abelian brane worlds: The heterotic string story," *JHEP* **10** (2005) 086 [hep-th/0510049].

[134] G. Honecker "Massive U(1)s and heterotic five-branes on K3," *Nucl.Phys.* **B748** (2006) 126–148 [hep-th/0602101].

[135] L. B. Anderson, Y.-H. He, and A. Lukas "Monad Bundles in Heterotic String Compactifications," *JHEP* **0807** (2008) 104 [0805.2875].

[136] L. Carlevaro and D. Israel "Heterotic Resolved Conifolds with Torsion, from Supergravity to CFT," *JHEP* **1001** (2010) 083 [0910.3190].

[137] J. Distler "Notes on N=2 sigma models," [hep-th/9212062].

[138] A. Adams "Orbifold Phases of Heterotic Flux Vacua," [0908.2994].

[139] A. Adams, A. Basu, and S. Sethi "(0,2) duality," *Adv.Theor.Math.Phys.* **7** (2004) 865–950 [hep-th/0309226].

[140] K. Dasgupta, G. Rajesh, and S. Sethi "M theory, orientifolds and G - flux," *JHEP* **9908** (1999) 023 [hep-th/9908088].

[141] J.-X. Fu and S.-T. Yau "The Theory of superstring with flux on non-Kahler manifolds and the complex Monge-Ampere equation," *J.Diff.Geom.* **78** (2009) 369–428 [hep-th/0604063].

[142] J.-X. Fu, L.-S. Tseng, and S.-T. Yau "Local Heterotic Torsional Models," *Commun.Math.Phys.* **289** (2009) 1151–1169 [0806.2392].

[143] C. M. Hull and E. Witten "Supersymmetric sigma models and the heterotic string," *Phys. Lett.* **B160** (1985) 398–402.

[144] C. Hull and P. Townsend "World sheet supersymmetry and anomaly cancellation in the heterotic string," *Phys.Lett.* **B178** (1986) 187.

[145] D. Tong "NS5-branes, T duality and world sheet instantons," *JHEP* **0207** (2002) 013 [hep-th/0204186].